

# PROCEEDINGS

OF THE PAKISTAN ACADEMY OF SCIENCES:

**A. Physical and Computational Sciences**

ISSN Print: 2518-4245

ISSN Online: 2518-4253

Vol. 53(4), December 2016



PAKISTAN ACADEMY OF SCIENCES  
ISLAMABAD, PAKISTAN

# PAKISTAN ACADEMY OF SCIENCES

Founded 1953

**President:** Anwar Nasim  
**Secretary General:** Zabta K. Shinwari  
**Treasurer:** M.D. Shami

*Proceedings of the Pakistan Academy of Sciences*, published since 1964, is quarterly journal of the Academy. It publishes original research papers and reviews in basic and applied sciences. All papers are peer reviewed. Authors are not required to be Fellows or Members of the Academy, or citizens of Pakistan.

## Editor-in-Chief:

Abdul Rashid, Pakistan Academy of Sciences, Islamabad, Pakistan; [editor@paspk.org](mailto:editor@paspk.org)

## Discipline Editors:

**Chemical Sciences:** Peter Langer, University of Rostock, Rostock, Germany; [peter.langer@uni-rostock.de](mailto:peter.langer@uni-rostock.de)

**Chemical Sciences:** Syed M. Qaim, Universität zu Köln D-52425, JÜLICH, Germany; [s.m.qaim@fz-juelich.de](mailto:s.m.qaim@fz-juelich.de)

**Computer Sciences:** Sharifullah Khan, NUST, Islamabad, Pakistan; [sharifullah.khan@seecs.edu.pk](mailto:sharifullah.khan@seecs.edu.pk)

**Engineering Sciences:** Fazal A. Khalid, University of Engineering & Technology, Lahore, Pakistan; [vc@uet.edu.pk](mailto:vc@uet.edu.pk)

**Mathematical Sciences:** Muhammad Sharif, University of the Punjab, Lahore, Pakistan; [msharif.math@pu.edu.pk](mailto:msharif.math@pu.edu.pk)

**Mathematical Sciences:** Jinde Cao, Southeast University, Nanjing, Jiangsu, China; [jdcao@seu.edu.cn](mailto:jdcao@seu.edu.cn)

**Physical Sciences:** M. Aslam Baig, National Center for Physics, Islamabad, Pakistan; [baig77@gmail.com](mailto:baig77@gmail.com)

**Physical Sciences:** Stanislav N. Kharin, 59 Tolebi, Almaty, Kazakhstan; [staskharin@yahoo.com](mailto:staskharin@yahoo.com)

## Editorial Advisory Board:

David F. Anderson, The University of Tennessee, Knoxville, TN, USA; [anderson@math.utk.edu](mailto:anderson@math.utk.edu)

Ismat Beg, Lahore School of Economics, Pakistan; [ibeg@lahoreschool.edu.pk](mailto:ibeg@lahoreschool.edu.pk)

Rashid Farooq, National University of Sciences & Technology, Islamabad, Pakistan; [farooq@sns.nust.edu.pk](mailto:farooq@sns.nust.edu.pk)

R. M. Gul, University of Engineering & Technology, Peshawar, Pakistan; [rmgul@uetpeshawar.edu.pk](mailto:rmgul@uetpeshawar.edu.pk)

M. Asghar Hashmi, The Islamia University of Bahawalpur, Pakistan; [mhashmi@iub.edu.pk](mailto:mhashmi@iub.edu.pk)

Aynur Keskin Kaymakci, Selcuk University, Konya, Turkey; [akeskin@selcuk.edu.tr](mailto:akeskin@selcuk.edu.tr)

T. I. Khan, Qatar University, Doha, Qatar; [tkhan@qu.edu.qa](mailto:tkhan@qu.edu.qa)

Zhou Lang, Nanchang University, Nanchang, Jiangxi, 330031, China; [lzhou@ncu.edu.cn](mailto:lzhou@ncu.edu.cn)

Shaukat Mahmood, Mirpur University of Science & Technology, Mirpur, Pakistan; [shau\\_meph@yahoo.com](mailto:shau_meph@yahoo.com)

Waqar Mahmood, University of Engineering & Technology, Lahore, Pakistan; [waqar@uet.edu.pk](mailto:waqar@uet.edu.pk)

Onaiza Maqbool, Quaid-i-Azam University, Islamabad, Pakistan; [onaiza@qau.edu.pk](mailto:onaiza@qau.edu.pk)

Nadeem Mufti, University of Engineering & Technology, Lahore, Pakistan; [namufti@uet.edu.pk](mailto:namufti@uet.edu.pk)

Adele Maria Muscolo, University Mediterranea di Reggio Calabria, Italy; [amuscolo@unirc.it](mailto:amuscolo@unirc.it)

Naveed K. Piracha, John Carroll University, University Heights, OH, USA; [npiracha@jcu.edu](mailto:npiracha@jcu.edu)

Martin C. Richardson, University of Central Florida, FL, USA; [mcr@creol.ucf.edu](mailto:mcr@creol.ucf.edu)

Mudasser Faraz Wyne, National University, San Diego, CA, USA; [mwyne@nu.edu](mailto:mwyne@nu.edu)

Muhammad Younas, Oxford Brookes University, Oxford, OX33 1HX, UK; [m.younas@brookes.ac.uk](mailto:m.younas@brookes.ac.uk)

**Annual Subscription:** Pakistan: Institutions, Rupees 2000/- ; Individuals, Rupees 1000/-

Other Countries: US\$ 100.00 (includes air-lifted overseas delivery)

© *Pakistan Academy of Sciences*. Reproduction of paper abstracts is permitted provided the source is acknowledged. Permission to reproduce any other material may be obtained in writing from the Editor-in-Chief.

The data and opinions published in the *Proceedings* are of the author(s) only. The *Pakistan Academy of Sciences* and the *Editors* accept no responsibility whatsoever in this regard.

**HEC Recognized, Category X; PM&DC Recognized**

Published by **Pakistan Academy of Sciences**, 3 Constitution Avenue, G-5/2, Islamabad, Pakistan

Tel: 92-5 1-920 7140 & 921 5478; Fax: 92-51-920 6770; Website: [www.paspk.org](http://www.paspk.org)

Printed at **PanGraphics (Pvt) Ltd.**, No. 1, I & T Centre, G-7/I, Islamabad, Pakistan

Tel: 92-51-220 2272, 220 2449 Fax: 92-51-220 2450 E-mail: [pangraph@gmail.com](mailto:pangraph@gmail.com)



# PROCEEDINGS

## OF THE PAKISTAN ACADEMY OF SCIENCES:

### A. Physical and Computational Sciences

## CONTENTS

Volume 53, No. 4, December 2016 Page

### Research Articles

- Enhanced Performance of Consensus Fault-tolerant Schemes for Decentralized Unmanned Autonomous Vehicle System 363  
— *Naeem Khan, Aitzaz Ali, and Wasi Ullah*
- Identification of Factors Affecting Modal Shift in Lahore 373  
— *Sulaiman Majeed and Zahara Batool*
- Generating EXPRESS Data Models from SBVR 381  
— *Imran Sarwar Bajwa, Nadeem Sarwar, and M. Asif Naeem*
- CFD Analysis to Study the Effect of Geometry in Flow Behavior of Wing Structure with Additional Riblets 391  
— *Muhammad Zia Ullah Khan, Rumeel A. Bhutta, Tahir Asif, Muhammad Farooq, and Adnan Qamar*
- Palm and Finger Segmentation of High Resolution Images using Hand Shape and Texture 401  
— *Momna Asghar, Irfan Arshad, Imtiaz Ahmad Taj, Gulistan Raja, and Ahmad Khalil Khan*
- An Empirical Study and a Framework for Effective Risk Management in Scrum 417  
— *Muneeb Ali, Yasir Hafeez, and Bushra Hamid*
- Fabrication and Identification of Graphene Layers on Silicon Dioxide and Flexible PMMA Substrates 431  
— *Zeba Khanam, Ibtisam Riaz, Adeel Rasheed, and Rashid Jalil*
- Product and Exponential Product Estimators in Adaptive Cluster Sampling under Different Population Situations 447  
— *Muhammad Shahzad Chaudhry, and Muhammad Hanif*
- Matter Wave Travelling Dark Solitons in a Coupled Bose-Einstein Condensate 459  
— *Muhammad Irfan Qadir and Sumreen Naz*
- Characterizing Semirings using Their Quasi and Bi-Ideals 469  
— *Mohammad Munir, and Mustafa Habib*

### Obituaries

- Prof. Dr. Muzaffer Ahmad 477  
Prof. Dr. Syed Qasim Mehdi 478

**Instructions for Authors** 479

---

**Submission of Manuscripts:** Manuscripts may be submitted as E-mail attachment at [editor@paspk.org](mailto:editor@paspk.org). Authors must consult the **Instructions for Authors** at the end of this issue or at the Website: [www.paspk.org](http://www.paspk.org)





# Enhanced Performance of Consensus Fault-tolerant Schemes for Decentralized Unmanned Autonomous Vehicle System

Naeem Khan\*, Aitzaz Ali, and Wasi Ullah

\*Electrical Engineering Department, University of Engineering and Technology Peshawar, Bannu Campus, Pakistan

**Abstract:** This paper addresses schemes for fault detection and isolation in a semi-decentralized environment. Now-a-days, sensor fault and failure are prevalent issues in numerous wireless sensor networks. We propose a few algorithms based on simple phenomenon of data fusion. Initially, a mutual consensus has been built among followers (e.g., Unmanned Autonomous Vehicles in this case) who are tracking a combine target. Having known the followers, relative positions with respect to target, a median is computed by each follower. This median is then shared with immediate and extended neighbours to compare with their estimated values about the same target position. If estimation is beyond the prescribed limits, the follower (sensor) is diagnosed as faulty, otherwise is considered healthy. Three different types of induced faults are discussed here: (i) follower – target or line of communication fault; (ii) follower – follower or communication with neighbour fault; and (iii) simultaneously these two faults. The scenario wherein eight followers are tracking a combine target in circular fashion has been considered to elaborate these faults.

**Keywords:** Median, FDI, data fusion, sensor faults, target tracking

## 1. INTRODUCTION

In the modern era the use of sensors is increasing day by day. Sensors are very useful as they measure physical quantities and convert them into signals [1]. These signals are then observed by observers or instruments which can be processed further for controlling purposes. As the world is moving towards autonomy and sensors are the core devices to give the feature any autonomous system, autonomous research is prevailing day by day [2]. However, majority of sensors are electronic devices and are vulnerable to faults and failures. The fault/failures may be because of electronic malfunctioning, manufacturer defect or bad weather condition etc. An important issue of a typical sensor network is to detect and report the locations of targets e.g. Tanks, land mines, etc, in the presence of faulty sensor measurements [3].

The requirements for sensor reliability,

availability, and security are growing significantly due to the growing trends towards autonomous system. An effective mean to assure the reliability and security of a sensor is to detect faulty sensors. To avoid system's failure and smooth operation due to sensor fault, system must handle and accommodate faulty sensors [4]. For example, in modern flight control system, sensor failures may cause severe problems which need to be accurately detected and isolated as soon as possible. Towards this end, various schemes have been presented in [5 - 6] and reference therein for Fault Detection and Isolation (FDI). In this connection, algorithms in Gaussian noisy environments use Kalman filter for estimation [7] or low-pass or high-pass filters [8-9]. A few of them address wireless sensor networks which use Bayesian technique [10], maximum likelihood scheme [7], or voting approaches [8] to observe and remove faulty UAV from the network. In [11], the authors have claimed that under a

mild assumption the proposed decentralized scheme is capable of almost detecting faulty sensors, even if half of the neighboring sensors are faulty. Other addresses wireless sensor networks which use Bayesian technique [10], maximum likelihood scheme [12], voting approaches [13] or residual generation technique [14] to observe and remove faulty UAV from the network. A decentralized technique for fault detection has been proposed [11]. This technique was proved to detect fault(s) under some assumptions in the event bisected UAV are erroneous. Task-oriented consensus algorithm have also been developed and implemented by various scholars including the presented work in the literature [15]. The technique in [9] employs two observations,  $d_{lm}(t)$  and  $\Delta d_{lm}^{\Delta t}$  where  $d_{lm}(t)$  is the difference between two consecutive readings “ $l$ ” and “ $m$ ” at instant  $t$  and  $\Delta d_{lm}^{\Delta t}$  is the change of  $d_{lm}(t)$  over a defined time span  $\Delta t$ . In the event, more than half of the tracking devices  $m \in N_l$  are such that their readings are less than allowed brink reading, then the reading “ $l$ ” is decided as acceptable and is subsequently used for diagnosing other sensors as good or faulty. “Although this scheme has claimed to be probabilistically attractive, it is noted that the two measures are not sufficient for detecting a group of faulty sensors all together in a faulty zone. For instance, one can easily consider a situation in which a faulty sensor  $l$  has its  $m$  neighboring sensors faulty, and therefore  $d_{lm}(t) = \Delta d_{lm}^{\Delta t} = 0$  for a particular time period and diagnosing the faulty sensor as good.”

The current work resolve the above mentioned issue by developing a decentralized, consensus scheme for a generalized network scenario of target and followers, where in target is tracked down by the followers. The proposed scheme guarantees accurate fault detection and isolation if there exists any faulty sensor in the network, thus assuring successful tracking of the target which is the primary objective of the generalized scenario.

## 2. PROBLEM STATEMENT

The objective of this paper is to track a combine target in a decentralized network while maintaining a specific formation  $\mathfrak{R}$ . When all the

sensors are healthy (no fault), the formation may be maintained by just keeping the relative distances constant with respect to target. However, when a sensor/UAV is unable to follow the target due to any abnormal condition, how to track the target and maintain that specific formation  $\mathfrak{R}$  is the issue address in this paper.

## 3. PROBLEM SCENARIO

Among the eight (08) follower UAVs, the corresponding target position estimated by  $l^{th}$  UAV is denoted by  $p_l(t)$ . It is assumed that position sensor reading follows Gaussian distribution due to which estimated target position information deviates from the actual target position  $p(t)$ . The deviation is standard deviation  $\sigma$  relative to the actual target position  $p(t)$ . Each UAV shares its information with all other UAVs (neighbours) within its sensor range. It is because each UAV should act according to the very similar information to keep the predefined formation  $\mathfrak{R}$  throughout the mission. Let the number of faulty sensors  $f$  in the network is less than half of the total sensors in network, i.e.,  $f < n/2$  where  $n$  is the total number of sensors in the network. It is assumed that for the  $l^{th}$  UAV to track the target, it must first estimate the target position  $a_l(t + \Delta t)$ . Once the  $l^{th}$  UAV has this information it can easily change its current position  $b_l(t)$  to  $b_l(t + \Delta t)$  to maintain the initial formation  $\mathfrak{R}$  relative to target position by using

$$b_l(t + \Delta t) = a_l(t + \Delta t) + b_l(0) - a_l(0)$$

Where

$b_l(t + \Delta t)$  is  $l^{th}$  UAV position at time  $t + \Delta t$ ,  $a_l(t + \Delta t)$  is target position at time  $t + \Delta t$ ,  $b_l(0)$  is  $l^{th}$  UAV initial position at time  $t = 0$ , and  $a_l(0)$  is target initial position at time  $t = 0$ .

## 4. PROPOSED ALGORITHMS

The proposed fault tolerant scheme consists of three algorithms:

1. Semi-decentralized data fusion algorithm [11, 16]

2. LOC (Line Of Communication) FDI algorithm [16]
3. CN (Communication with Neighbour) fault detection algorithm.

The LOC is a link between an UAV and target through which the UAV measure target position. On the other side, a CN is a medium two between UAVs through which they share their target position information with each other.

#### 4.1 Semi-decentralized Data Fusion Algorithm

The Semi-decentralized data fusion algorithm is employed by each UAV to update target position information and then change its position accordingly. The equation that summarizes Semi-decentralized data fusion algorithm [10] is

$$a_l(T) = (1 - \beta)a_l(T - 1) + \sum_{m \in M_l^r} [c_{lm}(T - r)p_m(T - r)] \quad (1)$$

Where  $a_l$  is estimated target position by  $l^{\text{th}}$  UAV,  $b_l$  is  $l^{\text{th}}$  UAV position information,  $r$  is the number of links with neighbors,  $p_m$  is  $m^{\text{th}}$  UAV sensor information and  $M_l^r$  is the set of  $l^{\text{th}}$  UAV and its  $r$ -neighbors which can be reached from  $l^{\text{th}}$  UAV through  $r$  links. The number of faulty sensors  $f$  in the set  $M_l^r$  must be such that  $f < r/2$  and  $c_{lm}$  is [1]

$$c_{lm}(T - r) = \frac{\beta e^{-\gamma} |p_l(T - r) - p_j(T - r)|}{\sum_{m \in M_l^r} e^{-\gamma} |p_l(T - r) - p_j(T - r)|} \quad (2)$$

In the above equation,  $\beta$  and  $\gamma$  are constant parameters. Its values are  $0 < \beta < 1$  and  $\gamma > 0$ , where  $p_l$  is the median of target position information of the  $l^{\text{th}}$  UAV sensor information and its neighbors readings. Initially when sensors are not diagnosed for fault yet, let all the sensors are healthy and non of the sensor is faulty thus making  $r$  equal to 1 i.e.  $r = 1$ .

#### 4.2 LOC Fault Detection and Isolation Algorithm

The above discussed Semi-decentralized data fusion algorithm is employed by UAV to estimate

the target position information, using this information, an UAV estimates its new position and move to that new position but at the same time the LOC (Line Of Communication) fault detection and isolation algorithm also operates in order to detect for faulty sensors in the network and isolate them from the network. This scheme follow two steps: First, it finds the global median of target position from the estimated target position ( $s$ ) information of the UAVs belonging to the set  $M_l^r$  over  $l^{\text{th}}$  UAV within a fixed tolerance; Secondly, that global median is then propagated to the UAVs belonging to the set  $M_l^r$  in order to determine faulty UAVs (those UAVs which have discrepancies with the global median beyond the fixed tolerance) and non-faulty UAVs.

In the first step of LOC FDI algorithm, the set of UAVs is  $M_l^r$  which is used to find the global median of target position information by gathering the target position information from the UAVs of set  $M_l^r$ , must satisfy the condition of  $f < n/2$  i.e. the number of faulty sensors  $f$  in the set  $M_l^r$  must be less than half of the total sensors  $n$  in that set. It is because one needs  $f + 1$  similar information i.e.  $|p_l - p_m| \leq 2\sigma$  in order to find the correct global median of target position information. If the set  $M_l^r$  does not satisfy the condition  $f < n/2$  or the set  $M_l^r$  does not have  $f + 1$  similar information then global median cannot be calculated from that set. In such case, the concept of extended neighbor is utilized i.e. extended neighbors are added to the set  $M_l^r$  and then global median is computed. In short, any UAV requires at least three similar information in order to find correct global median of target position information.

In the second step of LOC FDI algorithm, the found global median is distributed among the UAVs belonging to the set  $M_l^r$  to diagnose for faulty and healthier sensors. If the difference  $|G.Med - p_l|$  exceeds  $2\sigma$  the sensor is diagnosed as faulty. Once the sensor is diagnosed as faulty its information is replaced by global median in order to prevent faulty information from entering into the data fusion algorithm thus

assuring that faulty sensors are isolated from the network.

### 4.3 CN (Communication with Neighbor) Fault Detection Algorithm

Beside semi-decentralized data fusion algorithm and LOC FDI algorithm i.e. CN fault detection algorithm also operates to disclose CN fault in the network. CN fault is a fault in those sensors through which UAVs communicate with its neighbors. If CN fault exists between any two UAVs then these UAVs may not be able to share their target position information and global median information with each other. So detection of such fault is important in order to enhance the accuracy of target tracking network.

#### (i) Semi-decentralized data fusion algorithm

Determine number of neighbors  $r$  for  $l^{th}$  UAV,  $M_l^r$  and  $c_{lm}(t - (r-1)\Delta t)$  for  $m \in M_l^r$

- $a_l(t + \Delta t) = (1 - \beta)a_l(t) + \sum_{m \in M_l^r} c_{lm}(t - (r-1)\Delta t)p_m(t - (r-1)\Delta t)$
- $b_l(t + \Delta t) = a_l(t + \Delta t) + a_l(0) + b_l(0)$

#### (ii) LOC fault detection algorithm.

$\in M_l|_s$  = set of sensors (UAVs) that have similar information and can be reached from  $l^{th}$  UAV.

if

$$|\in M_l|_s \geq F + 1$$

$$G.Med_l = median(\Pi_l)$$

While

$$|\in M_l|_s < F + 1$$

if

$$G.Med_m = found$$

$$G.Med_l = G.Med_m$$

$$\text{else } \in M_l = \in M_l \cup \sum_{m \in M_l^r} \in M_m$$

$$G.Med_l = median(\Pi_l)$$

if

$$|G.Med_l - p_l(t)| > 2\sigma$$

$l^{th}$  UAV sensor has LOC fault

else  $l^{th}$  UAV sensor is non-faulty

#### (iii) LOC fault detection algorithm.

$\in M_l|_s$  = set of sensors (UAVs) that have similar information and can be reached from  $l^{th}$  UAV.

if

$$|\in M_l|_s \geq F + 1$$

$$G.Med_l = median(\Pi_l)$$

While

$$|\in M_l|_s < F + 1$$

if

$$G.Med_m = found$$

$$G.Med_l = G.Med_m$$

$$\text{else } \in M_l = \in M_l \cup \sum_{m \in M_l^r} \in M_m$$

$$G.Med_l = median(\Pi_l)$$

if

$$|G.Med_l - p_l(t)| > 2\sigma$$

$l^{th}$  UAV sensor has LOC fault

else  $l^{th}$  UAV sensor is non-faulty

## 5. SIMULATION RESULTS

The above three tables show the proposed semi-decentralized data fusion algorithm, LOC fault detection algorithm and CN fault detection algorithm respectively.

Fig. 1 represents the general scenario that has been considered to testify the proposed algorithms. In the Figure, the red box at the center represents the target which is tracked by eight UAVs represented by blue boxes. The black lines

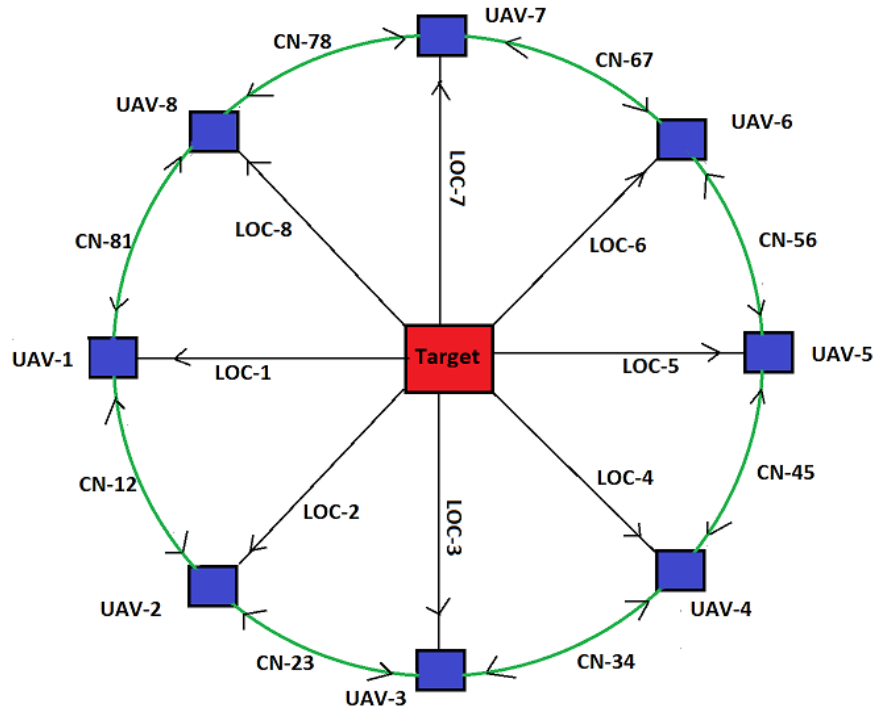


Fig. 1. Formation of UAVs to track the target.

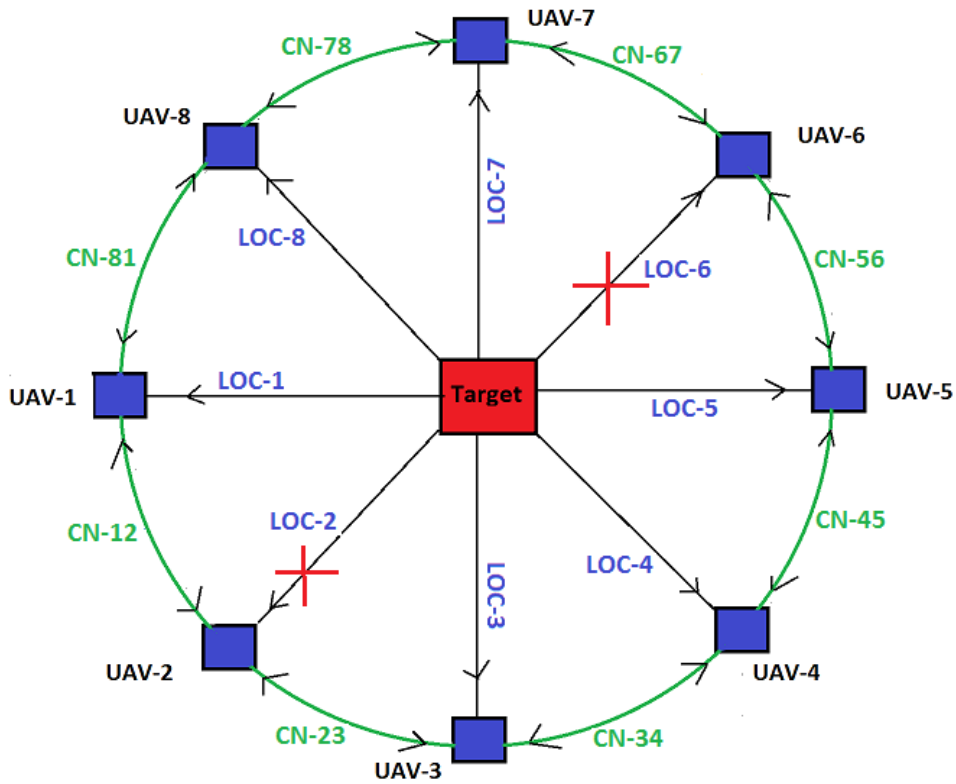


Fig. 2. Line of communication faults in UAV 2 and UAV 6.

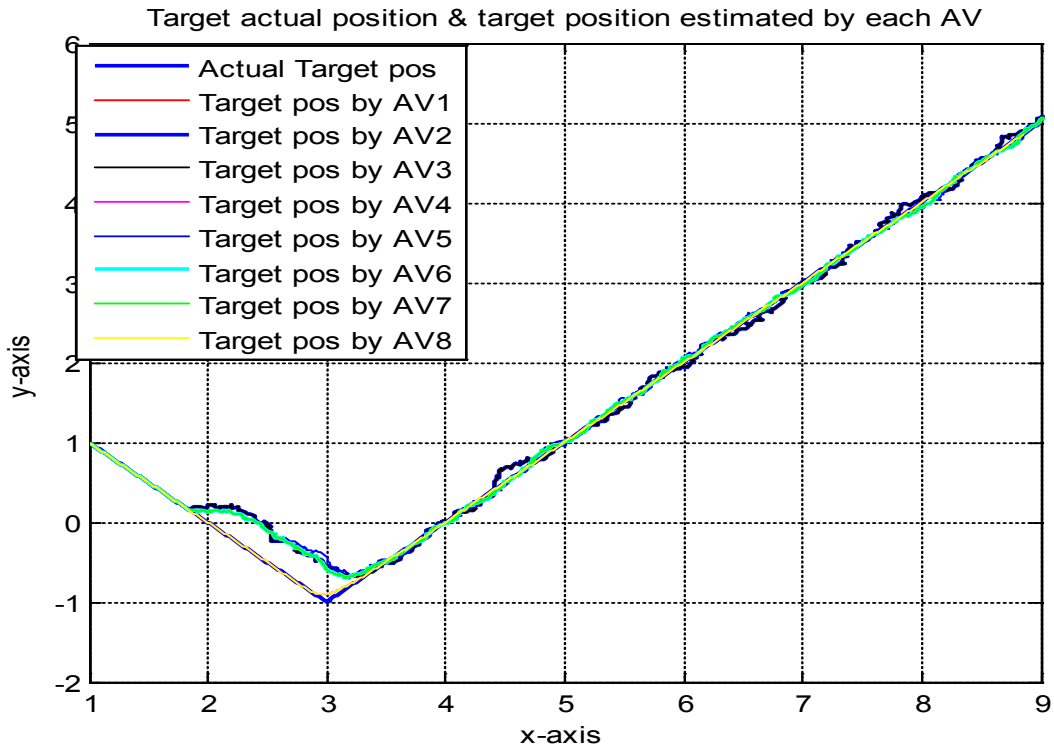


Fig. 3. Actual target position and estimation of target position by all UAVs.

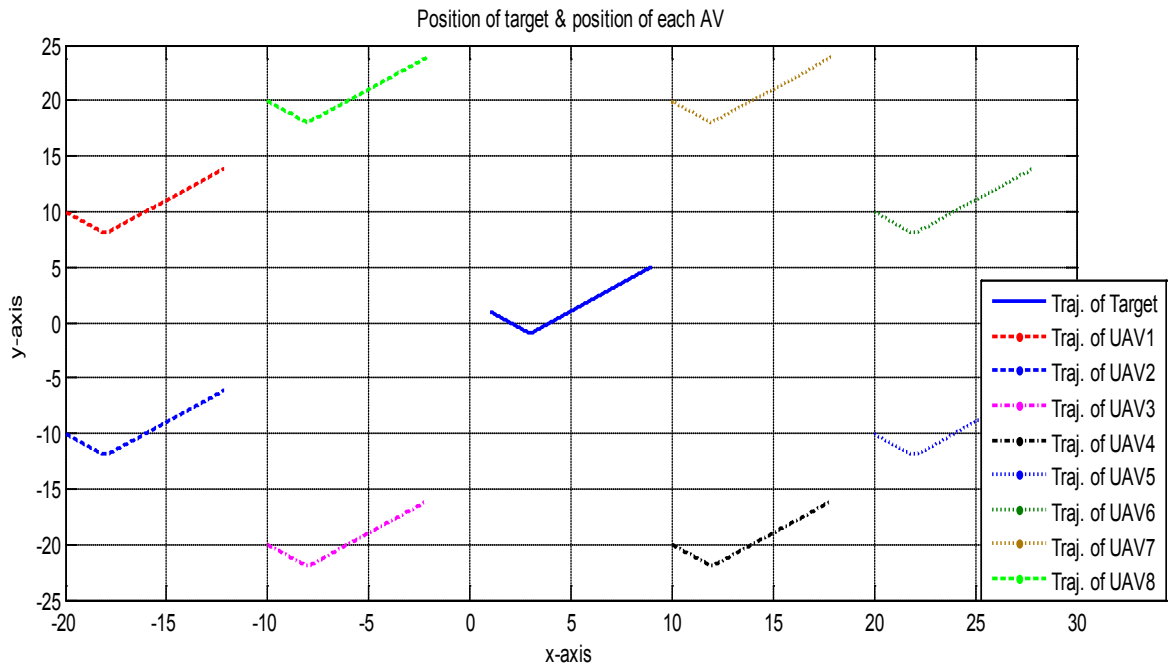


Fig. 4. Trajectories of target and UAVs (top view).

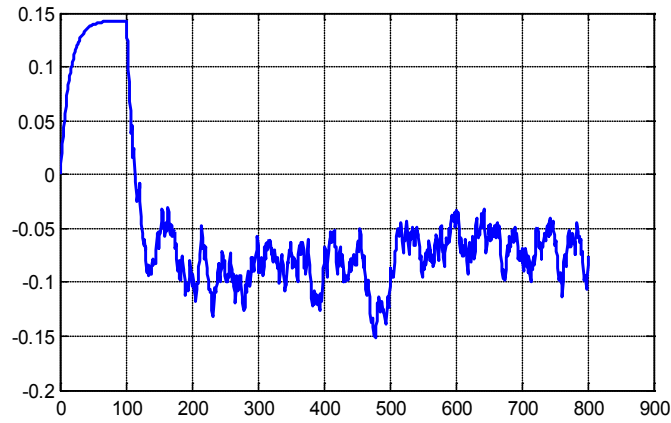


Fig. 5. Maximum possible deviation of UVA2 along Y-axis in the presence of LOC fault.

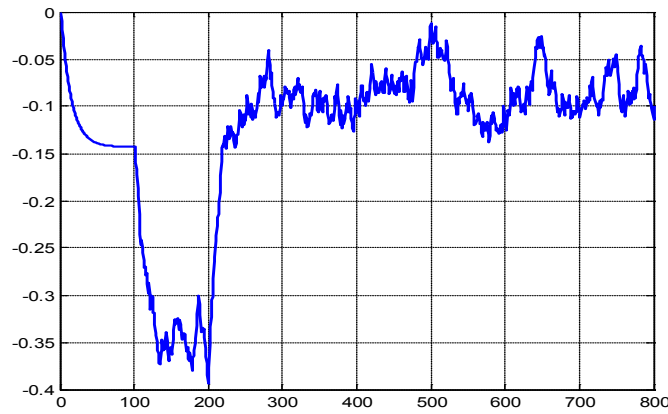


Fig. 6. Maximum possible deviation of UVA6 along Y-axis in the presence of LOC fault.

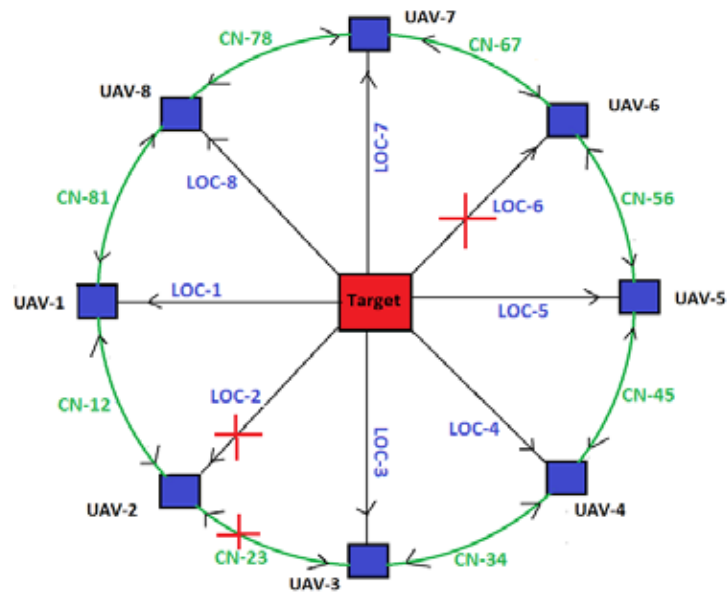


Fig. 7. Scenario for simultaneous LOC and CN faults.

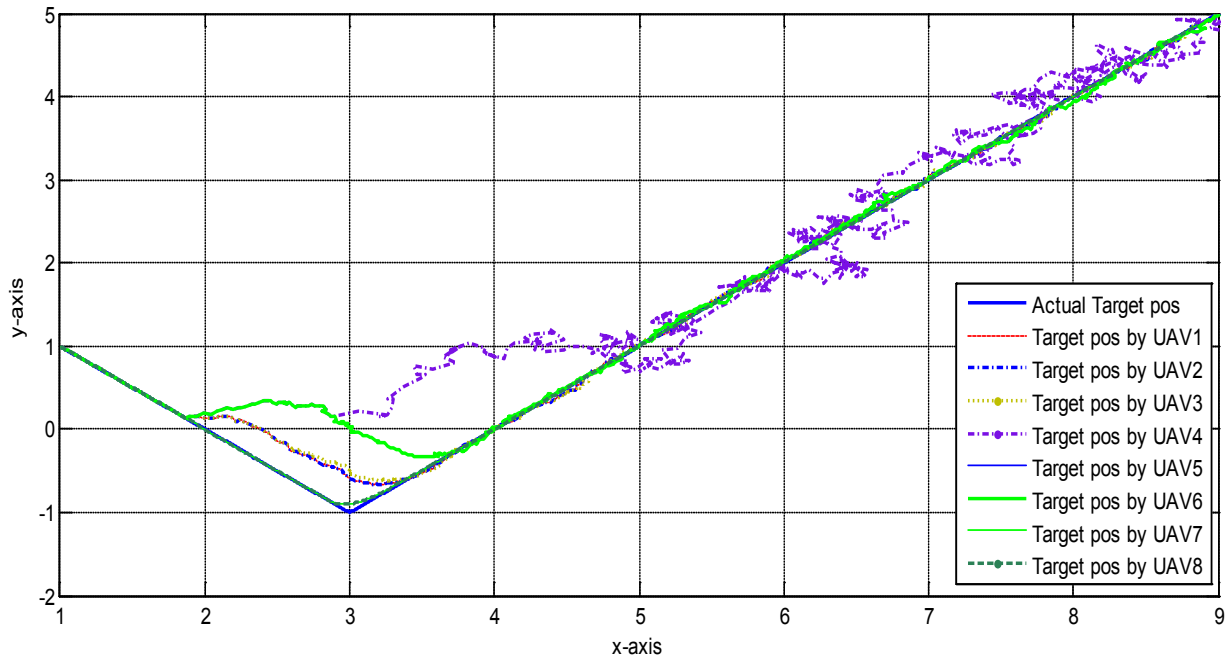


Fig. 8. Target actual trajectory and trajectories of UAVs for the scenario of Fig. 7.

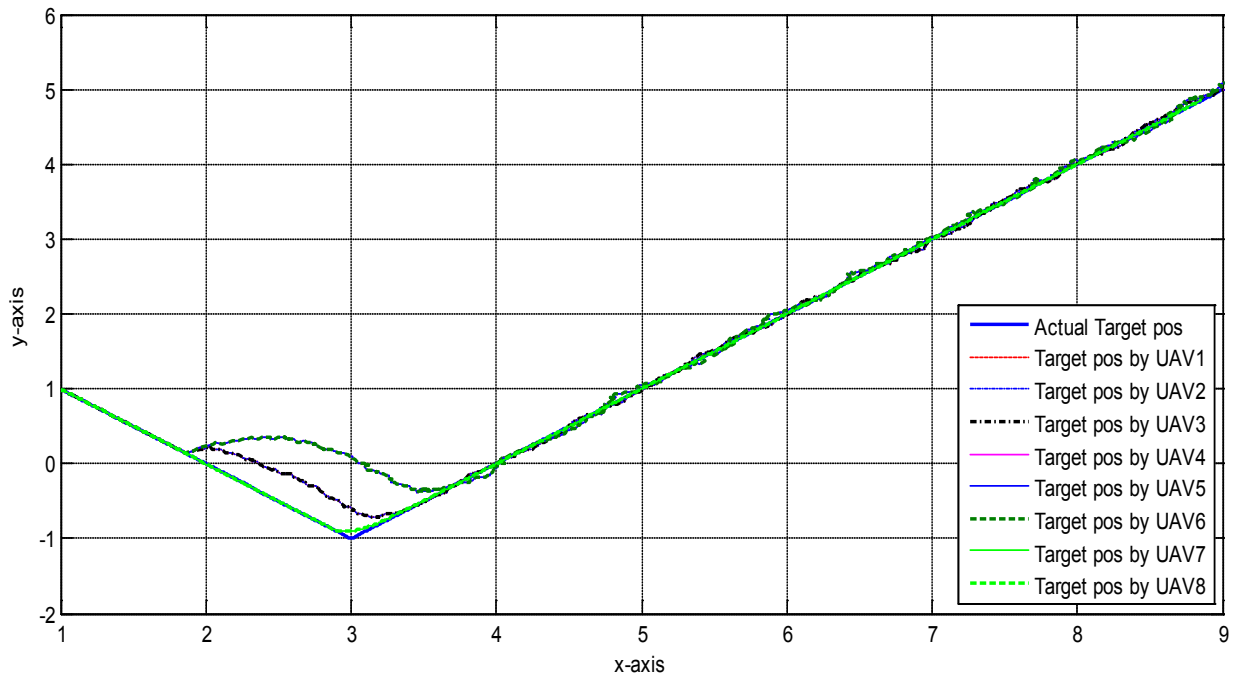


Fig. 9. Target actual position and target position estimated by each UAV using LOC and CN FDI algorithms simultaneously.

represent LOC links (connecting each UAV with target) through which each UAV senses the target position and track it down. The green lines (among successive UAVs) represent CN links through which each UAV communicate with its neighbor sharing its own target position information. Let the target enters into a bad weather condition zone where UAV 2 and UAV 6 cannot sense the actual target position as shown in Fig. 2. In this scenario, UAV 2 and UAV 6 are unable to track the target, leading to the failure of mission because of faulty sensor's information about target position. The simulation results are shown for the faulty scenario (double LOC fault). Due to the employment of LOC algorithm, as shown in Fig. 3 that UAV 2 and UAV 6 are still tracking the target in the presence of sensor faults. This is due to the operation of semi-decentralized data fusion algorithm and LOC FDI algorithm which forces both faulty UAVs to track the target, stay confined to the trajectory and maintains the initial distance constant throughout the mission.

It can also be confirmed that the trajectories of UAV 2 (represented by blue line) and UAV 6 (represented by green line) deviates from the exact path at the instant of fault occurrence in the system. Once the fault is diagnosed, the LOC-FDI algorithm causes to remove the reading of faulty UAVs/sensors from computing the global median. Fig. 4 shows a clear picture of trajectories of the target and the follower UAVs claiming that UAV 2 and UAV 4 (represented by red lines) are tracking the target accurately though their sensors cannot sense the target position.

Fig. 5 and 6 show the distances of UAV 6 from the target along X and Y axes increase at the instant of fault occurrence. However, upon diagnosing the fault and employing LOC-FDI algorithm, both the UAVs maintain the initial distance relative to target. Hence, the deviation does not exceed the allowed threshold limit of  $\pm 0.15$ . The deviation results are similar for both UAVs.

Consider another scenario where both LOC and CN faults occur simultaneously as shown below in Fig. 7. The LOC fault exists in UAV 2 and UAV 6 whereas UAV 2 and UAV 3 have CN fault which prevents information flow between them. Since UAV 2 is suffering from LOC fault (and cannot sense the target) and at the same time, it suffers from CN fault, hence it should not be able to track the target accurately. The simulation

results in Fig. 8 clearly shows that UAV 2 is unable to track the target accurately as it is suffering from both LOC and CN faults shown by blue line below.

Implementing the proposed LOC and CN-FDI algorithms simultaneously have resulted in superior performance. The affected UAV 2 is tracking the target with better result as shown in Fig. 9.

## 6. SUMMARY

In this paper, the proposed scheme designed for multi sensor target tracking network comprises of three algorithms: semi-decentralized data fusion algorithm, LOC fault detection and isolation algorithm and CN fault detection and isolation algorithm. The main theme is finding of global median from healthy (non-faulty) sensor readings using semi-decentralized algorithm. This global median is utilized to trace faulty and non-faulty sensors using Line-of-communication FDI algorithm and Communication-with-neighbor FDI algorithm.

## 7. REFERENCES

1. Stephen, A.D. *Wiley Survey of Instrumentation and Measurement*. John Wiley & Sons (2007).
2. Mele, A.R. *Autonomous Agents: From Self-Control to Autonomy*. Oxford University Press, doi:10.1093/0195150430.001.0001. Oxford Scholarship Online. (1995).
3. Ding, M., F. Liu, A. Thaeler, D. Chen, & X. Cheng, X. Fault-tolerant target localization in sensor networks. *EURASIP Journal on Wireless Communications and Networking* 7 (1): 1-9 (2007).
4. Fábrega, A.J.S., J.M.B. Caro, P.J.A. Herrera, & D.M. Santos. Fault detection methods based on bounded error and dynamic threshold techniques. *International Journal of Adaptive Control and Signal Processing* 30(2): 256-270 (2016).
5. Alwi, H., C. Edwards, & A. Marcos. Fault reconstruction using a LPV sliding mode observer for a class of LPV systems. *Journal of the Franklin Institute* 349(1): 510-530 (2012).
6. Grenaille, S., D. Henry, & A. Zolghadri. A method for designing fault diagnosis filters for LPV polytopic systems. *Journal of Control Science and Engineering* 1(6): 1-11, (2008).

7. Ren, W., R.W. Beard, & D.B. Kingston. Multiagent Kalman consensus with relative uncertainty. In: *Proceedings of the American Control Conference*, p. 1865–1870 (2005).
8. Saber, R.O. & J.S. Shamma. Consensus filters for sensor networks and distributed sensor fusion. In: *Proceedings of 44th IEEE Conference on Decision & Control and European Control Conference*, p. 6698-6703 (2005).
9. Spanos, D. P., R.O. Saber, & R.M. Murray. *Dynamic consensus on mobile networks*. In: *Proceedings of the 16th IFAC World Congress*, p. 1-6 (2005).
10. Lokesh, B.B. & N. Nalini. Bayesian network based fault tolerance in distributed sensor networks. *Journal of Telecommunication and Information technology* 4(14): 44-52 (2014).
11. Kim, Y.S. D.W. Gu & I. Postlewaite. *Fault-tolerant Cooperative Target Tracking in Distributed AV Network*. IFAC, Seoul Korea, p. 8878 - 8883 (2008).
12. Kuang, X. & H. Shao. Maximum likelihood localization algorithm using wireless sensor network. In: *1<sup>st</sup> IEEE International Conference on Innovative Computing, Information and Control ICICIC*, p. 263-266 (2006).
13. Bass, J.M., G.L. Shabgahi, & S. Bennett. Experimental comparison of voting algorithms in cases of disagreement. In: *Proceeding of the 23rd Euromicro Conference*, p. 516-523 (1997).
14. Wan, Y. & Y. Hao. Integrated design of residual generated and evaluation for fault detection of networked control system, *International Journal of Robust Nonlinear Control* 26(3): 519-544, (2015).
15. Chen, X. Hu, Y. & X. Guangyan. A study on the multiple UAVs cooperative Fire Fighting based on consensus algorithm, *International Journal of Control and Automation* 8(8): 309-324 (2015).
16. Postlewaite, I., D.W. Gu, Y.S. Kim, K. Natesan, M. Kothari, N. Khan, & R. Omar. A Robust fault-tolerant tracking scheme. *Realising Network Enable Capability, RNEC08*, p. 12-17 (2008).



# Identification of Factors Affecting Modal Shift in Lahore

Sulaiman Majeed<sup>1,\*</sup>, and Zahara Batool<sup>2</sup>

<sup>1</sup>Transport Department, Government of the Punjab, Lahore, Pakistan

<sup>2</sup>Department of Transportation Engineering, University of Engineering & Technology,  
Lahore, Pakistan

**Abstract:** The popularity of Metro Bus System (MBS) on the whole is increasing in different cities of developing countries that are looking for cost effective sustainable mass transit solutions. One such example is Lahore, which is under grave influence of poor urban public transportation system. To improve this, MBS was introduced on one of its busiest corridors from Shahdara to Gajjumatta in 2013. The idea proved to be a great success since it started achieving its objectives i.e. to shift the commuters from their self owned vehicles or para-transit system to a mass transit system. It is very efficient, comfortable and cost effective public transport service. This study aimed at studying the key indicators that influence possible modal shift that can be achieved as a result of extension of MBS from Shahdara to Kala Shah Kaku (KSK). For the rationale to fulfill this research, a road user perception interview survey was conducted in the study area. A Model is developed using binary logistic regression for MBS and Qingqi. The possible modal shift from Qingqi is also studied. It is estimated that 89% of the commuters are willing to shift from Qingqi to the proposed MBS. These potential commuters primarily belonged to lower-middle income group and their mode choice is predominantly influenced by travel time, travel distance and cost. Travel time was found to be the most significant variable. It is suggested that providing mass transit system with low fares and minimum headway may be a great success on this corridor.

**Keywords:** Metro bus system, binary logistic regression, qingqi, public transport, modal shift, public transport

## 1. INTRODUCTION

In developing as well as in developed countries of the world improvement of public transport system has become a key concern in transportation planning. In Pakistan, existing condition of Public Transport (PT) is poor mainly in metropolitan city of Lahore and Karachi.

Lahore is Punjab's provincial capital and the second largest urban centre of Pakistan where 22 percent urban population of Punjab resides [1]. According to the Punjab Development Statistics [2], total number of vehicles registered in Lahore to date is 3.992million in recent past, a rapid growth in population and vehicle ownership in city has been observed which has resulted into traffic congestion. Only 16% of city's total trips are made on public transport which is the lowest percentage among all south Asian cities [3].

The introduction of sustainable mass transit system is one of the solutions that reduce traffic congestion and accidents rate. MBS in PT planning is favoured in many Asian developing cities because of its lower investment cost and flexible implementation over rail system [4]. A great deal of research has gone into investigating planning, performance, and operation of Bus Rapid Transit (BRT); however, relatively less has been done to assess whether its introduction has actually had an appreciable effect on transit use [5].

In order to cope with the ever increasing traffic congestion in Lahore city, MBS has been introduced in 2013. According to a few academics and professionals a very formal definition for BRTS is: "Bus transit designed as an integrated system of distinct buses and a separate infrastructure with considerable independence from other traffic,

allowing higher speed, reliability and safety than the Bus Transit System (BTS)” [6]. It has dedicated corridor from Northern suburb of Lahore i.e. Shahdara to south-east direction Gajjumatta. According to Punjab Mass Transit Authority, Shahdara station has highest daily ridership of 25,672. The introduction of MBS has reduced travel time and travel cost for passengers. A large amount of people make trips from nearby cities/villages like Rana Town, Sheikhpura, Muridke, Imamia Colony, Kamoki, etc. for work and educational purposes.

As Lahore city is expanding on the Grand Trunk (G.T.) road towards Gujranwala and various residential societies like S.A. Garden etc are now developing on north bound of Shahdara Station towards Muridke. It is now been proposed to extend MBS Lahore to this side of the city, i.e., Shahdara to KSK (study area). This research is initiated with a scope to identify the key parameters that influence commuter’s modal shift from Qingqi to MBS.

## 2. MATERIALS AND METHODS

An understanding of the attitude and behaviour of commuters is a necessary condition in the creation of an effective transportation system intended to encourage more efficient urban public transportation [7].

For primary data collection, a road user perception survey was conducted at Shahdara Mor and KSK Toll Plaza. The population of the study area was calculated by adding population of all Union Councils that lie in a range of 500 m from the G.T. Road on both sides after extrapolating census population of 1998. A sample of 288 commuters were interviewed using W.G. Cochran method for 95% confidence interval of the estimated population [8]. Each commuter was given seven choice sets where he/she had to select the different current modes of travel along with the option of proposed extended Metro Bus System. The approach of survey conducted in the field is based on Stated Preference (SP) and this lead to the development of model for the proposed extension of Lahore MBS. The survey was scheduled in order to cover the morning, noon and evening peaks.

Binary logistic regression analysis was employed using various attributes and commuter’s preference to estimate the relative importance of the proposed MBS attributes. The methodology utilized is outlined in detail in Ben-Avika and Lerman [9]. Logit models determine the significance of mode choice based on attributes on each individual. This can be expressed as:

$$P_q(\text{Qingqi to BRTS Mode}) = \frac{e^{U_{\text{Qingqi}}}}{\sum (e^{U_{\text{Qingqi}}} + e^{U_{\text{BRTS}}})}$$

In order to study travel characteristics of the commuters, questions were asked like total travel time, preferable mode of transport, alternative available modes of transport, cost of the total trip, the total distance travelled etc. For detailed study and analysis, secondary data was also collected from sources included Lahore Urban Transport Master Plan Study by JICA [10].

### 2.1 Study Area

The study area for this research is adjacent area to proposed corridor for the extension of Lahore MBS from Shahdara to KSK as shown in Fig. 1.

The marked centreline shows proposed extended route’s starting point from Shahdara Mor and ending at KSK. It has typical mixed land use pattern that passes near many industrial and educational Institutions along with KSK Interchange which connects this corridor (G.T. Road) with Motorway M-2. The length is 9 km for proposed corridor.

### 2.2 Existing Condition of Public Transport

The situation of Public Transport system of Shahdara towards KSK on G.T. road is poor. Lahore Transport Company (LTC) is operating two bus routes B-49 and B-49-A. Ridership of these bus routes was calculated using boarding and alighting survey, starting from Shahdara Mor to KSK Toll Plaza in both directions. The calculated daily ridership was about 4,373 in both directions of this area. The estimated commuter ridership of PT in this stretch was 15,397. Only 31% PT users have waiting time less than 5 minutes at bus stops. Due to higher waiting time, the most popular mode of PT is Qingqi/Motorcycle Rickshaw. The

usage of this mode is about 49%. As a result less passengers use LTC buses and other PT modes despite of high potential of PT users in this area. The existing mode of travel of study area is shown in Fig. 2.

### 2.3 Data Collection

This research covers socio-economic factors that can affect trip characteristics and mode choice decision. Therefore, household type, trip patterns and their characteristics and personal demographics were selected. A deep rooted and intense relationship exists between the socio-economic characteristics and the travel demand of the commuters. For example, study of Surat City, India identified that Income, Gender, Trip Length, Trip Frequency, Travel Time and Travel cost are major factors that cause variation in modal shift behavior of various modes to MBS [11]. In order to determine the potential of modal shift, traffic counts alongwith PT vehicle boarding and alighting survey were conducted at Shahdara Mor and KSK Interchange for through traffic from Shahdara towards KSK. Further, LTC buses vehicle occupancy survey was done and MBS user perception survey at Shahdara Station of MBS Lahore was conducted. Also PT and private vehicle users were asked about their willingness to shift to MBS if it is extended to KSK.

### 2.4 Statistical Technique

Binary logistic regression analysis technique is used to develop models in order to study which attributes were significant in predicting the choice of transportation mode. As the willingness to shift to MBS is dichotomous, this approach helps to study about the relationship of independent variables on dependent variables.

The utility equation was developed after the data analysis in SPSS. These equations are developed for various modes including the MBS. Calculated willingness of the commuters to shift from local public transport modes available to the extended proposed MBS corridor was computed for assessing the possible modal shift if the project of proposed MBS extension is executed. Another analysis is done in SPSS to study the impact of trip behaviour / characteristics and different individual

on the utility value of a particular mode including the MBS. This study was done using the binary regression model prediction about the change in the public transportation system with reference to the modal sharing are further analyzed by the options selected for choice set by each respondent.

## 3. RESULTS AND DISCUSSION

Based on the user interview survey in the study area, the results showed that the majority of commuters were male of age between 14 to 30 years. It is important to note that in Pakistan, mostly male members of the household support their families especially in lower and middle income class group of the society.

Children below 14 years make trips on the decision of their parents and it is also difficult to interview them. Therefore they were not considered in the survey. Average Annual Daily Traffic (AADT) was calculated from Traffic counts surveys. These were conducted for three days (one weekend and two weekdays), at Shahdara Mor and KSK Interchange. It was estimated about 11,774 for through traffic from KSK to Shahdara, for through traffic from Shahdara to KSK 14,681 and total through traffic between KSK and Shahdara was estimated 26,455. Out of these 13,113 were Qingqis. It shows that this mode is the most used mode in the study area. Also 89% of Qingqi users were willing to shift to MBS proposed extension.

### 3.1 Sample Characteristics

The user perception survey showed that most of the individuals belong to lower middle group having monthly income in the range of Rs. 5000 to Rs. 20,000 per month. Share of such respondents were observed to be around 51 percent from the sample collected using SPSS. Motorcycle is owned by about 35 percent individuals. It clearly shows that this mode is very common and most of the people prefer to use it as compared to other modes.

Majority of the individuals of the study area works in private sector about 48 percent, while the representation of students is second highest about 17 percent. This shows that the commuters travelling on the proposed corridor are mostly either working

in private sector or are students.

When studying the modal split by the trip purpose, for work trips, majority of the people are using Qingqi and only minority group are using private car and auto-rickshaw. For educational trips, the usage of Qingqi is highest again about 46.5%.

Comparing the public transport (auto-rickshaw, Qingqi, mini-bus and bus) users with their household availability, about 66 percent of them can be considered as captive travellers of public transport with no vehicle ownership. As vehicle ownership increases, the chances of using public transport also decrease. The vehicle owned in a household is used by the head of the household in the most of the cases while remaining members rely on the public transport.

### 3.2 Attitude towards Lahore MBS

A user perception survey was conducted at Shahdara Station of Lahore MBS to assess perception of MBS users. It was found that 83% users were satisfied with punctuality of MBS. About 88.5% agreed that

MBS is safe and 65% said that MBS is affordable. Around 39% MBS users prefer MBS over private / conventional PT because of its accessibility. The Fig. 3 shows the attributes which attracted conventional PT / private vehicle users towards MBS.

Further, it was found that 45% passengers use MBS for work trips. About 97% agreed that MBS should be extended to KSK. Around 23.6% and 23.0% are willing to pay an additional fare of Rs. 5 and Rs. 10 respectively in case MBS is extended from Shahdara to KSK.

### 3.3 Model for Qingqi

Using stated preference approach, user perception interview survey was carried out in the study area. As the commuters state their preference after perceiving cost of travel, travel time and travel comfort etc. The variables used for the binary logistic model are the proposed extended MBS attributes and the current travel choice attributes as given in Table 1.

**Table 1.** Input variables.

Variable	Description
Travel Time (TT)	Total travel time for the trip (Walk time to MBS stop + In-vehicle Time)
Travel Cost (TC)	Total cost of the one way trip
Trip Length (TL)	Distance from origin to destination for Home work trips or Home Education trips
Income Group (IG)	Individual Monthly Income
*Traveler's Occupation (TO)	Occupation of a person – 0: Dependent, 1: Independent
ASC	Alternative (Mode) Specific Constant

\*Traveler's occupation consists of two categories; dependent includes students, housewife and jobless while independent includes government job, private job, business and labour.

**Table 2.** Model results in SPSS.

Independent Variable	Estimate (B)	Standard Error (S.E.)	Sig. (Z)	P-value
TO	-0.199	0.665	0.764	0.819
IG	0.000	0.000	0.017	1.000
TL	0.246	0.119	0.039	1.279
TT	-0.164	0.049	0.001	0.849
TC	0.036	0.062	0.558	1.037
ASC	4.784	1.498	0.001	119.566

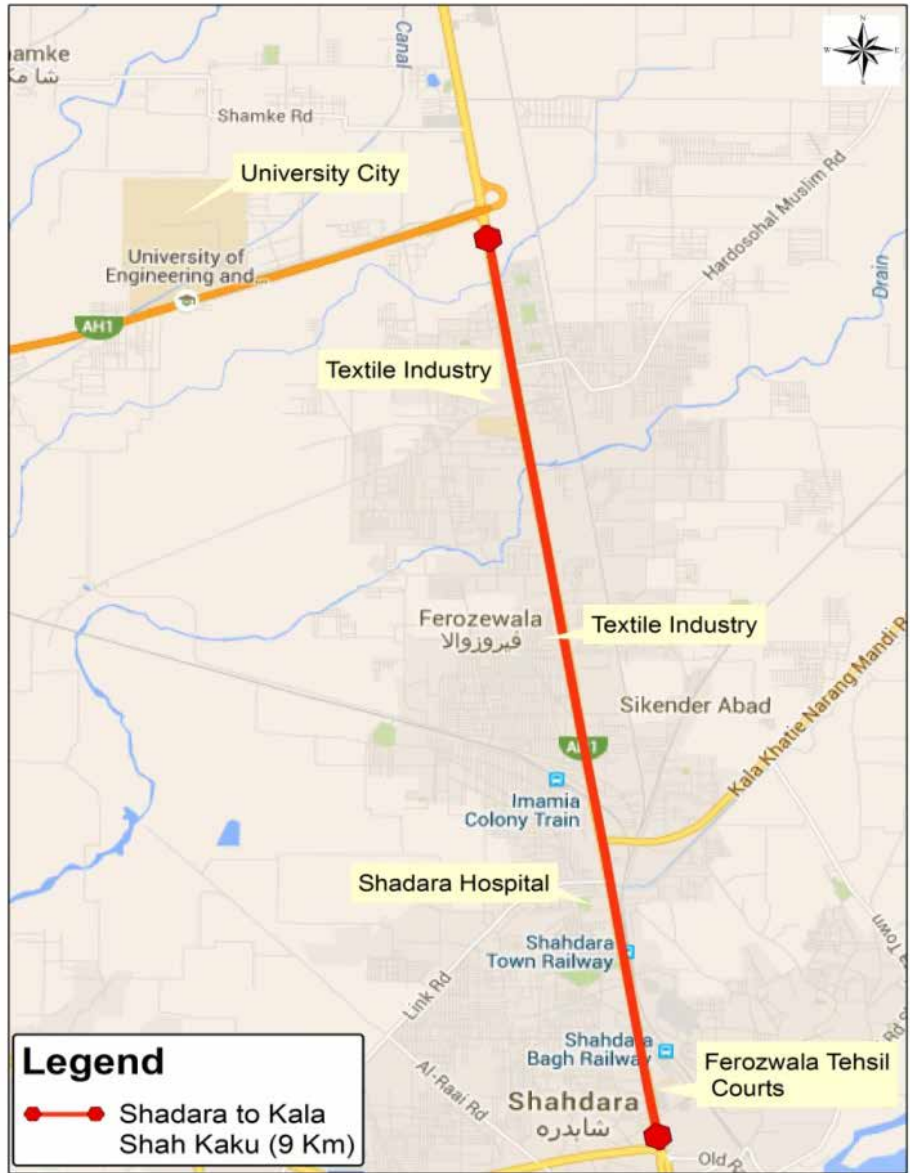


Fig. 1. Location map of the proposed extended metro bus corridor.

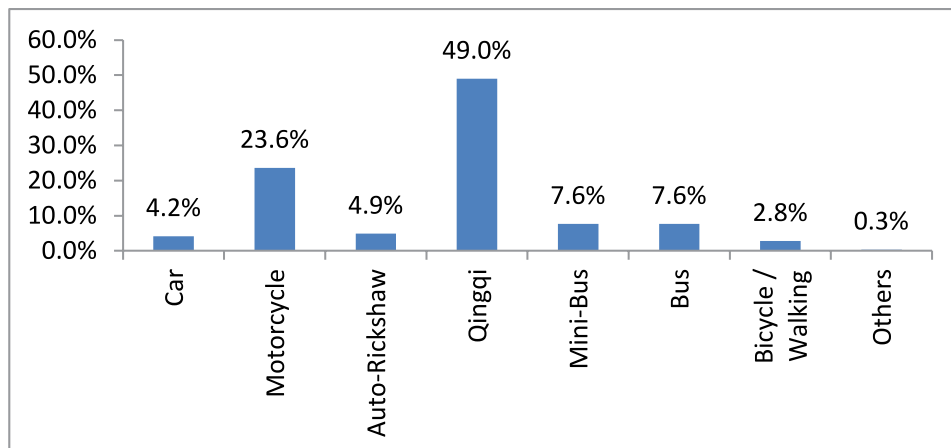


Fig. 2. Existing mode of travel in study area.

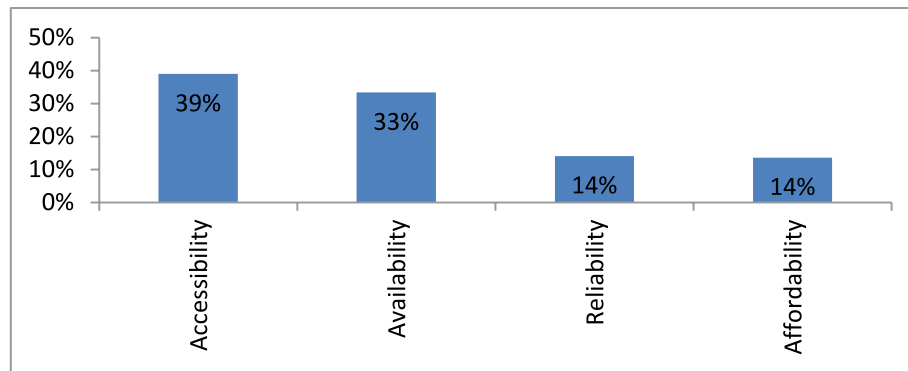


Fig. 3. Attributes that caused modal shift to MBS.

The binary logit analysis was employed to model the attributes and preferences of the commuters through their stated choices. The utility functions, derived out of the choice sets help to observe the relative attractiveness of each alternative, for a given trip. The contribution of each attribute to a utility of an alternative is indicated by the sign of its coefficients. A positive value indicates a positive impact on the utility and opposite applies to negative value. The correlation of various attributes was analyzed in SPSS. Depending upon the value of regression coefficient selection of the attribute / choice set was done for derivation of utility equation.

The inclusion and exclusion of the variables is dependent on their significance test. If the parameter of a variable is giving very low significance test results, they are excluded. Based on this theory various models were developed which are described below.

The utility expression was used to determine the total utility of the MBS in comparison with Qingqi. In this case a high utility value indicates that the commuters preferred the MBS more and thus the MBS will be more attractive to its potential users. On the other hand, a lower Utility value indicates that the commuters preferred the MBS less meaning that the MBS will be less attractive to its potential users i.e. the commuters.

$$U_Q = ASC + (\beta_O \times \text{Occupation}) + (\beta_{MI} \times \text{Monthly Income}) + (\beta_{TL} \times \text{Trip Length}) + (\beta_{TC} \times \text{Travel Cost}) + (\beta_{TT} \times \text{Total Travel Time})$$

Here,  $\beta_O$  = Utility parameter for Occupation

$\beta_{MI}$  = Utility Parameter for Monthly Income

$\beta_{TL}$  = Utility Parameter for Distance Travel

$\beta_{TC}$  = Utility Parameter for Travel Cost

$\beta_{TT}$  = Utility Parameter for Travel time

ACS = Alternative Specific Constant

Nagelkerke R-square 0.315

Cox and Snell R-square 0.155

The estimated logit is obtained from the following equation:

$$U_Q = 4.784 - (0.199 \text{ Occupation}) + (0.246 \text{ Trip Length}) - (0.164 \text{ Total Travel Time}) + (0.036 \text{ Travel Cost})$$

This utility function derived out of the choice sets, helps to assess the relative attractiveness of the option, indicated by the sign of the coefficients of the attributes. Qingqi is the most accessible and cheaper mode of public transport in Pakistan but its design is not proper. This mode is causing noise and air pollution. Also it is involved in majority of accidents in Lahore city. The drivers of Qingqi mostly belong to poor families and uneducated. There is no provision of side mirrors in this mode which is a major flaw.

The models developed of other modes of transportation i.e. bus, auto-rickshaw, car and wagons showed that trip cost is the most significant factor for mode choice. The model for Qingqi shows that the monthly income, travel distance and total travel time are the most significant parameters, in order to encourage the modal shift. The results show that commuters prefer the use of Qingqi as public transport because of its lesser travel time

and cheaper cost. Modal shift of this mode can be achieved more than 90% by providing a service like metro bus which has good quality service, lesser travel time and low fares too. In developing countries like Pakistan, commuters prefer cost of travel over time and comfort because of lower household income. However, this pattern is in contrast with developed world where commuters give maximum value to travel time.

#### 4. CONCLUSIONS

The conclusions of this study were as under:

- Most used PT mode in this corridor is motorcycle rickshaw / Qingqi and it has the highest modal shift possibility of 89%.
- Total travel time is found to be the most significant attribute in modal shift to MBS.
- Income of the commuters of study area has no effect on the modal shift as mostly Qingqi users belongs to lower middle income group
- Trip length has a positive coefficient, shows that for longer trips modal shift towards MBS is expected to be higher
- Travel cost has small estimate value as the cost of Qingqi and proposed MBS is same. It doesn't have much effect on modal shift in the study area.

#### 5. ACKNOWLEDGEMENTS

We express our gratitude to Engr. Usman Sheikh, Highway Engineer, Osmani & Company (Pvt.) Ltd. for sharing his wisdom and expertise which greatly helped in this research.

#### 6. REFERENCES

1. Riaz, Haq. *Urbanization in Pakistan Highest in South Asia. [Blog comment]*, Retrieved from <http://www.riazhaq.com/2009/09/urbanization-in-pakistan-highest-in.html> (2009).
2. Punjab Development Statistics. Bureau of Statistics, Government of the Punjab, Lahore, 388 pp. (2016).
3. Imran, M. Public Transport in Pakistan: A critical overview. *Journal of Public Transportation* 12(2): 53-77 (2009).
4. Jaensirisak, S. & P. Klungboonkrong. Why Bus Rapid Transit (BRT) is interested by Transport Planners and Travellers in Thailand. *Proceedings of the Eastern Asia Society for Transportation Studies* 7: 266-274 (2009).
5. Robert, David. *An Ex Post Evaluation of the Ridership Impacts of the Viva Bus Transit System*. MSc thesis, University of Toronto, Toronto, Canada (2011).
6. Vuchic, V.R. *Urban Transit Systems and Technology*. John Wiley & Sons, New York, 256 pp. (2007).
7. Vedagiri, P. & V.T. Arasan. Estimating modal shift of car travellers to bus on introduction to bus priority system. *Journal of Transportation System Engineering and Information Technology* 9(6): 120-124 (2009).
8. Cochran, W.G. *Sampling Techniques*, 3<sup>rd</sup>ed. John Wiley and Sons, New York (1977).
9. Ben-Avika, M. & S.R. Lerman. *Discrete Choice Analysis: Theory to Travel Demand*. The MIT Press, Cambridge, Massachusetts, USA (1985).
10. Government of the Punjab. *The Project for Lahore Urban Transport Master Plan (LUTMP) in the Islamic Republic of Pakistan*. Final Report. ALMEC Corporation Oriental Consultant Co. Ltd., Japan International Cooperation Agency (2011).
11. Kumar, R. & F. Electricwala. Impact of proposed modal shift from private users to bus rapid transit system: An Indian city case study. *International Journal of Civil, Structural, Construction and Architectural Engineering* 8(6): 663-667 (2014).





# Generating EXPRESS Data Models from SBVR

Imran Sarwar Bajwa<sup>1,\*</sup>, Nadeem Sarwar<sup>1</sup>, and M. Asif Naeem<sup>2</sup>

<sup>1</sup>Department of Computer Sciences & Information Technology,  
The Islamia University of Bahawalpur, Bahawalpur 63100, Pakistan

<sup>2</sup>School of Computer and Mathematical Sciences,  
Auckland University of Technology, Auckland, 1142, New Zealand

**Abstract:** EXPRESS is a standard graphical documentation for data models. It is a helpful buddy to the EXPRESS dialect for showing element and sort definitions, connections and cardinality. This graphical documentation underpins a subset of the EXPRESS dialect. One of the preferences of utilizing EXPRESS over EXPRESS is that the structure of an information model can be exhibited in a more reasonable way. In software engineering the graphical representation of the software structure is very necessary because understanding of coding is very difficult. Semantic Business Vocabulary Rules (SBVR) specifications many authors have done model to model transformation. SBVR2EXPRESS is also possible. In this study we propose an EXPRESS data model using Natural language. That model manually implements on two case studies and generate the EXPRESS diagram using SBVR rules. That diagram full fills the all software requirement of the Software engineers. Model representation is very helpful to develop large scale of systems like, Aerospace, medical science and other industries where the representation of system working is very important. This work is very helpful to the Data manger and IT managers to represent their organization structure.

**Keywords:** EXPRESS, SBVR, natural language rules

## 1. INTRODUCTION

The field of exploration and real issues of learning space are exhibited, highlights the tended to research issue, and portrays the examination inspirations and the significant exploration targets. In Data Modeling language Different types of Data Modeling languages have been available, There are two types of Modeling Languages these are textual and graphical. In Textual modeling language is use standard keywords associated by natural language expression and phrases or variables make computer explainable terms. Diagram technique with named symbols are use in Graphical Modeling language to represent concepts and lines that join the arbitrary signs and show the connection between them and various elements represent by using graphical notations. The EXPRESS [2] is an example of a textual modeling language and graphical modeling language. The EXPRESS-G and EXPRESS (International Standard Organization 10303-11)

are international standard nonspecific purpose data modeling language [3, 4].

## 2. RELATED WORK

Ma and Wang [3] focused on the components of EXPRESS representing the data base modeling with possibility distribution and FUZZY sets are extended and integrating such EXPRESS FUZZY data base models. The EXPRESS FUZZY models are mapped to object oriented FUZZY data base by using formal techniques is being presented. The data access standard interface requirements are investigated for functioning the EXPRESS defined information in database [3]. Similar to this work, Zhao and Liu [4] developed a technique which is based on ontology for interoperable meaning and logic of model knowledge. Two languages namely OWL and SWRL for web semantics are used to develop information model of product. They disused

EXPRESS language as traditional language they presented information model of EXPRESS oriented product using representation technique. They introduce the importance of representing technique is configured from EXPRESS to SWRL/OWL [4, 5]. Another similar work was [6] implementation of an EXPRESS model on a database vault, questioned upon and controlled. They introduce a product advancement stage which aids creators to make EXPRESS models, to produce a proportional database composition and to control this mapping. Likewise they can make an introductory EXPRESS model utilizing EXPRESS-G. EXPRESS code is then created and further altering embraced utilizing a particular EXPRESS proofreader. They can likewise imagine the legacy chain of importance of the complete pattern. The EXPRESS pattern is changed over to an article situated database framework and got to by means of a STEP Data Access Interface (SDAI). They portray every segment of the advancement stage furthermore inspect the conceivable improvements. The ISO STEP particulars plan to give a viable means by which item data can be imparted, traded in the middle of utilizations and ventures. EXPRESS is a modeling language inside the STEP particulars and it is utilized to portray item information [6].

Kahn et al. [11] describe a structure for controlling EXPRESS models and the objective is to hold the STEP idea of the direct mapping of a data model to a usage, yet to do as such in a manner that empowers elective execution techniques to be received. In this structure, called STEPWISE, permits the client to point out controls and model changes keeping in mind the end goal to change over models from one structure into an alternate [11]. Similarly, Sukys et al. [12] presented transformation framework to transform questions in structured language SBVR to SPARQL queries for ontologies defined in Web Ontology Language (OWL) 2.0 and supplemented with semantic web rules SWRL. This transformation depends on OWL 2 ontology related with corresponding SBVR vocabulary and rules. They considers a family of transformations and metamodels required for relating ontologies, rules, SPARQL queries and real business data supported by computerized information systems, as well as establishes requirements for harmonizing

the coexistence and preserving semantics of these different representations [12].

A process for planning change was presented as a medium for capturing structural and behavioral qualities of a model change [19], that supports layouts which, when instantiated, naturally create proportional formal specification with investigation capacities. They demonstrated with a little illustration, UML Class to Relational Database change, and verification utilizing Alloy, and the improvement of model changes is normally an specially appointed action in MDE. Changes are designing items and can be created in a decently composed manner, in the same way as other programming items, and model change advancement methodology can deliver changes communicated in various styles, change designs can be utilized to strengthen such distinctive properties to be developed.

López-Ortega [14] introduced a system, which is utilized to turn upward the meaning of element and relations of the operation information and to make the acclimating Data Manipulation Language (DML) articulations execute and afterward the mapping tenet of EXPRESS information [14] style to social database, including fundamental information sort, object information sort and legacy, is depicted. The mapping method bantered about can be utilized as a part of all STEP information constructions, and STEP is an item demonstrating approach that considers all the peculiarities of an item, including geometry and hierarchical information [16]. Another technique was developed that was based on ontology for interoperable meaning and logic of model knowledge. Two languages namely OWL and SWRL for web semantics are used to develop information model of product. They disused EXPRESS language as traditional language they presented information model of EXPRESS oriented product using representation technique. They introduce the importance of representing technique is configured from EXPRESS to SWRL/OWL [17]. A methodology was presented for changing business rules (BR) made in regular tongue (Natural Language) [18]. All the related work discussed in this section highlights that there is currently no approach available to generate EXPRESS models from natural language or SBVR text.

### 3. PRELIMINARIES

#### 3.1 EXPRESS Data Modeling Language

A standard language for modeling material extracted from software products is called EXPRESS and the exchange type of model STEP (10303) standard in ISO is formalized for EXPRESS and the evolved standard is 10303-11. The problem domain representation into EXPRESS model is achieved through different schemas which are used for grouping elements having similar semantic and persistence. The different data types including plain types e.g. String or integer containers e.g. LIST or SET, enumerations and data types defined by users are assisted by EXPRESS language entity types is a key type in EXPRESS language to define the elements and constraints [2].

Information Modeling is a system used to portray and analyze data necessities anticipated that would backing the business structures inside the degree of looking at information systems in affiliations and the technique of data showing incorporates capable data modelers working almost with business accomplices, As well as potential customers of the information structure.

#### 3.2 Semantic Business Vocabulary Rules

SBVR is an openly accessible determination from the Object Management Group [1] expected the premise for a prescribed and documented characteristic dialect revelatory depiction of a complex substance, for example, a commercial, SBVR is prearranged to validate difficult agreeability standards, for example, operational principles for an undertaking, security strategy,

standard consistence, or administrative agreeability rules.

#### 3.3 Model Transformation

A model change, in model-driven designing is an automatable method for guaranteeing that a group of models is reliable, in an exact sense which the product architect can characterize and the point of utilizing a model change is to spare exertion and lessen lapses via computerizing the building and adjustment of models where conceivable. A model change may be composed in a broadly useful programming dialect; however specific model change dialects are additionally accessible.

## 4. USED APPROACH

#### 4.1 SBVR to EXPRESS Transformation Framework

In this framework, we extract the SBVR specifications then find the SBVR elements and describe them individually then implement them on EXPRESS metamodel elements which are finding from EXPRESS metamodel using transformation rules as shown in Fig. 1. Here, the researcher compares both metamodel elements and describe them individually and extract them.

#### 4.2 Semantic Analysis of SBVR Specifications

To distinguish the SBVR vocabulary, semantic part naming is performed and Semantic part marking or topical part marking is a shared methodology utilized as a part of shallow semantic parsing, and the SBVR components, for example, thing

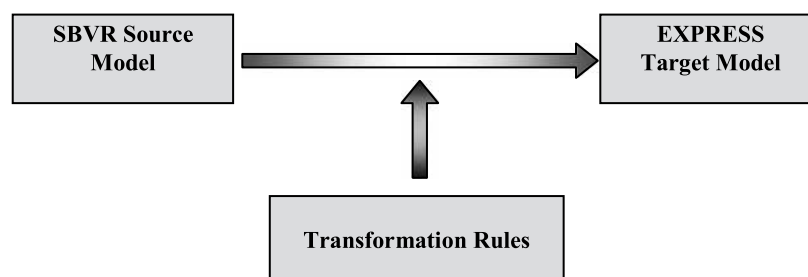


Fig. 1. SBVR to EXPRESS transformation framework.

idea, singular idea, article sort, verb ideas are distinguished from the SBVR data.

### 4.3 Extracting SBVR Elements

By using the following conservative of mappings are used to extract of SBVR elements is as following:

#### 4.3.1. Extracting Noun Concept

Different methods are used to describe the noun and noun phrases in English language, In old-fashioned syntax, nouns are imparted to be words that mention to individuals, things, places, or immaterial concepts and while up-to-date morphology discover this classification to be challenging because it depend on generic nouns such as objects to exactly define what a noun is, in our community thoughtful of what nouns are complies to the old-fashioned meaning but In SBVR, the mutual noun phrase (co-actors, actors, recipients, thematic things,) or nouns, are plotted as the object types e.g. employee, tools, , chair, etc.

#### 4.3.2. Extracting Individual Concepts

Here, each single type of individual concepts has exactly one unique element, which is the instance of the proper nouns (recipients, co actors, actors and thematic objects) and distinct concept, is plotted to the distinct ideas. In the distinct noun concept ‘Bahawalpur’ is a one instance and it is a specific state in the Punjab of Pakistan. The General concepts, Individual noun concepts, Verb concepts, noun concept and concept type are also defined individual concepts.

#### 4.3.3. Extracting Fact Types

In SBVR fact types (kinds of facts, such as “Employee works for Department”) are explain obligation the subordinate and exploit verbs are characterized as Association, Property, Property association, Partitive verb ideas to building a Fact Types. Examples of fact-based representation of a database schema, the information structure implied

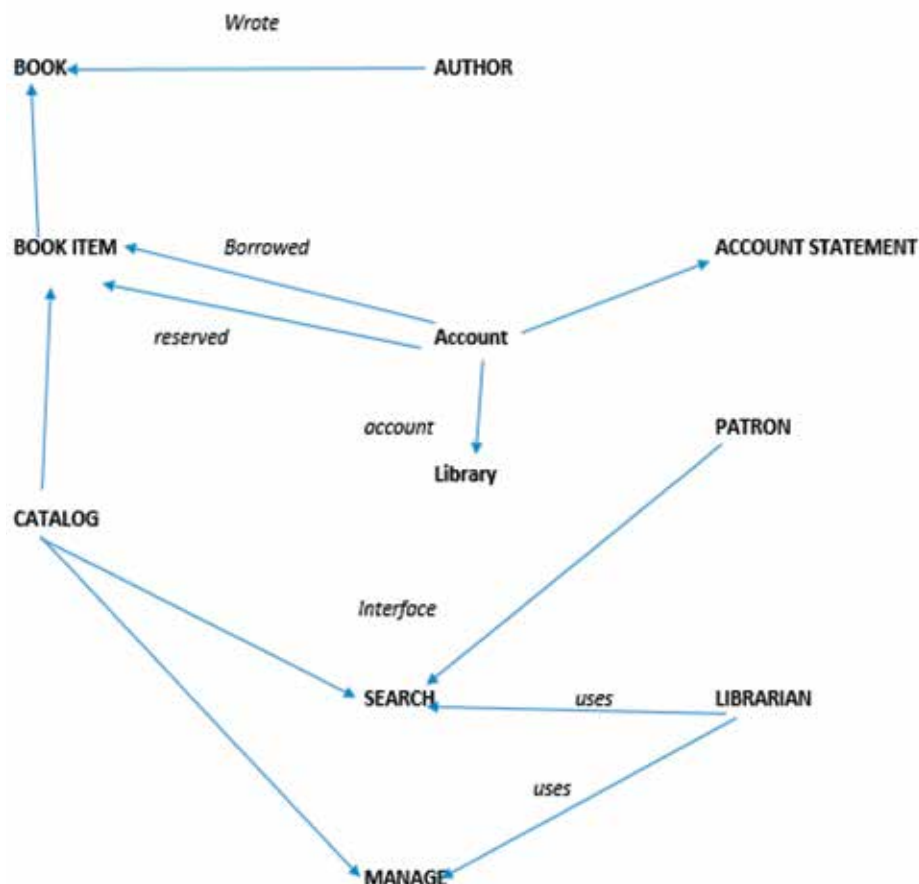


Fig. 2. Output EXPRESS model.

by the database schema can be expressed as a set of fact types and constraints as follows, using the capitalized mix fix notational style described earlier: Types of individuals are Employee, Car, Employee Number, Employee Name and Car Registration Number.

#### **4.3.4. Extracting Characteristics**

In SBVR, trademark which is key to comprehension an idea. An idea has an inferred trademark just on the off chance that it takes after by sensible ramifications from some blend of consolidations of attributes by ideas and/or structural standards that the trademark is constantly ascribed to every example of the idea. Furthermore clarify parallel verb idea, unitary thing idea and individual thing idea. Every example of every trademark sort is a trademark. The augmentation of the trademark sort “shading” incorporates the attributes ‘thing is blue’, ‘thing is red’, ‘thing is green” and so forth. The core package contains all of the generally required modeling elements of EXPRESS, along with some basic metamodel artifacts, and it is the foundation on which all of the other packages are built.

The Core Package is the minimal implementation of the EXPRESS metamodel, and the Core package contains all of the generally required modeling elements of EXPRESS, such as scopes and naming concepts, schemas, data types, entities, attributes, and relationships along with domain constraints. The Core package also includes the abstract classes Expression and Instance, which serve as linking points for detailed models contained in other packages.

#### **4.1.5 Transforming SBVR to EXPRESS**

Semantic Business Vocabulary Rules are transformed to the EXPRESS and present the rules of transformation. The all elements of the EXPRESS model is mapped with the elements of SBVR by using rules of transformation and the above section is already discussed the extraction of SBVR specifications which are used in this transformation. The following section describes the transformation method of mapping SBVR elements with element of EXPRESS data models:

#### **4.3.6. Mapping Verb Concepts to Methods**

In this section we transform or map verb concepts (action verbs) of the SBVR are related to a noun concept are transformed and Verb concepts map to fact types, each fact type being a set of possible ground facts that can be formulated based on the verb concept and that use reference schemes to identify, for each fact, each thing that fills each role.

#### **4.3.7. Mapping Noun Concept to EXPRESS Class**

In the Semantic Business Vocabulary Rule, entirely the Noun Concepts are transformed to EXPRESS classes in an EXPRESS Core Package model. The idea is the importance of a thing or thing expression.

#### **4.3.8. Mapping Individual Concepts to Objects**

In this phase transform all individual concepts and its sub elements of Semantic Business Vocabulary Rule to the objects in an EXPRESS Core model and all the general, individual, noun concepts, verb concepts and concept types are mapped to object and with its elements. Individual noun concepts logically map to singleton types of individuals. Each single type of individual has exactly one element, which is the instance of the individual noun concept.

#### **4.3.9 Mapping Definitional Rule to Global Rule**

A Schema Element denoting a collection of Named Rules for the interaction of the Extents of one or more Entity Types and It corresponds to the RULE declaration in EXPRESS; Every Global Rule is also an Algorithm Scope and may define Common Elements and Variables.

#### **4.3.10. Mapping Characteristics to Attribute**

The concept of SBVR element characteristics is mapped with the element of EXPRESS element Attribute. The characteristic “driver is of age” by this meaning: “the age of the driver is at least the EU-Rent Minimum Driving Age.” In this element dualistic verb concept, unitary noun concept and individual noun concept are also sub elements are mapped with the sub elements of Attribute like. Entity Definition, Inverse attribute, explicit attribute, Derived attribute and Base type.

## 5. IMPLEMENTATION

Our aim was to define computerized transformations from natural language to an EXPRESS model. In this thesis, we focused on model to model transformation from a SBVR specification to an EXPRESS model and proposed text to model transformations. We made the assumptions that the input SBVR specification is consistent and complete. Our approach was divided into two steps:

- Firstly, extracting SBVR elements. SBVR elements are extracted using NL2SBVR tool [9]; and
- Defining applied Business Rules transformations to the control flow of the identified elements of EXPRESS and top21otentiallyrefinethem.

## 6. CASE STUDIES

The following case study will help us to generate the EXPRESS data model by using SBVR rules and system requirements:

*“A library issues loan items to student. Each student is known as a member and is issued a membership card that shows a unique member number. Along with the membership number other details on a student must be kept such as a name, address, and date of birth. The library is made up of a number of subject sections. Each section is denoted by a classification mark. A loan item is uniquely identified by a barcode. There are two types of loan items, language tapes, and books. A language tape has a title language (e.g., French), and level (e.g., beginner). A book has a title, and author(s). A student may borrow up to a maximum of 8 items. An item can be borrowed, reserved or renewed to extend a current loan. When an item is issued the customer’s membership number is scanned via a barcode reader or entered manually. If the membership is still valid and the number of items on loan less than 8, the book barcode is read, either via the barcode reader or entered manually. If the item can be issued (e.g. not reserved) the item is stamped and then issued. The library must support the facility for an item to be searched and for a daily update of records.”*

### 6.1 SBVR Vocabulary Generation

The SBVR specification (output of NL2SBVR tool) was given as input to the SBVR2EXPRESS tool that is an Eclipse plugin implemented in java as a proof of concept. The following text is shown in SBVR Structured English notation [1] that represents each SBVR vocabulary type in predefined different colours. The SBVR specification after extracting SBVR vocabulary is as follows:

“A library issues loan items to each student. Each student is known as a member and is issued a membership card that shows a unique member number. It is necessary that the membership number and other details on a student must be kept such as a name, address, and date-of-birth. The library is made up of a number of subject sections. Each section is denoted by a classification-mark. A loan item is identified by a bar-code. There are exactly two types of loan items, language tapes, and books. A language tape has a title-language, and level. A book has a title, and author(s). It is a possibility that each student may borrow up to at most 8 items. It is a possibility that each item can be borrowed, reserved or renewed to extend a current loan. When an item is issued the student’s membership-number is scanned via a barcode reader or entered manually. If the membership is valid and the number of items on loan at most 8, the book’s bar-code is read, either via the barcode reader or entered manually. It is possibility that if the item can be issued the item is stamped and then issued. It is necessary that the library must support the facility for an item to be searched and for a daily update of records.”

Afterwards, the extracted SBVR vocabulary was mapped to the EXPRESS elements. Following information was extracted in OO analysis phase:

### 6.2 SBVR Based Software Requirements

For this situation study Library information Management System is an (invented) books library, utilized as a contextual analysis as a part of the SBVR determination. The business prerequisites for Library information Management System incorporate the accompanying:

- Authors wrote different books
- Books have different types
- Different catalogue has record of books

- Each book has account in library
- Each student has account in library
- Librarian searches the records of students and books
- Librarian manages the records of students and books

**6.3 SBVR Rules Generation**

**SBVR Rule:** It is necessary that each student *has* exactly one account.

**SBVR Rule:** It is necessary that each catalogue *includes* exactly one book.

**SBVR Rule:** It is necessary that the Librarian *manage* each account

**SBVR Rule:** It is necessary that each Patron *uses* exactly all accounts.

**SBVR Rule:** It is obligatory that the Book *issuance of a book is* at most 2 months.

**6.4 Generated EXPREES Diagram**

EXPRESS generated Library information Management System diagram is shown in Figure 2

**7. EXPERIMENTS & RESULTS**

Our assessment strategy is taking into account three things and technique that are portrayed. For

the evaluation purpose, we have used three metrics: Precision, Recall and F-Measure.

**8. RESULTS AND DISCUSSION**

There were seven sentences in the used case study problem. The largest sentence was composed of 58 words and the smallest sentence contained 18 words. The average length of all sentences is 26. The major reason to select this case study was to test our tool with the complex examples. The correct, incorrect, and missing SBVR elements are shown in Table 3.

Results of each SBVR element describe in above Table separately. According to our evaluation methodology, Table 4 shows sample elements are 54 in which 48 are True 04 are False and 02 are error SBVR elements. The above table describes the Recall and precision of examples for generating EXPRESS data model. In Table 4, the average recall for SBVR software requirements are premeditated 96.42% while average precision is calculated 93.10%. The normal F-value is figured 84.90% that is encouraging for introductory analysis. We can't hope to measure up our outcomes to whatever other apparatus as no other device is accessible that can produce EXPRESS information model using SBVR.

**Table 1.** Plotting semantic business vocabulary rules and express metamodel elements.

Elements of SBVR Metamodel	mapped to	Elements of EXPRESS Metamodel
Individual Concept	→	Object
Noun Concept	→	Class
Verb Concept	→	Methods
Business Rule	→	Schema
Definitional Rule	→	Global Rules
Characteristic	→	Attribute
Elementary Concepts	→	Base Type
Constraints	→	Constraints
PartitiveFactType	→	Generalization
Associative FactType	→	Association
CategorizationFactType	→	Aggregation
Quantification	→	Cardinalities

**Table 2.** List of Generated SBVR vocabulary.

Category	Count	Details
Noun Concept	08	Student, library, subject section, section, loan items, language tapes, books, car movement, receiving branch, geographical movement type.
Verb Concepts	06	Membership, bar code, records, reader, item, records, issued, receiving branch
Individual Concepts	08	Borrowed, issued, manually, Author, title, searched, car group, movement-id, rental car, movement-id
Characteristics	03	Renewed served , extend, searched, stamped
Quantifications	05	Unique, scanned, valid, daily, reader, in-country car movement.
Constraints	08	Manually, facility, read, title language, membership, tapes, borrowed, one-way car, movement
Associative Fact Types	06	Section, department, class, catalogue, sending branch.
Partitive Fact Types	04	Possibility, manually, round-trip car movement
Categorization Fact Types	06	At most, stamped, record, international car movement

**Table 3.** Recall and Precision of examples for EXPRESS model from case study.

Type/Metrics	$N_{example}$	$N_{True}$	$N_{False}$	$N_{error}$	Rec%	Prec%
Software Requirements	54	48	04	02	96.42	93.10

**Table 4.** Evaluation results.

Input	$N_{example}$	$N_{True}$	$N_{False}$	$N_{error}$	Rec%	Pre%	F-Value
Sample 1	48	40	6	2	84.32	87.28	80.76
Sample 2	50	45	4	1	83.56	84.41	83.43
Sample 3	45	35	5	5	84.28	86.50	82.66
Sample 4	54	48	4	2	85.43	85.84	84.68
Average					84.26	85.98	84.90

## 9. CONCLUSIONS AND FUTURE WORK

This paper deals with the generation of EXPRESS models from SBVR details to EXPRESS Core Package components. This generation begins with the SBVR parsing and by utilizing ordinary NLP methodologies and second issue of change of SBVR metamodel components to EXPRESS metamodel components was tended to by utilizing model change innovation. SiTra library was utilized

with the end goal of the model change. Moreover, the mechanized article arranged investigation of SBVR particulars of programming necessities was finished. The outcomes demonstrate that the displayed methodology is a superior approach when contrasted with the other accessible methodologies. Our tool SBVR2EXPRESS gives a higher exactness when contrasted with other accessible NL-based tools, what's more better precision,

SBVR has likewise empowered to concentrate OO data, for example, affiliation variety, collections, speculations and occurrences as other NL-based apparatuses can't process and concentrate this data.

The possible future development of the extracted SBVR elements and transformation to EXPRESS elements is mapping to its graphical representation. In this paper, all work that we have planned were not completed, we transform only a few elements of both metamodels. Mapping of other elements are remaining and we will do it further in future. After the complete transformation it will further helpful and use full in the field of Data modelling and representation of data in graphically with notations. Our focus on the exact and complete model transformation between EXPRESS and SBVR

## 10. REFERENCES

1. OMG. *Semantics of Business Vocabulary and Rules (SBVR)*, v.1.2. Object Management Group, Available: <http://www.omg.org/spec/SBVR/1.2/pdf> (2013).
2. OMG.EXPRESS Information Modeling Language, v1.1 Object Management Group, Available: <http://www.omg.org/spbec/EXPRESS/1.1> (2014).
3. Ma, Z.M., & H. Wang. STEP implementation of Imperfect EXPRESS Model in Fuzzy object-oriented Databases. *Fuzzy Sets and Systems* 157(12): 1597-1621 (2006).
4. Zhao, W., & J.K. Liu. OWL/SWRL Representation Methodology for EXPRESS-driven Product Information Model: Part I. Implementation methodology. *Computers in Industry* 59(6): 580-589 (2008).
5. Barbau, R., S. Krifa, S. Rachuri, & A. Narayanan. OntoSTEP: Enriching product model data using ontologies. *Computer-Aided Design* 44(6): 575-590 (2012).
6. Goh, A., S. Hui, & B. Song. An Integrated Environment for Product Development using STEP/EXPRESS. *Computers in Industry* 31(3): 305-313 (1996).
7. Afreen, H., I.S. Bajwa, & B. Bordbar. SBVR2UML: A Challenging Transformation. *Frontiers of Information Technology (FIT)*, Islamabad, Pakistan. December 19-21, 2011, p. 33-38 (2011).
8. Reynares, E., M. Caliusco, & M. Galli. SBVR to OWL 2 mappings: An Automatable and Structural-Rooted Approach. *Clei Electronic Journal* 17(3): 3-7 (2014).
9. Bajwa, I.S., Lee, M.G., & Bordbar, B. SBVR Business rules generation from natural language specification. In: *AAAI Spring Symposium: AI for Business Agility*, California, USA. March 21-23, 2011, p. 2-8 (2011).
10. Bajwa, I.S., B. Behzad & G.L. Mark. SBVR vs. OCL: A Comparative Analysis of Standards. In: *IEEE 14th International Multitopic Conference (INMIC)*, Karachi, Pakistan. December 22-24, 2011, p. 261-266 (2011).
11. Kahn, H., N. Filer, A. Williams, & N. Whitaker. A generic framework for transforming EXPRESS information models. *Computer-Aided Design* 33(7): 501-510 (2001).
12. Sukys, A., L. Nemuraitė, & B. Paradauskas. Transformation framework for SBVR based semantic queries in business information systems. In: *Second International Conference on Business Intelligence and Technology (BUSTECH)*, Nice, France. July 22-27, 2012, p. 1-6 (2012).
13. Skersys, T., L. Tutkute, & R. Butleris. Extending BPMN business process model with SBVR business vocabulary and rules. *Information Technology and Control* 41(4): 356-367 (2012).
14. López-Ortega, O. A Java Application based on an EXPRESS model for sharing flexible manufacturing resources data. In: *8th IEEE International Conference on Emerging Technologies and Factory Automation*, Vol. 2. Berlin, Germany. October 15-18, 2011, p. 3-11 (2011).
15. Kluza, K., & K. Honkisz. From SBVR to BPMN and DMN models: Proposal of translation from rules to process and decision models. In: *International Conference on Artificial Intelligence and Soft Computing*. Venice, Italy. June 13-14, 2016, p. 453-462. (2016).
16. Jonko, P., B. Feuto, & Walid El Abed. From natural language business requirements to executable models via SBVR. In: *International Conference on Systems and Informatics (ICSAI)* Yantai, China. May 19-20, 2012, p. 2453-2457 (2012).
17. Al Khalil, F., M. Ceci, K. Yapa, & L. O'Brien. SBVR to OWL 2 mapping in the domain of legal rules. In: *International Symposium on Rules and Rule Markup Languages for the Semantic Web*. New York, USA. July 6-9, 2016, p. 258-266 (2016).
18. Luo, Y., M. Van den Brand, & A. Kiburse. Safety case development with SBVR-based controlled language. In: *International Conference on Model-Driven Engineering and Software Development* 2013. Barcelona, Spain. February 19-21, 2013, p. 3-17 (2013).
19. Sani, A.A., P.A.C. Fiona, & P.F. Richard. Model transformation specification for automated formal verification. In: *5th Malaysian Conference on Software Engineering (MySEC2011)*, Bahru, Malaysia. December 11-13, 2011, p. 76-81 (2011).





# CFD Analysis to Study the Effect of Geometry in Flow Behavior of Wing Structure with Additional Riblets

Muhammad Zia Ullah Khan<sup>1</sup>, Rumeel A. Bhutta<sup>1</sup>, Tahir Asif<sup>2,\*</sup>,  
Muhammad Farooq<sup>2</sup>, and Adnan Qamar<sup>2</sup>

<sup>1</sup>Mechanical Engineering Department,  
COMSATS Institute of Information Technology, Sahiwal, Pakistan

<sup>2</sup>Mechanical Engineering Department,  
University of Engineering & Technology, Lahore, Pakistan

**Abstract:** Drag reduction have always been the most important area of interest for a decade with many advancement in it, there has been continuous research on the flow behavior of wing with different geometric combination. Previous studies suggest that Riblets are 7% effective given that they are made with correct sizing. According to test conducted shows the near same result of drag reduction up to 5%. In the present research CFD techniques were used to analyze the flow pattern, where geometry was changed in addition to Riblets named as add-ins. Pressure effect and corresponding velocity dynamics were studied. Each reformed airfoil was analyzed using CFD techniques. A structured grid mesh was used. Governing equation were identified to model exact behavior and numerical computation was performed using FEA software. Simple algorithm and second order upwind scheme for pressure discretization, second order upwind scheme for momentum and energy was used. Changing geometric shape shifts pressure regions and more control is obtained on lift. Value extraction zone selected is outer cross-sectional area in close approximation to wing profile using commercially available computational package.  $\Delta P$  at point 0.05 for design 1,2 and 3 at  $0^\circ$  is 5400 Pa, 7000 Pa and 100 Pa, at  $15^\circ$  on far location is 26000 Pa, 4000 Pa and 8000 Pa where on close location is 35000 Pa, 18000 Pa and 5000 Pa which shows good feasibility for first two designs. Design 1 and 4  $\Delta P$  at 0.05 is 500 Pa and 4000 Pa. Singular geometric alteration yields better result than plural, any modification to rear section does not affect the flow separation. By doing these amendments on desired points can increasing fuel economy rate for jets and commercial air planes.

**Keywords:** Addition of riblets, computational modeling, velocity profile, wing geometry analysis

## Nomenclature

P	Density	$\tau_{ij}$	Stress tensor
t	Time	$u_i$	Orthogonal velocities
$V_x, V_y, V_z$	Velocities	$\mu$	Dynamic viscosity
P	Pressure	$\mu_e$	Effective viscosity
R	General gas constant	$\lambda$	Second coefficient of viscosity
T	Temperature	$\mu m$	Micrometre

## 1. INTRODUCTION

Riblets are small patches on the surface of wing that makes a turbulent flow unidirectional. Riblet and their ratio effectiveness depends on protrusion size [1, 2]. Micro protrusions have significant effect in friction and viscous drag reduction, it is worth studying that how the flow behavior change if these small protrusion are added to the down side of the wing. V-grooved shaped riblet proved to most efficient [3, 4], study of NACA 0012 showed 4.3%

drag reduction [5] while in [6] drag reduction of 4% to 7% on flat surfaces. Sand paper strip was used to give micro structured effect at the leading edge of airfoil NACA 0012 showing adverse effect on velocity [7] like other studies consideration was given to the upper section of airfoil, where amalgamation of riblets and gurney flaps gives no positive result [4, 8]. Since riblets are considered as an auxiliary change to the structure to enhance flow behavior, its transition from laminar to turbulent

increasing overall efficiency of airfoil, and any structure change in airfoil geometry is ranked on how it effects these variables. The variation in local velocity profile for hairy surface is similar to the surface with riblets [9] as velocity profile passages away from surface reducing skin friction. Numerical drag reductions were not verified by the experimental data [10]. Same hairy like effect was tested based on owl wing surface by using two velvet like surfaces concluded that separation bubble does not depend on the angle of attack and enhances the aerodynamic performance of wing [8]. This phenomena helps birds to fly with best efficiency but cannot be imitative for practical applications. Rice and butter wing effect introduced by Bixler and Bhushan, anisotropic flow leading to low drag was found due to aligned shingle-like scales in butterfly wings and sinusoidal grooves in rice leaf [11]. Same results were found when microstructure inspired by shark-skin is tested [12].

Ribbed coating of polymeric film bonded to the upper and lower surface of wing, lateral and vertical aerodynamics are effected by coating also it proved to have negligible effect on longitudinal aerodynamic moments [13]. Biologically inspired microstructures where are useful but on other hand hard to implement practically on large scale. Experiment by [14] on NACA 0012 airfoil by the use of Miro-Riblet Film (MRF) showed that it decreases the overall height of vortices increasing the drag force on wing. Riblets were found to be as good passive controller in reduction of secondary flow where observed setup had riblets placed in front of wing [15]. Solitary use of riblets becomes ineffective once dirt and weather parameters are introduced into the practical equation [16].

Up to authors' knowledge recent literature in this area focuses on effect of riblets in upper section of airfoil. In this very research change in airfoil geometry in lower section of wing termed as add-in, is studied, paralleled with normal structure, structure with riblet and with combination of riblet and add-in. Simple yet effective technique of CFD is used to study such geometric changes. Airfoil used for this is of Boeing 737 MIDSPAN cross sectional area. All these simulation are scaled down to one fifty of their original model as most of the parameters estimating the pressure gradient,

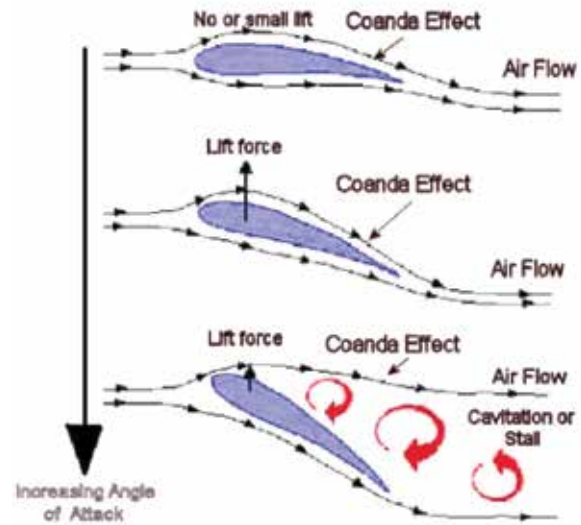


**Fig. 1.** Flow behavior and properties associated with it [22].

velocity and turbulence association are all being dimensionless and would not affect the overall result aiding to characterize and identify pressure with change in design, add in contribution to overall behavior, best optimal location for add-in.

Different shapes invokes different behaviors in Riblets [17], Fig. 1 rotating wing about an axis perpendicular to direction of flow and considering rear edge to be origin, as angle of rotation increases more frontal area comes in contact with air which generates vortices to the upper side of wing and if angle escalates wing will reach a condition known as stall where it no longer generates lift and same case can be considered with add-ins.

## 2. METHODS

### 2.1. Theoretical Formulation

Laws of conservation of momentum, mass and energy are used to explain the fluid flow behaviors [18]. These are then solved in term of differential equations. Assumptions are to be made in order to solve such equations as laminar flow, one phase existence. Keeping these assumptions the governing equations are:

$$\frac{\partial \rho}{\partial t} + \frac{\partial(\rho V_x)}{\partial x} + \frac{\partial(\rho V_y)}{\partial y} + \frac{\partial(\rho V_z)}{\partial z} = 0 \quad (i)$$

Equation (i) is continuity equation which can be deduced form law of conservation of mass [19]. For

simulation above equation is solved by replacing the rate of change of density ( $\rho$ ) with that of rate of change of pressure (P) according to which density changes with pressure. Equation (ii) specifies this as,

$$\frac{\partial \rho}{\partial t} = \frac{\partial \rho}{\partial P} \frac{\partial P}{\partial t} \quad (ii)$$

Where P is the pressure. Since air is assumed to be ideal gas, then the evaluation of the derivation of density can be done from the equation of state by equation (iii) as,

$$\rho = \frac{P}{RT} \Rightarrow \frac{\partial \rho}{\partial t} = \frac{1}{RT} \quad (iii)$$

R and T are gas constant. Air being a Newtonian fluid so the relationship between rate of deformation of fluid and stress can be described by equation (iv) as:

$$\tau_{ij} = -P\delta_{ij} + \mu \left( \frac{\partial u_i}{\partial x_j} + \frac{\partial u_j}{\partial x_i} \right) + \delta_{ij} \lambda \frac{\partial u_i}{\partial x_i} \quad (iv)$$

Where  $\tau_{ij}$  is stress tensor,  $u_i$  are orthogonal velocities  $\mu$  is dynamic viscosity and  $\lambda$  is the second coefficient of viscosity. This relationship is simplified after solving and neglecting some term for compressible fluid for x, y and z component respectively we get three equations,

$$\begin{aligned} \frac{\partial \rho V_x}{\partial t} + \frac{\partial(\rho V_x V_x)}{\partial x} + \frac{\partial(\rho V_y V_x)}{\partial y} + \frac{\partial(\rho V_z V_x)}{\partial z} \\ = \rho g_x - \frac{\partial \rho}{\partial x} + R_x + T_x + \frac{\partial}{\partial x} \left( \mu_e \frac{\partial V_x}{\partial x} \right) \\ + \frac{\partial}{\partial y} \left( \mu_e \frac{\partial V_x}{\partial y} \right) + \frac{\partial}{\partial z} \left( \mu_e \frac{\partial V_x}{\partial z} \right) \end{aligned} \quad (v)$$

$$\begin{aligned} \frac{\partial \rho V_y}{\partial t} + \frac{\partial(\rho V_y V_x)}{\partial x} + \frac{\partial(\rho V_y V_y)}{\partial y} + \frac{\partial(\rho V_y V_z)}{\partial z} \\ = \rho g_y - \frac{\partial \rho}{\partial y} + R_y + T_y + \frac{\partial}{\partial x} \left( \mu_e \frac{\partial V_y}{\partial x} \right) \\ + \frac{\partial}{\partial y} \left( \mu_e \frac{\partial V_y}{\partial y} \right) + \frac{\partial}{\partial z} \left( \mu_e \frac{\partial V_y}{\partial z} \right) \end{aligned} \quad (vi)$$

$$\begin{aligned} \frac{\partial \rho V_z}{\partial t} + \frac{\partial(\rho V_z V_x)}{\partial x} + \frac{\partial(\rho V_z V_y)}{\partial y} + \frac{\partial(\rho V_z V_z)}{\partial z} \\ = \rho g_z - \frac{\partial \rho}{\partial z} + R_z + T_z + \frac{\partial}{\partial x} \left( \mu_e \frac{\partial V_z}{\partial x} \right) \\ + \frac{\partial}{\partial y} \left( \mu_e \frac{\partial V_z}{\partial y} \right) + \frac{\partial}{\partial z} \left( \mu_e \frac{\partial V_z}{\partial z} \right) \end{aligned} \quad (vii)$$

Where  $\mu_e$  is the effective viscosity; in the instant case effective viscosity is the dynamic viscosity.

Energy equation solution is not required as flow behavior is studied. All these equation are used by FEA package to stimulate flow. All the terms for z distribution are neglected due to 2D analysis and other reason for this is that introducing another dimension to the analysis complicates the deduction of flow behavior which is not required.

### 2.2. Modeling Conditions

Fig. 2 shows the cross-section of the geometries with location of riblet and add-in on upper and lower portion of airfoil for all designs, used for the present analysis, and along with it is the mesh produced situation which consist of structural mesh of 77188 nodes and 38129 elements around and on the plane. Domain fifteen times the airfoil form

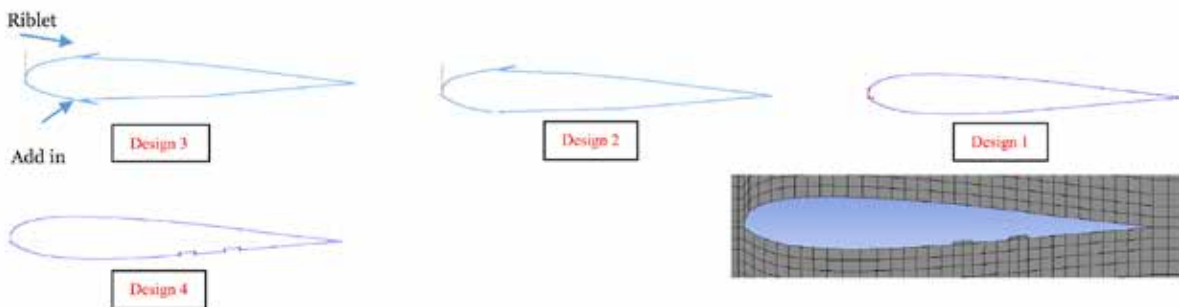


Fig. 2. Wing cross-sections showing different changes (Design 1-4).

origin to upper and lower Y axis limit, seven times to front and twenty five times to back, to capture proper flow on leaving regime. Inlet boundary condition of 330m/s, outlet is set to gauge pressure. No slip condition on outer walls of domain. These boundary conditions are being used one by one which change in shape and angle of attack.

### 2.3. Analysis Factor

Analysis was carried out with simple algorithm and second order upwind scheme for pressure discretization, second order upwind scheme for momentum and energy too. Neglecting atmospheric extreme weather conditions like snow or volcano eruption[16], using air as working fluid with its respective flow properties. Relaxation factors are taken to be default values of pressure 0.3, density 1, body forces 1, momentum 0.7 and turbulent kinetic energy 0.8. Convergence criterion set for 0.001 for continuity, x-momentum and y-momentum. Initial velocity is 330m/s. Boundary condition for pressure is zero gauge.

## 3. RESULTS AND DISCUSSION

Fig. 3-5, pressure and flow behavior with each profile is different as lift is a force generated by turning a moving fluid. Fig. 3, pressure dispersal around the airfoil is symmetric for  $0^\circ$  with change in angle from  $0^\circ$  to  $15^\circ$  variations starts to occur and force per unit area on the tip increases. Molecules close to surface have little or no motion due to skin friction drag and is same on upper and lower surface in case of  $0^\circ$  at  $15^\circ$  they stay attached to

lower surface but separation on molecular layer is observed on upper surface same as in [20], which shows parting from wing surface but molecules remain attached to upper flow boundary forming a smooth layer of flow followed by vortices region. Flow then stabilizes in regime after. Fig. 4, alteration in wing profile on upper surface depicts no significance visual flow pattern modification for  $0^\circ$  in terms of  $\Delta P$  when compared to not modified wing; however molecule separation from surface layer becomes substantial. Rotated to  $15^\circ$ , pressure uncertainty increases with small pressure bubble area formation at rear section acting as unit area force normal to surface downwards. Nevertheless this rotation shows positive results it also add more momentum to leaving air molecules making then to ring around one center forming big vortices on amended region. Formation point of these vortices is tip addition which no longer let the incoming layer over top surface to remain attach and as layer passes tip it starts to separate due to high velocity, where decrease in height of vortices is linked to high drag [14].

Fig. 5, same alteration in design on both surfaces shows symmetrical behavior of flow in terms of pressure and velocity, flow flinches to separate into small layers where particles of air on layer exhibiting coanda effect are collinear with the modified tip. This is the extreme point for flow disturbance and is symmetric to plane parallel to flow and passing through chord length. Comparison of Fig. 3-5, with no change flow behaves in its natural pattern, with change in one side natural pattern on that side is different where unchanged side of that very design

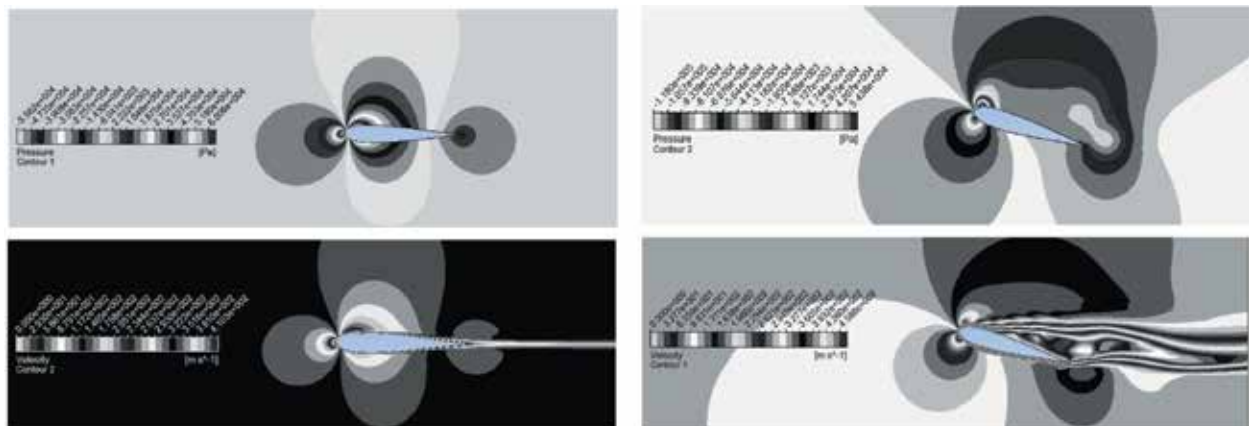


Fig. 3. Design 1 pressure (top) and velocity (below) Contour at  $0^\circ$  (left) and  $15^\circ$  (right) angle of attack.

still portrays the old natural behavior. Change on both sides pattern of side amended early simply gets mirrored with same results but now they are on the upper and lower side of the wing. From this study it is deduced that air foil that follows

this mirror characteristics along chord length will produce no or little change when riblet and add-in are used combined. A better understanding of it can be observed by center of pressure (CoP) theory which is used to stabilize any object moving in fluid

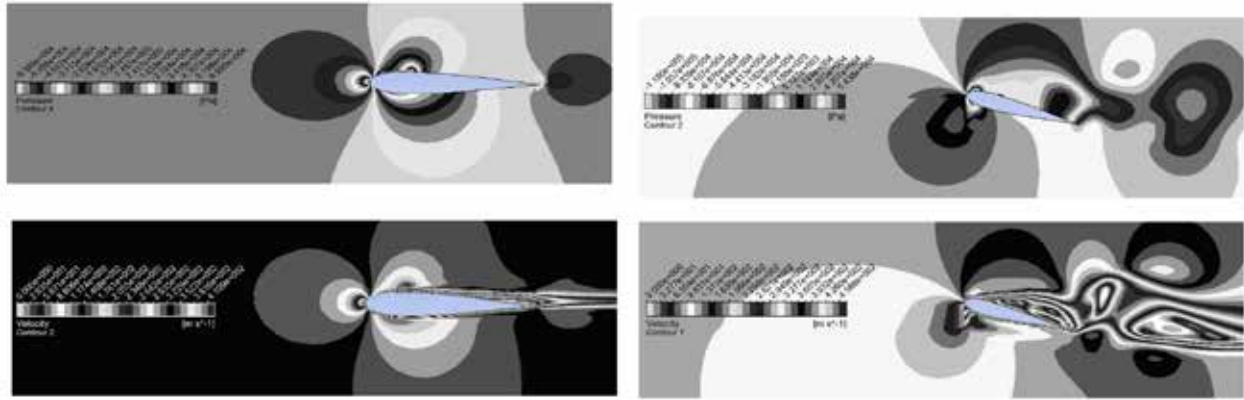


Fig. 4. Design 2 pressure (top) and velocity (below) Contour at 0° (left) and 15° (right) angle of attack.

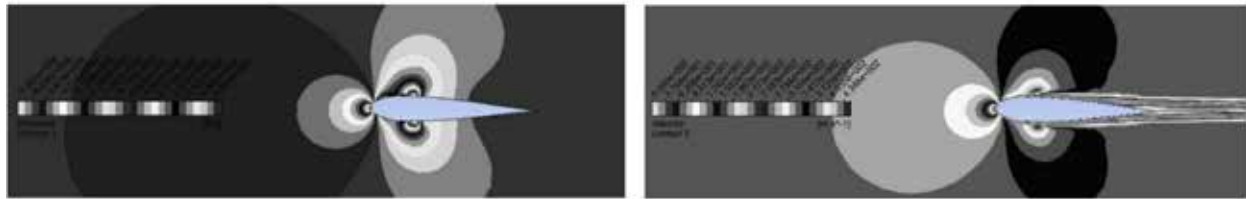


Fig. 5. Design 3 pressure (top) and velocity (below) contour at 0°.

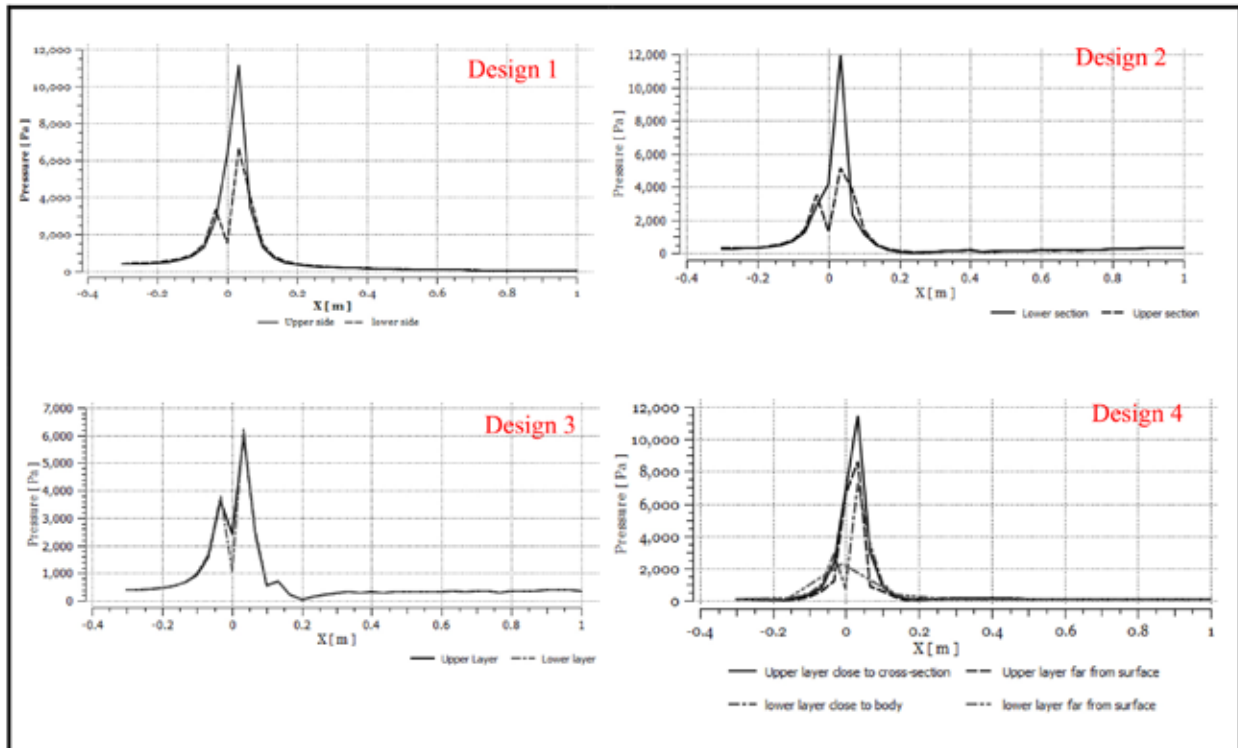


Fig. 6. Pressure distribution around the airfoil at 0° attack angle.

as CoP changes which change in angle of attack so pattern of flow behavior will change according to it. Aerodynamic force is integration of pressure times surface area, lift and drag are the resolved components of this force, which acts through the center of pressure in flight. Increasing  $\theta$  from  $0^\circ$  to  $15^\circ$  shifts CoP close to wing tip and thus producing more lift at the tip section. Fig. 3-5, CoP shift is same due to the fact that this protrusion size in practical is in  $\mu\text{m}$  so any kind of groove would not affect this transferal, as long as the air foil under study is same.

Fig. 6 shows that the pressure distribution on the nodes close and far on the both upper and lower side of the wings, on x-axis is the distance along which pressure varies. Graphs are generated for different geometric conditions for comparing the results and developing a proper conclusion. Legends show the discrimination between the upper and lower side flow on airfoil. Fig. 6 design 1 upper side riblet causes more disturbance in the flow in term of pressure  $P$  and region where  $-0.2 < x < 0.3$ , is reverse flow which generates a little vacuum and is the cause of negative values.

### 3.1. Transverse Flow Assessment of Design 1, 2 and 3

Design 1 represents the tip type cross-section for the riblet on the upper side of the airfoil. Addition of riblet in shapes effects flow and pressure associated with it. Lower section defines the lower portion of wing and upper section defines upper layer close to wing bounding entities. Pressure shifts at upper section in region in between  $-0.2$  to  $0.2$ , having low values as compared to pressure at lower region. Variation in pressure raises the overall lift of wing.

Fig. 6 design 3 is graph between pressure  $P$  and distance  $s$ . It shows pressure dissemination in simple wing along x-direction, on regions enveloped by it at upper and lower portion on stated cross-section. Zero on x-axis represents tip of wing. Pressure increases as approaching air towards wing influences in region adjacent to wing tip. At tip sudden pressure drop followed by a peak pressure value. Gain in pressure is then reduces as flow enter the later region of wing from  $0.05$  m to  $0.2$  m, sliding over wing surface with high velocity. Both upper and lower layer have same curve paradigm.

After comparing designs in Fig. 6 graphs four designs at  $0^\circ$  angle of attack we find that the difference in pressure on the upper and lower side of airfoil is much greater for Design 1 while considering pressure difference at 0 point in graph. Whereas Design 2 pressure is at maximum of  $12000$  Pa higher than other designs.

Fig. 7 design 3 altered angle of attack to  $15$  degree with this change pressure elevates to triple the amount as compared to  $0$  degree gave the same effect that of use of rough strip at leading edge [7]. Pressure divergence in upper and lower layer close to surface is in relation of low to high respectively. A spike in the negative direction in Fig. 7 design 1 shows a vacuum and reverse flow generation which is also visible on the contour visuals in Fig. 3. It can be seen that lower section of the wings have high pressure on the tip lower side of the wing as compared to upper side, indirect more lift as  $P_{\text{lower}} > P_{\text{upper}}$ . Fig. 3 design 4, upper close layer and far layer section pressure increases and to the point  $0$  to  $0.05$  and then decreases showing the same characteristics like design 1 in the upper section as the geometry is alike as far the lower section design 4 shifting in behavior for region far from cross section with an increase in pressure at the edge of the wing and having lower pressure around regions in close contact with the airfoil showing a  $5\%$  increase then design 1 at  $0^\circ$  attack angle.

Three peak values were observed which changes from design 1-3. First two designs have peak values at point  $0$  with a negative peak value followed by it. Pressure change for design 1 in Fig. 7 does not chart a smooth curve instead an abrupt change occurs along the flow direction generating some low pressure region below gauge pressure value. This phenomena is also observed with design 2 at  $15^\circ$  yet unlike design 1 curve change is not sudden but it first decreases then stabilizes for some distance between point  $0$  to  $0.05$  and then it descends again up to  $0.1$  and goes tends towards stabilizing again, this is the case in lower section of wing. In upper region pressure is in negative as soon as air particles comes in contact with wing tip pressure values decreases indication of vacuum in upper wing section and as the flow leaves the wing it stabilizes joining with the incoming flow from the lower side of the wing. Design 1 and 2 at  $15^\circ$  exhibit

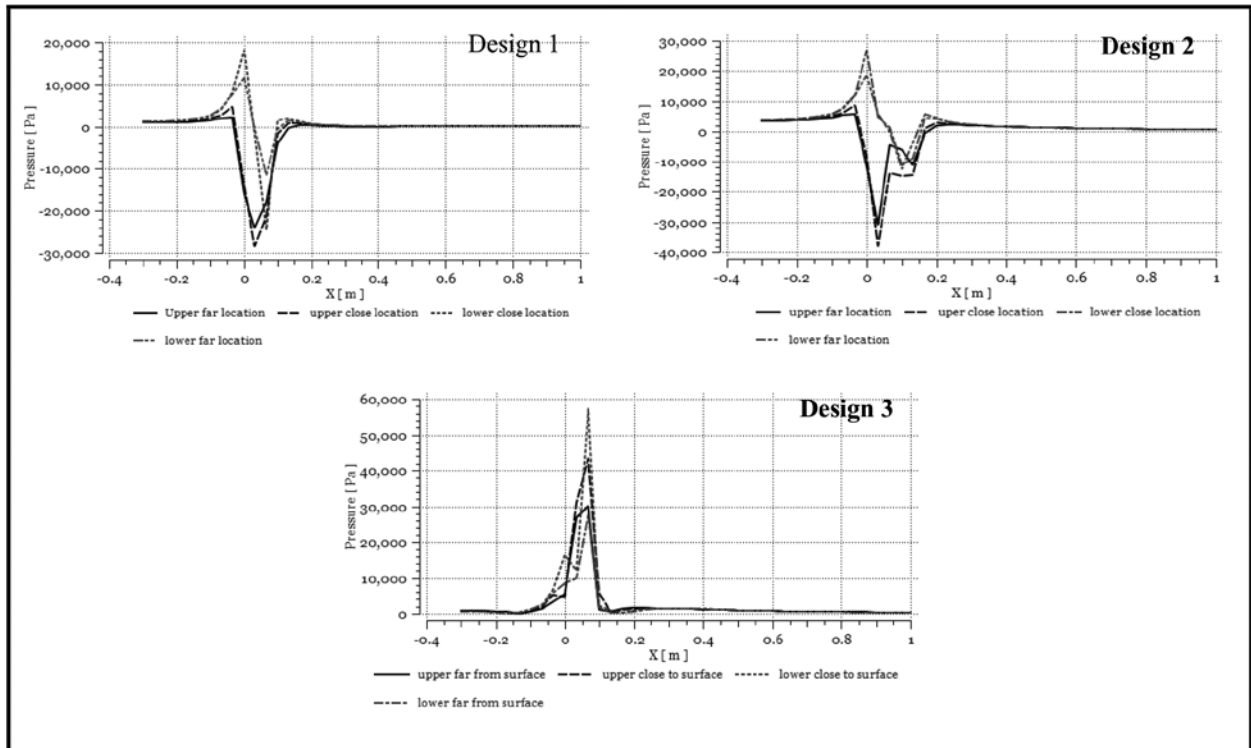


Fig. 7. Pressure distribution around the airfoil at  $15^\circ$  attack angle.

the same behavior but with different flow values. Design 3 in Fig. 7 have symmetric riblet and add-in, with a curve following the same behavior as of preceding graphs, to understand different behavior values taken for design were all positive and close comparison of all the layers showed that both upper layer had low value of 30000 Pa and 41000 Pa at point 0.05 while that of both lower layers had peak values reaching 54000 Pa at same point. Curve flow is abrupt same before graph.

Data values are extracted from the graph to evaluate each design behavior under specific location which is in table 1. Design 1-3 points 0, 0.05 and 0.1 along the flow direction are selected to assess pressure difference. Design 1-3 at point 0 gave pressure value of 4400 Pa, 2500 Pa and 1500 where at point 0.05 it gave 5400 Pa, 7000 Pa and 100 Pa and at 0.1 it had 100 Pa, 200 Pa and 0 Pa. At same point 0 all design have descending pressure values conversely at point 0.05 design 2 displayed an increase in pressure value this was due to alteration made to the foil. Derivative to point 0.1 with same analogy, on basis of this observation design 3 gives poor feasibility then design 1 and 2. With an increase in angle from  $0^\circ$  to  $15^\circ$  pressure

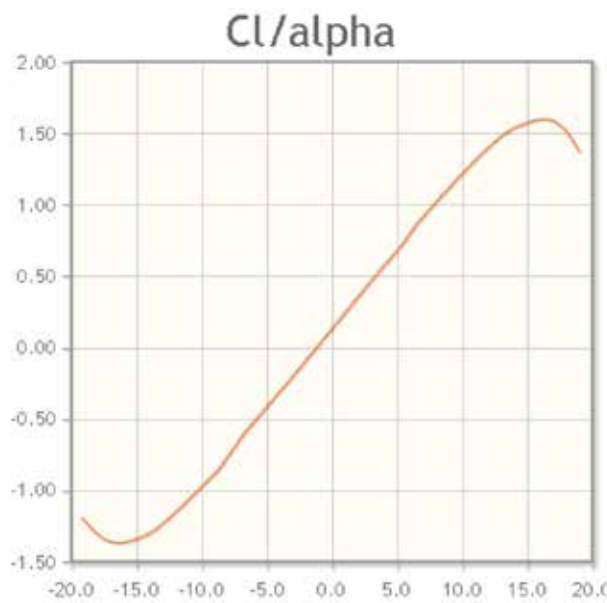
values elevated in surrounding regime far from wing surface, at point 0 gave pressure value of 27000 Pa, 32000 Pa and 4000 where at point 0.05 it gave 26000 Pa, 4000 Pa and 8000 Pa and at 0.1 it had 4000 Pa, 18000 Pa and 200 Pa. Comparing those data values design 3 falls under poor feasibility due to low pressure difference in between locations. Regime far from wing surface gave low pressure values when compared to regime that is close to wing surface which are as at point 0 gave pressure value of 32000 Pa, 39000 Pa and 11000 where at point 0.05 it gave 35000 Pa, 18000 Pa and 5000 Pa and at 0.1 it had 2000 Pa, 6000 Pa and 2000 Pa with poor feasibility for design 3 as it had truncated pressure at point 0 when equated with other designs at the same angle.

### 3.2. Transverse Flow Assessment of Design 1 and 4

Fig. 6, design 4 and design 1 make comparison of simple wing and wing with Add-in on lower side. For this comparison only upper layer close to cross-section and lower layer close to body is considered for Design 4 case to evaluate pressure difference at different points shown in Table 1 and were establish

**Table 1.** Comparison of airfoil at different angles along with practicability.

Geometry	Angle of attack	Pressure difference (Pa) at points			Feasibility
		(0 point)	(0.05 point)	(0.1 point)	
Design 1	0°	4400	5400	100	Good
Design 2	0°	2500	7000	200	Good
Design 3	0°	1500	100	0	Poor
<i>Pressure Difference on Surrounding Regime far from Wing Surface</i>					
Design 1	15°	27000	26000	4000	Good
Design 2	15°	32000	4000	18000	Good
Design 3	15°	4000	8000	200	Poor
<i>Pressure Difference on Surrounding Regime close to Wing Surface</i>					
Design 1	15°	32000	35000	2000	Good
Design 2	15°	39000	18000	6000	Good
Design 3	15°	11000	5000	2000	Poor
<i>Pressure Difference on Upper Layer close to Cross-section and Lower Layer close to Body</i>					
Design 1	0°	4300	500	100	Good
Design 4	0°	6200	4000	100	Better then Design 1

**Fig. 8.** Effect of angle of attack on lift co-efficient for Boeing 737 MIDSPAN Airfoil [23].

to be as at point 0 pressure value of 4300 Pa, 6200 Pa where at point 0.05 it gave 500 Pa, 4000 Pa and at 0.1 it had 100 Pa, 100 Pa. Pressure transformation in design 4 is smooth as it does not descends ascends with high gap between values unlikely than design 1 for which values were fluctuating with more gap in between them. Thus, proving design 4 at 0° to be

better than design 1.

Graph in Fig. 8 was generated using Xfoil online software to predict the effect of angle of attack on coefficient of lift. Maximum effective value of lift is in range of 15 degrees to 17 degrees. Increasing angle more than that decreases wing efficiency and tilted wing greater than 17 introduces frontal face drag parameter to the equation.

#### 4. CONCLUSIONS

Four different alterations were done to airfoil in term of geometric point of view; each reformed airfoil was analyzed using CFD techniques. A structured grid mesh was used as it gives more stable result instead of hybrid or tetrahedral mesh topology. Flow behavior of air molecules were studied when subjected to different design changes along with attack angle change from 0° to 15° rotating wing about an axis perpendicular to direction of flow and considering rear edge to be origin. Coanda effect, stall condition, pressure distribution, air molecule flow behavior with first initial contact till final, wing design optimization and its effect of likelihood with-in the designs under study were premeditated. Each design was compared on the basis of pressure values covering the air foil surrounding regime.

Changing conventional wing sections into new ones changes the flow pattern, but as for the sake of observation protrusion were kept to big size, which different changes Coanda effect and stall properties can be controlled and Riblets along with add-in have proven to be valuable to study such cases. Concept of CAM for riblet manufacturing which can be instigated to the add-in segment.

It is concluded that, theoretically add-in was a good approach in seeking better aerodynamic results but practically they could be of problem in extreme weather conditions like snow or volcano eruption where ash or small particles can get stuck in to these small protrusions. which is rare event like bird strike and were excluded being a rare parameter from analysis but an enhance mechanical system needs to be devised which can control the patching when it is needed to overcome such problems. Table 1 singular design change was feasibly good as paralleled to plural alteration. V-grooved shaped riblet of 100 $\mu$ m in height when tested for turbine wing design showed an improvement of 6% alike shape is integrated for our study and found near analogous result .Where it is seen that when add-in is introduced near the tail, decreases the overall pressure directly effecting efficiency. Table 1 comparison show wing with add-in (square) better than simple wing with point 0 pressure value of 4300 Pa, 6200 Pa where at point 0.05 it gave 500 Pa, 4000 Pa and at 0.1 it had 100 Pa, 100 Pa. Hence, this shows that additional geometric changes make positive effect in some cases given that they are made on specific location like in front section or rear section. More work needs to be done in respect to study 3D cases of such problems; a practically good solution can lead to better fuel efficiency.

## 5. REFERENCES

- Duan, L. & M.M. Choudhari. *Effects of Riblets on Skin Friction in High-Speed Turbulent Boundary Layers*. NASA Langley Research Center, Hampton, VA, USA (2012).
- Sareen, A., R.W. Deters, S.P. Henry, & M.S. Selig. Drag reduction using riblet film applied to airfoils for wind turbines. *Journal of Solar Energy Engineering* 136(2): 021007-021007-8 (2014).
- Chamorro, L., R. Arndt, & F. Sotiropoulos. Drag reduction of large wind turbine blades through riblets: Evaluation of riblet geometry and application strategies. *Renewable Energy* 50: 1095-1105 (2013).
- Li, Y. & J. Wang. Experimental studies on the drag reduction and lift enhancement of a delta wing. *Journal of Aircraft* 40(2): 277-281 (2003).
- Han, M., H.C.Lim, Y.G. Jang, S.S. Lee, & S.J. June. Fabrication of a micro-riblet film and drag reduction effects on curved objects. In: *12th International Conference on TRANSDUCERS, Solid-State Sensors, Actuators and Microsystems*, , 8-12 June, Boston, USA, 1: 396-399 (2003).
- Walsh, M.J. Turbulent boundary layer drag reduction using riblets. In: *The American Institute of Aeronautics and Astronautics, Aerospace Sciences Meeting 1* (1982).
- Kim, S., J. Kim, J. Park, & J. Choi. Measurements in the wake of an airfoil with regular roughness on the upper surface near the leading edge. *Proceedings of the Institution of Mechanical Engineers, Part G: Journal of Aerospace Engineering* 220(3): 203-208 (2006).
- Klän, S., S. Burgmann, T. Bachmann, M. Klaas, H. Wagner & W. Schröder. Surface structure and dimensional effects on the aerodynamics of an owl-based wing model. *European Journal of Mechanics - B/Fluids* 33: 58-73 (2012).
- M. Bartenwerfer & D. Bechert. The viscous flow on hairy surfaces, In: *6<sup>th</sup> European Drag Reduction Working Meeting, Eindhoven/Nederland*, p. 21–22 (1991).
- Bechert, D., M. Bruse, W. Hage & R. Meyer. Fluid Mechanics of Biological Surfaces and their Technological Application. *Naturwissenschaften* 87(4): 157-171 (2000).
- Bixler, G. & B. Bhushan. Bioinspired rice leaf and butterfly wing surface structures combining shark skin and lotus effects. *Soft Matter* 8(44): 11271-11284 (2012).
- Martin, S. & B. Bhushan. Fluid flow analysis of a shark-inspired microstructure. *Journal of Fluid Mechanics* 756: 5-29 (2014).
- Konovalov, S., Y. Lashkov & V. Mikhailov. Effect of longitudinal riblets on the aerodynamic characteristics of a straight wing. *Fluid Dynamics* 30(2): 183-187 (1995).
- Lee, S. & Y. Jang. Control of flow around a NACA 0012 airfoil with a micro-riblet film. *Journal of Fluids and Structures* 20(5): 659-672 (2005).
- Kairouz, K. & H. Rahai. Turbulent junction flow with an upstream ribbed surface. *International Journal of Heat and Fluid Flow* 26(5): 771-779 (2005).
- Abbas, A., J. de Vicente & E. Valero. Aerodynamic technologies to improve aircraft performance. *Aerospace Science and Technology* 28(1): 100-132 (2013).
- Grüneberger, R., F. Kramer, E. Wassen, W. Hage,

- R. Meyer & F. Thiele. Influence of wave-like riblets on turbulent friction drag. *Nature-Inspired Fluid Mechanics* 311-329(2012).
18. ANSYS14.5 manual, article 7.1 (2014).
  19. Welty, J.R., C.E. Wicks, G. Rorrer & R.E. Wilson. *Fundamentals of Momentum, Heat and Mass Transfer*. John Wiley & Sons, New York (2009).
  20. Boiko, A.V., V.V. Kozlov, V.V. Syzrantsev & V.A. Shcherbakov. Riblet control of the laminar-turbulent transition in a stationary vortex on an oblique airfoil. *Journal of Applied Mechanics and Technical Physics* 37(1): 69-79 (1996).
  21. Saggu, J. & J. Fielding. An integrated CAD/CAM method for the design and construction of aircraft wing components. *Computers in Industry* 12(2): 123-130(1989).
  22. Anon. [Image] Available at: [http://www.formula1-dictionary.net/coanda\\_effect.html](http://www.formula1-dictionary.net/coanda_effect.html) (2016) [Accessed 4 Feb. 2016].
  23. Xfoil Online Software. BOEING 737 MIDSPAN AIRFOIL - Boeing Commercial Airplane Company model 737 airfoils.Co-efficient of Lift VS Angle of Attack. < <http://airfoiltools.com/airfoil/details?airfoil=b737b-il#polars> >[Accessed 4 Feb. 2016].



# Palm and Finger Segmentation of High Resolution Images using Hand Shape and Texture

Momna Asghar<sup>1</sup>, Irfan Arshad<sup>1,\*</sup>, Imtiaz Ahmad Taj<sup>2</sup>,  
Gulistan Raja<sup>1</sup>, and Ahmad Khalil Khan<sup>1</sup>

<sup>1</sup>Electrical Engineering Department,  
University of Engineering and Technology, Taxila, Pakistan

<sup>2</sup>Electrical Engineering Department,  
Capital University of Science and Technology, Islamabad, Pakistan

**Abstract:** Amongst the diverse range of available biometric systems, hand based security system is considered as the oldest one. This paper focuses on dealing with high resolution images obtained from the HP scanner. The main advantage associated with this work is the ability to utilize the normal scanner for palm as well as for fingerprint acquisition so that the high cost associated with the palm and fingerprint scanner can be reduced. The proposed method is of significant importance since single image of hand is used to extract both the hand-shape and palm print. A robust methodology, based on fusion of contour and the texture approach has been proposed. To capture the contour of the hand, B-Spline curve has been used. Whereas, for the texture based approach Fourier transform followed by edge detectors has been employed. In order to attain the better accuracy of detection, HOG (Histogram of Oriented Gradients) descriptor is used for feature extraction.

**Keywords:** Hand based system, high resolution images, segmentation, biometric systems, palm-print.

## 1. INTRODUCTION

Personal authentication has gained much importance in the current information systems, including access control in confidential areas, electronic payments, securing computer's or smart phone's data, etc. Amongst the other developed systems, biometrics has played a vital role for the security purposes [1]. The commonly measured traits are fingerprints, hand shape, gait, palm-print, face, voice, etc. Amongst the other existing biometrics, human hand is considered as the oldest technology [2] and it has gained researcher's attention because of its permanence, uniqueness and reliability [3]. Palm print, hand vein, knuckle point, fingerprint and hand geometry are usually extracted from hand. These features are reliable and stable throughout the life span, after a person reaches his adulthood [4]. At this time, mostly the acquisition devices are working on low resolution

and some of them use pegs or guidance peripherals for the image acquisition [5, 6].

Most of the previous work in this field has been done on the low resolution images. This paper focuses on dealing with high resolution images obtained from the HP scanner. Thus, cutting off high cost associated with the palm scanners. This paper proposes a novel approach to segment out the whole hand into palm and fingers without extracting any landmark points or using pegs.

The several steps involved in the development of proposed method are as follows: First, utilize the hp scanner for hand scanning. Secondly, in order to deal with different posture of hand, it was decomposed into palm and fingers. Third, the landmark points were avoided because the finger valleys are not reliable for different poses of hand. Finally, instead of traditional approaches

used for the representation of hand geometry using geometrical measurements, geometry of all parts of a hand like palm and the fingers are represented separately. With the intentions of avoiding the touching of the fingers, users should stretch their hand slightly during scanning.

## 2. RELATED WORK

In literature, many approaches have been proposed for the palm-print and fingerprint recognition purposes. Early studies employed the peg based systems to provide assistance for the placement of user's hand [7, 8]. It is not user friendly as well as unreliable since pegs can deform the image severely. Mostly palm-print databases were background restricted [5]. Jain et al. [9] and Oden et al. [10] used hand image taken at low resolution as well as the pegs to restrict the movement of hand. The obtained results were quite promising. Recently proposed contact-less palm-print systems have used monotone dark backgrounds to avoid the segmentation [11]. Palm segmentation plays a vital role in system's performance, since better segmentation results can lead to better selection of region of interest (ROI) thus, increases the recognition rates [12]. Neves et al. [13] presented a biometric identification technique using palm image. Through the identification of human palm using the textural and geometrical data obtained from the Local Binary Pattern (LBP) method, a Palm-Print Authentication System (PPAS) was implemented, the approach was tested on 50 images and the results were quite effective. Afsal et al. [14] used the fuzzy entropy to calculate the maximum uncertainty in the information. It uses fuzzy function to extract the maximum possible information from the palm images, since it is full of uncertainties.

Using detection techniques based on skin color, segmentation can't be done in cluttered environment because of same chrominance values. Multimodal systems have attracted the attention of the researchers. Recently [1, 15-17], have developed some techniques for the implementation of multimodal systems. Zhu et al. [18] proposed a multi-modal system based on palm-print, knuckle point, finger geometry, and features by fusing

them at decision stage to enhance the efficiency of the matching module along with the accuracy of recognition. G. Amayeh et al. [19] segmented the hand using a tough, iterative procedure by utilizing the morphological operators. They employed Zernike moments for the representation of the geometry of each segmented part. Afterwards, the hand image is separated into 6 sections i.e. palm and the finger's region. Higher order Zernike moments are used for the representation of geometry of all parts of hand. Feature extraction using the landmarks has been very successful but it needs a reference image for comparison of detected landmarks with the reference landmarks [20]. Some researchers employed Component-based approach using region descriptors comprises of high order Zernike moments for hand-based verification and identification [21] to improve efficiency and speed, along with the ease of use. Wu et al. [22] used hierarchical method to develop the feature vectors taken from centroids of various areas of hand. The quality of hand image was not so satisfactory and it was affected by the illumination device which can also affect the accuracy of the system.

Geometric metrics like length, width, Euclidean, and weighted Euclidean have been used for the feature extraction, but these methods are not so efficient because they are more prone to errors [23]. Rahman et al. [24] proposed a new hand approach based on the geometry, using Distance-based Nearest Neighbor (DBNN) algorithm and the Complete Graph Theory (CGT). Han et al. used the NIR camera and NIR LEDs in which segmentation is considered as a part of hardware [25]. Wang [26] implemented a technique using both hand-tracking and gesture recognition on FGPA using combination of YCbCr color space and region growing algorithms, including morphological operations for the noise removal. Another novel approach based on scattering wavelet transform (SWT) was proposed by Saranraj et al. [27]. They extracted the discriminative features from the palm image that were considered most useful in the matching process, then simple Euclidean distance based matching was employed.

Comparing the methods of visible light with the approaches using infrared light [28], the results show that the latter performs well. The method

employed by Morales et al. [28] improved the performance of image acquiring device, but it raises another flaw in it. They used a template of palm to assist the users in placing their hand on the image acquisition device; it reduces the flexibility of hand along with the practical application of hand based verification system.

Kumar et al. [29] used the combination of palm print and the hand shape signature to develop a peg free recognition system, but their computational cost was quite high. An ordinary flat-bed scanner was used for the image acquisition, user could place its hand freely and naturally on the scanner. Amayeh et al. [30] developed an approach by employing a simple lighting table and a VGA (video graphics array) resolution CCD camera, without involving pegs. The camera was directed perpendicular to the direction of the table. It produces a binary, noise and shadow free image of hand. Sato et al. [31] pointed out the problem of extraction of the exact palm-region from the images with large deformation, using a contact-less palm recognition method. They proposed a system using 3D measurements with diffraction grating laser. Aishwarya et al. [32] presented a novel system that detects the bio-metric traits utilizing the liveness detection method and the weber's local descriptor algorithm; thus reducing the spoofing methods, simply employing the Euclidean distance formula both false acceptance and false rejection rates are reduced.

The paper proceeds as: the image acquisition device and pre-processing steps are discussed in section 3. Then section 4 analyzes the active approach suggested in the paper, by proposing a robust approach comprises of the fusion of geometrical features and the texture of hand. In section 5, the extraction method for palm and fingers is described. Section 6 includes the presentation of the results on the new hand database along with its comparison with other existing techniques. In the end, section 7 concludes the paper with a brief dialogue along with the suggested future work.

### 3. IMAGE ACQUISITION AND PRE-PROCESSING

To confirm the validity and efficiency of the proposed

technique, a new database has been developed. For this purpose, a normal high resolution scanner has been used as shown in Fig. 1. Images at the resolution of 1200 ppi have been taken from this device. Images are captured by placing the hand on the scanner with the fingers stretched. No guidance assembly like pegs is used to restrict the placement of hand on the device. Size of images obtained at the resolution of 1200 ppi (pixels per inch) is  $7,000 \times 6000$  pixels.



Fig. 1. HP scanner used for hand scanning.

Some samples of hand captured from the high resolution hp scanner are given in Fig. 2. Since, the imaging is peg free, thus, it is accepted by the public easily. To decrease the computational cost of the system the size of the image is reduced to  $1800 \times 1300$  pixels and later on, restored to its original value.

### Pre-Processing

Images taken from the scanner need some preprocessing steps to make them more feasible for use. First, the images are converted into grey scale by Eq. (1) [18].

$$G(\text{row}, \text{col}) = 0.587 * C_{\text{Green}}(\text{row}, \text{col}) + 0.299 * C_{\text{Red}}(\text{row}, \text{col}) + 0.114 * C_{\text{Blue}}(\text{row}, \text{col}) \quad (1)$$

where  $C_{\text{Green}}(\text{row}, \text{col})$ ,  $C_{\text{Red}}(\text{row}, \text{col})$ , and  $C_{\text{Blue}}(\text{row}, \text{col})$  are used to show the color constituents of green, red, and blue, respectively.

In order to enhance the contrast of the images, contrast stretching is used. The equation governing this process is given in Eq. (2).

$$I_{\text{Norm}} = (I - I_{\text{min}}) \frac{I_{\text{newmax}} - I_{\text{newmin}}}{I_{\text{max}} - I_{\text{min}}} + I_{\text{newmin}} \quad (2)$$

## 4. PROPOSED WORK

A segmentation algorithm has been proposed here, that can extract as well as utilize the palm-print and fingerprint at the same time. Segmentation of hand

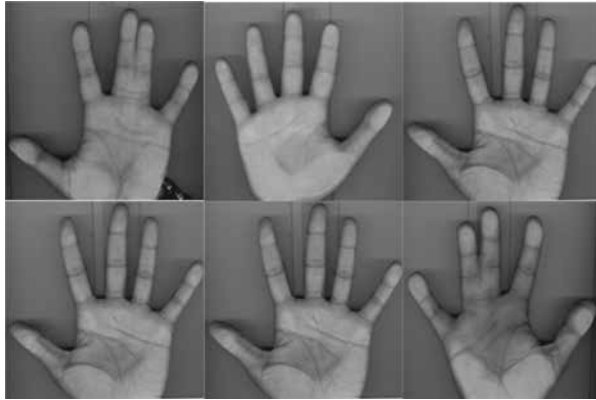


Fig. 2. Images form database scanned by hp scanner.

into its different regions can be made robust by sensing the landmarks on the silhouette of hand, but this approach is more susceptible to errors. Thus the overall efficiency of the system is reduced. The proposed methodology is given in Fig. 3.

#### 4.1 Texture Based Approach

Texture based approach is implied to separate out the background from the hand image. It involves the following steps: First, the Fourier transform of enhanced image is calculated. It helps in determining the frequency components of image. Through visual inspection, it is found that there exists a certain band of frequencies which correspond to the desired part of the image. Therefore, Gaussian Band-pass filter has been applied on the transformed images to

extract the band of frequencies which are suitable for the enhancement of image. It helps in making the outer boundary of the hand noticeable by removing the undesirable frequency components from it.

Since the image is 2D so there is a need to use the two 1D Gaussian functions, as given by Eq. (3).

$$G(x, y) = \frac{1}{2\pi\sigma^2} e^{-\frac{x^2+y^2}{2\sigma^2}} \quad (3)$$

Afterwards, there is a need of a threshold value, that can be used effectively and efficiently to separate the desired area from the background.

In order to get the adaptive threshold value for the pixels of the image that are outside the hand silhouette i.e. the background pixels, an analysis is performed. Since in the generalized automatic system, it is required to extract the region of interest from a huge number of databases. The value of the threshold relies upon the intensity values of all pixels, and then the best value is chosen as the threshold. For this purpose many techniques have been used like histogram. But Otsu's [33] method for threshold has proven itself a good candidate for the choice of a threshold value. Since this method assumes that the image belongs to two pixel classes i.e. foreground and the background, it computes the best threshold value that separates the two classes such that their intra-class variance is insignificant. The pseudo code for Otsu's method for threshold is

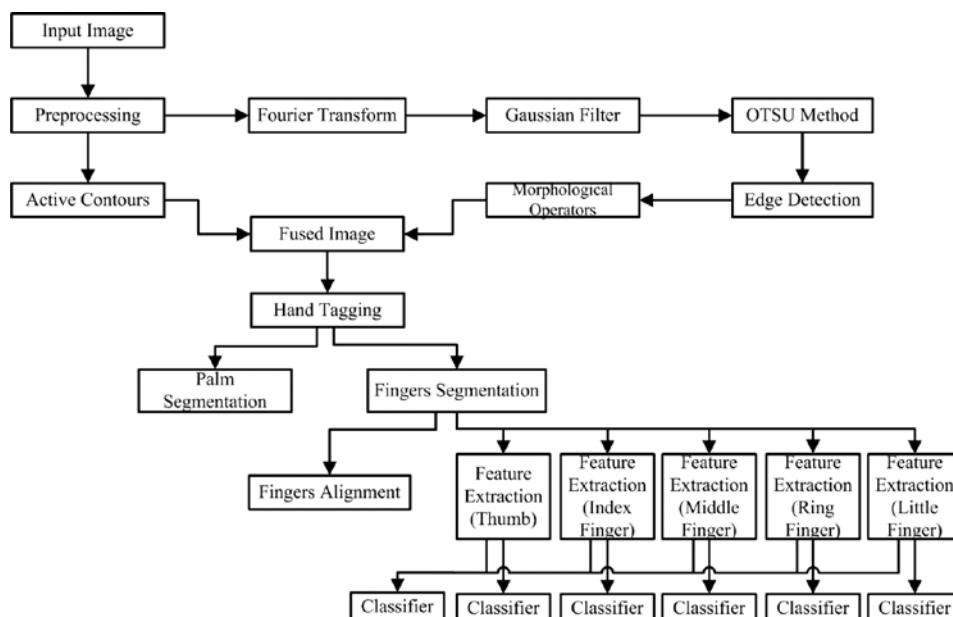


Fig. 3. Proposed algorithm for palm-print and fingerprint segmentation.

given in Table 1.

**Table 1.** Otsu algorithm for thresholding.

Otsu's Algorithm Pseudo code	
1.	Compute the histogram and the pixel counts for each level of intensity.
2.	Initialize $\omega_i$ and $\mu_i$
3.	Go through all possible thresholds $T=[0,255]$ .
4.	Update $\omega_i$ and $\mu_i$
5.	Compute $\sigma_i^2(T) = \omega_1(T) \cdot \omega_2(T) \cdot [\mu_1(T) - \mu_2(T)]^2$
6.	Required value of threshold is the maximum value of $\sigma_i^2(T)$ .

$\omega_i(T)$ = Number of pixels in class i
$\mu_i(T)$ = Mean pixel intensity in class i
$\sigma_i^2(T)$ = Inter class variance

After making the choice of the threshold value, sobel edge detection operator is convolved with filtered image (that contains the certain band of frequencies) to obtain the hand response in horizontal, vertical and diagonal directions, shown in Eq. (4). The edges obtained from it generally correspond to the wrinkles and shape of the hand. To eliminate the little bogus borders from the background of the hand silhouette, the edged image needs smoothing.

$$G_{hor} = \begin{bmatrix} -1 & -2 & -1 \\ 0 & 0 & 0 \\ 1 & 2 & 1 \end{bmatrix}, \quad G_{vert} = \begin{bmatrix} -1 & 0 & 1 \\ -2 & 0 & 2 \\ -1 & 0 & 1 \end{bmatrix},$$

$$G_{dia\_pos} = \begin{bmatrix} 0 & 1 & 2 \\ -1 & 0 & 1 \\ -2 & -1 & 0 \end{bmatrix}, \quad G_{dia\_neg} = \begin{bmatrix} -2 & -1 & 0 \\ -1 & 0 & 1 \\ 0 & 1 & 2 \end{bmatrix} \quad (4)$$

where  $G_{dia\_pos}$  and  $G_{dia\_neg}$  are at -45 and +45 respectively. To remove the unwanted edges and the borders from the image, morphological operations like erosion, dilation, opening and thinning with structuring element given in Fig. 4 are applied to provide the best solution. They remove the spurious

objects as well as fill the gaps present in the image.

1	1	1
1	X	1
1	1	1

**Fig. 4.** Structuring element used for morphological operations.

### 4.2 Geometric Based Approach

Although threshold value selected from Otsu's method is giving satisfactory results but for some images, it is unable to find all parts of hand. Figure 5 shows the resultant image after applying the threshold and the morphological operators, some fingers are not segmented correctly due to the similarity of their pixel values with the background. Hence, use of Snakes as an active contour model has been introduced to extract the silhouette of hand. Therefore, remaining parts of the hand can be filled accurately. This method encompasses two stages, namely, Snake based Background Removal (SBR) and Snake based Hand Localization (SHL). SBR is employed to remove the background from the image whereas SHL is used for the localization of hand silhouette.

Generally, the basic goal of most active-contour algorithms is the extraction of a homogeneous region in an image, whilst the goal of most anisotropic-diffusion algorithms is the smoothing of the values within the homogeneous region, not across the boundaries. The most widely used mathematical models addressing both goals



**Fig. 5.** Incorrect segmentation results.

is of Mumford and Shah [34-35], they proposed a variation problem of minimizing a function that includes a piece-wise smooth model of an image. The proposed function incorporated a geometric term, penalizing the Hausdorff measure of a set in which certain discontinuities would be acceptable.

The basic concept behind the evolution of active contours is to reduce the difficulty encountered during the adjustment of a contour while using the explicit representations, for example chain codes. Since, these explicit representations don't provide the susceptible computational manipulations results, therefore active contours (in two dimensional space) has been defined in the form of rectangular mask, to get the required contour, in this case its hand. This approach helps in the segmentation of those images having homogeneous but statistically different foreground and backgrounds. The active contour  $C_i$  is defined by Eq. (5).

$$C_i = \{(r, c) \in \mathbb{R}^2 \mid \Phi(r, c) = 0\} \quad (5)$$

where,  $\Phi$  defines a scalar field when the level set of active contours is zero. After initializing the contour,  $C_i$  ceases to modify itself. In this way, the difficulty of adjusting  $C_i$  to the data input (here, it is the hand image) stops to modify  $\Phi$ , so there is a need to define the Signed Distance Function (SDF) for  $\Phi$  which assigns negative sign to  $\Phi$  when the mask is in the inner side of the contour as shown in Eq. (6):

$$\phi(r, c) = (-1)^{I(r, c) \in \text{int}(C_i)} \min_{(r', c')} \|(r, c) - (r', c')\| \quad (6)$$

where  $\text{int}(C_i)$  shows the interior of the contour and  $\|$  is the sign function. Hence, it becomes as Eq. (7)

$$\phi(r, c) < 0 \leftrightarrow (r, c) \in \text{int}(C_i) \quad (7)$$

Active contours, without edges have been implemented in this paper, proposed in [36]. It is constructed by using the curve evolution techniques, segmentation function of Mumford and Shah [34-35] technique and the level sets. It has ability to detect those objects which doesn't contain the strong gradient at the boundaries. It has the advantage that the problem of minimal partition in the formulation of level set becomes

the mean curvature flow problem. Thus, stops the evolution of contour at the desired edge. Another advantage of this approach is that the initialization of initial curve doesn't affect the efficiency and it automatically detects the interior contour.

Active contours integrates the information of local-adaptive neighborhood image with the help of adapted spatial morphological opening and closing operations utilizing general neighborhood structuring elements. Incorporation of the general adaptation in local-neighborhood information resulted in the robustness of active contours model to the non-uniformity. It also helps in the solution of the minimized energy function through morphological approximations, thus increasing the stability and the contour evolution speed. Consequently, a general spatially adapted information combining morphological active contours without edges are generalized, i.e., prone to non-uniformity and noise and there is no need of re-initialization. The resultant images after the application of active contours are shown in Fig. 6.

### 4.3 Fusion Process

Similar to the texture based approach, geometric based approach is susceptible to some errors, like the fingers are not completely segmented from the hand and also the finger tips are not segmented correctly. Therefore, there is a need to fuse the results obtained from the region based and the geometrical features. The fusion is done by using the logical OR operator using Eq. (8).

$$I_{fusion} = I_{texture} \parallel I_{geometrical} \quad (8)$$

It helps in combining the both results. The resultant fused image is given in Fig. 7. A robust methodology is needed to separate the palm and the fingers from the hand image.

### 4.4 Hand Classification

Hand can be classified as left or right by extracting four points from it. All of the extracted points are the tips of fingers. An algorithm described in section 5.2 can be used for the determination of correct peak points. The proposed system is quite flexible since it allows the user to use both hands. The detected hands can be stored separately in the database which reduces the searching database to

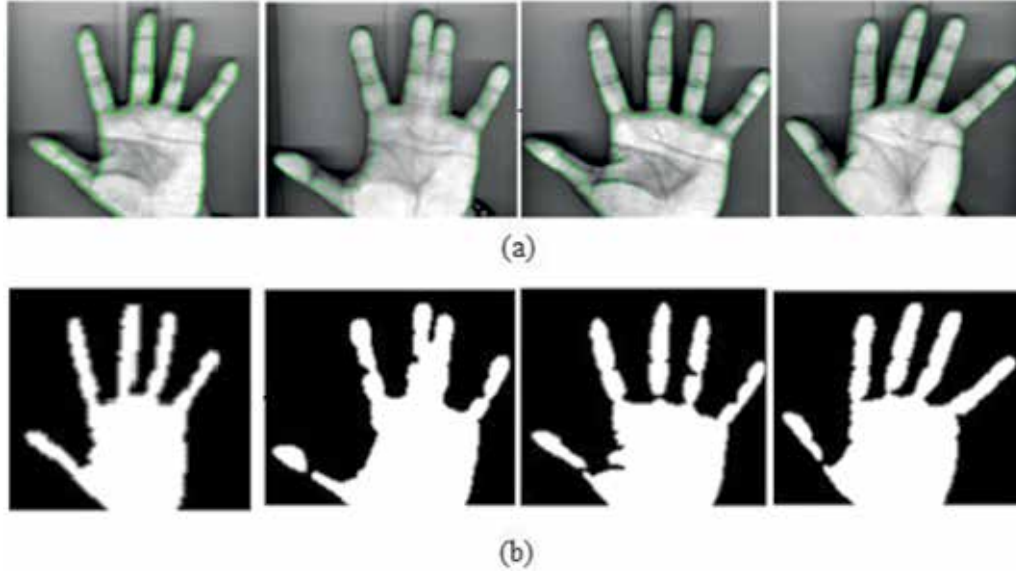


Fig. 6. Segmented images using active contours: (a) Detected boundary images; (b) Resultant segmented images.

half, thus speeds up the recognition process. Fig. 8 shows the fingertips of left and right hand.

Eqs. (9) and (10) are used for the classification of hand.

Left hand determination:

$$\begin{aligned}
 &x_1 > x_2 \text{ AND } x_1 > x_3 \text{ AND } x_1 > x_4 \text{ AND } x_1 > x_5 \\
 &> x_5 \text{ AND } y_1 < y_2 \text{ AND } y_1 < y_3 \text{ AND } y_1 < y_4 \text{ AND } y_1 < y_5
 \end{aligned}
 \tag{9}$$

Right hand determination:

$$\begin{aligned}
 &x_5 > x_1 \text{ AND } x_5 > x_2 \text{ AND } x_5 > x_3 \text{ AND } x_5 > x_4 \\
 &> x_4 \text{ AND } y_5 > y_1 \text{ AND } y_5 > y_2 \text{ AND } y_5 > y_3 \text{ AND } y_5 > y_4
 \end{aligned}
 \tag{10}$$

where,  $x_1$  to  $x_5$  are the horizontal coordinates and  $y_1$

to  $y_5$  are the vertical coordinates of the fingertips.

## 5. PALM & FINGERS SEGMENTATION USING PROPOSED ALGORITHM

### 5.1 Palm Segmentation

Palm is the source of abundant information and the complex part of hand. Mostly researchers have used the algorithm which searches for the maximum inscribed circle in the whole image and then by drawing the rectangle around that circle the palm region is separated [18]. Although this is an effective method for the palm detection, but this approach has a drawback associated with it, that it is much time consuming. Since the circle modifies itself again and again it raises the computational cost of the overall system. Therefore, with the propose

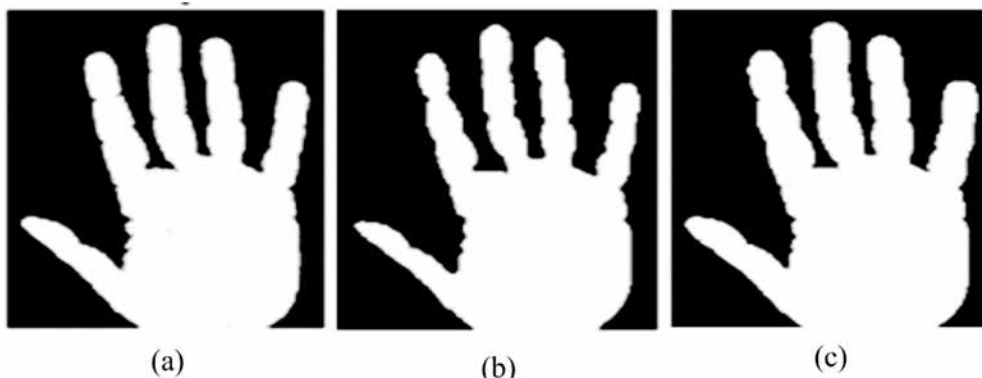
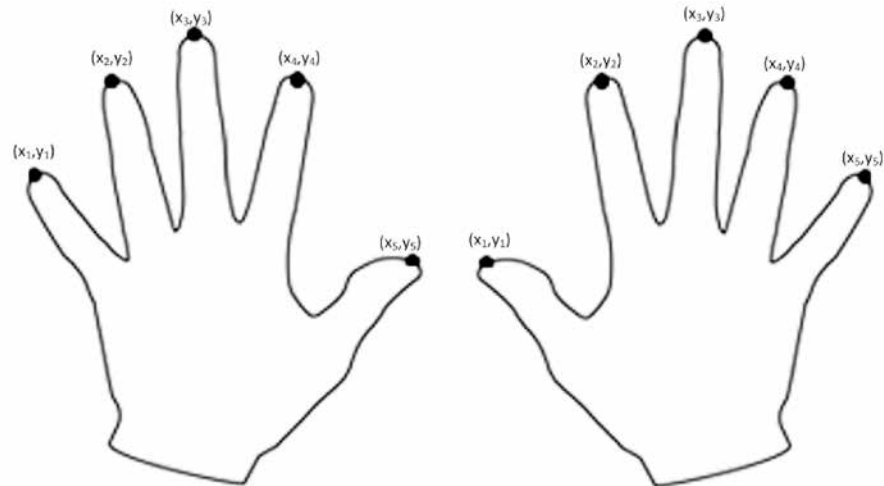


Fig. 7. Fusion process: (a) Resultant image obtained from texture based analysis; (b) Active contours result; (c) Resultant fused image.



**Fig. 8.** Right and left hand fingertips.

method for improving the processing speed of the algorithm, the palm is segmented from the whole hand by detecting the largest finger valley point. The valley points are calculated using Eq. 11.

$$v_k = \operatorname{argmin} ( \| \zeta - h_c \| ) \quad (11)$$

where,  $\zeta = c(f_n, f_{n+1})$  is the portion of edge from finger-tip  $f_k$  and  $f_{k+1}$ , with  $n = \{l, r, m, L\}$  that means little, ring, middle and index finger and  $h_c$  is the contour of hand [37]. The palm extracted from the image along with the bounded box is shown in Fig. 9.

## 5.2 Fingers Segmentation

After separating the palm region from the whole hand, the remaining part of the image comprises of fingers. There is a need to separate these fingers from each other. Thumb can be easily separated from the other four fingers as it is not connected to any of them. Thumb is removed from the image

by assigning it a different label and then separating that particular label from the image. The separation of other four fingers from each other is a tricky job. For that purpose again finger valley points have been searched throughout the image. The valley point is the area where the y coordinate of the image first decreases and then increases in its magnitude. The approach used here for locating the valley points is to find the minimum sum in the vertical direction and then on that particular column a search window of 100 pixels is employed. It searches for the exact valley point by starting from the x-100 coordinate to x+100. If the searched area has the property that the y coordinate first decreases then increases the inflexion point is chosen as the valley point. The required point can be found easily and accurately because the segmented image with sharp edges has been improved by the morphological operators. Finally, on the basis of these valley points the fingers are separated from each other. The image after the removal of palm is given in Fig. 10 (a) and

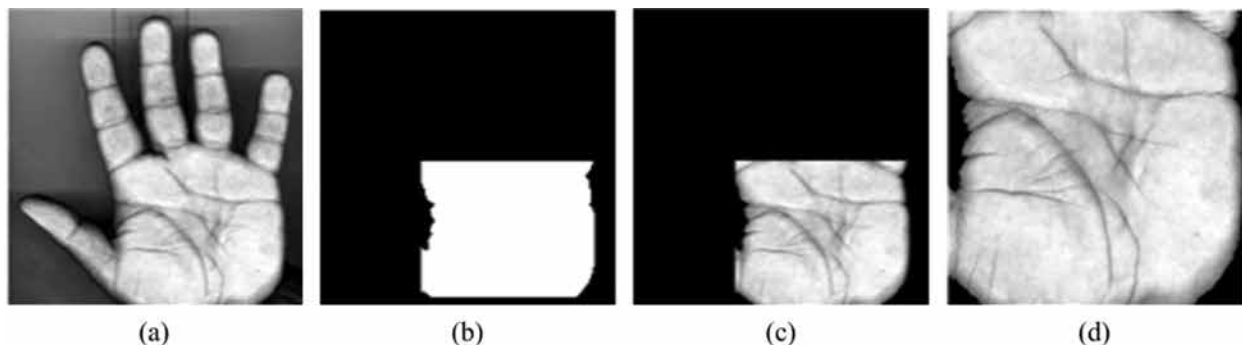


**Fig. 9.** Palm segmentation: (a) Pre-processed image; (b) Extracted palm; (c) Segmented palm from pre-processed image; (d) Bounded box of palm.

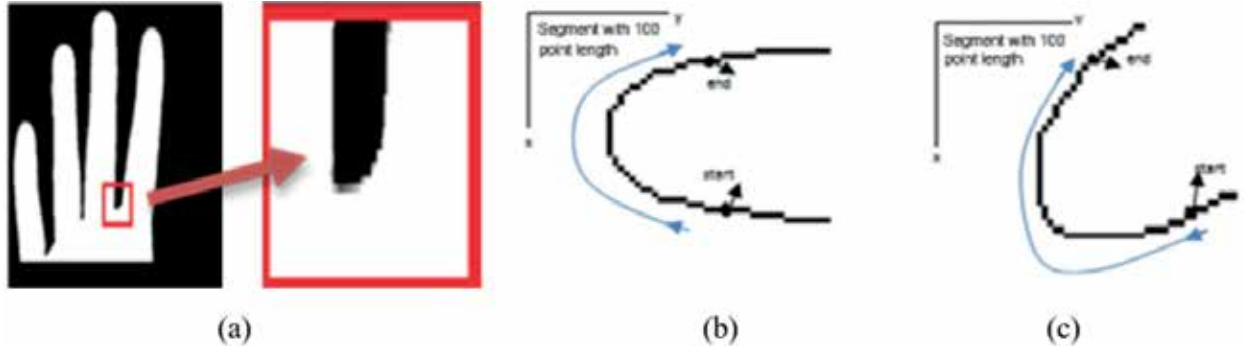


**Fig. 10.** Fingers and Valley point Detection Scheme: (a) Fingers and valley point; (b) and (c) Valley-point detection scheme for different postures of hand.

the search process examples are displayed in the Fig. 10 (b) and (c). Figure 11 shows the segmented fingers using proposed method.

Afterwards, there is a need to tag these fingers i.e. thumb, middle, ring, index and little finger. To do this, geometrical features of fingers must be calculated. These features can be length, width, and variance of width, orientation, variance of orientation and the angular distance amongst the fingers. The better the features, the better will be the classification.

### 5.3 Feature Extraction

Feature extraction involves the process of extracting the features detail from the image. The geometrical features of hand include finger length, area, curvature, thickness, and width. The Histograms of oriented Gradient (HoG) is an alternative method to encrypt the image to find visual descriptor's vector. The examples are Lowe's SIFT [38], Dalal and Triggs' HoG [39], Berg's geometric blur and shape context [40], and Riesenhuber and Poggio's

C1 [41]. Histogram of Gradients feature (HoG) parameters are much more appropriate than the SIFT feature, for generic object identification. HoG consists of the Scale Invariant Feature Transform (SIFT). It uses the orientations and the magnitude of gradients around the critical locations to compute the histogram of these points. It is defined as a weighted histogram in which each bin of histogram assembles the sum from the gradient points of the particular location having the particular orientation. The image gradient is computed using 1D discrete derivative kernel in both the vertical and the horizontal directions, the kernels are given in Eq. 12. [39].

$$[-1 \ 0 \ 1] \text{ and } [-1 \ 0 \ 1]^T \tag{12}$$

The magnitude and the corresponding orientation of each pixel is given in Eq. 13 and Eq. 14.

$$g_{mag}(x, y) = \sqrt{g_x^2(x, y) + g_y^2(x, y)} \tag{13}$$

$$\theta(x, y) = \tan^{-1} \left( \frac{g_y(x, y)}{g_x(x, y)} \right) + \frac{\pi}{2} \tag{14}$$

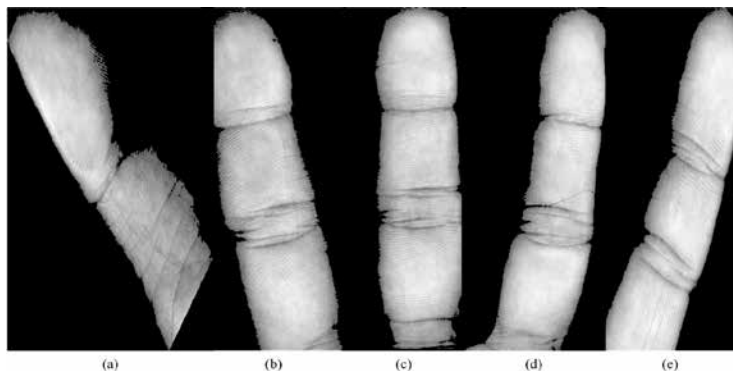


**Fig. 11.** Segmented fingers: (a) Thumb; (b) Index finger; (c) Middle finger; (d) Ring finger; (e) Little finger.

where  $g_y(x, y)$  and  $g_x(x, y)$  are gradient values in the vertical and the horizontal direction, respectively. The total numeral of bins present in the histogram of image are used for the quantization of orientations (nine orientations in this case).

The cells are grouped into blocks to normalize the strength against various contrast and illumination. These blocks overlap with one another, thus each bin is contributing its orientation more than once. In every block of histogram, the sum of all magnitudes in a particular direction is computed. To normalize these histograms, histogram is divided by the total sum of all orientations using Eq. 15, so that a normalized value between 0 and 1 can be obtained.

$$f_i = \frac{v_i}{\sqrt{\|V_i\|^2}} \quad (15)$$

$F = \{f_1, f_2, \dots, f_n\}$  is the resultant HoG feature vector. The feature set of HoG comprises of the histograms constructed inside a rectangular section on the given input image. The toolbox used for the implementation of HOG is VLFEATROOT [42]. Fig. 12 shows the results of HoG.

#### 5.4 Orientation

The orientation of each finger of the hand is different from each other. To align all the fingers in a particular direction, further processing can be carried out from them. Since the device used for the image acquisition does not use any peripheral devices therefore, the fingers can have any orientation in any direction.

In literature, many approaches have been presented for the alignment of the orientation of hand and fingers. In this case, the image can only be

acquired in a particular direction, there is no need to take into account the orientation of hand. Kumar et al. [43] used an inertial matrix to find the large Eigen value corresponding to the ellipse's main axis that fits into the region of hand. Another technique uses the hand silhouette of the binary image for the application of chain codes. Both the hand valleys and the finger tips are extracted and on the basis of the middle finger's key point a rotation process is performed. It gives the maximum angular variation of only 20%. Therefore, it is not a good method to be used in the unpaired system.

The method used for the alignment of fingers in literature is 'Image registration' in which the central finger or any pre-defined finger from the database is used as a base and all the other fingers are aligned according to that finger. In this case, since the size of the image is quite large and the image registration process cannot be carried out as it increases the computation cost of the system. For this purpose, first the orientation of each finger is found by the orientation finding method of image cropping, then on the basis of values of orientation, a search process is used that aligns the fingers in the erect direction. The orientation of each finger is found with respect to the x-axis. The resultant and the original orientation of fingers are given in Fig. 13. The contour of each finger is rotated by using Eq. 16.

$$\begin{bmatrix} x' \\ y' \end{bmatrix} = \begin{bmatrix} \cos\theta & -\sin\theta \\ \sin\theta & \cos\theta \end{bmatrix} \begin{bmatrix} x \\ y \end{bmatrix} \quad (16)$$

Where,  $x$  and  $y$  are the central co-ordinates of the contour of finger. The orientation alignment is used i) to extract the finger tips easily ii) to obtain the fingerprints region.

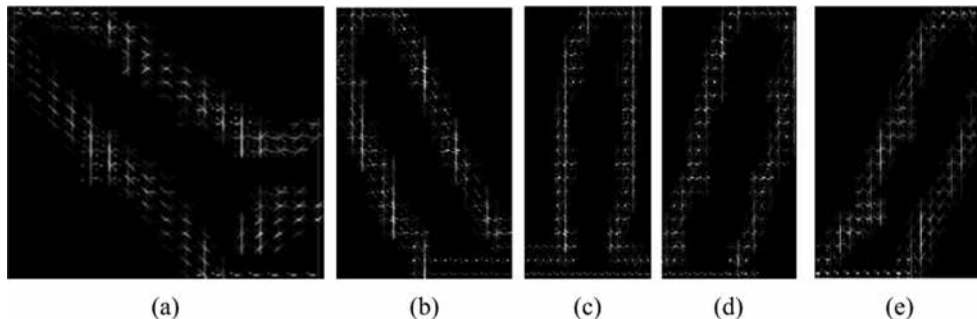


**Fig. 12.** HOG on binary images: (a) Thumb; (b) Index finger; (c) Middle finger; (d) Ring finger; (e) Little finger.

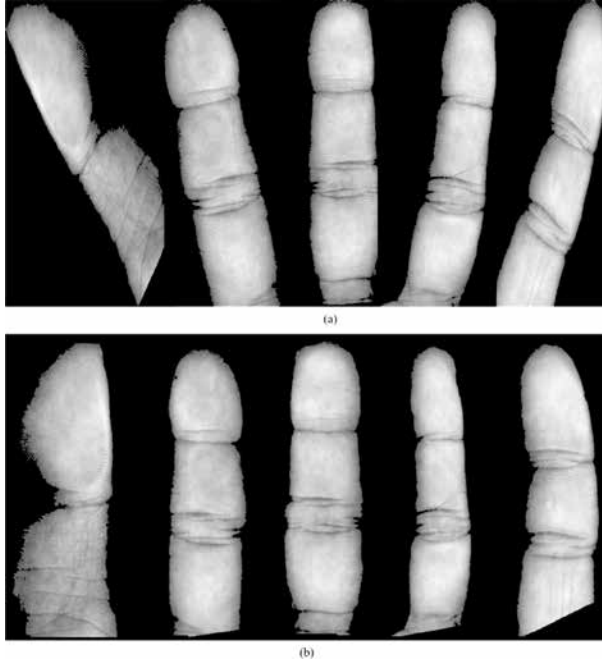


**Fig. 13.** Fingers alignment: (a) Original orientation; (b) After alignment using HoG.

## 6. RESULTS AND DISCUSSIONS

### 6.1 Error Rate Analysis

In this paper, we used k-NN classifier for the decision making that whether the finger is classified correctly or not. The features are distributed using the k-NN classifier, which operates on a non-parametric method for the classification and regression. It employs the minimum Euclidean distance among the test feature vectors and all other sample training data. In the regression stage of k-NN classifier, the output value is taken by averaging the values of its  $k$ -nearest neighbors.

On the basis of this classification, False Acceptance and False Rejection error rates are computed. The error probabilities are denoted as: P (FAR) and P (FRR).

The total probability of FAR is the given in Eq. 17.

$$P (FAR) = \prod_{i=1}^n P(FAR) \quad (17)$$

where, P (FAR) is the probability of a False Accept Rate. Similarly, for the False Reject Rate (FRR) is given in Eq. 18.

$$P (FRR) = 1 - \prod_{i=1}^n (1 - P(FRR)) \quad (18)$$

where, P (FRR) is the probability of a False Reject rate.

### 6.2 Experimental Results

To validate the results of this research, database of 100 persons was collected. The database consists of 400 hand images, four images per person, obtained from the high resolution HP scanner at the resolution of 1200 ppi, using peg free arrangement. The hand images were collected from the persons of age between 16 to 55 years. The image acquisition process was carried out while making sure that 1) The fingers are far apart from each other and 2) the upper lid of the scanner is closed. The automatic segmentation of palm and fingers was achieved through proposed algorithm discussed in Section 4.

Palm is separated from the image, only fingers are used for the classification purpose. The reason behind its usage is to tag the fingers. The size of the fingers, in the image, is reduced to  $600 \times 500$  pixels. Thus, HoG can be applied effectively and efficiently. The size of the feature vector obtained is  $10,540 \times 1$ . The subjects were trained on the basis of these feature vectors and the classification was done using 2 out of 4 images as a database images whereas the other 2 images are used for the classification to increase the identification rate. It allows the fair combination by using the same training and test data. All the reported experimental results are carried out using Matlab. The system used is Intel Atom, Dual Core CPU, 1 GB RAM, 500 GB HD and Windows 7(32 bit) operating system.

Figure 14 displays the identification rate with respect to the various numbers of fingers extracted from the images present in the database, the range of images varies from 1 to 400. The inspection of the identification rate curve shows that results better than 96.9% can be achieved by increasing the database size. Figure 14 helps in determination of the accuracy with which each finger is classified by k-NN classifier.

The accuracy of detection of each finger is shown by a bar graph given in Fig. 15, whereas, ROC of all fingers and of each finger separately is plotted in Fig. 16 and Fig. 17, respectively.

Table 2 shows the performance of the proposed

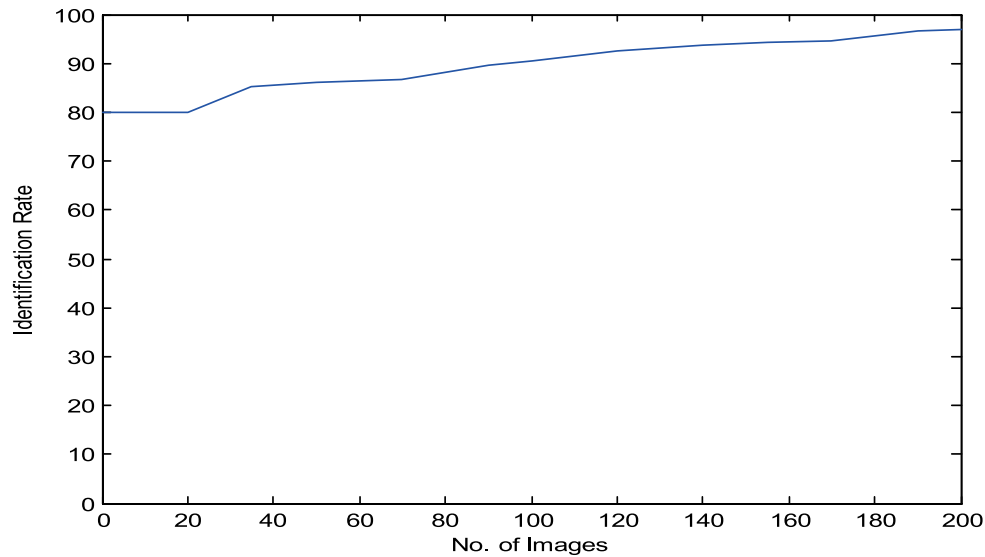


**Fig. 14.** Identification rate

method. It validates that the proposed solution can perform well in the given scenario. Hence, it can control the access privileges on a large scale. The previous results show that the image quality effects the identification rate. Since the device used here provides the high resolution images thus there is no flaw in the system due to image quality.

The Equal Error Rate (EER) of each finger is

**Table 2.** Performance properties.

Performance Properties	
Total images	400
Identification Rate	96.9%
FAR	0.0309
FRR	0.0312
EER	0.0311

separately given in Table 3, whereas the comparison with other existing techniques is given in Table 4.

## 7. CONCLUSIONS

A bi-modal biometrics system, based on the features of hand, has been proposed. The proposed scheme combines the efficacy of hand geometry and the palm prints with the high precision of fingers geometry. The results of the geometric and texture based approach are combined at the fusion stage to segment out the hand image. Since the segmentation process includes the separation of palm and fingers from the hand image, hence their features are not related to each other. For further study these feature vectors has been implemented independently to increase the system performance. The features extracted from the fingers can be

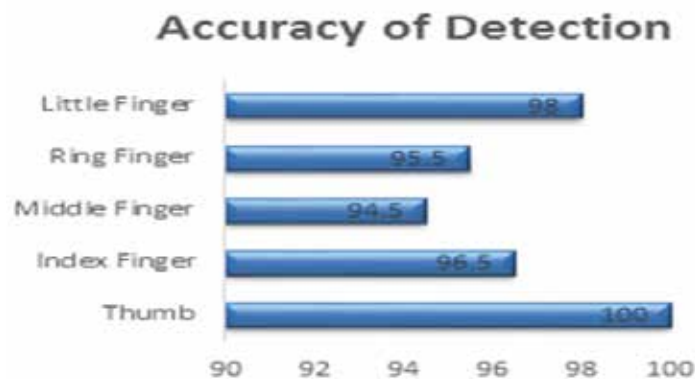


**Fig. 15.** Graph representing the accuracy of detection of each finger.

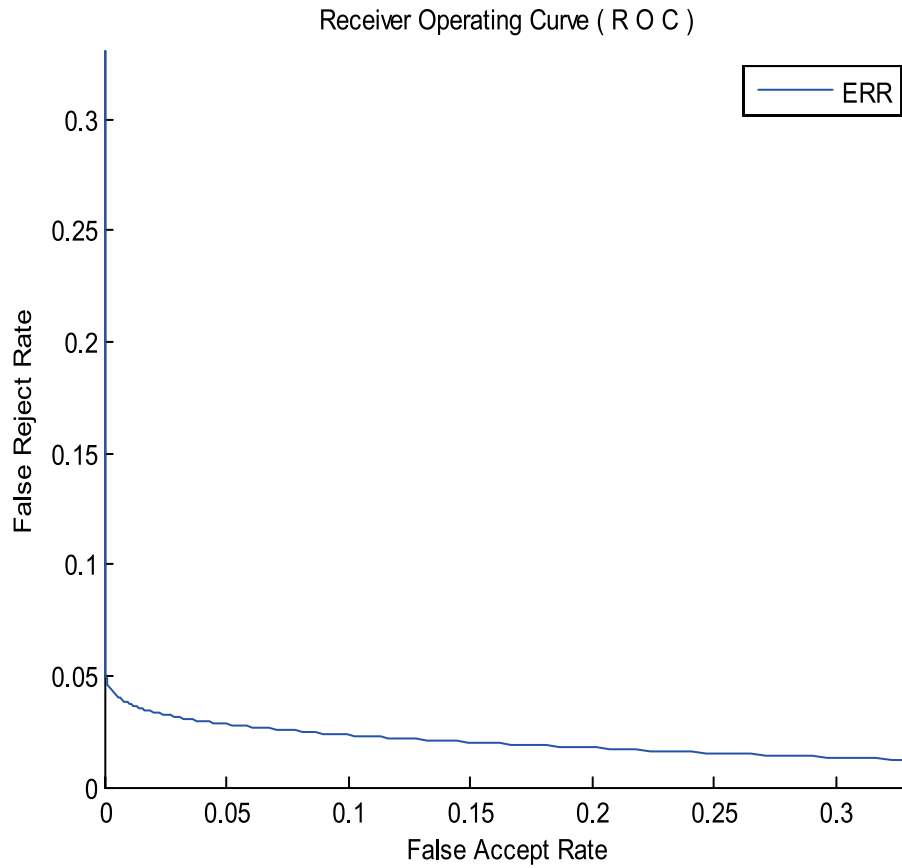


Fig. 16. Receiver operating characteristics.

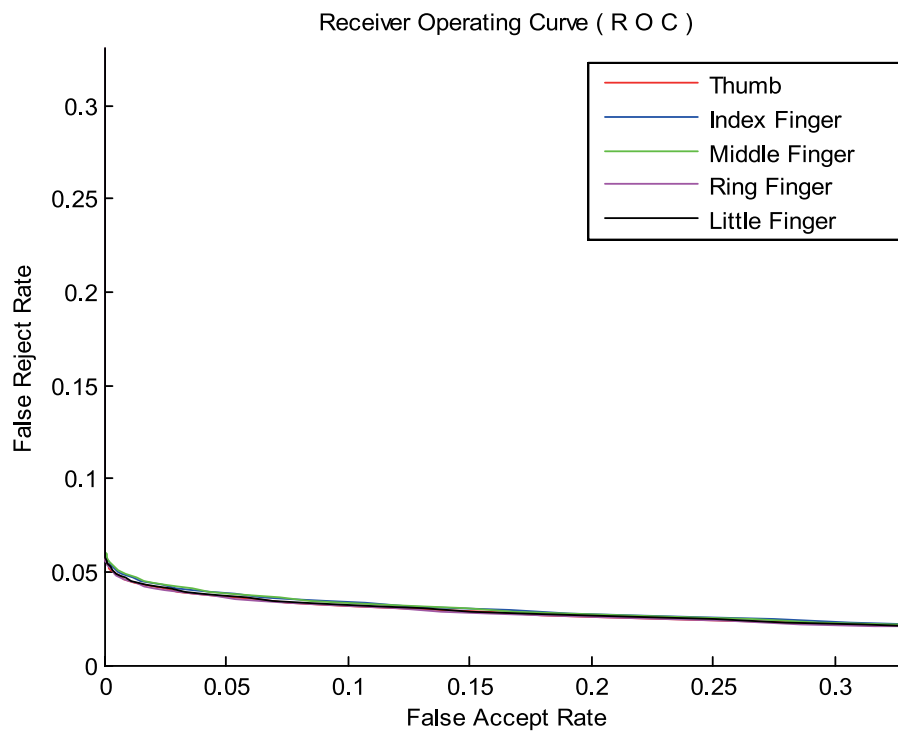


Fig. 17. Receiver operating characteristics for each finger.

**Table 3.** Finger wise EER computation.

Fingers	Thumb	Index Finger	Middle Finger	Ring Finger	Little Finger
EER	0.0375	0.0383	0.0415	0.0376	0.0392

**Table 4.** Comparison of proposed algorithm with existing methods available in literature.

Algorithms	# of people	Samples per person	Approach	Features	Performance	Recognition rate
Sanchez-Reillo et al. [44]	200	20	Various distances, GMMs, RBF	Hand/finger measurements	FAR=0.066 FRR =0.09	—
Woodard et al. [45]	42	2	Normalized correlation coefficient	Singe and Fused Fingers, linear regression technique	EER = 0.055	94
Fouquier [46]	750	6	Symmetric Kullback	Finger geometry measurement	EER = 0.0421	—
Proposed	100	4	HoG & k-NN	Geometrical features	FAR = 0.0309 FRR= 0.0312 EER = 0.0311	96.9

easily used for the tagging of fingers by using k-NN classifier, which classifies and identifies the fingers accurately. The experimental results show that these segmented images can be used effectively and efficiently for the development of the other stages of the fully automatic hand-based security system. Future work includes: 1) To carry out an advance research to increase the accuracy of the system; 2) Modification of pre-processing step so the significant characteristics of the image can be extracted; and 3) Investigation of methods that may reduce the computational cost of the system.

## 8. REFERENCES

- Jain, A.K., A. Ross & S. Prabhakar. An introduction to biometric recognition. *IEEE Transactions on Circuits and Systems for Video Technology* 14(1): 4-20 (2004).
- Hand-based biometrics. *Biometric Technology Today* 11(7): 9-11 (2003).
- Duta, N. A survey of biometric technology based on hand shape. *Pattern Recognition* 42(11): 2797-2806 (2009).
- Yörük, E., H. Dutagaci & B. Sankur. Hand biometrics. *Image and Vision Computing* 24(5): 483-497 (2006).
- Zhang, D., W.-K. Kong, J. You & M. Wong. Online palmprint identification. *IEEE Transactions on Pattern Analysis and Machine Intelligence* 25(9): 1041-1050 (2003).
- Wang, J.-G., W.-Y. Yau, A. Suwandy & E. Sung. Person recognition by fusing palmprint and palm vein images based on Laplacian palm representation. *Pattern Recognition* 41(5): 1514-1527 (2008).
- Sidlauskas, D.P. HAND: give me five. *IEEE Spectrum* 32(2): 24-25 (1994).
- Peng-di, H., S. Jun-sheng & X. Guang-hui. An associated extraction method of palmprint principal lines. In: *7<sup>th</sup> IEEE International Conference on Image and Graphics (ICIG) Shandong, P.R. China, 26-28 July 2013*, p. 448-452 (2013).
- Jain, A.K., A. Ross & S. Pankanti. A prototype hand geometry-based verification system. In: *Proceedings of 2<sup>nd</sup> Conference on Audio and Video based Personal Authentication (AVBPA), Washington, USA, 22-24 March 1999*, p. 166-171 (1999).
- Oden, C., A. Ercil & B. Buke. Combining implicit polynomials and geometric features for hand recognition. *Pattern Recognition Letters* 24(13): 2145-2152 (2003).
- I.I.o.T.D. *Biometrics Research Laboratory*. Iit delhi touchless palmprint database version 1.0. <http://web.iitd.ac.in/ajaykr/DatabasePalm.htm>
- Murat, A. & M. Ekinci. AAM-based palm segmentation in unrestricted backgrounds and various postures for palmprint recognition. *Pattern Recognition Letters* 34(9): 955-962 (2013).
- L. A. P. Neves, D. J. Müller, F. Alexandre, P. M. G. Trevisani, P. S. Brandi & R. Junqueira. Hand recognition using texture histograms a proposed technique for image acquisition and recognition of the human palm. In: *9<sup>th</sup> IEEE International Conference on Computer Vision Theory and Applications (VISAPP), Lisbon, Portugal, 5-8 January 2014*, 3: p. 180-185 (2014).

14. Afsal S., A.K. Rafeeq, J. Jijo, S. Ahmed & F. Sayeed. A novel approach for palm print recognition using entropy information features. In: *IEEE International Conference on Wireless Communications, Signal Processing and Networking (WiSPNET)*, Chennai, India, 23-25 March 2016, p. 1439-1442 (2016).
15. Hong, L. & A. Jain. Integrating faces and fingerprints for personal identification. *IEEE Transactions on Pattern Analysis and Machine Intelligence* 20(12): 1295-1307 (1998).
16. Toh, K.A. & W.-Y. Yau. Combination of hyperbolic functions for multimodal biometrics data fusion. *IEEE Transactions on Systems, Man, and Cybernetics, Part B (Cybernetics)* 34(2): 1196-1209 (2004).
17. Wang, Y., T. Tan & A.K. Jain. Combining face and iris biometrics for identity verification. In: *4<sup>th</sup> International Conference on Audio and Video Based Biometric Person Authentication (AVBPA)*, Guildford, UK, 9-11 June 2003, p. 805-813 (2003).
18. Zhu, L.Q. & S.Y. Zhang. Multimodal biometric identification system based on finger geometry, knuckle print and palm print. *Pattern Recognition Letters* 31(12): 1641-1649 (2010).
19. Amayeh, G., G. Bebis, A. Erol & M. Nicolescu. A Component-Based Approach to Hand Verification. In: *IEEE International Conference on Computer Vision and Pattern Recognition (CVPR)*, Minnesota, USA, 17-22 June 2007, p. 1-8 (2007).
20. Guo, J.M., C.H. Hsia, Y.F. Liu, J.C. Yu, M.H. Chu & T.N. Le. Contact-free hand geometry-based identification system. *Expert Systems with Applications* 39(14): 11728-11736 (2012).
21. Gholamreza, A., G. Bebis, A. Erol & M. Nicolescu. Hand-based verification and identification using palm-finger segmentation and fusion. *Computer Vision and Image Understanding* 113(4): 477-501 (2009).
22. Wu, X., D. Zhang & K. Wang. Palm line extraction and matching for personal authentication. *IEEE Transactions on Systems, Man, Cybernetics, Part A: Systems and Humans* 36(5): 978-987 (2006).
23. Singh, A.K., A.K. Agrawal & C.B. Pal. Hand Geometry Verification System: A Review. In: *IEEE International Conference on Ultra Modern Telecommunications & Workshops(ICUMT)*, Saint Petersburg, Russia, 12-14 October 2009, p. 1-7 (2009).
24. Rahman, A., F. Anwar & S. Azad. A simple and effective technique for human verification with Hand Geometry. In: *IEEE International Conference on Computer and Communication Engineering, (ICCCE)*, Kuala Lumpur, Malaysia, 13-15 May 2008, p. 1177-1180 (2008).
25. Han, Y., Z. Sun, F. Wang & T. Tan. Palmprint recognition under unconstrained scenes. In: *Proceedings of 8<sup>th</sup> Asian conference on Computer vision (ACCV)*, Tokyo, Japan, 18-22 November 2007, p. 1-11 (2007).
26. Wang, Z. Hardware implementation for a hand recognition system on FPGA. In: *IEEE International Conference on Electronics Information and Emergency Communication (ICEIEC)*, Beijing, China, 14-16 May 2015, p. 34-38 (2015).
27. Saranraj, S., V. Padmapriya, S. Sudharsan, D. Piruthiha & N. Venkateswaran. Palm print biometric recognition based on Scattering Wavelet Transform. In: *IEEE International Conference on Wireless Communications, Signal Processing and Networking (WiSPNET)*, Chennai, India, 23-25 March 2016, p. 490-495 (2016).
28. Morales, A., M.A. Ferrer, F. Díaz, J.B. Alonso & C.M. Travieso. Contact-free hand biometric system for real environments. In: *16<sup>th</sup> IEEE European Signal Processing Conference (EUSIPCO)*, Lausanne, Switzerland, 25-29 August 2008, p. 1-5 (2008).
29. Kumar, A. & D. Zhang. Personal recognition using hand shape and texture. *IEEE Transactions on Image Processing* 15(8): 2454-2461 (2006).
30. Amayeh, G., G. Bebis, A. Erol & M. Nicolescu. Peg-free hand shape verification using high order zernike moments. In: *IEEE Conference on Computer Vision and Pattern Recognition Workshop (CVPRW)*, New York, USA, 17-22 June 2006, p. 40-40 (2006).
31. Sato, T., S. Aoyama, S. Sakai, S. Yusa, K. Ito & T. Aoki. A contactless palm recognition system using simple active 3D measurement with diffraction grating laser. In: *IEEE Asian Conference on Pattern Recognition (ACPR)*, Okinawa, Japan, 5-8 November 2013, p. 542-546 (2013).
32. Aishwarya, D., M. Gowri & R.K. Saranya. Palm print recognition using liveness detection technique. In: *IEEE International Conference on Science Technology Engineering and Management (ICONSTEM)*, Chennai, India, 30-31 March 2016, p. 109-114 (2016).
33. Otsu, N. A threshold selection method from gray-level histograms. *IEEE Transactions on Systems, Man, and Cybernetics* 9(1): 62-66 (1979).
34. Mumford, D. & J. Shah. Optimal approximations by piecewise smooth functions and associated variational problems. *Communications on Pure and Applied Mathematics* 42(5): 577-685 (1989).
35. Mumford, D. & J. Shah. Boundary detection by minimizing functionals. In: *IEEE Conference on Computer Vision and Pattern Recognition (CVPR) San Francisco, CA, 19-23 June 1985*, p. 22-26 (1985).
36. Chan, T.F. & L.A. Vese. Active contours without edges. *IEEE Transactions on Image Processing* 10(2): 266-277 (2001).
37. Santos, A., C. Avila, J. Casanova & G. Pozo.

- Invariant Hand Biometrics Feature Extraction. In: *6<sup>th</sup> Chinese Conference on Biometric Recognition (CCBR)*, Beijing, China, 3-4 December 2011, p. 108-115 (2011).
38. Lowe, D.G. Distinctive image features from scale-invariant keypoints. *International Journal of Computer Vision* 60(2): 91-110 (2004).
39. Dalal, N. & B. Triggs. Histograms of oriented gradients for human detection. In: *IEEE Computer Society Conference on Computer Vision and Pattern Recognition (CVPR)*, San Diego, CA, 20-25 June 2005, p. 886-893 (2005).
40. Berg A.C., T.L Berg & J. Malik. Shape matching and object recognition using low distortion correspondences. In: *IEEE Computer Society Conference on Computer Vision and Pattern Recognition, (CVPR)*, San Diego, CA, 20-25 June 2005, p. 26-33 (2005).
41. Maximilian R. & T. Poggio. Hierarchical models of object recognition in cortex. *Nature Neuroscience* 2(11): 1019-1025 (1999).
42. Vision lab features library. *Histogram of Oriented Gradients: An overview*. <http://www.vlfeat.org/overview/hog.html>
43. Kumar, A., D.C.M. Wong, H.C. Shen & A.K. Jain. Personal verification using palmprint and hand geometry biometric. In: *Proceedings of 4<sup>th</sup> International Conference on Audio and Video Based Biometric Person Authentication (AVBPA)*, Guildford, UK, 9-11 June 2003, p. 668-678 (2003).
44. Sanchez-Reillo, R., C. Sanchez-Avila & A. Gonzalez-Marcos. Biometric identification through hand geometry measurements. *IEEE Transactions on Pattern Analysis and Machine Intelligence* 22(10): 1168-1171 (2000).
45. Damon, L.W. & J.F Patrick. Finger surface as a biometric identifier. *Computer Vision and Image Understanding* 100(3): 357-384 (2005).
46. Fouquier, G., L. Likforman, J. Darbon & B. Sankur. The biosecure geometry-based system for hand modality. In: *IEEE International Conference on Acoustics, Speech and Signal Processing (ICASSP)*, Hawaii, USA, 15-20 April 2007, p. 1-801-804 (2007).



# An Empirical Study and a Framework for Effective Risk Management in Scrum

Muneeb Ali\*, Yasir Hafeez, and Bushra Hamid

University Institute of Information Technology,  
PMAS-Arid Agriculture University, Rawalpindi, Pakistan

**Abstract:** Now a day, agile methods are broadly used for software development. The agile methods are expected to provide virtuous outcomes and producing better quality software products that achieves the customer requirements. In view of the contemporary scenario, it is clear that secure and better quality software products are foremost apprehension. This research study deals with risk management within the scrum framework. The purpose of this research was to propose and validated a framework developed that produces quality product. The continuous approach of scrum overlooks the risk issues which can result in changes and cost expansion. To mitigate this risk, a free scrum model is proposed. This model is produced by combining the activities of risk management and in scrum methodology. A case study has been employed to evaluate proposed framework for mitigating risks effectively in scrum process. We used a qualitative approach with structured interviews, to validate the proposed work. We have explored both the existing principle theory for risk management and the results of different empirical studies to build the framework. On the said base, we have drawn up vindicated proposals for the framework. Results of case study has shown that the proposed framework is suitable for the developing a quality software product. By employing the risk management activities into scrum methodology, as per proposed framework, there is a promising scrum model to control risk. This also ensures software quality along with benefits of cost reduction, experience gained and customer satisfaction. This framework has implications with the effective risk management in scrum way of development and provide valuable insights for risk management scrum. The case study provides direction for future research and lesson learned. It will also provide assistance to apply effective principles of risk management in scrum to develop high quality software product. Our future research will be directed toward the generalization of this framework. The proposed framework activities will be applied on different agile methodologies and other case studies will be conducted, so the results can be generalized.

**Keywords:** Agile, scrum, software quality, risk management, risk register

## 1. INTRODUCTION

Mainstream organizations are improving the process of software development in order to achieve better quality products. Scrum is considered the best agile methodology for agile application development [1]. The scrum focuses on continuously delivery of the software product. It is an iterative and incremental agile software development model for managing development of software products. Scrum is more concerned with deliver software in short term. This result in compromising the quality of product by ignoring the risk and security issues identification and mitigation.

In traditional software development, the risk management is done by applying different techniques and tools. These tools and techniques restrict the decision making regarding the risks [2]. The main objective of risk management is to determine the potential issues before it occurs, so its avoidance or mitigation can be planned accordingly. The objectives can be achieved by handling the problems as per required across the life of the software development. Risk management is manifold and complex in traditional software development [3].

Agile way of software development may process

software faster but how they cater our quality requirements. It provides the ability to respond quickly to change, frequent deliveries of working software and close customer collaboration. On the other hand, this agility can cause overlooking the potential threats. We know from traditional software development that risk registers is an approach to maintain quality in the software product. The technique is effective with the traditional software development, because the gathered in the beginning of project. In agile, due to close collaboration the requirement changing become a major loop hole for risks.

The recent trend shows that scrum is the most employed agile method of software development. The purpose behind using scrum model is to deliver the required software to the customer by making teams that work in short cycles, iteration by iteration. Scrum is more concerned with the project management and expects that the self-organizing team pulls any needed practices into the process via the mechanism of variation.

In Scrum software development, the security and risk management are not considered essential from the start of development process. Security of product has become an essential part of the end product. It can be concluded that risk management from the first phases of development should be introduced. The process of risk management should continue throughout the development cycle. Scrum

development framework emphasis on providing the maximum benefits with in less the time. Effective risk management can be achieved by employing these activities:

1. Identification of risk, risk analysis and prioritizing the identified risks on severity basis.
2. Planning and Implementation.
3. Monitoring and Review to verify risk are treated and removed.
4. Imminent Analysis of risk.

### 1.1. Research Objectives

Software development projects are exposed to risk like incomplete requirements, non-traceable requirements, time limitations, unrealistic schedule, communication and technology change [4]. These issues of project development can be addressed by applying effective risk management.

It could be argued that the technical issues are of less important than managerial issues in software development projects. The reasons for the failure of projects are usually management foibles rather than technical mistakes [5].

Risk can be identified in scrum but the cause of risk, factors to evaluate risk and practices to handle the risk, cannot be identified [6]. These arises a need to develop a framework for scrum method that incorporates effective risk management process to handle the above mentioned issues.

## 2. LITERATURE REVIEW

Risk is usually considered as possibility of loss. Shapira (March, 1987) presented the view of risk as variation in possible outcomes. Risk is considered for negative outcomes of the project by 80 percent of the manager [1]. The probability of risk occurrence and impact of risk are the factors that enhance the priority for risk handling.

According to Janus et al. [7] there seems to be no traditional Quality Assurance in Agile Software Development, even though Agility promises to deliver high Quality Software. The lack of quality assurance in agile methodology enhances the probability of risk occurrences. Alharbi et al. [8]

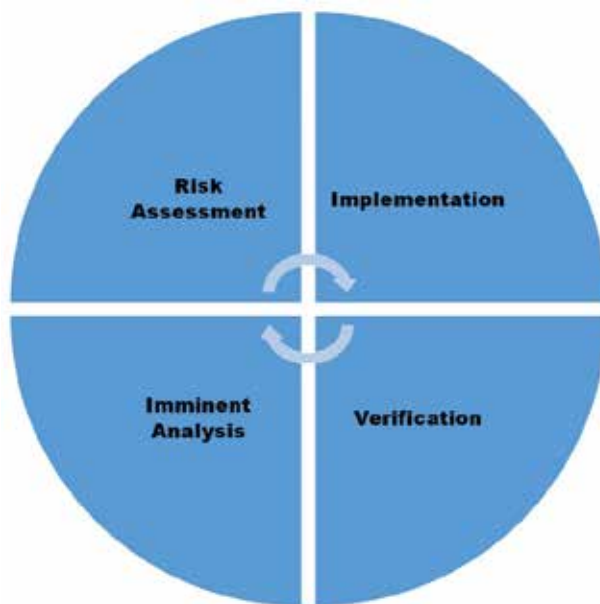


Fig. 1. Effective risk management.

explored that risk register should be used with in scrum in order to improve quality of the product. They claimed that use of risk register doesn't affect the agility of a project. The risk assessments of every sprint will be maintained in the risk register. The register will be used to monitor the occurrence of risk during every sprint.

Panday et al. [9] described a model for the risk management in the software development process. The presented risk management model controls the known and unknown issues or risks during the development process of software. Pohl et al. [10] presented a secure model for scrum. The security issues should be considering during the course of entire process of development. Their model emphasis on incorporating security issues into practice without affecting the principles of scrum method.

Wanderley et al. [11] conducted a study which support the fact that risk management contributes toward the success of the IT project. The study was conducted on publications from 1999 to 2007 and selected 29 publications with empirical data. After analysis of those research studies it was concluded that risk management has impact on the IT projects.

Offshore software development has become very popular because of its cost effectiveness. It benefits by pooling labor from countries having low wages. Islam et. al. [12] has addressed to the threats associated with this trend. There are certain challenges to overcome such as geographical, communicational and cultural differences. The author has proposed tailored risk management framework to overcome these risks. The researcher proposed that risk should be assessed and managed at earlier stages, so its size of loss will be nominal. For the said purpose, goals are linked with the risks in a relational model. For goals KAOS extension has been employed. For validation, case study has been conducted on framework (GSRM). The results showed better management of risk after integration of framework.

According to Ylimannela et al. [13], Agile development is based on short iteration cycles, which allow and respond to changes in business environment. Using agile development is itself risk management at project level. He has created a model

to manage risks in agile development environment. The suggested model has been proposed in order to address the problem arose during the interviews. The suggested model is based on existing models and interviews.

For managing risk in a formal way the team, the product owner or Scrum master can:

1. Use burn down chart for risk [13].
2. Prioritize the outrageous risk requirements first in the upcoming sprint [14].
3. Risk board can be used with two colors of notes [15].
  - i. Red notes: Describes the risks
  - ii. Yellow ones: Describes risk responses
4. Employee a risk registers [16].

### 2.1. Critical Factors

There are different dimensions in which risk can be classified such as organizational, people, process, and technical.

1. Organizational Factor
  - i. Cultural differences
    - a. Too traditional
    - b. Too political
  - ii. Large organizational size
  - iii. Lack of commitment or proper management
  - iv. Lack of logistical support
  - v. Intellectual property rights
2. People
  - i. Lack of expertise
  - ii. Lack of project management competency
  - iii. Lack of team coordination
  - iv. Conflict of individuals / groups
  - v. Depraved customer relationship
3. Process
  - i. Undefined scope
  - ii. Undefined requirements
  - iii. Lack of frozen/ agreed requirements
  - iv. Improper planning
  - v. Lack of progress tracking mechanism
  - vi. Lack of customer involvement
4. Technical
  - i. Lack of ample set of correct scrum practices
  - ii. Inappropriate use of technology and tools

## 3. MATERIALS AND METHODS

Risk management hold worth, if it is not only

identified and communicated in start, but also, a proper sequence of activities should be involved throughout the development cycle. Our finding from the literature review conducted on the base of below mentioned research questions have indicated the need of consolidated conceptual framework.

### 3.1 Research Questions

RQ1: How the Risk management is integrated in scrum methodology?

RQ2: What are the critical factors for effective risk management procedures in scrum methodology?

RQ3: What standards and practices are employed in scrum methodology for risk management?

By addressing these research question, we are able to identify the essential activities of risk management that can amalgamate with scrum methodology. The identified critical factors has enlighten the existing challenges to be addressed. The outcomes of RQ3 are the current industrial practices of risk management in scrum.

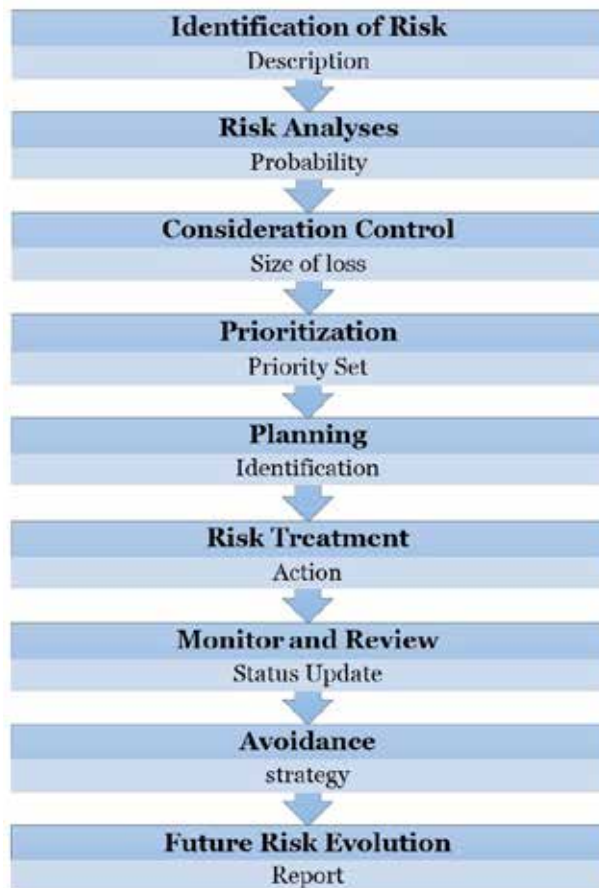


Fig. 2. Risk management activities.

In this research study we have proposed a framework that helps the software engineers to develop a quality product by managing risk. To achieve this, we have determined a complete process of risk management mapped on the scrum. Our proposed model involved of four major activities for risk management.

Given below is a brief description of the said above risk management activities.

### 3.2. Risk Assessment

It is one separate thing to identify and outline list of potential issues, whereas it is an entirely different matter to address them. This is where assessment comes to play its role.

The identification activity in product backlog stage of scrum framework is used to detect the security and risk issues. The identified issues are listed and tagged as well.

The vision of customer is converted into manageable chunks and prioritize in the product backlog. A short description regarding the identified issue is sorted in the register. During the refining of the product backlog these issues (identified during the product backlog) are analyzed for the validation of potential risk. The potential issues are then priorities according to their impact. The issues related to security and risks are marked by the tags.

#### 3.2.1 Identification of Risk

The base step of risk assessment is risk identification. The team of stakeholders review all items of backlog within the scope of project. The review is formulated from different perspective of various categories of risk. These results in a list of identified potential risk that could have a significant negative impact on the success of project.

The risk that can effect project goals, are identified, classified and report these risks. The outcome of identification process is a list of risks [14]. The resultant risk list depends on project and the environment. For small, noncomplex projects (low-budget projects), there are few risks with little ambiguity. For large, complex projects (high-budget projects), there are effect by uncertain environment. The risks can provide for the risk assessment and risk control process. The mitigation of these risks

can be performed by listing and flagging each item with color. These colors are assigned according to the priority of the risk.

### **3.2.2 Risk Analysis**

When the risks have been documented and all items are analyzed. The cause of the risk analysis is to evaluate the loss possibility and magnitude of each software risk item. The contribution is the software risk statement and situation developed in the appreciation phase.

After the completion of risk assessment, risk analysis is conducted to identify the chances of occurrence and, if so, when the risk is likely to occur in the overall time-line of project. There are several conventional methods that can be employed for the risk analysis, such as cost risk analysis, reliability analysis, decision analysis, and schedule analysis.

### **3.2.3 Consideration Control**

Consideration Control is calculation of losses. Possible action to reduce or remove such threats are considered. Possible risk factors are identified in each item, for instance business, technical and nontechnical features of product and any other areas that effect the goals of product development.

## **3.3 Implementation**

During every Sprint of scrum, Sprint planning results into two artifacts; sprint goal and sprint backlog. During the sprint planning meeting the solutions for tagged issues are identified. The identified solution is listed according to the tag no assigned to the issue. The consideration control on marked issues is done to evaluate the size of loss. The size of loss expected in result of that issue entered in the register. Finally the issues are treated accordingly the solution identified in the planning meeting.

### **3.3.1 Prioritization**

The integrities of identified risk can be identified by the prioritization of risk. Exposure is the product of the possibility of incurring a loss due to the risk and the potential magnitude of these losses. On complex and large projects i.e. high-cost projects that are usually environment uncertain.

It would be much difficult, to provide a plan or strategy for catering the effects of potential risk, in

every phase of the project. By assigning each risk, with a risk priority value, the stakeholders now have a road-map for catering threats. Risk effects are catered by contriving contingency plans for the task with highest to the lowest risk priority factor.

### **3.3.2 Response Planning**

The approaches to deal with risk are identified in this step.

Three strategies for risk planning are introduced:

1. Avoidance: Attempt to minimize the possibilities of risk [17].
2. Minimization: Attempts to decrease the impact of risk.
3. Control: Actions are implemented to reduce the impact of the risk.

### **3.3.3 Risk Treatment**

The strategy is used to mitigate consequence of risk acceptance and transfer. Risk treatment is related to tendency for taking risks. Behavior towards taking risks may change over time through training, education and experience. The threshold of taking risk by organization depends upon the stable risk treatment. As a consequence, competitive control of organization may increase.

## **3.4 Verification**

During the daily scrum meeting the rectified issues are monitored and reviewed. Status of the issues is updated during the meeting.

### **3.4.1 Monitor and Review**

In response of every risk item monitoring and review take place. This tracking helps to achieve the goals of risk management processes. Execution of risk management is ensured by evaluating the risk treatment activity is performed throughout the project development.

## **3.5 Imminent Analysis**

### **3.5.1 Future Analysis**

During the sprint review this is ensured that the issues identified at start of the scrum are catered. If the treated issues are no longer threat for future, a brief report is prepared consisting of the issues that occurred in each sprint. If the same issue has any

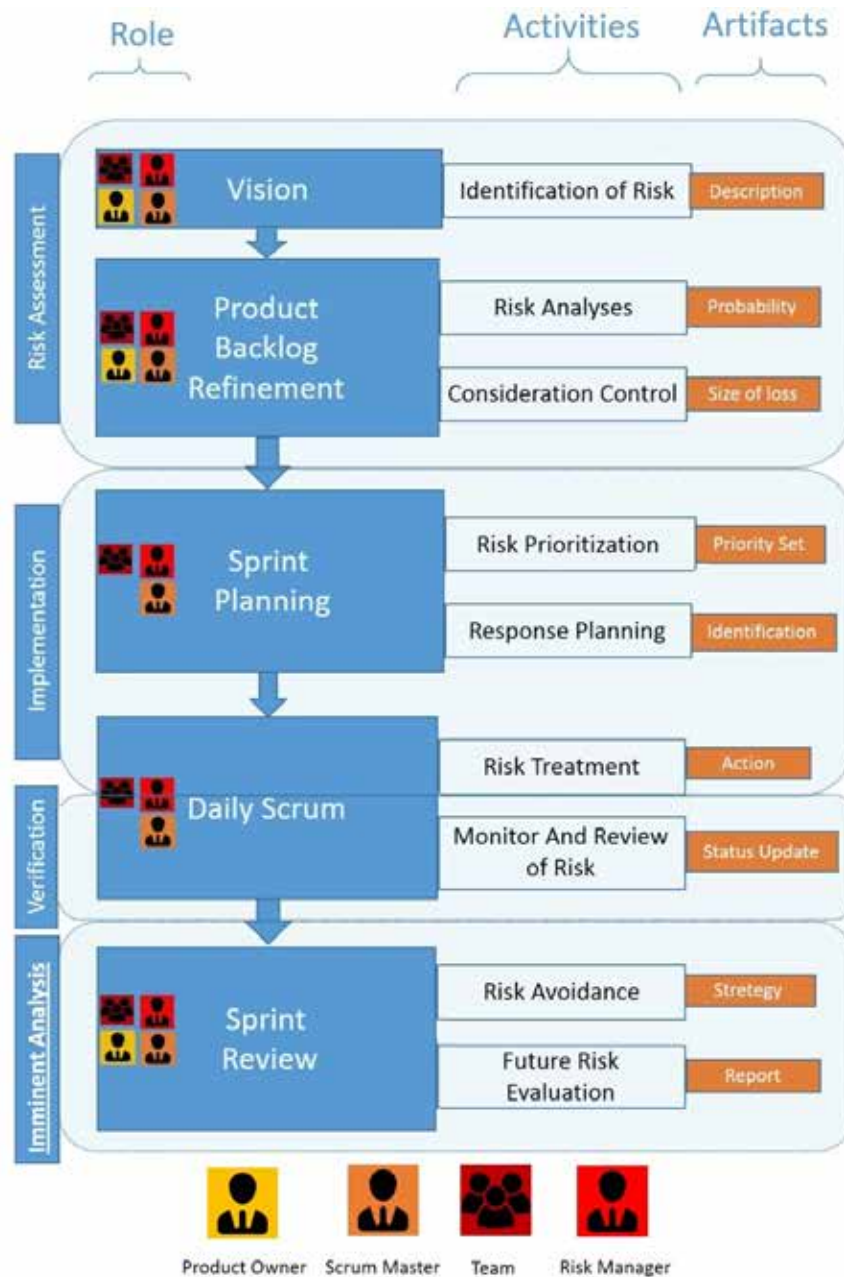


Fig. 3. Risk management in scrum.

chance of reoccurrence in sprint, the team refers the issue to next sprint1 and so on.

### 3.5.2 Avoidance strategy

It is known that the most efficacious risk avoidance plan is to establish effective communication throughout the life cycle of project. Oftentimes, scrum master fail to keep the entire stakeholder in the loop about the project.

Formal risk avoidance methods depend upon understanding the user requirements, obtaining domain information and effective communication

[18]. These factors ensure that the plan will achieve project objectives.

### 3.6 Future Risk Evaluation

Directions for future occurrence of risk will be discussed and gap of the risk treatment are identified. All the information gathered during the development process is analyzed to predict the chances of occurrence of each risk item. At the time of sprint review and retrospective of scrum, a report is prepared then all the learned instructions

are acknowledged. This information stored in the information repository for making decision in future projects.

In Scrum software development the risk management is not considered essential from the start of development process. The proposed framework mitigates the risk after performing proper assessment, its implementation, verification and analysis for future aspects. Fig. 2 represents the proposed model.

Every activity performed in scrum contributes toward the management of risk. The risks will be identified in the vision activity of scrum. Followed by, analyses of the identified risk items. During analysis the risk occurrence, the size of loss and its priority is determined. These activities come under the risk assessment phase and are performed during the creation and refinement of product backlog. The prioritized risks are then treated according to a proper plan framed during the daily scrum. The treated risk are then review to confirm its removal in daily scrum meetings. The review is conducted on daily basis so its effects can be monitored, and in-case plans for mitigation can be altered accordingly. This will minimize the cost of treating the risk. The sprint review is open for more risk to be identified and listed accordingly with the retrospective. The progress of the project is then shared with stakeholders.

**3.7 Validation**

Case study has been used as a research method [19]. While designing the study, we emphasized on human sense making and how the mechanisms of risk management were understood by the participants involved. The research method is selected to collect experiences which could be used to improve performance of the corresponding

projects. The project selected under this umbrella is a new development of company’s internal web application. The web application is collection of several different level of tracking phases.

The data from stakeholders and project participants was collected by conducting semi-structured interviews. During interview, notes were created in such a way that attendants were able to comment and make corrections as and if required. This case study is performed on web development project in global Soft tech Company. The company’s head office is in Europe, but it has offsite activities in several locations in Asia like Pakistan. The agile methods are use in company from past 10 years and it is common to have project of different nature i.e. large scale small scale, distributed etc.

The interviews conducted were from 15 participants including all stakeholders. The interviews comprised questions of 9 in total, out of which 6 questions were related to the experience and background. In other questions, issues and suggestion were gathered. While interviews project participants and stakeholders were directed to concentrate on all possible aspects of the theme.

The data gathered from interviews was analyzed qualitatively. While performing the qualitative analysis, issues identified by the interviewee was counted. A meeting with the participants was organized, in the first half of meeting participants were able to comment on each issues. In the second half of the meeting, improvement regarding the raised issues, were voted for further actions and study. However, here, we have reported the core findings and leaving the rest analysis for further studies.

**3.8 Proposed Model in Action**

The case study was completed in 5 months. The

**Table 1.** Scrum in action.

Event	Sprint 1	Sprint 2	Sprint 3	Sprint 4	Sprint 5
Sprint Planning	4 hour/week	6 hour/week	8 hour/week	10 hour/week	12 hour/week
Daily Scrum	15 min/day	15 min/day	15 min/day	15 min/day	15 min/day
Sprint Review	2 hour/week	3 hour/week	4 hour/week	5 hour/week	6 hour/week
Sprint Retrospective	1 hour/week	2 hour/week	3 hour/week	4 hour/week	5 hour/week

**Table 2.** Risk identification.

Identification by	Risk
Customer	Resistance to change by End Users
	Delay in delivery
	Conflicts between End Users
Product owner	Frequently changing requirements
	Effective identification of System requirement
	Vague and Incorrect system requirements
Team	Project complexity
	Use of new and immature technology
	Less experience and technical complexities
Risk Manager	Project planning and control
	Inexperience team
	Failure to manage end user expectation
	Failure to gain user commitment

team has to go through five sprint to complete the project. Following are the schedules of the conducted case study.

The stakeholders have to conduct session of

sprint planning of 40 hours in total, the daily scrum meeting timing in total of 27.5 hours in total, the sprint review was conducted in total of 20 hours and the sprint retrospective 15 hours in total project.

The stakeholder of the said case project gathered during the activities of vision and in review. A few of risk identified by the stakeholders are mentioned in Table 2.

The evaluation of these items, results in the priority set (Table 4), size of expected loss ranked in 1-10 (Table 5) and planning (Table 6) how to mitigate the risk items.

For every risk item a proper mitigation plan has been formulated. The description of plan for a few selected risk item are shown in Table 7.

Each risk item is considered a separate entity and treated (Table 8) according to the priority set of the risk. The process of evaluation of the risk item is performed in the daily scrum meeting.

These item are treated during the daily scrum and afterwards, the mitigation of each item is monitored and verified (Table 9).

These items are reviewed (Table 10) in final so their future occurrence can be avoided. The future benefits (Table 11) are also considered at the end of the project, so the artifacts can be used for future planning.

**Table 3.** Risk description.

Risk	Description
Resistance to change by End Users	End User may be hesitant towards the change
Delay in delivery	Project complexities
Conflicts between End Users	End user may have different vision about the same requirement.
Frequently changing requirements	Customer with foggy vision.
Effective identification of System requirement	Requirement gathering in agile manner.
Vague and Incorrect system requirements	May acquire ambiguous requirements.
Project complexity	Interdependencies or Interconnections
Use of new and immature technology	Technology is introduced in the same year, less support available
Less experience and technical complexities	Lack of expertise.
Project planning and control	Un-experienced Scrum Master
Inexperience team	Team have no hands on practices for the technology.
Failure to manage end user expectation	User requirement, budget and timeline clashes
Failure to gain user commitment	Un-interested users and with less awareness of technology.

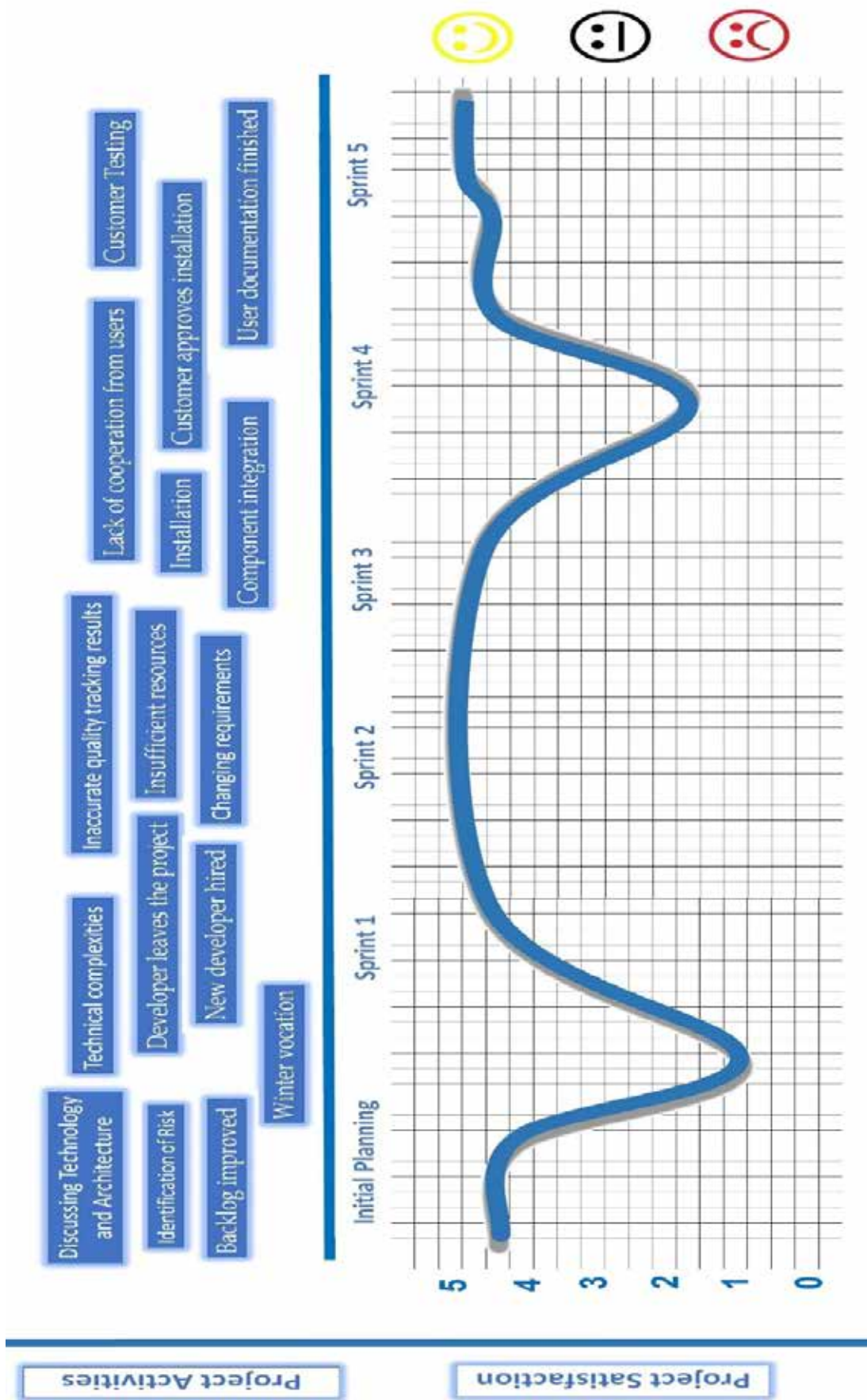


Fig. 4. Case study results.

**Table 4.** Risk analysis.

<b>Risk</b>	<b>Probability</b>
Resistance to change by End Users	70%
Delay in delivery	40%
Conflicts between End Users	20%
Frequently changing requirements	50%
Flaws in identification of System requirement	40%
Vague and Incorrect system requirements	20%
Project complexity	40%
Use of new and immature technology	80%
Less experience and technical complexities	30%
Project planning and control	50%
Inexperience team	30%
Failure to manage end user expectation	30%

**Table 5.** Consideration control.

<b>Risk</b>	<b>Size of loss</b>
Frequently changing requirements	8
Failure to manage end user expectation	8
Use of new and immature technology	6
Project planning and control	6
Flaws in identification of System requirement	6
Resistance to change by End Users	5
Project complexity	5
Less experience and technical complexities	5
Vague and Incorrect system requirements	4
Conflicts between End Users	4
Inexperience team	3
Delay in delivery	3
Failure to gain user commitment	2

**Table 6.** Risk prioritization.

<b>Risk</b>	<b>Prioritization</b>
Use of new and immature technology	Red
Resistance to change by End Users	Red
Failure to gain user commitment	Orange
Frequently changing requirements	Orange
Project planning and control	Orange
Project complexity	Orange
Flaws in identification of System requirement	Orange
Delay in delivery	Orange
Less experience and technical complexities	Purple
Inexperience team	Purple
Failure to manage end user expectation	Purple
Conflicts between End Users	Purple
Vague and Incorrect system requirements	Purple

**Table 7.** Risk planning.

<b>Risk</b>	<b>Planning</b>
Use of new and immature technology	Look for alternatives and Training
Resistance to change by End Users	Development of interest
Failure to gain user commitment	Development of interest
Frequently changing requirements	Freezing requirements
Project planning and control	Experience Scrum Master
Project complexity	Experience Team
Flaws in identification of System requirement	Use of Requirement Technique
Delay in delivery	Proper scheduling
Less experience and technical complexities	Employing experts
Inexperience team	Employing experts
Failure to manage end user expectation	Use of Prototyping
Conflicts between End Users	Rectify conflicting requirements
Vague and Incorrect system requirements	Remove ambiguous requirement

**Table 8.** Risk treatment.

<b>Risk</b>	<b>Treatment</b>
Use of new and immature technology	Used mature technology
Resistance to change by End Users	Conducted session to brief the ease of use.
Failure to gain user commitment	Engage in project for interest development.
Frequently changing requirements	Developed requirement documents
Project planning and control	Employing experience Scrum Master
Project complexity	Conducted training
Flaws in identification of System requirement	Effective requirement engineering
Delay in delivery	Scheduled Events
Less experience and technical complexities	Employed experts
Inexperience team	Employed experts
Failure to manage end user expectation	Used Model to verify the design
Conflicts between End Users	Improved requirement analysis
Vague and Incorrect system requirements	Improved requirement analysis

**Table 9.** Monitor and review of risk.

<b>Risk</b>	<b>Monitor</b>	<b>Review</b>
Use of new and immature technology	√	√
Resistance to change by End Users	√	√
Failure to gain user commitment	√	√
Frequently changing requirements	√	√
Project planning and control	√	√
Project complexity		√
Flaws in identification of System requirement	√	√
Delay in delivery		√
Less experience and technical complexities	√	√
Inexperience team		√
Failure to manage end user expectation	√	√
Conflicts between End Users	√	√
Vague and Incorrect system requirements	√	

**Table 10.** Future risk evaluation.

<b>Risk</b>	<b>Future Evaluation</b>
Use of new and immature technology	Foresee the technological changes.
Resistance to change by End Users	Training session planning.
Failure to gain user commitment	Engage in project for interest development.
Frequently changing requirements	Consider developed requirement documents a baseline
Project planning and control	Planning and management of future activities
Project complexity	Utilizing gained Expertise
Flaws in identification of System requirement	Effective employing of requirement engineering
Delay in delivery	Improved Scheduled experience
Less experience and technical complexities	Keeping employees upto-date with new technologies
Inexperience team	Conducting in house tanning and workshops
Failure to manage end user expectation	Managing a design Repository
Conflicts between End Users	Employing experience in requirement communication
Vague and Incorrect system requirements	Employing experience in requirement analysis

**Table 11.** Benefits of risk management

<b>Risk</b>	<b>Future Evaluation</b>
Use of new and immature technology	Knowledge to choose the technology.
Resistance to change by End Users	Experience to conducted session.
Failure to gain user commitment	Designs for user interest programs
Frequently changing requirements	Requirement documents Repository
Project planning and control	Assets for future
Project complexity	Expertise
Flaws in identification of System requirement	Effective employing of requirement engineering
Delay in delivery	Improved Scheduled experience
Less experience and technical complexities	Assets for future
Inexperience team	Assets for future
Failure to manage end user expectation	Design Repository
Conflicts between End Users	Experience in requirement analysis
Vague and Incorrect system requirements	Experience in requirement analysis

#### 4. RESULTS AND DISCUSSION

On the subject of our research questions, we were able to get confirmation that risk management in scrum is likely improved using the proposed framework. The web development project is completely functional and no risk issues in any sprint of scrum were reported. While performing the study more improvement needs were highlighted rather than working issues. None of the identified issues was so severe that it would have suffered the working of project.

Conclusion drawn on the base of working is that framework has worth of use. The process management and stakeholders' involvement issues

were mainly identified. This gives a contrary impact, but while observing in detail it became vibrant that some skills are required for adjusting Scrum to risk free environment.

#### 5. CONCLUSIONS

The success of project can be increased by effective risk management practices. The uncertainties are considered as the risk of the project that result in cost expansion and reduce the quality of product. Timely decision is vital for controlling the risk issues. The roles involved in the development of project should be able to identify these issues without any problem. In our research study we have employed

risk management activities in a Scrum model. This enables to identify the risk by marking the issues and maintaining repositories for future reference. Thus risk issues can be identified and tracked at any stage of sprint. We have conducted a case study and results have shown that by adopting secure and risk free scrum model a quality software product can be produced. Our future research will be directed toward the generalization of this framework. The proposed framework has been developed and evaluated for collocated environment. However, in future we will extend our work in distributed environment, so the results can be more significant.

## 6. ACKNOWLEDGEMENTS

We thank every person at our institution who contributed in the study or offered views for improvement of the study.

## 7. REFERENCES

1. Malik, M.U., H. Nasir, & A. Javed. An efficient objective quality model for agile application development. *International Journal of Computer Applications* 85(8): 19-24 (2014).
2. Cerpa, N., & J.M. Verner. Why did your project fail?. *Communications of the ACM* 52(12): 130-134 (2009).
3. McManus, J. Risk management in software development projects. *Routledge*, London (June 25, 2012).
4. Bali, V. & S. Bali. *Software Engineering*. S.K. Kataria and Sons Publishers, New Delhi, India, p. 269-278 (2008).
5. Reddaiah, B., S.P. Ravi, & L.S. Movva. Risk management board for effective risk management in scrum. *International Journal of Computer Applications* 65(12): 16-23 (2013).
6. Garvey, P.R. *Analytical Methods for Risk Management: A System Engineering Perspective*. Chapman-Hall/CRC Press, Taylor & Francis Group, Boca Raton (2008).
7. Janus, A., R. Dumke, A. Schmietendorf, & J. Jäger. The 3c approach for agile quality assurance. In: *3rd International Workshop on Emerging Trends in Software Metrics (WETSOM)*, Zurich, Switzerland, p. 9-13 (2012).
8. Alharbi, E.T., & M.R.J. Qureshi. Implementation of risk management with SCRUM to achieve CMMI requirements. *International Journal of Computer Network and Information Security* 6(11): 20-25 (2014).
9. Pandey, P.K.D. Development of risk management model for secure software product. *South Asia Journal of Multidisciplinary Studies* 1(3): <http://gjms.co.in/index.php/SAJMS/article/view/840> (2015).
10. Pohl, C., & H.J. Hof. Secure Scrum: Development of secure software with SCRUM. *Ninth International Conference on Emerging Security Information, Systems and Technologies*, Venice, Italy [https://www.researchgate.net/publication/277307837\\_Secure\\_Scrum\\_Development\\_of\\_Secure\\_Software\\_with\\_Scrum](https://www.researchgate.net/publication/277307837_Secure_Scrum_Development_of_Secure_Software_with_Scrum) (2015).
11. Wanderley, M., J. Menezes, C. Gusmão, & F. Lima. Proposal of risk management metrics for multiple project software development. *Procedia Computer Science* 64: doi:10.1016/j.procs.2015.08.619, 1001-1009 (2015).
12. Islam, S., & Houmb, S. H. Towards a framework for offshore outsource software development risk management model. *Journal of Software*, San Bernardino, California 6(1): 38-47 (2011).
13. Ylimannela, V. A Model for risk management In Agile software development. March 2012 <http://www.cloudsw.org/under-review/a6f468c9-4857-4206-96ee-f67df0583d41> (Accessed: 22 April, 2016).
14. Layton, M.C. How to manage risk within Agile management - for dummies. *Agile Project Management for Dummies*, May-2012. <http://www.dummies.com/how-to/content/how-to-manage-risk-within-agile-management.html> (Accessed: 17 Jan, 2016).
15. Veethil. S.T. Risk management in Agile. Scrum alliance. <https://www.scrumalliance.org/community/articles/2013/2013-may/risk-management-in-agile> (Accessed: 17-Jan-2016).
16. Odzaly, E. E., & Des Greer, D. S. Lightweight risk management in Agile projects. In: *Conference: 26th Software Engineering Knowledge Engineering Conference (SEKE)*, Vancouver, Canada: doi: 10.13140/2.1.4681.0882 (2014).
17. De Bakker, K., A. Boonstra, & H. Wortmann. Does risk management contribute to IT project success? A meta-analysis of empirical evidence. *International Journal of Project Management* 28(5): 493-503 (2010).
18. Hijazi, H., Alqrainy, S., Muaidi, H., & Khmour, T. Risk factors in software development phases. *European Scientific Journal* 10(3): <http://www.ejournal.org/index.php/esj/article/view/2624> (2014).
19. Runeson, P., & Höst, M. Guidelines for conducting and reporting case study research in software engineering. *Empirical Software Engineering* 14(2): 131-164 (2009). doi:10.1007/s10664-008-9102-8.





# Fabrication and Identification of Graphene Layers on Silicon Dioxide and Flexible PMMA Substrates

Zeba Khanam, Ibtisam Riaz\*, Adeel Rasheed, and Rashid Jalil

Nanotechnology Research Center, Department of Physics,  
University of Engineering and Technology, Lahore, Pakistan

**Abstract:** Graphene is a “wonder material” and rapidly rising star in all fields of physics. This strictly two-dimensional material exhibits exceptionally high crystal quality and band structure. Graphene, building block of all graphitic materials, has emerged as an interesting material of the 21st century. This two-dimensional, single-layer sheet of  $sp^2$  hybridized carbon atoms has attracted tremendous attention and research interest, owing to its exceptional physical properties, such as high mobility, good thermal stability, excellent mechanical strength and high transparency. These properties make graphene a material of interest for many applications, for example in the fields of electronics, optoelectronics, photonics, composites as well as sensors. There are a number of methods for fabricating and characterizing graphene. Here in this work, graphene has been synthesized via micromechanical cleavage method and characterized via various techniques. Graphene is fabricated on oxidized silicon ( $Si/SiO_2$ ) and polymethyl methacrylate (PMMA) substrates.  $Si/SiO_2$  is a rigid substrate while PMMA is transparent, flexible and a versatile polymeric material having applications in flexible electronics. Micromechanical cleavage method is reproducible and large numbers of high quality graphene flakes were obtained by using this method on these two substrates. The graphene layers thus produced have been identified and characterized using optical microscopy, AFM and Raman spectroscopy showing single layer, bilayer, tri-layer and multi-layer graphene.

**Keywords:** Graphene, two-dimensional material, fabrication, micromechanical cleavage

## 1. INTRODUCTION

Graphene is made up of a single atom thick carbon layer arranged in a honeycomb-like lattice. Graphene is the thinnest, strongest and hardest material available so far. In recent times, graphene has attracted the huge attention of scientific fraternity in all areas of academic and industrial research due to its unique set of properties. Graphene is trying to replace the previously existing modern material i.e. silicon which was set to change the face of research and technology. Due to its rapid popularity it can be said that Graphene is going to change the future of technology even making invisibility a reality [1-3].

Graphene is the first material in the new class of 2D materials. Although it was supposed that 2D materials cannot exist without 3D base until 2004. But this assumption has changed with the

experimental discovery of graphene [4] by Geim and Novoselov [5]. Theoretically, graphene has been studied for sixty years [6-8] but there were some difficulties in isolating single layer. If we go back in the distant past, we are surprised to know that graphene also existed in ancient times. Because everyone while using an ordinary lead pencil probably produce graphene-like structures without knowing it (because graphite consists of stacked graphene sheets). So we can say that graphene was existed in past in the form of different carbon materials such as graphite, fullerenes and carbon nanotubes [9]. But in 2004, it was discovered as a single isolated layer [4]. After its discovery it became evident that graphene is the building block of all graphitic materials. It can be wrapped up into 0D fullerenes, rolled into 1D nanotube or stacked

into 3D graphite [9].

Crystal structure of graphene consists of single layer of carbon atoms undergo hybridization with angle between each bond is  $120^\circ$  and the carbon distance is 0.142 nm. There are two carbon atoms per unit cell in a hexagonal honeycomb lattice of graphene [10]. The two dimensional linear network of carbons with no cross linking makes graphene flexible and stretchable. The electronic band structure of graphene considers only the electrons in the 2 orbitals. These electrons give rise to the  $\pi$  band and account for the transport properties of graphene. The conduction and valence band touches at the  $K$  and  $K'$  points at the border of the first Brillouin zone which specifies that graphene has no band gap, and it is therefore called as a zero-gap semiconductor [5] or a semi metal [5].

Graphene has several useful electronic, optical, mechanical and thermal properties. Graphene has a charge carrier mobility  $\sim 200,000$   $\text{cm}^2/\text{Vs}$  [4] compared to the other semiconductor materials. Graphene is an optically transparent material. Single layer of graphene can absorb only 2.3% of light while 97.7% of light is transmitted [11]. Transparency of graphene reduces with increasing number of layers as 2.3% per layer [11]. In 2009, Le et al showed that graphene has breaking strength over 100 times greater than a hypothetical steel film of the same thickness, with a Young's modulus of 1 TPa [12]. Therefore, graphene; having the breaking strength of  $42 \text{ Nm}^{-1}$  and the Young's modulus of 1.0 TPa; is suggesting the strongest material ever measured [13]. Graphene is the superconductor of heat. It has highest thermal conductivity 3080–5300  $\text{W/mK}$  [4] compared to the other carbon materials.

These properties of graphene make it an attractive choice for use in advanced applications. Graphene is a single atom thick flat sheet of carbon. Therefore, electrons and holes move much faster through it than through other materials. This property makes graphene a suitable candidate to replace silicon as an electronic material and can be used in high frequency transistor applications [14–16]. Graphene has also replaced semiconductors in photo detectors. Graphene with zero band gap has wide spectral range from ultraviolet to infrared [17]. While other semiconductor photo detectors

have limited detecting spectral width. Graphene's high operating bandwidth makes it suitable for high-speed data communications [17]. Mechanical flexibility, electrical and optical properties (low sheet resistance and high transparency) make graphene an attractive choice for flexible electronic devices [3]. It is used as a transparent conductive coating in electronic products such as touch screen displays, organic light emitting diodes, etc. Due to its high strength properties, it is used in composite materials [13] such as body armour for military personnel, vehicles and aircrafts. Due to its good electrical conductivity, it is used to coat aircraft surface to prevent from lightning strikes. Due to its high demand in a number of applications, we have fabricated graphene over Si/SiO<sub>2</sub> and PMMA substrates using micromechanical cleavage method and characterized it using optical microscopy, AFM and Raman spectroscopy.

## 2. MATERIALS AND METHODS

There are different methods to fabricate graphene. However, micromechanical cleavage was the first method by which single layer of graphene was discovered. The same method was used in our experiment. The steps used are as follows:

Two types of substrates were used for graphene fabrication, one was Si/SiO<sub>2</sub> and the other was PMMA which is transparent and flexible. Si/SiO<sub>2</sub> was used with two thicknesses, 90 nm and 290 nm. While the thickness, length and width of PMMA rectangular bar was 3 mm, 43 mm and 15 mm respectively.

The substrates were cleaned using standard cleaning method discussed below.

### 2.1 Standard Cleaning

The steps involved shown in Fig. 1 are as follows: Si/SiO<sub>2</sub> substrate was rinsed with Acetone and then IPA and dried with Nitrogen gas. Acetone removed the protective resist coating and IPA dissolved excess Acetone from the substrate. After baking at  $120^\circ\text{C}$  the substrate was cleaned.

Fig. 2 shows the cleaning process of the PMMA substrate. PMMA being reactive with acetone

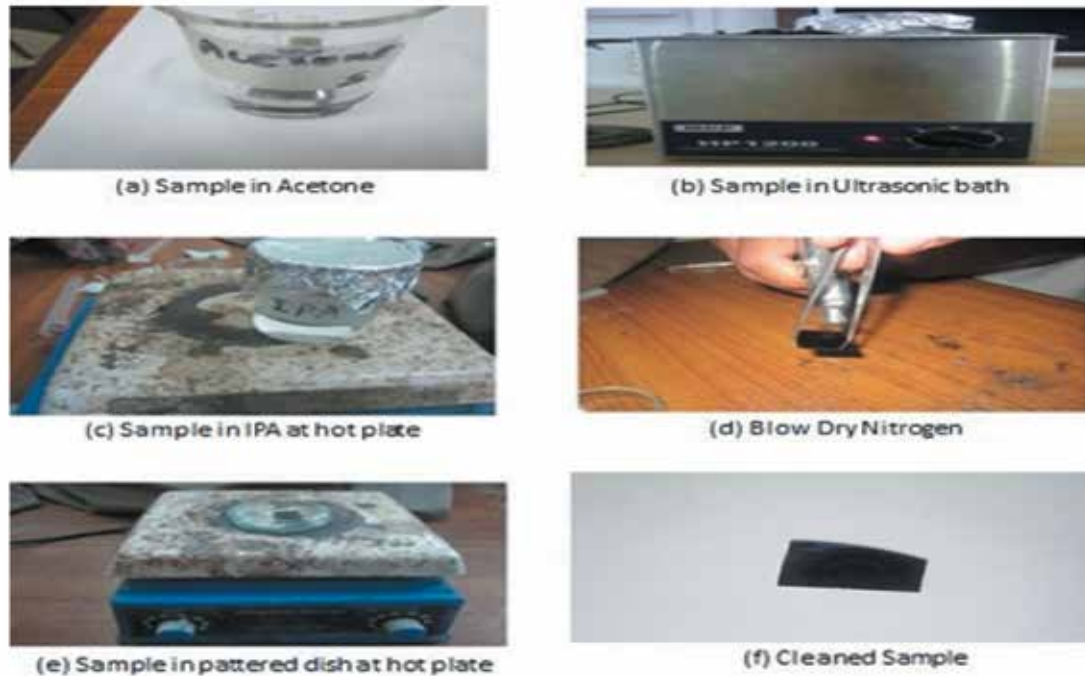


Fig. 1. Standard cleaning method used for Si/SiO<sub>2</sub> substrate.

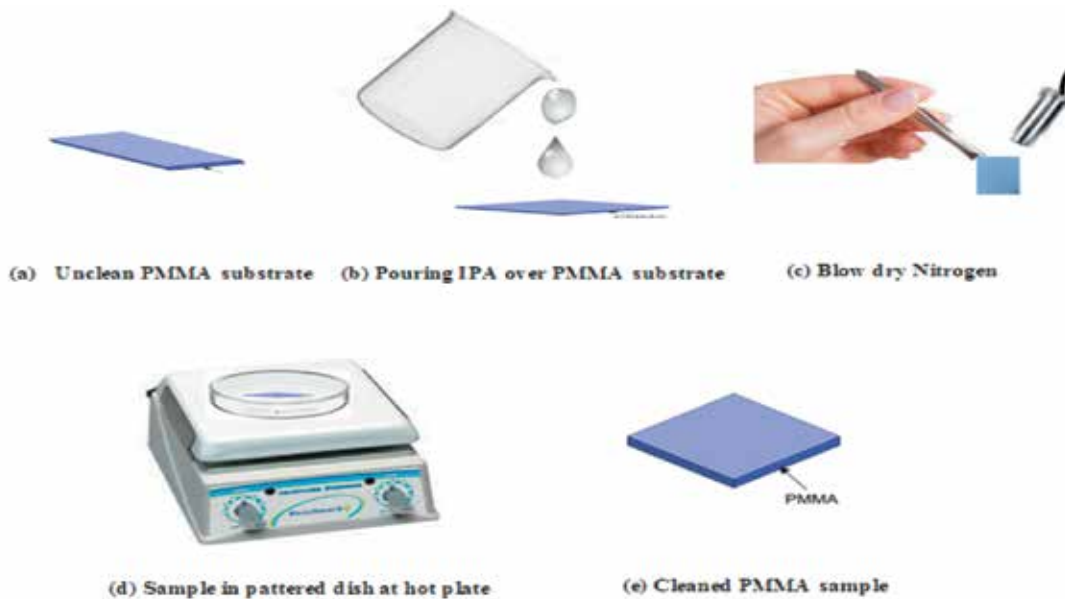


Fig. 2. Schematic of standard cleaning method for PMMA substrate.

only rinsed with IPA and dried with gas. Now the samples were ready for micromechanical cleavage.

## 2.2 Micromechanical Cleavage Method

Geim and Novoselov [4] used adhesive tape to fabricate single layer graphene by cleavage. Cleavage is also known as Mechanical exfoliation.

Achieving single layers typically involves multiple exfoliation steps, each fabricating a slice with fewer layers, until only one remains. The graphene prepared by this method is of high quality with no defects and differ considerably in size and thickness, where the sizes range from few to hundreds of micron [4]. Our experiment was based on the same cleavage method.

The steps involved in this method were as follows:

A tape was taken and a piece of graphite was emplaced over it. By multiple folding and peeling the tape, the graphite piece was exfoliated into multiple thinner graphite flakes covering the entire tape surface.

Then the tape was put over the pre-cleaned Si/SiO<sub>2</sub> and PMMA substrates and pressed hard with thumb several times to ensure close contact between the flakes and the substrate and left for 1 hour. The sample, Si/SiO<sub>2</sub> with attached tape, was then immersed in Acetone solution for two to three minutes. Tape was left the surface and taken out with tweezer. Then the sample was transferred from Acetone to Fresh Acetone beaker and baked for three to five minutes at 58 to 60 °C. The PMMA rod with graphite tape was immersed into deionized (DI) water at 70 °C and was left for 10 minutes. The tape was removed mechanically. Both samples were then transferred to separate IPA solutions and baked again for five minutes at 50 °C. After that the samples were dried out with nitrogen gas. The sample with Si/SiO<sub>2</sub> substrate was then baked at hot plate at 120 °C for 15 minutes. While the sample with PMMA substrate was baked in microwaves oven at 50-60 °C for 15 minutes. This whole process removed the adhesions due to the tape. The samples were then picked up and left for some time until they maintained the room temperature. Finally, one last peeling with unused tape was performed to remove the thicker flakes and the substrates were left with graphene sheets and other thin graphitic layers. The steps involved for fabrication over Si/SiO<sub>2</sub> and PMMA are shown in Fig. 3 and Fig. 4, respectively.

### 3. RESULTS AND DISCUSSION

The samples prepared by the experiment, discussed above, are then characterized by three techniques: optical microscopy, AFM and Raman spectroscopy. The results obtained are discussed below.

#### 3.1 Optical Microscopy

The optical microscopy is the first immediate technique that is used for graphene flake identification. It is used to image various layers

since it is the cheapest, non-destructive and readily available in laboratories. Optical microscope provides low resolution due to the light diffraction limit. Therefore, it could not provide conclusive evidence that a given flake was single, double or multilayer but by using the colour difference or reflection variations with image with back ground we can say that the layer is monolayer, bilayer or multilayer.

Fig. 5 to Fig. 12 illustrate main findings of this study. These figures show graphene viewed in an optical microscope (OLYMPUS, MM6C-AF-2) under normal, white-light illumination with different magnifications used in reflection mode on top of a Si/SiO<sub>2</sub> substrate.

Two samples were prepared having a number of graphene flakes over 90 nm and 290 nm Si/SiO<sub>2</sub> substrates. The graphene flakes fabricated over 90 nm Si/SiO<sub>2</sub> substrate are shown in Fig. 5 to Fig. 9 at three magnifications, i.e., (a) 20x, (b) 50x, and (c) 100x. Single layer, bilayer, tri-layer and multi-layer graphene can be identified by contrast analysis which shows that on 90 nm Si/SiO<sub>2</sub> substrate, single layer shows the grey color while multilayer goes towards the white. Single layer graphene are encircled.

The graphene flakes fabricated over 290 nm Si/SiO<sub>2</sub> substrate are shown in Fig. 10 to Fig. 12 at three magnifications: (a) 20x, (b) 50x, and (c) 100x. Single layer, bilayer, tri-layer and multi-layer graphene can be identified by contrast analysis which shows that on 290 nm Si/SiO<sub>2</sub> substrate, single layer shows the purple color and multilayer goes towards the blue. The encircled regions of optical micrograph indicate the single layer graphene of different flakes.

Graphene fabricated over PMMA substrate is shown in Fig. 13 to Fig. 16. The graphene flakes are easily identified on a PMMA substrate because the flakes add an additional optical path for the light reflected off the substrate surface (effective). Typically the colour of graphitic flakes is dark grey (thin flakes) to white grey (thick flakes) on PMMA substrate. In general, the optical contrast of single layer graphene depends on the substrate.

To obtain a better contrast we used the optical

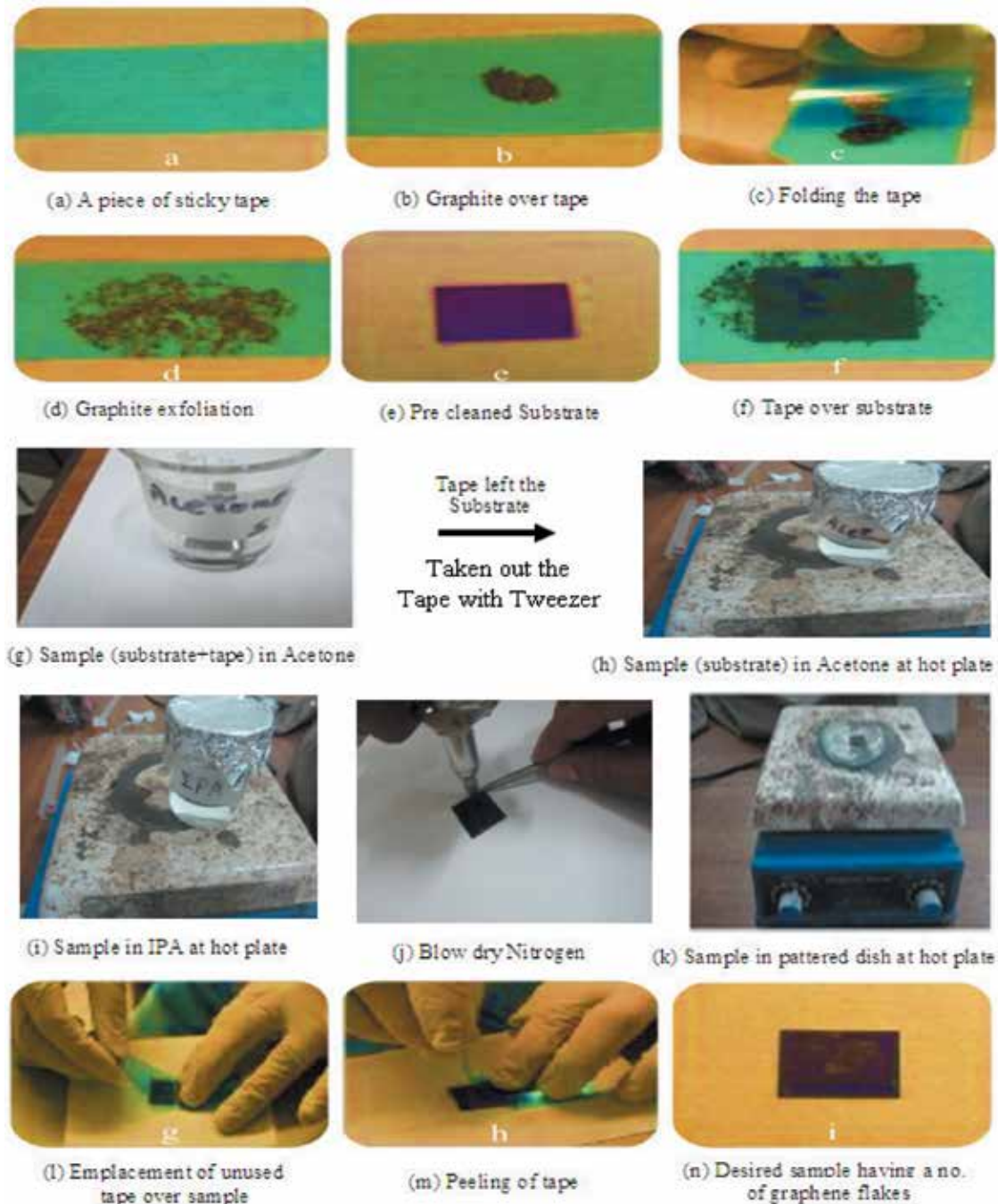


**Fig. 3.** Schematic of micromechanical cleavage method to fabricate graphene on Si/SiO<sub>2</sub> substrate.

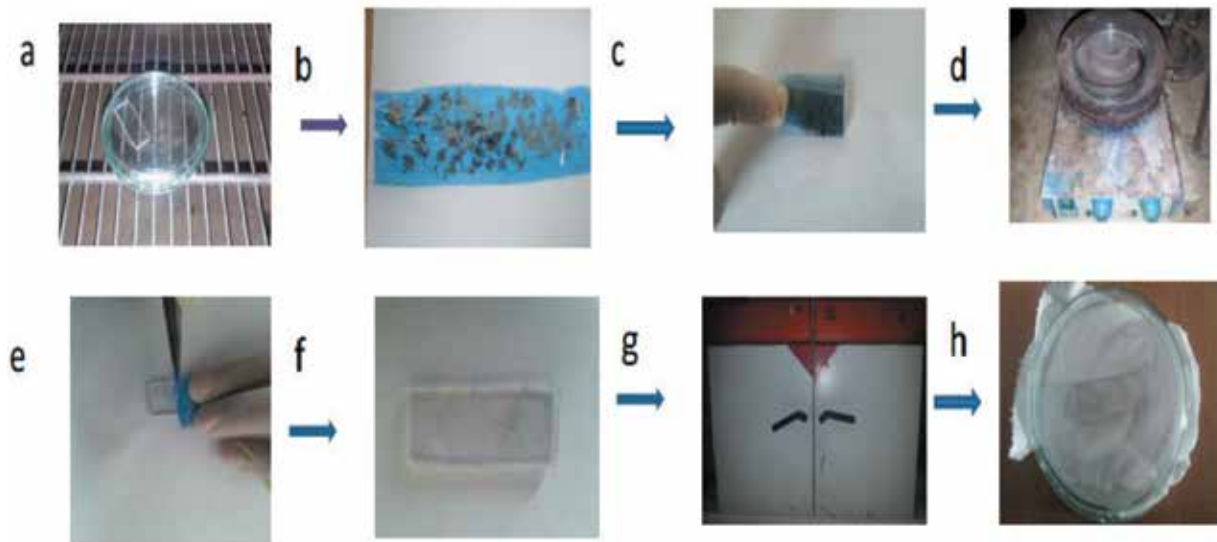
filters. Fig. 14 illustrates the improvement in image quality using the optical filters with different wavelengths in optical microscopy. Different images of graphene flake at different magnification level using different filters are shown in Fig. 15 and Fig. 16.

### 3.2 Atomic Force Microscopy (AFM)

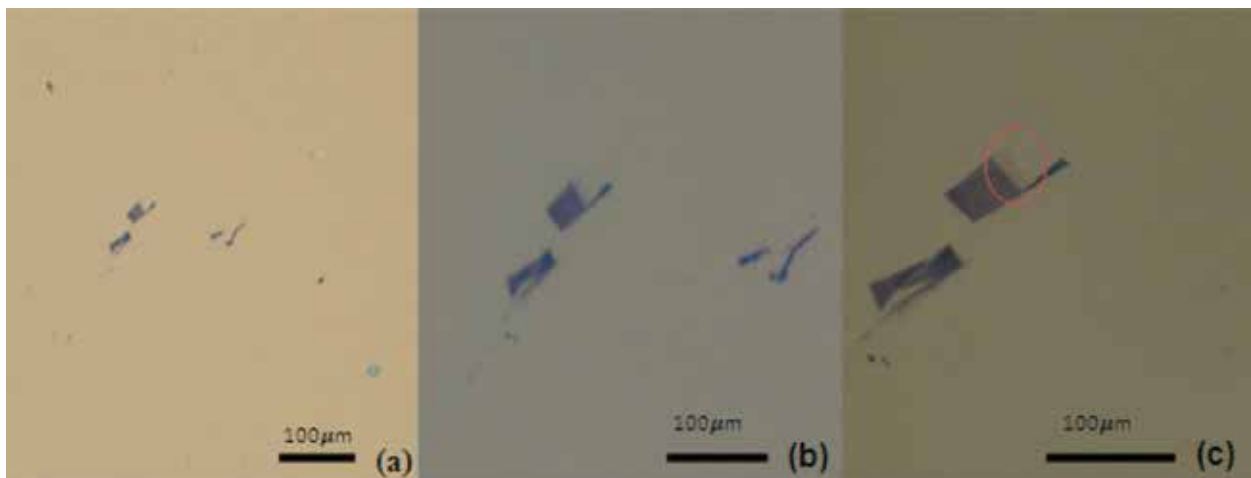
This technique of imaging can successfully

determine the layer thickness at the nanometer scale. AFM images were observed under tapping mode in which cantilever tip touch the surface only for a short time, thus avoiding the issue of lateral forces [18] and drag across the surface. This enables tapping mode to image soft, fragile and adhesive surfaces without damaging them while work under contact mode allows the damage to occur.

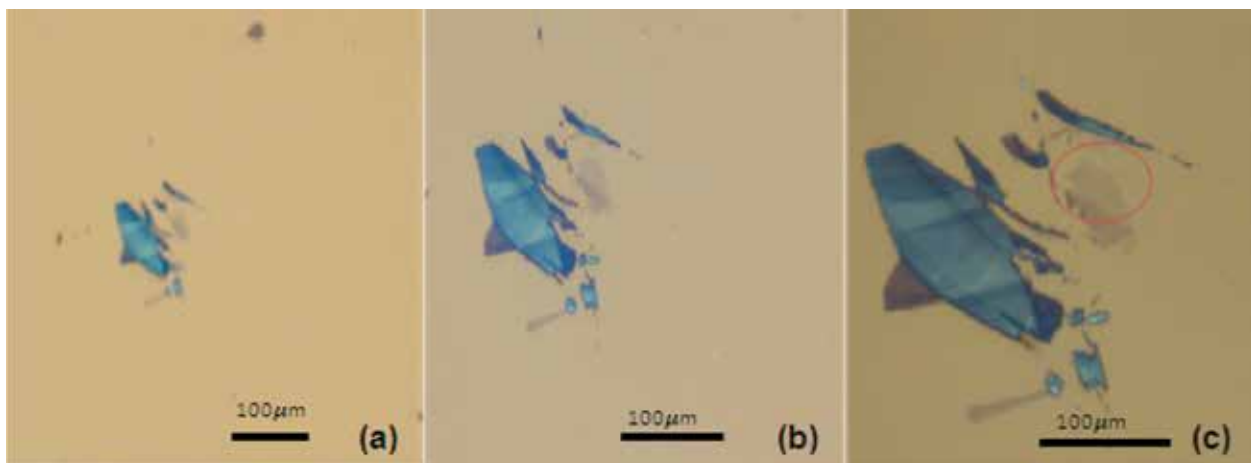
Graphene flakes are analyzed by using AFM.



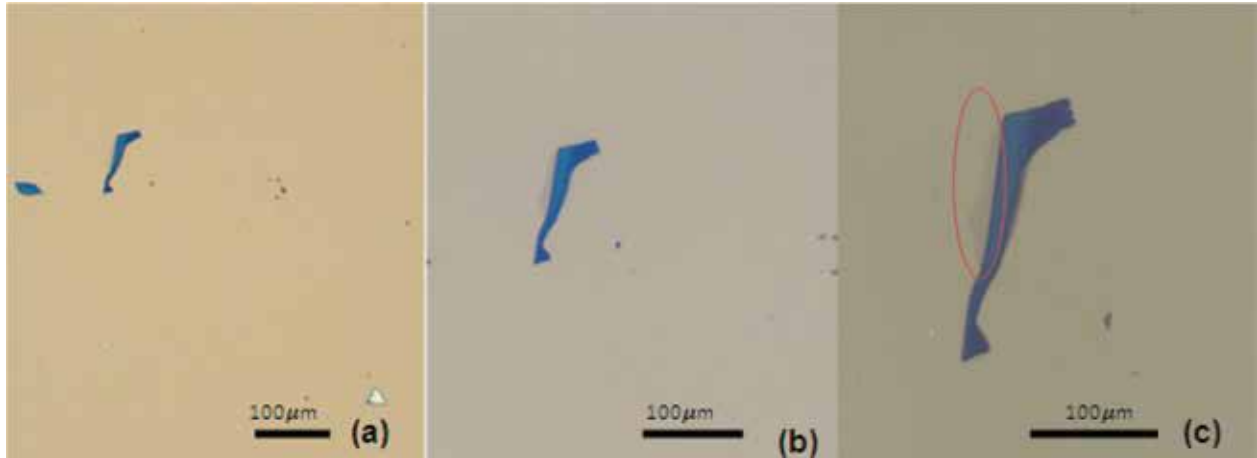
**Fig. 4.** Schematic for the fabrication of graphene on PMMA substrate.



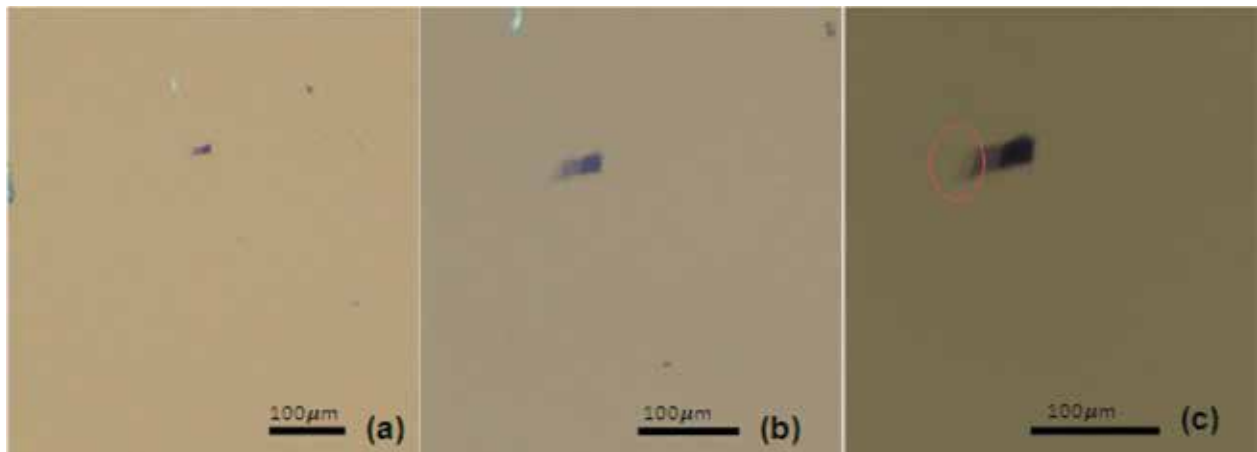
**Fig. 5.** Optical image of first flake over 90nm Si/SiO<sub>2</sub> substrate at: (a) 20x; (b) 50x; (c) 100x.



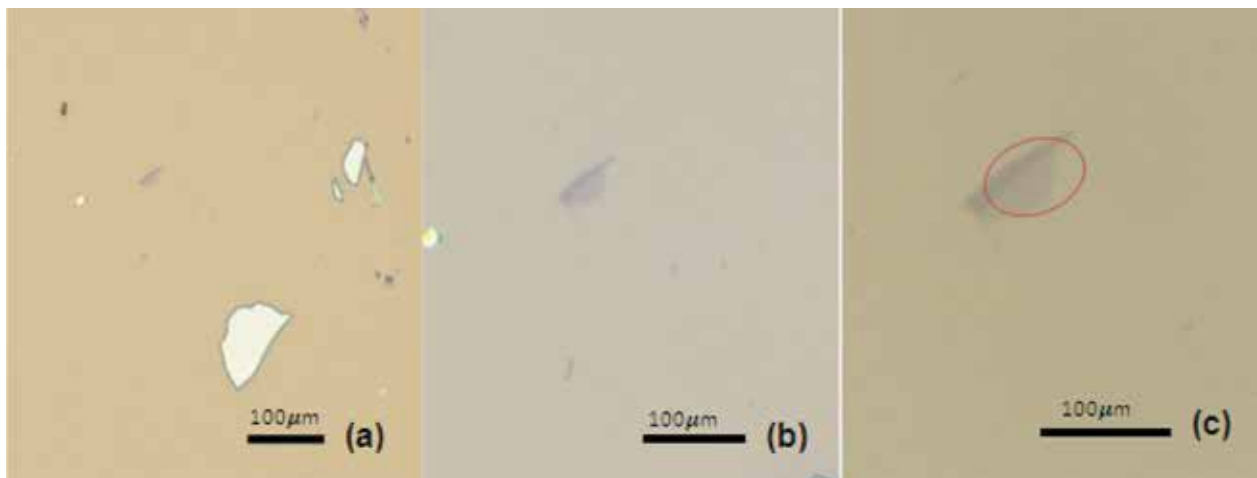
**Fig. 6.** Optical image of second flake over 90nm Si/SiO<sub>2</sub> substrate at: (a) 20x; (b) 50x; (c) 100x.



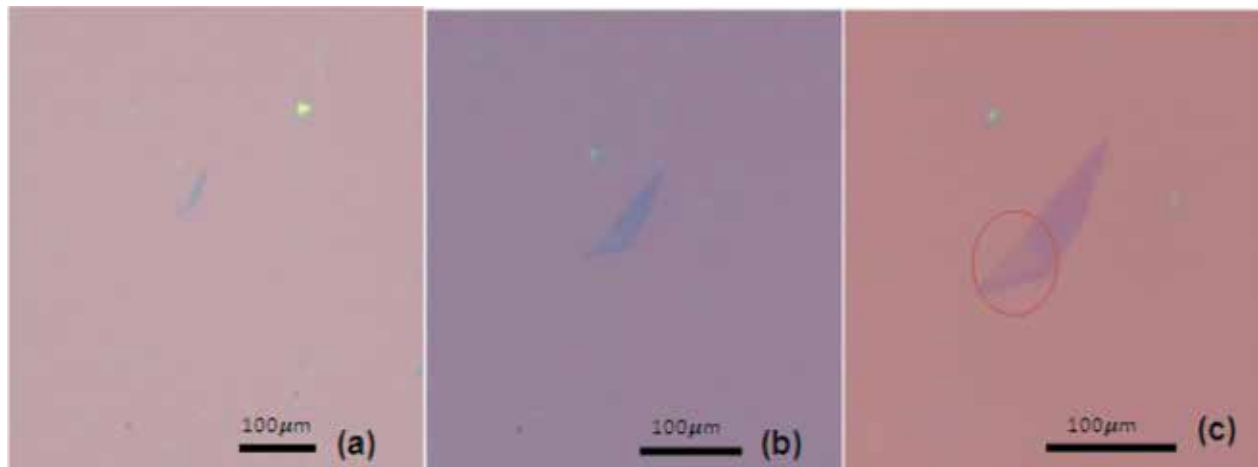
**Fig. 7.** Optical image of third flake over 90nm Si/SiO<sub>2</sub> substrate at (a) 20x (b) 50x (c) 100x.



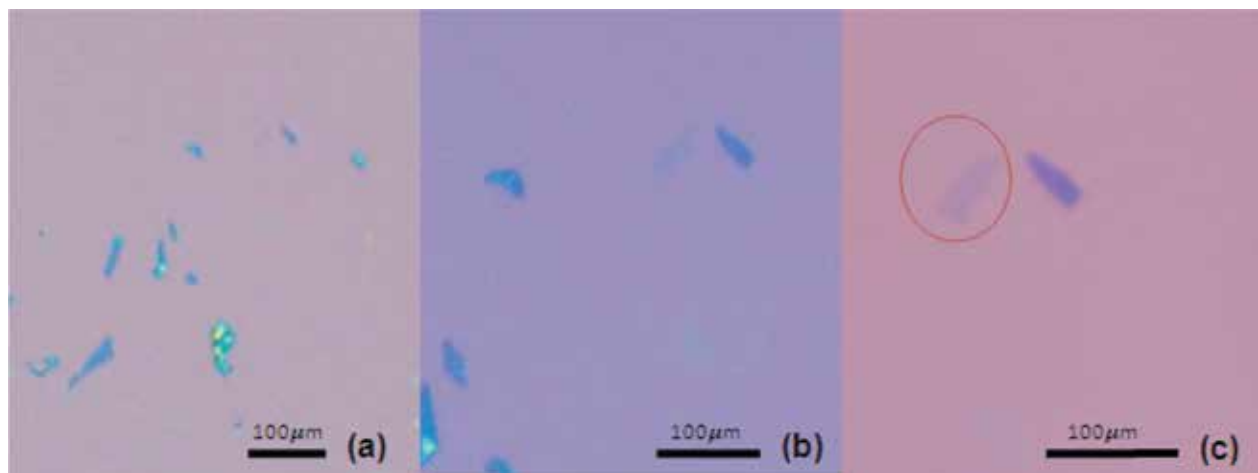
**Fig. 8.** Optical image of fourth flake over 90nm Si/SiO<sub>2</sub> substrate at: (a) 20x; (b) 50x; (c) 100x.



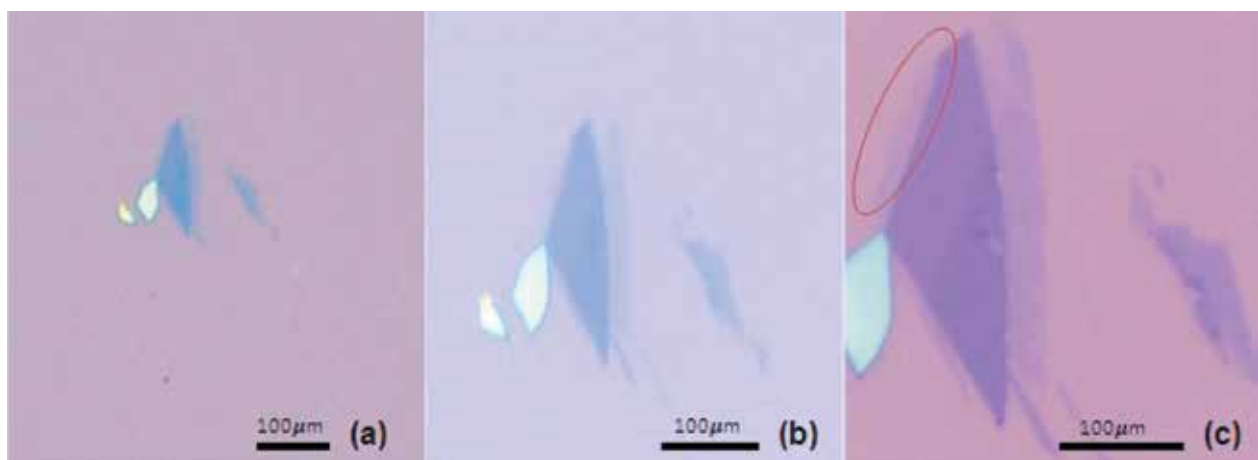
**Fig. 9.** Optical image of fifth flake over 90nm Si/SiO<sub>2</sub> substrate at: (a) 20x; (b) 50x; (c) 100x.



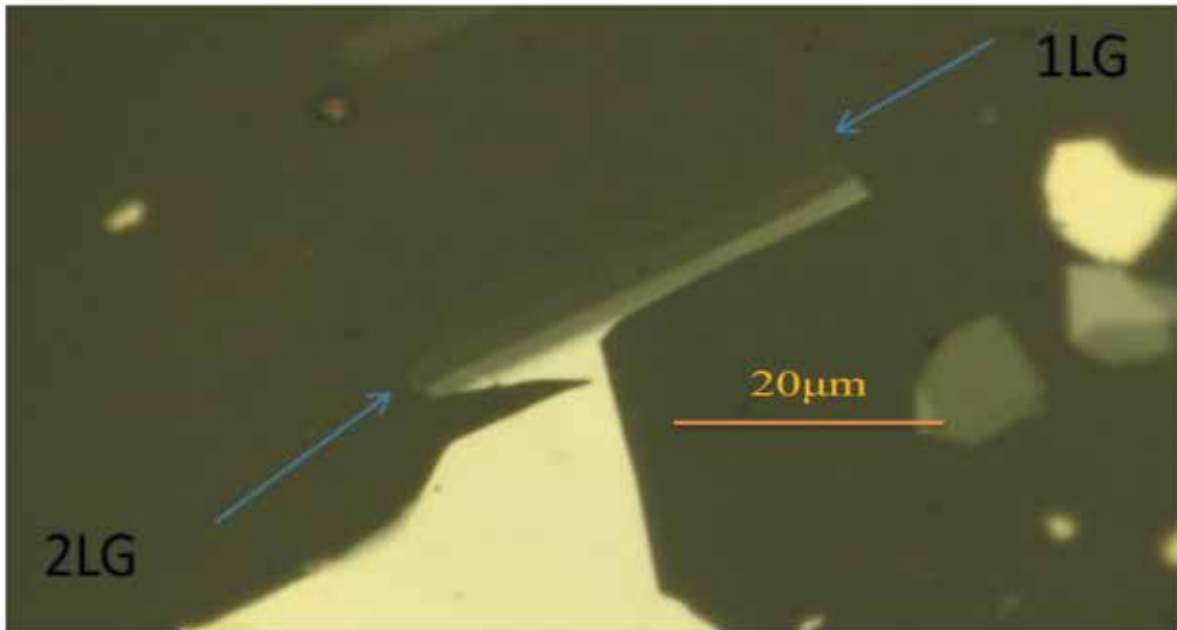
**Fig. 10.** Optical image of first flake over 300nm Si/SiO<sub>2</sub> substrate at: (a) 20x; (b) 50x; (c) 100x.



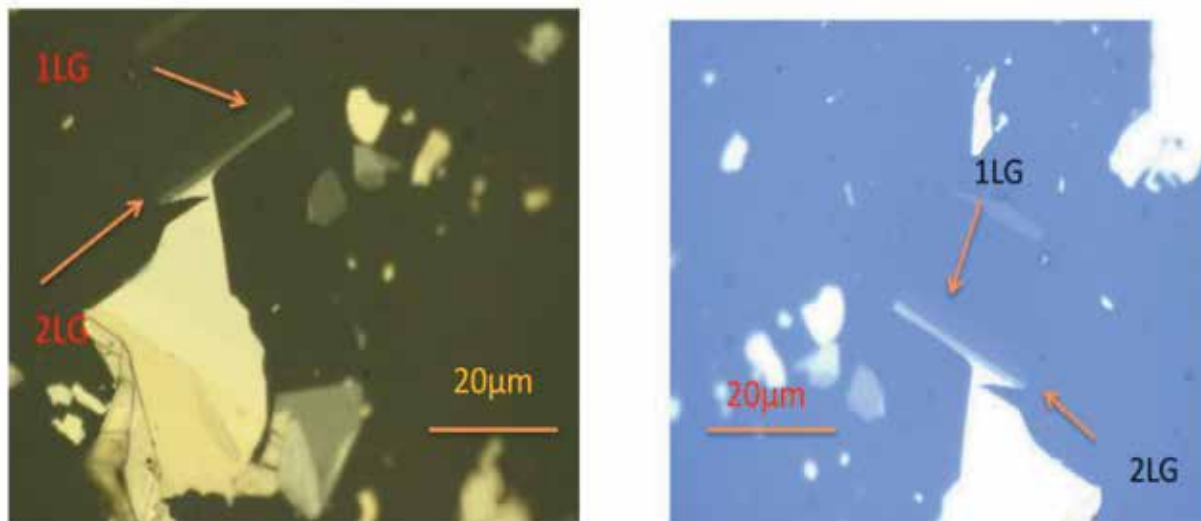
**Fig. 11.** Optical image of second flake over 300nm Si/SiO<sub>2</sub> substrate at: (a) 20x; (b) 50x; (c) 100x.



**Fig. 12.** Optical image of third flake over 300nm Si/SiO<sub>2</sub> substrate at: (a) 20x; (b) 50x; (c) 100x.



**Fig. 13.** Optical image for single (1LG), bi-layer (2LG) and few-layer graphene on PMMA substrate at 100x.



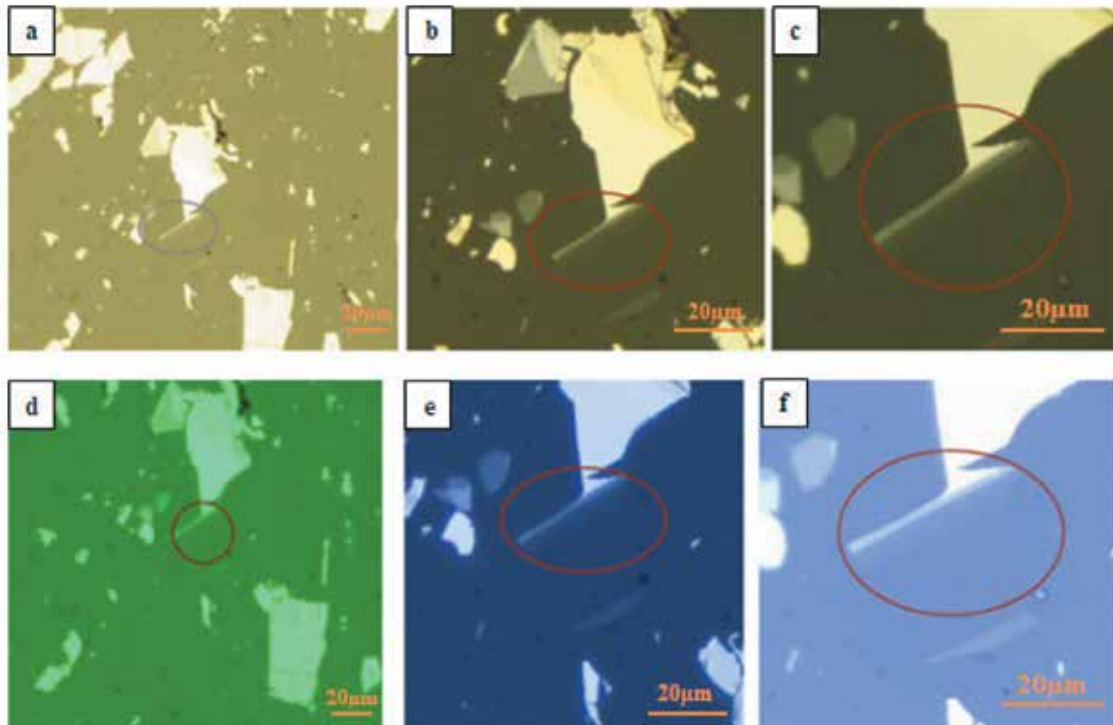
**Fig. 14.** Improvement in the optical contrast of graphene flakes using optical filter.

Fig. 17 shows the AFM analysis of graphene flake prepared on Si/SiO<sub>2</sub> substrate. When cantilever passes over the desired portion represented by the square box in Fig. 17(a), image contrast as Fig. 17(b) was obtained. By analyzing the folded region, step height of graphene layer over the substrate was obtained. The graph of Fig. 18 represents the height profile which can be used to find the number of layers. The average of these peaks is about 0.3

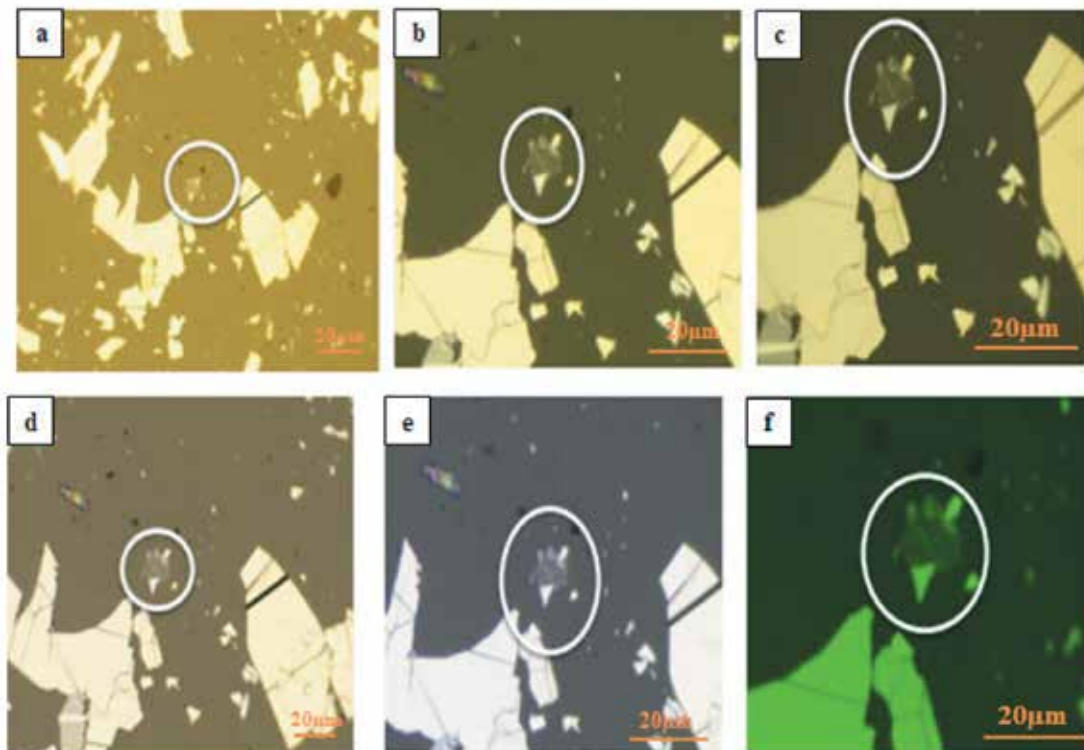
nm which clearly indicates that it is a single layer.

Fig. 19 shows the AFM analysis of another graphene flake prepared on Si/SiO<sub>2</sub> substrate. In this case, step height of about 1.0 nm was obtained which clearly shows ~ 3 layers over the substrate.

The atomic force microscopy (AFM) measurement is the most direct way to identify the number of layers of graphene. However, this is cumbersome for imaging large area graphene



**Fig. 15.** Optical images of graphene flake on PMMA substrate: (a) at 20x using white light; (b) at 50x using white light; (c) at 100x using white light; (d) at 20x with green filter; (e) at 50x with blue filter; (f) at 100x with blue filter.



**Fig. 16.** Optical images of graphene flake on PMMA substrate: (a) at 20x using white light; (b) at 50x using white light; (c) at 100x using white light; (d) at 20x with LB145 filter; (e) at 50x with LB145 filter; (f) at 100x with GB530 filter.

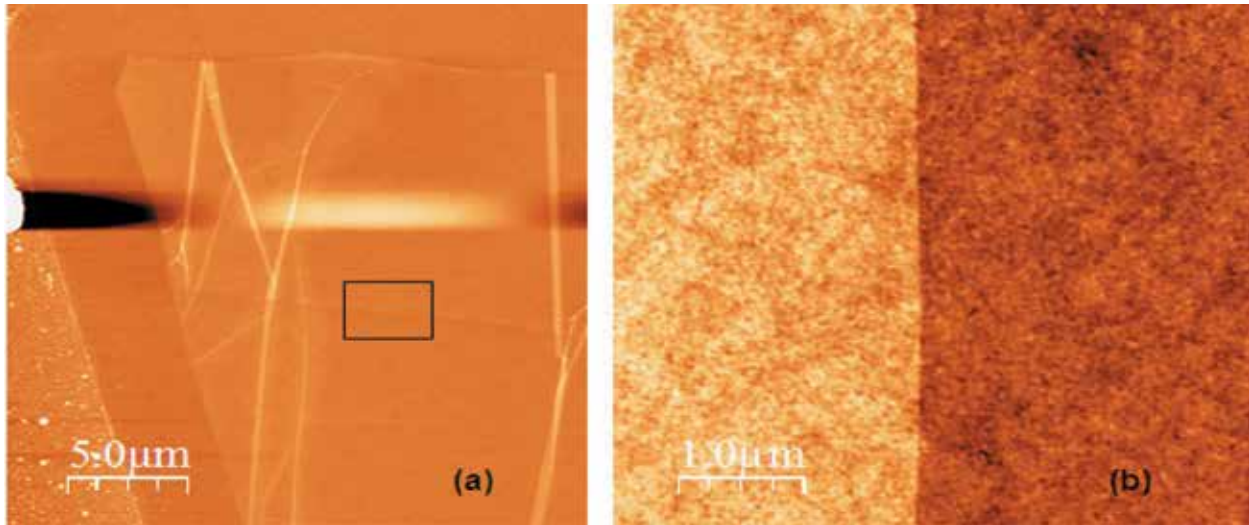


Fig. 17. AFM analysis of graphene flake.

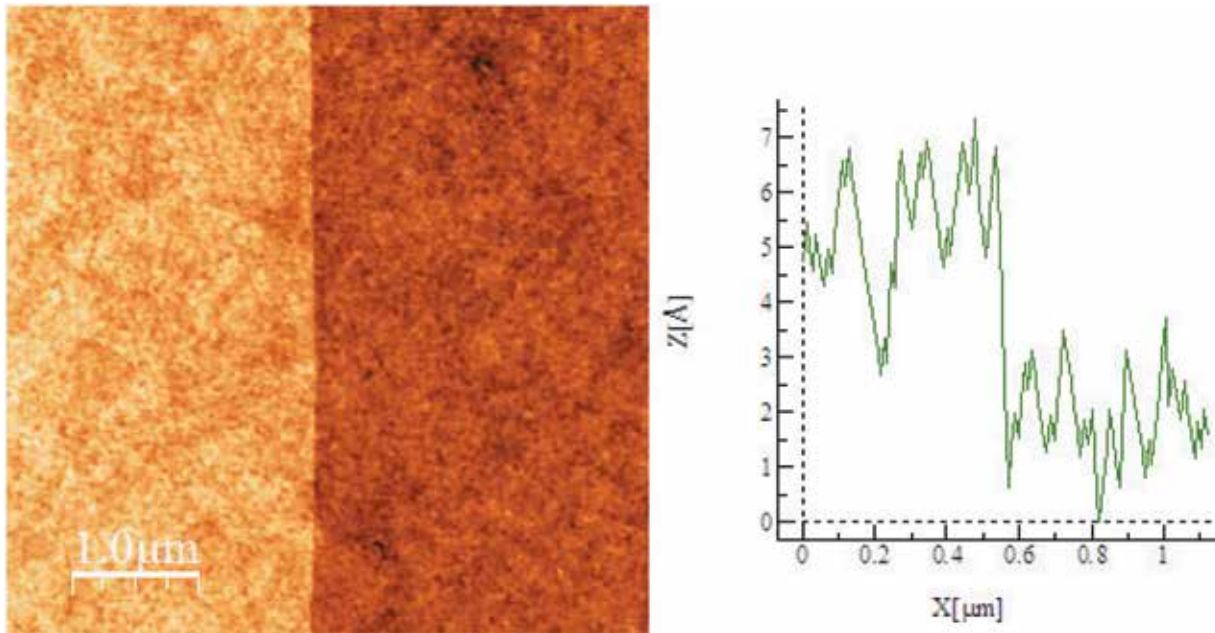


Fig. 18. Step height  $\sim 0.3$  nm (1 layer).

and also this method has a very slow throughput. Therefore, Raman spectroscopy was used because it not only determines the number of layers but also the structure of graphene.

### 3.3 Raman Spectroscopy

Raman spectroscopy is a spectroscopic technique based on inelastic scattering of monochromatic light, usually from a laser source. Inelastic scattering means that the frequency of photons in monochromatic light changes upon interaction with a sample. Raman study of single layer, bi-layer and

multilayer graphene has been reported for the first time in 2006 [19]. This is quick and unambiguous technique to provide the information about the number of layers of graphene.

In our experiment, high quality monolayer graphene was prepared on Si/SiO<sub>2</sub> by Micromechanical cleavage. Fig. 20 shows the Raman spectra of single layer graphene on Si/SiO<sub>2</sub>. Two bands (G band and 2D band) were observed on Raman spectra of graphene flake. G band is used to determine the number of graphene layers. When the layer thickness increases, the band position

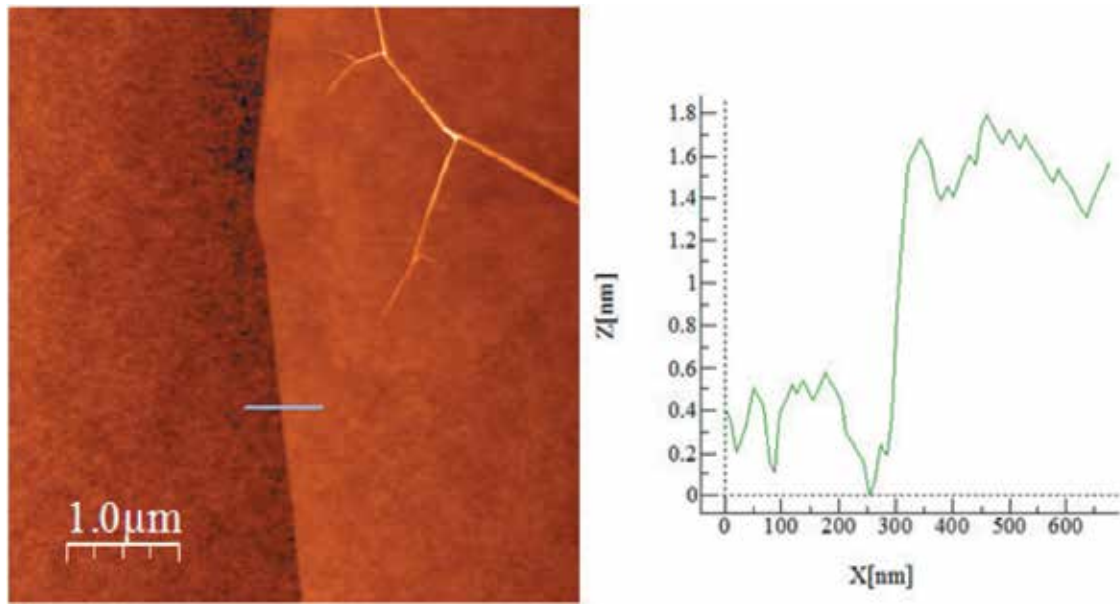


Fig. 19. Step height  $\sim 1.0$ nm (3 layers).

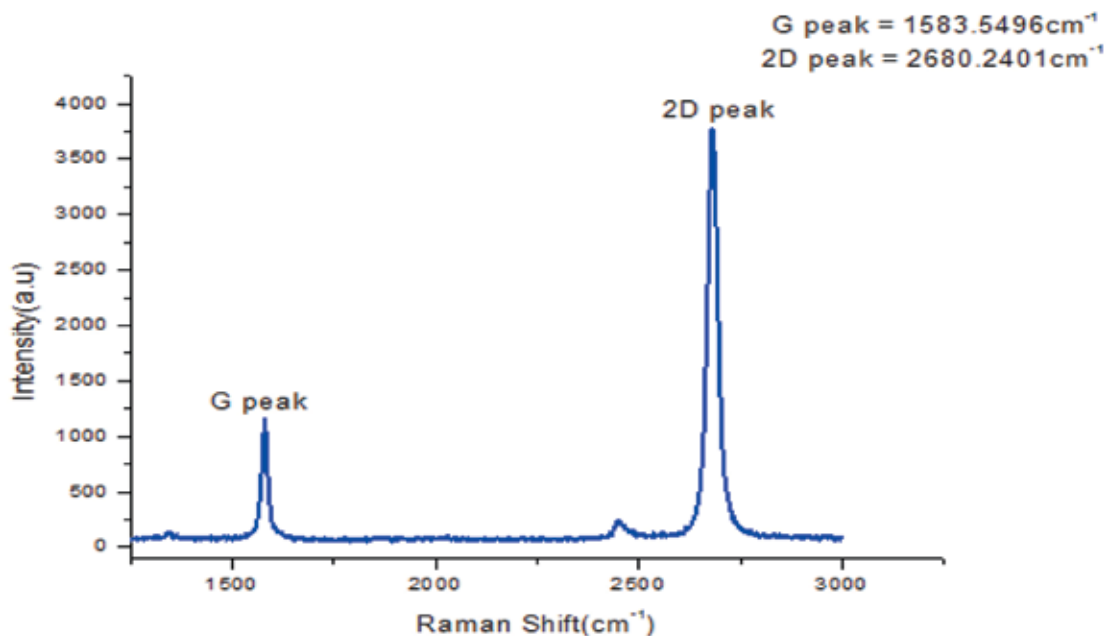


Fig. 20. Raman spectra of single layer graphene on Si/SiO<sub>2</sub> substrate.

shifts to lower intensity [19]. The G peak position is another important parameter which is sensitive to doping and strain. Doping causes the higher shift while strain causes the lower shift. 2D band which is also used to determine the number of graphene layers; however the differences between single and bilayer graphene in this band are more complex than that observed with the G-band. There is a general shifting to higher wave numbers as the layer

thickness increases, but the more noticeable change in the band shape as 2D band splits and becomes more complex for two or more layers. With single layer graphene, there is only one component to the 2D-band, but with bilayer graphene, there are three components to the 2D-band [20]. The 2D peak conventionally called G' peak in the Raman spectra of graphene layers. The intensity of the 2D peak is greater than G peak in single layer of graphene,

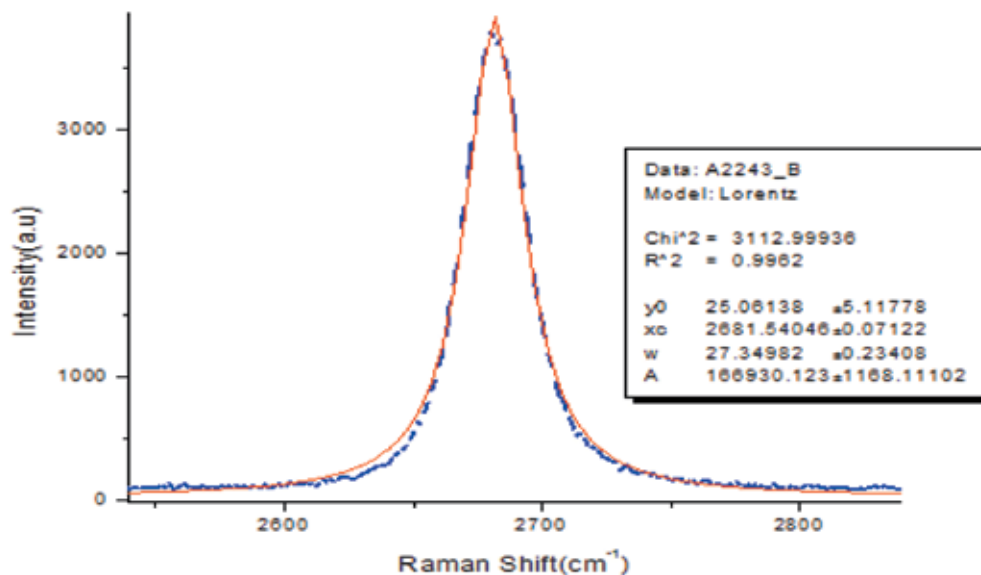


Fig. 21. Determination of width of 2D band by Lorentz fitting.

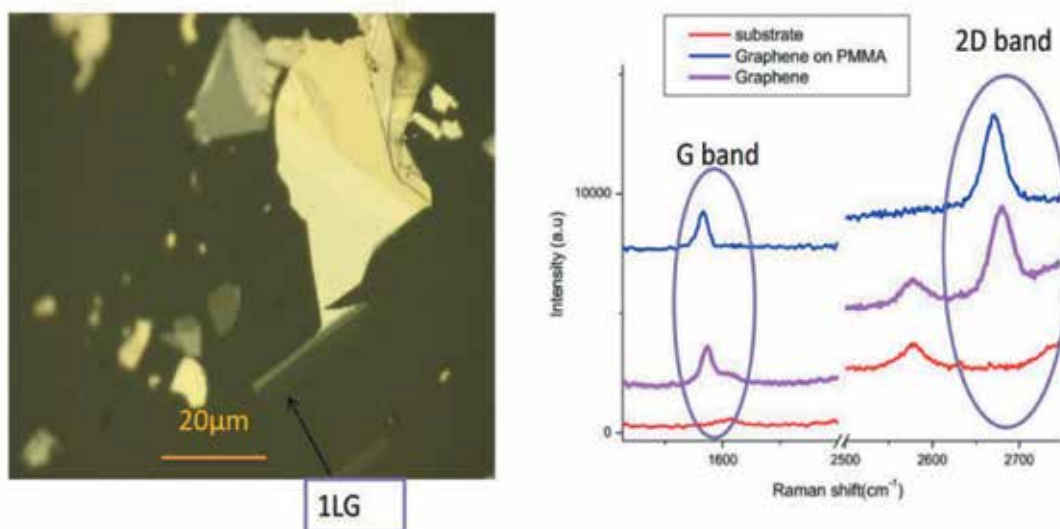


Fig. 22. Raman spectra of monolayer graphene (1LG) over PMMA substrate.

but as the number of graphene layers increased, its intensity decreased. Number of layers can be better examined by using the width of 2D peak. As the number of graphene layer increases, its width (FWHM) increases [20].

In our experiment, the peak position of G and 2D band for graphene fabricated over Si/SiO<sub>2</sub> were respectively located at 1583.54 cm<sup>-1</sup> (very close to the actual value for single layer ~ 1580 cm<sup>-1</sup> [21] and is doped) and 2680.24 cm<sup>-1</sup> (very close to the

actual value for single layer ~ 2700 cm<sup>-1</sup> [21]).

We used Lorentzian curves to fit the spectra and obtained the FWHM of 2D band as shown in Fig. 21. The FWHM of 2D band was 27.34 cm<sup>-1</sup> indicates that it is single layer [20, 22-23].

The Raman spectra of the graphene fabricated over PMMA using laser of 514 nm wavelength is shown in the Fig. 22. The prominent G peak appears at 1580 cm<sup>-1</sup> and 2D peak (G' peak) at 2680 cm<sup>-1</sup> in the monolayer of graphene. The same peak was obtained on Si/SiO<sub>2</sub> substrate, which means

that these peaks are independent of the substrates. The intensity of the G line changes with the number of graphene layers. After applying the Lorentzian in origin we have found that  $30\text{ cm}^{-1}$  is FWHM in monolayer and  $50\text{ cm}^{-1}$  in bilayer graphene over PMMA substrate.

#### 4. CONCLUSIONS

Samples of graphene have been fabricated on oxidized silicon (with 90 nm and 290 nm oxide thickness) and PMMA substrate by using micromechanical cleavage method. Micromechanical cleavage method is reproducible and yield large number of high quality graphene flakes successfully.

The graphene layers thus produced have been successfully identified and characterized using optical microscopy showing single layer, bilayer, tri-layer and multi-layer graphene by contrast analysis which shows that on 90 nm Si/SiO<sub>2</sub> substrate single layer shows the grey color and multilayer goes towards the white, on 300 nm Si/SiO<sub>2</sub> substrate single layer shows the purple color and multilayer goes towards the blue. But on PMMA substrate thin flakes show the dark grey color and thick flakes go towards the white grey. By using optical filters image quality is improved and better contrast can be obtained.

Two graphene flakes identified by optical microscopy were selected for AFM analysis. The graphene flake fabricated on 90 nm Si/SiO<sub>2</sub> substrate shows the step height  $\sim 0.3\text{ nm}$  (very close to the actual value of single layer  $\sim 0.335\text{ nm}$ ) indicates that it is single layer. The other fabricated on 300 nm Si/SiO<sub>2</sub> substrate shows the step height  $\sim 1.0\text{ nm}$  (very close to the actual value of three layers  $\sim 1.005\text{ nm}$ ) indicates that it is tri layer over the substrate.

Raman spectroscopy was performed for graphene fabricated on 90nm Si/SiO<sub>2</sub> substrate and PMMA substrate. Raman spectrum for Si/SiO<sub>2</sub> substrate shows two peaks named as G peak and 2D peak at the positions  $1583.54\text{ cm}^{-1}$  (very close to the actual value that is  $\sim 1580\text{ cm}^{-1}$ ) and  $2680.24\text{ cm}^{-1}$  (very close to the actual value that is  $\sim 2700\text{ cm}^{-1}$ ), respectively. The same peaks were

obtained for PMMA substrate named as G peak and 2D peak at the positions of  $1580\text{ cm}^{-1}$  and  $2680\text{ cm}^{-1}$  respectively. It suggests that underlying substrate does not change the graphene peaks that are G and 2D. Lorentz curve fit was applied to 2D peak to determine the width of peak as 2D width is helpful in counting the number of graphene layers. Our results give the FWHM of about  $27.34\text{ cm}^{-1}$  for graphene sampled on Si/SiO<sub>2</sub> showing mono layer. For graphene sampled on PMMA, FWHM of about  $30\text{ cm}^{-1}$  and  $50\text{ cm}^{-1}$  were obtained showing mono layer and bilayer.

#### 5. ACKNOWLEDGEMENTS

This research was supported by the Nanotechnology Center, Department of Physics, University of Engineering and Technology Lahore, Pakistan.

#### 6. REFERENCES

1. Blake, P. & E.W. Hill. Making graphene visible. *Applied Physics Letters* 91:1–4 (2007).
2. Bonaccorso, F. & Z. Sun. Graphene photonics and optoelectronics. *Nature Photonics* 4: 611–622 (2010).
3. Bae, S. & H. Kim. Roll-to-roll production of 30-inch graphene films for transparent electrodes. *Nature Nanotechnology* 5: 574–578 (2010).
4. Novoselov, K.S. Electric field effect in atomically thin carbon films. *Science* 306: 666–669 (2004).
5. Avouris, P. Graphene: electronic and photonic properties and devices. *Nano Letters* 10: 4285–4294(2010).
6. Wallace, P.R. The band theory of graphite. *Physical Review Letters* 71: 622–634 (1947).
7. McClure, J.W. Diamagnetism of graphite. *Physical Review Letters* 104: 666–671 (1956).
8. Slonczewski, J.C. & P.R. Weiss. Band structure of graphite. *Physical Review Letters* 109: 272–279 (1958).
9. Geim, A.K. & K.S. Novoselov. The rise of graphene. *Nature Materials* 6: 183–191 (2007).
10. Castro Neto, A.H. The electronic properties of graphene. *Reviews of Modern Physics* 81: 109–162 (2009).
11. Nair, R.R. Fine structure constant defines transparency of graphene. *Science* 320: 1308–1308 (2008).
12. Lee, C. & X. Wei. Measurement of the elastic properties and intrinsic strength of monolayer graphene. *Science* 321: 385–388 (2008).
13. Huang, X. & X. Qi. Graphene-based composites. *Chemical Society Reviews* 41: 666–686 (2011).

14. Lin, Y.M. 100-GHz transistors from wafer-scale epitaxial graphene. *Science* 327: 662 (2010).
15. Wu, Y. & Y. Lin. High frequency, scaled graphene transistor on diamond like carbon. *Nature* 472: 74-78 (2011).
16. Liao, L. & Y.C. Lin. High speed graphene transistors with a self-aligned nanowire gate. *Nature* 467: 305-308 (2010).
17. Novoselov, K.S. & V.I. Falko. A roadmap for graphene. *Nature* 490: 192-200 (2012).
18. Wang, Y. Understanding tapping-mode atomic force microscopy data on the surface of soft block copolymers. *Surface Science* 530: 136-148 (2003).
19. Ferrari, A.C. & J.C. Meyer. Raman spectrum of graphene and graphene layers. *Physical Review Letters* 97: 1-4 (2006).
20. Park, J.S. & A. Reina. G' band raman spectra of single, double and triple layer graphene. *Carbon* 47: 1303-1310 (2009).
21. Vidano, R.P. Observation of raman band shifting with excitation wavelength for carbons and graphites. *Solid State Communications* 39: 341-344 (1981).
22. Malard, L.M. & M.A. Pimenta. Raman spectroscopy in graphene. *Physics Reports* 473: 51-87 (2009).
23. Graf, D. & F. Molitor. Spatially resolved raman spectroscopy of single- and few-layer graphene. *Nano Letters* 7: 238-242 (2007).





# Product and Exponential Product Estimators in Adaptive Cluster Sampling under Different Population Situations

Muhammad Shahzad Chaudhry<sup>1\*</sup>, and Muhammad Hanif<sup>2</sup>

<sup>1</sup>Department of Statistics, Government College University, Lahore, Pakistan

<sup>2</sup>National College of Business Administration & Economics, Lahore, Pakistan

**Abstract:** In this paper, the product and exponential product estimators have been proposed for estimating the population mean using population mean of an auxiliary variable, when there is negative correlation between the variables, under adaptive cluster sampling (ACS) design. The expressions for mean squared error (MSE) and bias of the proposed estimators have been derived. Two simulated populations are used and simulation studies have been conducted out to reveal and match the efficiencies of the estimators. The proposed estimators have been matched with conventional estimators and estimators in ACS. The simulation results showed that the proposed product and exponential product estimators are more efficient as compare to conventional as well as Hansen-Hurwitz and ratio estimators in ACS.

**Keywords:** Auxiliary information, simulated population, transformed population, bivariate normal distribution, negative correlation, expected final sample size, comparable variance, estimated relative bias

## 1. INTRODUCTION

Sampling selects a part of population of interest to gain information about the whole. Data are often produced by sampling a population of individuals or objects. The inferences made will rely on the statistics gained from the data so these inferences can only be as good as the data. The sampling design refers to the method used to select the sample from the population. Deprived sampling design can produce deceptive conclusions. In conventional sampling designs the sample size is determined prior to the survey. In these designs the sampling units are independent on observations gathered throughout the survey.

A main problem that arises in survey sampling is estimation of the density of rare and clustered population, such as plants, birds and animals of scarce and dying out species, fisheries, patchy minerals exploration, toxic waste concentrations, drug addicted, and AIDS patients. The traditional random sampling designs may be inefficient and frequently not succeed to offer samples with useful information for rare population, because it is possible that the majority of the sampled elements give no information [1].

The Adaptive Cluster Sampling (ACS) design is appropriate for the scarce and bunched population. In ACS, a first sample is selected with a usual sampling design then the vicinity of every element selected in first sample is considered. If the observed values of the study variable satisfy a specific condition  $C$ , say  $y_i > C$  then the additional units in the neighbourhood of the  $i$ th units is sampled. Each neighbouring element is included and investigated if the predefined condition  $C$  is fulfilled and the procedure keep on until a new unit does not satisfy the condition. It is a type of network sampling, which provides improved estimates as compared to conventional designs in case of clustered rare population. All the units studied (including the initial sample) compose the final sample. The set consisting on those elements that met the condition are called a network. The elements that are fails to fulfil the condition are called edge units. Clusters are grouping of networks and edge units.

Thompson [2] first proposed the idea of the ACS scheme and introduced modified Hansen-Hurwitz [3]

and Horvitz-Thompson [4] form estimators. Dryver [5] established that ACS performed extraordinary in univariate situation but in the multivariate setting, the efficiency of ACS depended on the relationship of the variables. The simulation results for actual data of blue-winged and red-winged showed that Horvitz-Thompson [4] form of estimator was the mainly efficient estimator in certain conditions. Dryver and Chao [6] proposed the conventional ratio estimator in ACS and also proposed two more ratio estimators.

### ***Adaptive Cluster Sampling Process***

Consider a fixed population of  $N$  elements labelled  $1, 2, 3, \dots, N$  are denoted as  $u = \{u_1, u_2, \dots, u_N\}$ . Consider a small initial sample of size  $n$  which is selected from  $N$  by simple random sample without replacement (srswor). The first sample is chosen by traditional sampling process in an ACS procedure and then the predefined neighbouring units for all the units of the first sample are considered for a particular condition  $C$ . If any of the elements in the first sample satisfy condition  $C$  there neighbouring elements are included to the sample and observed. In general, if the characteristic of interest is found at a particular area then we continue to locate around that area for more information. Further, if any neighbouring unit satisfies the condition then its neighbourhoods are also sampled and the process goes on. This iterative process stops when the new unit does not satisfy condition  $C$ . The vicinity can be decided in two ways. The sampling element and four neighbouring elements are known as the first-order neighbourhood denoted by east, west, north, and south. The first-order neighbouring elements and the elements northeast, northwest, southeast, and southwest are known as second-order neighbourhood. There are in total eight neighbourhood quadrats including the first-order neighbourhood and the second order neighbourhood. All the units including the initial sample composed the final sample.

A network consists of elements that satisfy the specified condition (usually  $y = 1$ ). The networks of size one are those elements which fail to meet the predefined condition  $C$  in the first sample. The edge units are those which do not satisfy the specified criteria. A cluster is a mixture of network units with associated edge units. Clusters may have overlapping edge units. The networks do not have common elements such that the union of the networks becomes the population. Thus, it is possible to partition the population of all elements in a form of exclusive and entire networks. The networks related to clusters can be denoted by  $A_1, A_2, A_3, \dots, A_n$  or they can be shown with darker lines around the quadrats. These may be shaded as well. The edge units can be denoted with open circles ( $\circ$ ). The entire region is partitioned into  $N$  rectangular or square units of equal size that can be set in a lattice system. The rectangular or square units are called quadrats. The units  $(u_1, u_2, \dots, u_N)$  form a disjoint and comprehensive partition of the entire area so that units labels  $(1, 2, \dots, N)$  categorise the position of  $N$  quadrats. In ACS the population is measured in terms of quadrats only.

## **2. MATERIALS AND METHODS**

### **2.1 Some Estimators in Simple Random Sampling**

Let  $N$  be the entire number of elements in the population. A random sample of size  $n$  is selected by using srswor. The study variable and auxiliary variable are represented by  $y$  and  $x$  with the population means  $\bar{Y}$  and  $\bar{X}$ , population standard deviation  $S_y$  and  $S_x$  and coefficient of variation  $C_y$  and  $C_x$  respectively. Also let  $\rho_{xy}$  denote population correlation coefficient between  $X$  and  $Y$ . The sample means of the study and auxiliary variables are denoted by  $\bar{y}$  and  $\bar{x}$  respectively. Cochran [7] and Robson [8] proposed the classical ratio and classical product estimators, respectively, for estimating the population mean stated as follows:

$$t_1 = \bar{y} \left[ \frac{\bar{X}}{\bar{x}} \right], \quad (1)$$

and 
$$t_2 = \bar{y} \left[ \frac{\bar{x}}{\bar{X}} \right]. \quad (2)$$

The mean squared error (MSE) of the estimators (1) and (2) are given by:

$$\text{MSE}(t_1) \approx \theta \bar{Y}^2 \left[ C_y^2 + C_x^2 - 2\rho_{xy} C_x C_y \right], \tag{3}$$

and 
$$\text{MSE}(t_2) \approx \theta \bar{Y}^2 \left[ C_y^2 + C_x^2 + 2\rho_{xy} C_x C_y \right], \tag{4}$$

respectively. Where  $\theta = \frac{1}{n} - \frac{1}{N}$ . The ratio and product estimators are design biased.

Bahl and Tuteja [9] proposed the exponential ratio and exponential product estimators to estimate the population mean are given by:

$$t_3 = \bar{y} \exp \left[ \frac{\bar{X} - \bar{x}}{\bar{X} + \bar{x}} \right], \tag{5}$$

$$t_4 = \bar{y} \exp \left[ \frac{\bar{x} - \bar{X}}{\bar{X} + \bar{x}} \right]. \tag{6}$$

The MSE and bias of the exponential ratio estimator  $t_3$  are as follows:

$$\text{MSE}(t_3) \approx \theta \bar{Y}^2 \left[ C_y^2 + \frac{C_x^2}{4} - \rho_{xy} C_x C_y \right], \tag{7}$$

$$\text{Bias}(t_3) \approx \theta \bar{Y} \left[ \frac{3}{8} C_x^2 - \frac{\rho_{xy} C_x C_y}{2} \right]. \tag{8}$$

The MSE and bias of the exponential product estimator  $t_4$  are given by:

$$\text{MSE}(t_4) \approx \theta \bar{Y}^2 \left[ C_y^2 + \frac{C_x^2}{4} + \rho_{xy} C_x C_y \right], \tag{9}$$

$$\text{Bias}(t_4) \approx \theta \bar{Y} \left[ -\frac{1}{8} C_x^2 + \frac{\rho_{xy} C_x C_y}{2} \right]. \tag{10}$$

### 2.2 Some Estimators in Adaptive Cluster Sampling

Let a preliminary sample of  $n$  elements is selected with a srswor from a finite population of size  $N$  categorized like  $1, 2, 3, \dots, N$ . The average  $y$ -value and average  $x$ -value in the network which includes unit  $i$

are  $w_{yi} = \frac{1}{m_i} \sum_{j \in A_i} y_j$  and  $w_{xi} = \frac{1}{m_i} \sum_{j \in A_i} x_j$  respectively. ACS can be considered as srswor when

the averages of networks are considered [1, 6]. The averages of networks are considered as transformed population. Transformed population is obtained with the replacement of the original values of the networks with the averages of the networks. In the case of transformed population is used, each sample of size one selected with srswor will be representative of the whole network if it intersect to any unit of a network. In the transformed population, the sample means of the study and auxiliary variables are

$\bar{w}_y = \frac{1}{n} \sum_{i=1}^n w_{yi}$  and  $\bar{w}_x = \frac{1}{n} \sum_{i=1}^n w_{xi}$  respectively. Consider  $C_{wy}$  and  $C_{wx}$  represents population

coefficient of variations of the study variable and auxiliary variable in the transformed population respectively and  $\rho_{wxy}$  represent population correlation coefficient between  $w_x$  and  $w_y$  in the ACS. Let us define,

$$\bar{e}_{wy} = \frac{\bar{w}_y - \bar{Y}}{\bar{Y}} \text{ and } \bar{e}_{wx} = \frac{\bar{w}_x - \bar{X}}{\bar{X}}. \tag{11}$$

Where  $\bar{e}_{wy}$  and  $\bar{e}_{wx}$  are relative sampling errors of the study variable and auxiliary variable respectively, such that:

$$E(\bar{e}_{wy}) = E(\bar{e}_{wx}) = 0 \text{ and } E(\bar{e}_{wx}\bar{e}_{wy}) = \theta \rho_{wxwy} C_{wx} C_{wy} \quad (12)$$

$$E(\bar{e}_{wy}^2) = \theta C_{wy}^2 \text{ and } E(\bar{e}_{wx}^2) = \theta C_{wx}^2 \quad (13)$$

Thompson [2] proposed an unbiased modified Hansen-Hurwitz [3] estimator for population mean in ACS and can be used as sampling done with replacement or without replacement. Elements that do not meet the condition  $C$  are ignored if these elements are not selected in the preliminary sample. In the form of  $n$  networks (which possibly will not be exclusive) overlapped by the preliminary sample (because transformed population is used, ACS becomes srswor and each unit selected will represent a whole network) is stated as follows:

$$t_5 = \frac{1}{n} \sum_{i=1}^n w_{yi} = \bar{w}_y \quad (14)$$

Where  $w_{yi} = \frac{1}{m_i} \sum_{j \in A_i} y_j$  is the average of the number of elements  $m_i$  in the network  $A_i$ .

The variance of  $t_5$  is given by:

$$Var(t_5) = \frac{\theta}{N-1} \sum_{i=1}^N (w_{yi} - \bar{Y})^2 \quad (15)$$

Dryver and Chao [6] proposed a modified ratio estimator to estimate the population mean in ACS is given by:

$$t_6 = \left[ \frac{\sum_{i \in s_0} w_{yi}}{\sum_{i \in s_0} w_{xi}} \right] \bar{X} = \hat{R} \bar{X} \quad (16)$$

Where  $\hat{R}$  is the sample ratio between  $w_{yi}$  and  $w_{xi}$ .

The MSE of  $t_6$  is given by:

$$MSE(t_6) = \frac{\theta}{N-1} \sum_{i=1}^N (w_{yi} - R w_{xi})^2 \quad (17)$$

Where  $R$  is the population ratio between  $w_{yi}$  and  $w_{xi}$ .

### 2.3 Proposed Estimators in Adaptive Cluster Sampling

The proposed modified classical product estimator in ACS with one auxiliary variable is stated as follows:

$$t_7 = \bar{w}_y \frac{\bar{w}_x}{\bar{X}} \quad (18)$$

Following the Bahl and Tuteja [9], the proposed exponential product estimator in ACS with one auxiliary variable is stated as follows:

$$t_8 = \bar{w}_y \exp \left[ \frac{\bar{w}_x - \bar{X}}{\bar{w}_x + \bar{X}} \right] \quad (19)$$

**2.3.1 Bias and Mean Square Error of Proposed Product Estimator  $t_7$**

Using (11) the estimator (18) may be written as follows:

$$t_7 = \bar{Y} (1 + \bar{e}_{wy}) \frac{\bar{X}(1 + \bar{e}_{wx})}{\bar{X}}, \tag{20}$$

so,  $t_7 = \bar{Y} [1 + \bar{e}_{wy} + \bar{e}_{wx} + \bar{e}_{wx}\bar{e}_{wy}]$ . (21)

Applying expectations on both sides of (21), and using the notations (12) we get as follows:

$$\text{Bias } t_7 = E(t_7 - \bar{Y}) = \bar{Y} \theta \rho_{wxwy} C_{wx} C_{wy}. \tag{22}$$

In order to derive MSE of (18), we have (23) by ignoring the term degree 2 or greater as follows:

$$t_7 = \bar{Y} [1 + \bar{e}_{wy} + \bar{e}_{wx}], \tag{23}$$

$$t_7 - \bar{Y} = [\bar{e}_{wy} + \bar{e}_{wx}]. \tag{24}$$

Taking square and expectations on the both sides of (24), the obtained as follows:

$$\text{MSE}(t_7) = E(t_7 - \bar{Y})^2 \approx \bar{Y}^2 (\theta C_{wy}^2 + \theta C_{wx}^2 + 2\theta \rho_{wxwy} C_{wx} C_{wy}). \tag{25}$$

**2.3.2 Bias and Mean Square Error of the Proposed Exponential Product Estimator  $t_8$**

Using (11) the estimator (19) may be written as follows:

$$t_8 = \bar{Y} (1 + \bar{e}_{wy}) \exp \left[ \frac{\bar{X}(1 + \bar{e}_{wx}) - \bar{X}}{\bar{X}(1 + \bar{e}_{wx}) + \bar{X}} \right], \tag{26}$$

$$t_8 = \bar{Y} (1 + \bar{e}_{wy}) \exp \left[ \frac{\bar{e}_{wx}}{2} (1 + \frac{\bar{e}_{wx}}{2})^{-1} \right], \tag{27}$$

or  $t_8 = \bar{Y} (1 + \bar{e}_{wy}) \exp \left[ \frac{\bar{e}_{wx}}{2} (1 - \frac{\bar{e}_{wx}}{2} + \frac{\bar{e}_{wx}^2}{4}) \right]$ , (28)

or  $t_8 = \bar{Y} (1 + \bar{e}_{wy}) \exp \left[ \frac{\bar{e}_{wx}}{2} - \frac{\bar{e}_{wx}^2}{4} \right]$ . (29)

Expanding the exponential term up-to the second degree, we get (29) as follows:

$$t_8 \approx \bar{Y} (1 + \bar{e}_{wy}) \left[ 1 + \frac{\bar{e}_{wx}}{2} - \frac{\bar{e}_{wx}^2}{4} + \frac{\bar{e}_{wx}^2}{8} \right]. \tag{30}$$

Simplifying, ignoring the terms with degree three or greater we get as follows:

$$t_8 - \bar{Y} \approx \bar{Y} \left( \bar{e}_{wy} + \frac{\bar{e}_{wx}}{2} - \frac{\bar{e}_{wx}^2}{4} + \frac{\bar{e}_{wx}^2}{8} + \frac{\bar{e}_{wy}\bar{e}_{wx}}{2} \right). \tag{31}$$

Applying expectations on both sides of (31) as follows:

$$\text{Bias}(t_8) = E(t_8 - \bar{Y}) \approx \bar{Y} \theta \left( -\frac{C_{wx}^2}{4} + \frac{C_{wx}^2}{8} + \frac{\rho_{wxwy} C_{wx} C_{wy}}{2} \right). \tag{32}$$

In order to derive MSE of (19), we have (32) as follows:

$$t_8 \approx \bar{Y} (1 + \bar{e}_{wy}) \exp \left[ \frac{\bar{e}_{wx}}{2} (1 - \frac{\bar{e}_{wx}}{2}) \right]. \quad (33)$$

Ignoring the terms with power two or greater, we get (33) as follows:

$$t_8 \approx \bar{Y} (1 + \bar{e}_{wy}) \exp \left[ \frac{\bar{e}_{wx}}{2} \right]. \quad (34)$$

Opening the exponential term, ignoring terms with power two or more we get (34) as follows:

$$t_8 \approx \bar{Y} (1 + \bar{e}_{wy}) \left[ 1 + \frac{\bar{e}_{wx}}{2} \right], \quad (35)$$

or 
$$t_8 - \bar{Y} \approx \bar{Y} \left( \bar{e}_{wy} + \frac{\bar{e}_{wx}}{2} + \frac{\bar{e}_{wx}\bar{e}_{wy}}{2} \right). \quad (36)$$

Taking square and expectations on the both sides of (36), and using notations (12 & 13) we get as follows:

$$\text{MSE}(t_8) = E(t_8 - \bar{Y})^2 \approx \theta \bar{Y}^2 \left( C_{wy}^2 + \frac{C_{wx}^2}{4} + \rho_{wxwy} C_{wx} C_{wy} \right). \quad (37)$$

### 3. RESULTS AND DISCUSSION

#### 3.1 Simulation Study

To evaluate and match the efficiency of suggested estimators with the already existing estimators, two different types of simulated populations are used and executed simulations for the comprehensive study. The condition C for included elements in the sample is defined. To get the transformed population, the y-values are acquired and averaged for keeping the sample network with respect to the condition and for every sample network parallel x-values are obtained and averaged, then y-values and x-values are replaced with their networks averages, accordingly. For the simulation study ten thousands iteration was executed to get MSE and bias for each estimator with the srswor and the initial sample sizes of 5,10,15,20 and 25 for populations 1 and 2. In ACS, the ultimate sample size is generally larger than the preliminary sample size. Let  $E(v)$  denote the expected final sample size in ACS, this is the sum of the probabilities of inclusion of all quadrats. The expected final sample size fluctuates from one sample to another sample in ACS. For the comparison, the sample mean from a srswor based on  $E(v)$  has variance using the formula stated as follows:

$$\text{Var}(\bar{y}) = \frac{\sigma^2(N - E(v))}{NE(v)} \quad (38)$$

The estimated relative bias is defined as:

$$\widehat{RBias}(t_*) = \frac{\frac{1}{r} \sum_{i=1}^r (t_*) - \bar{Y}}{\bar{Y}} \quad (39)$$

Where  $t_*$  is the value for the relevant estimator for sample  $i$ , and  $r$  is the number of iterations.

The estimated MSE of the estimated mean is given by:

$$\widehat{MSE}(t_*) = \frac{1}{r} \sum_{i=1}^r (t_* - \bar{Y})^2 \quad (40)$$

The percentage relative efficiency is given by:

$$PRE = \frac{Var(\bar{y})}{MSE(t_*)} \times 100 \tag{41}$$

**3.2 Population 1: Study Variable is Clustered and Auxiliary Variable is Binary**

Dryver and Chao [6] used blue-winged teal data (Fig. 1) collected by Smith et al. [10] as an auxiliary variable for proposed ratio estimators under ACS and compared their efficiency with conventional ratio estimator in srswor. Let  $y_i$  and  $x_i$  denote the  $i^{th}$  value for the variable of interest  $y$ , auxiliary variables  $x$  (say blue-winged teal), Dryver and Chao [6] generated the values for the variable of interest using the following two models:

$$y_i = 4x_i + \epsilon_i \quad \text{where} \quad \epsilon_i \sim N(0, x_i) \tag{42}$$

$$y_i = 4w_{xi} + \epsilon_i \quad \text{where} \quad \epsilon_i \sim N(0, w_{xi}) \tag{43}$$

0	0	3	5	0	0	0	0	0	0
0	0	0	24	14	0	0	10	103	0
0	0	0	0	2	3	2	0	13639	1
0	0	0	0	0	0	0	0	14	122
0	0	0	0	0	0	2	0	0	177

Fig. 1. Blue-Winged Teal data [10] for population.

The variability of the variable of interest  $y$  is proportional to the auxiliary variable itself in model (42) while it is proportional to the within-network mean level of the auxiliary variable in model (43). Therefore, the within network variances of the variable of interest in the networks are greatly bigger in the population produced with model (42). In this simulation study the blue-winged teal (BWT) is taken as the study variable  $y$ . To generate a data set for the auxiliary variable  $x$  (Fig. 2) that contributes high negative correlation (-0.999) correspond to the BWT data which is the variable of interest ( $y$ ), the following model is used:

$$x_i = (-1)y_i + \epsilon_i \quad \text{where} \quad \epsilon_i \sim N(0, y_i) \tag{44}$$

1	1	1	1	1	1	1	1	1	1
1	1	1	0	1	1	1	1	0	1
1	1	1	1	1	1	1	1	0	1
1	1	1	1	1	1	1	1	1	0
1	1	1	1	1	1	1	1	1	0

Fig. 2. Simulated  $x$  values, based on model (43) and using BWT data for population 1.

In model (44), the study variable  $y$  is treated as independent variable just to generate a data set for the auxiliary variable  $x$ . Then 50 is added to and divided by each value to avoid the maximum number of negative values and the remaining negative values are treated as zero. Doing so, the correlation decreases

to -0.442. Now changing the role of variables again (i.e., BWT is treated as study variable and not as an auxiliary variable) the condition for the variable of interest BWT is set as  $C \geq 10$  to added unit in the sample. There remaining only two networks with this condition but the correlation found to be -0.908 between the average values of the networks (Fig. 3, 4). Thus, there is a low correlation at a unit level but high correlation at the network level. Dryver and Chao [6] demonstrated that classical estimators in srswor execute well than ACS estimators for high correlation at unit level while execute poorer when contain the high correlation at network level.

0	0	3	5	0	0	0	0	0	0
0	0	0	19	19	0	0	2344.2	2344.2	0
0	0	0	0	2	3	2	0	2344.2	1
0	0	0	0	0	0	0	0	2344.2	2344.2
0	0	0	0	0	0	2	0	0	2344.2

Fig. 3. Transformed population-1 with average values of the networks (Wy).

1	1	1	1	1	1	1	1	1	1
1	1	1	0.5	0.5	1	1	0.33	0.33	1
1	1	1	1	1	1	1	1	0.33	1
1	1	1	1	1	1	1	1	0.33	0.33
1	1	1	1	1	1	1	1	1	0.33

Fig. 4. Transformed Population-1 with average values of the networks (Wx).

The variability of the auxiliary variable is proportional to the variable of interest in the model (44). The whole variance of the variable of interest is 3716168 whereas in the transformed population the variance decreased to 591498.701. The within network variance of the variable of interest for the network (10, 103, 13639, 14, 122, 177) is 30621746.971. An enormous part of whole variance is accounts by within network variance. Therefore, estimators in ACS are likely to be more efficient than the equivalent estimators in srs. The estimators in srs are more efficient than the estimators in ACS if within-network variances do not report a great part of the overall variance [6].

The comparative percentage relative efficiency (Table 1) of the ACS estimators is much higher than their counterpart SRS estimators. The proposed modified product  $t_7$  and exponential modified product estimator  $t_8$  in ACS has maximum percentage relative efficiency for the initial sample size and percentage relative efficiency starts increasing rapidly for comparable sample sizes. Thus, the proposed product estimator in ACS perform much superior than the other usual estimators, the ratio, and the Hansen-Hurwitz estimators in ACS when there is a high negative correlation among the study and the auxiliary variables, under the given conditions.

Table 1. Comparative percentage relative efficiencies for population1 based on E(v).

$\bar{y}$	$t_1$	$t_2$	$t_3$	$t_4$	$t_5$	$t_6$	$t_7$	$t_8$
100	59	146	79	123	110	72	158	137
100	81	117	91	109	113	88	143	130
100	88	109	95	105	123	96	152	135
100	93	106	96	103	138	114	168	151
100	95	104	98	102	159	134	189	171

The estimated relative bias (Table 2) of the estimators decreases as sample sizes increases in the ACS as well as in the srs. For ACS, as like srswor, it is suggested a bigger sample size for a small bias [11].

**Table 2.** Estimated relative bias for population 1 for different sample sizes.

n	E(v)	t <sub>1</sub>	t <sub>2</sub>	t <sub>3</sub>	t <sub>4</sub>	t <sub>5</sub>	t <sub>6</sub>	t <sub>7</sub>	t <sub>8</sub>
5	19.22	0.23	-0.17	0.12	-0.11	0	0.12	-0.12	-0.07
10	29.09	0.09	-0.09	0.04	-0.03	0	0.07	-0.05	-0.04
15	34.36	0.02	-0.05	0.03	-0.03	0	0.05	-0.03	-0.02
20	37.54	0.04	-0.03	0.02	0.00	0	0.02	-0.03	-0.01
25	39.90	0.02	-0.02	0.01	0.00	0	0.02	-0.01	-0.01

**3.3 Population 2: Study Variable is Rare Clustered and Auxiliary Variable is Abundant**

The population 2 (Fig. 5 & Fig. 6) has been generated from a bivariate normal distribution with the mean vector  $\mu$  and covariance matrix  $\Sigma$ , this is  $\begin{pmatrix} Y \\ X \end{pmatrix} \sim N(\mu, \Sigma)$ . In particular, we assumed  $\mu = (0,10)$  and  $\Sigma = \begin{pmatrix} 1 & -2 \\ -2 & 5 \end{pmatrix}$ . The condition C to included elements in the sample is  $y > 0$  for population 2. The correlation in the pair of random variables of the population was found to be -0.912. When negative values are assumed zeroes in simulated population the correlation reduces to -0.722. The correlation when the averages of the networks (Fig. 7, 8) assumed increases to -0.733.

0	0	0	0	0	0	0	0	2	0
0	0	0	0	1	0	2	0	1	1
0	1	2	0	0	1	1	0	1	1
0	1	0	0	0	1	1	0	1	0
2	0	1	0	0	0	1	2	0	0

**Fig. 5.** Simulated y values for population 2, based on bivariate normal distribution.

8	14	9	10	13	13	9	9	7	11
11	14	10	12	8	14	8	10	6	10
9	9	6	10	12	8	9	11	9	8
11	9	11	15	12	11	8	14	8	10
6	12	8	13	11	13	10	6	9	11

**Fig. 6.** Simulated x values for population 2, based on bivariate normal distribution.

0	0	0	0	0	0	0	0	1.16	0
0	0	0	0	1	0	1.29	0	1.16	1.16
0	1.33	1.33	0	0	1.29	1.29	0	1.16	1.16
0	1.33	0	0	0	1.29	1.29	0	1.16	0
2	0	1	0	0	0	1.29	1.29	0	0

Fig. 7. Transformed population-2 with average values of the networks (Wy).

8	14	9	10	13	13	9	9	8	11
11	14	10	12	8	14	8.57	10	8	8
9	8	8	10	12	8.57	8.57	11	8	8
11	8	11	15	12	8.57	8.57	14	8	10
6	12	8	13	11	13	8.57	8.57	9	11

Fig. 8. Transformed population-2 with average values of the networks (Wx).

The whole variance of the variable of interest is 0.459 while this variance reduced to 0.399 in the transformed population. The within network variances of the study variable for the network (1,1,3) is 0.333, for the network (1,1,2,1,1,2) is 0.238, and for the network (2,1,1,1,1,1) is 0.167. The network variances do not accounts a huge part of whole variance. The overall variance is found to be high as compare to the within network variances for the study variable. Thus, adaptive estimators are expected to perform worse than the comparable usual estimators. The usual estimators will be more efficient than the adaptive estimators if within-network variances do not account for a huge part of the overall variance [6].

The percentage relative efficiency (Table 3) of the ACS estimators is much lower than the SRS estimators, as expected. The usual product estimator has maximum percentage relative efficiency, while usual exponential product estimator has higher percentage relative efficiency than the other conventional and adaptive estimators in ACS. The bias of all the estimators decreases by increasing the sample size. The estimated relative bias is given in Table 4. The bias decreases by increasing the sample size as recommended that bias decreases for large sample sizes [11].

Table 3. Comparative percentage relative efficiencies for population 2 based on E(v).

$\bar{y}$	$t_1$	$t_2$	$t_3$	$t_4$	$t_5$	$t_6$	$t_7$	$t_8$
100	71.16	131.7	84.69	116.6	22.84	16.46	29.13	25.44
100	76.32	127.3	87.16	113.6	21.29	16.82	27.09	24.16
100	77.67	125.2	88.22	113.3	20.93	16.40	26.56	23.87
100	78.21	126.7	88.83	112.6	21.38	16.76	27.04	24.61
100	79.32	125.6	88.90	112.3	22.21	17.86	28.05	25.53

**Table 4.** Estimated relative bias for population 2 for different sample sizes.

N	E(v)	$t_1$	$t_2$	$t_3$	$t_4$	$t_5$	$t_6$	$t_7$	$t_8$
5	18.25	0.05	-0.05	0.02	-0.01	0	0.04	-0.04	-0.02
10	28.79	0.02	-0.02	0.01	-0.01	0	0.02	-0.02	-0.01
15	35.05	0.01	-0.02	0.00	-0.01	0	0.02	-0.01	0.00
20	39.03	0.01	-0.01	0.00	-0.01	0	0.01	-0.01	-0.01
25	41.82	0.00	0.00	0.00	0.00	0	0.00	-0.01	0.00

#### 4. CONCLUSIONS

The performance of proposed product estimator and exponential product is better than all the other estimators including conventional as well as Hansen-Hurwitz and ratio estimators in ACS sampling for population 1. The proposed estimators become more efficient as initial sample size increases for the population 1, under the given conditions. Thus, the proposed product estimator and proposed exponential product estimator should be employed for rare and clustered population when there is negative correlation between the study variable and the auxiliary variable. The product and exponential product estimators may be studied for the population variance for negatively correlated study and auxiliary variables in ACS. Moreover, some logarithmic form of estimators may also be derived as a future research in ACS.

#### 5. ACKNOWLEDGEMENTS

The authors are indebted to Yves G. Berger, University of Southampton, UK for the programming guidance to produce populations, simulations and precious suggestions about the upgrading of this paper.

#### 6. REFERENCES

1. Thompson, S. K. *Sampling*. Wiley, New York (1992).
2. Thompson, S.K. Adaptive cluster sampling. *Journal of American Statistical Association* 85: 1050–1059 (1990).
3. Hansen, M.M. & W.N. Hurwitz. On the theory of sampling from finite population. *Annals of Mathematical Statistics* 14: 333–362 (1943).
4. Horvitz, D.G. & D.J. Thompson. A generalization of sampling without replacement from a finite universe. *Journal of American Statistical Association* 47: 663–685 (1952).
5. Dryver, A.L. Performance of adaptive cluster sampling estimators in a multivariate setting. *Environmental and Ecological Statistics* 10: 107–113 (2003).
6. Dryver, A.L. & C.T. Chao. Ratio estimators in adaptive cluster sampling. *Environmetrics* 18: 607–620 (2007).
7. Cochran, W.G. The estimation of the yields of cereal experiments by sampling for the ratio of grain to total produce. *Journal of Agricultural Sciences* 30: 262-275 (1940).
8. Robson, D.S. Application of multivariate polykeys to the theory of unbiased ratio type estimators. *Journal of American Statistical Association* 52: 511-522 (1957).
9. Bahl, S. & R.K. Tuteja. Ratio and product type exponential estimator. *Information and Optimization Sciences* 12: 159-163 (1991).
10. Smith, D.R., M.J. Conroy, & D.H. Brakhage. Efficiency of adaptive cluster sampling for estimating density of wintering waterfowl. *Biometrics* 51: 777-788 (1995).
11. Lohr, S.L. *Sampling Design and Analysis*. Pacific Grove, Duxbury Press, CA (1999).





# Matter Wave Travelling Dark Solitons in a Coupled Bose-Einstein Condensate

Muhammad Irfan Qadir\* and Sumreen Naz

Department of Mathematics, University of Engineering & Technology,  
Lahore 54890, Pakistan

**Abstract:** We investigate the existence and stability of matter wave travelling coupled dark solitons in two effectively one-dimensional parallel coupled Bose-Einstein condensates. The system can be described by linearly coupled Gross-Pitaevskii equations. In particular, we have examined the effects of changing the value of coupling strength between the condensates over the stability of travelling coupled dark solitons. It is found that the travelling coupled dark solitons are unstable but the instability of the solutions can be defeated by having a control on the coupling strength.

**Keywords:** Bose Einstein condensate, Bose-Josephson junction, dark solitons, Josephson effect, stability.

## 1. INTRODUCTION

In the last decade of the 20th century, one of the magnificent and successful achievements in the field of quantum physics was the realization of Bose-Einstein condensates (BEC) of alkali atoms [1, 2]. The first prediction about BEC was made in early 1920s by Bose and Einstein. The atoms of BEC follow Bose statistics and are linked with the essential physical phenomenon such as superconductivity in metals and superfluidity in helium [3, 4].

Dilute atomic BEC is substantially a nonlinear system that possesses the solitary wave solutions. A soliton is a localized wave which strength itself and keeps its original form unchanged when moving with fixed velocity. Solitons originate due to the balance of dispersive and nonlinear effects in the medium. They can be either bright as localized height or dark as localized depth on a continuous background. The velocity of a soliton is directly associated with its height or depth as if it is either a bright or a dark soliton respectively. Individual solitons can collide and remain unchanged in velocity, amplitude and shape but possibly not for phase shift [5].

The study of matter wave dark solitons has been a delightful area of research. The criterion for the one dimensional dynamical stability of matter wave dark soliton was presented in [6]. The snake instability was suppressed by tightly encompassing the motion in the radial direction and keeping the mean field interaction of atoms smaller than the frequency. The investigation of vortices in BEC were exhibited both theoretically and experimentally in [7].

The notion of tunneling of electrons between two superconductors linked by a very thin insulator [8] was extended to the tunneling of atoms in BEC by Smerzi et al. [9, 10, 14] and is known as the Josephson

tunneling. The experimental realization of such tunneling for a single and a collection of small Bose-Josephson junction was presented in [12]. The concept of Bose-Josephson junction was extended to long Bose-Josephson junction [13, 14]. This idea was similar to long superconducting Josephson junction. It was suggested in [13] that atomic vortices can be viewed in weakly coupled BEC and that these atomic vortices are identical to Josephson fluxon in superconducting long Josephson junction [15]. Furthermore, it was depicted that these atomic vortices can be reversibly transformed to dark soliton and the transformation can be controlled through coupling strength.

In this study, we investigate the existence and stability of travelling dark solitons in two cigar-shaped coupled BEC. Specifically, we study the effects of variation in the value of coupling parameter on the stability of matter wave travelling dark solitons moving with a particular velocity in BEC.

The paper is formatted as follows. In section 2, we consider the coupled system of nonlinear Schrodinger equations describing BEC and find the matter wave travelling coupled dark soliton solution numerically. In section 3, we discuss the stability of the travelling soliton solution while changing the coupling strength. We conclude our results in section 4.

## 2. MATHEMATICAL MODEL AND DESCRIPTION

We consider a system of two parallel cigar-shaped coupled BEC with the repulsive intra atomic interactions. The system can be described by two one-dimensional coupled nonlinear Schrodinger equations which can be written as

$$i \frac{\partial Z_1}{\partial t} = -\frac{1}{2} \frac{\partial^2 Z_1}{\partial X^2} + \mu |Z_1|^2 Z_1 - \omega Z_1 - \gamma Z_2, \quad (1)$$

$$i \frac{\partial Z_2}{\partial t} = -\frac{1}{2} \frac{\partial^2 Z_2}{\partial X^2} + \mu |Z_2|^2 Z_2 - \omega Z_2 - \gamma Z_1, \quad (2)$$

where  $Z_1$  and  $Z_2$  denote the wave functions of atoms of two BEC. The variables  $X$  and  $t$  represent respectively the space and time variables.  $\mu$  is the nonlinearity coefficient and  $\gamma$  is the coupling strength between the condensates.  $\omega$  is the chemical potential which is the rate of change of energy with respect to the number of atoms. Both  $\gamma$  and  $\omega$  can be controlled experimentally using different techniques. Typically, they can be controlled by using a combination of lasers of different intensities.

Since the soliton solutions of equations (1) and (2) are translationally invariant, this property of translational invariance motivated us to study the existence and stability of matter wave dark soliton in a moving coordinate frame of reference. So, we substitute  $x = X - vt$  in equations (1) and (2) to obtain

$$i \frac{\partial Z_1}{\partial t} = -\frac{1}{2} \frac{\partial^2 Z_1}{\partial x^2} + \mu |Z_1|^2 Z_1 - \omega Z_1 - \gamma Z_2 + iv \frac{\partial Z_1}{\partial x}, \quad (3)$$

$$i \frac{\partial Z_2}{\partial t} = -\frac{1}{2} \frac{\partial^2 Z_2}{\partial x^2} + \mu |Z_2|^2 Z_2 - \omega Z_2 - \gamma Z_1 + iv \frac{\partial Z_2}{\partial x}, \quad (4)$$

where  $v$  represents the velocity of the soliton solutions.

For the steady state solutions, we substitute  $\frac{\partial Z_1}{\partial t} = 0 = \frac{\partial Z_2}{\partial t}$  in equations (3) and (4) and acquire

$$-\frac{1}{2} \frac{\partial^2 Z_1}{\partial x^2} + \mu |Z_1|^2 Z_1 - \omega Z_1 - \gamma Z_2 + iv \frac{\partial Z_1}{\partial x} = 0, \quad (5)$$

$$-\frac{1}{2} \frac{\partial^2 Z_2}{\partial x^2} + \mu |Z_2|^2 Z_2 - \omega Z_2 - \gamma Z_1 + iv \frac{\partial Z_2}{\partial x} = 0. \quad (6)$$

Since  $Z_1$  and  $Z_2$  are complex, we substitute  $Z_1 = a_1 + ib_1$  and  $Z_2 = a_2 + ib_2$  in equations (5) and (6) and after equating real and imaginary parts on both sides, we get the following equations

$$-\frac{1}{2} \frac{\partial^2 a_1}{\partial x^2} + \mu(a_1^3 + a_1 b_1^2) - \omega a_1 - \gamma a_2 - v \frac{\partial b_1}{\partial x} = 0, \quad (7)$$

$$-\frac{1}{2} \frac{\partial^2 b_1}{\partial x^2} + \mu(b_1^3 + a_1^2 b_1) - \omega b_1 - \gamma b_2 + v \frac{\partial a_1}{\partial x} = 0, \quad (8)$$

$$-\frac{1}{2} \frac{\partial^2 a_2}{\partial x^2} + \mu(a_2^3 + a_2 b_2^2) - \omega a_2 - \gamma a_1 - v \frac{\partial b_2}{\partial x} = 0, \quad (9)$$

$$-\frac{1}{2} \frac{\partial^2 b_2}{\partial x^2} + \mu(b_2^3 + a_2^2 b_2) - \omega b_2 - \gamma b_1 + v \frac{\partial a_2}{\partial x} = 0. \quad (10)$$

We discretize equations (7), (8), (9) and (10) to obtain

$$-\frac{1}{2} \left( \frac{a_{1,j-1} - 2a_{1,j} + a_{1,j+1}}{h^2} \right) + \mu(a_{1,j}^3 + a_{1,j} b_{1,j}^2) - \omega a_{1,j} - \gamma a_{2,j} - v \left( \frac{b_{1,j+1} - b_{1,j-1}}{2h} \right) = 0, \quad (11)$$

$$-\frac{1}{2} \left( \frac{b_{1,j-1} - 2b_{1,j} + b_{1,j+1}}{h^2} \right) + \mu(b_{1,j}^3 + a_{1,j}^2 b_{1,j}) - \omega b_{1,j} - \gamma b_{2,j} + v \left( \frac{a_{1,j+1} - a_{1,j-1}}{2h} \right) = 0, \quad (12)$$

$$-\frac{1}{2} \left( \frac{a_{2,j-1} - 2a_{2,j} + a_{2,j+1}}{h^2} \right) + \mu(a_{2,j}^3 + a_{2,j} b_{2,j}^2) - \omega a_{2,j} - \gamma a_{1,j} - v \left( \frac{b_{2,j+1} - b_{2,j-1}}{2h} \right) = 0, \quad (13)$$

$$-\frac{1}{2} \left( \frac{b_{2,j-1} - 2b_{2,j} + b_{2,j+1}}{h^2} \right) + \mu(b_{2,j}^3 + a_{2,j}^2 b_{2,j}) - \omega b_{2,j} - \gamma b_{1,j} + v \left( \frac{a_{2,j+1} - a_{2,j-1}}{2h} \right) = 0, \quad (14)$$

where  $j = 1, 2, \dots, N$ . The equations (11), (12), (13) and (14) represent a nonlinear system of algebraic equations. We employ Newton's method with the Neumann boundary conditions  $Z_{n,0} = Z_{n,1}$  and  $Z_{n,N} = Z_{n,N+1}$ ,  $n = 1, 2$ , to get the travelling coupled dark soliton solutions as depicted in Fig. (1).

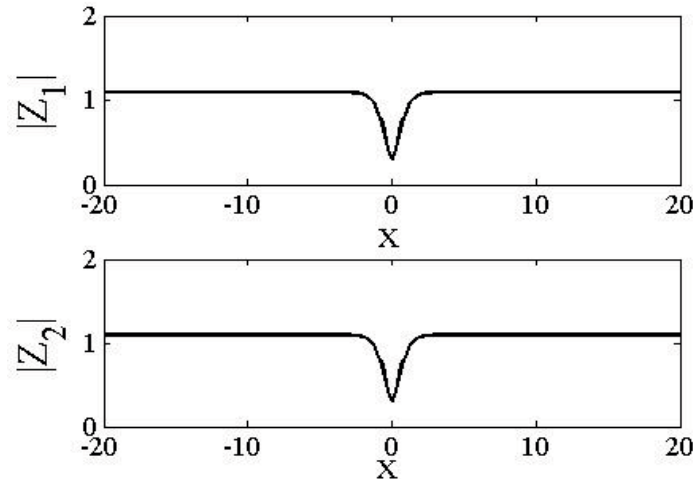


**Fig. 1.** Travelling Coupled dark soliton solution obtained numerically for the parameter values  $\mu = 1$ ,  $\omega = 1$ ,  $\gamma = 0.2$  and  $\nu = 0.3$ .

### 3. STABILITY OF TRAVELLING COUPLED DARK SOLITONS

For investigating the stability of travelling coupled dark solitons, we first assume that  $Z_1^{(0)}(x)$  and  $Z_2^{(0)}(x)$  are the steady state solutions of system of equations (3) and (4). We add very small perturbations  $p_1(x, t)$  and  $p_2(x, t)$  in these solutions  $Z_1^{(0)}$  and  $Z_2^{(0)}$  respectively, i.e.

$$Z_1(x, t) = Z_1^{(0)}(x) + p_1(x, t), \quad (15)$$

$$Z_2(x, t) = Z_2^{(0)}(x) + p_2(x, t). \quad (16)$$

We substitute the values of  $Z_1(x, t)$  and  $Z_2(x, t)$  in equations (3) and (4) and after doing linearization, we obtain

$$i \frac{\partial p_1}{\partial t} = -\frac{1}{2} \frac{\partial^2 p_1}{\partial x^2} + \mu (Z_1^{(0)})^2 \bar{p}_1 + 2\mu |Z_1^{(0)}|^2 p_1 - \omega p_1 - \gamma p_2 + i\nu \frac{\partial p_1}{\partial x}, \quad (17)$$

$$i \frac{\partial p_2}{\partial t} = -\frac{1}{2} \frac{\partial^2 p_2}{\partial x^2} + \mu (Z_2^{(0)})^2 \bar{p}_2 + 2\mu |Z_2^{(0)}|^2 p_2 - \omega p_2 - \gamma p_1 + i\nu \frac{\partial p_2}{\partial x}. \quad (18)$$

Here bar denotes the complex conjugate. Taking complex conjugate of equations (17) and (18), we get

$$-i \frac{\partial \bar{p}_1}{\partial t} = -\frac{1}{2} \frac{\partial^2 \bar{p}_1}{\partial x^2} + \mu \overline{(Z_1^{(0)})^2} p_1 + 2\mu |Z_1^{(0)}|^2 \bar{p}_1 - \omega \bar{p}_1 - \gamma \bar{p}_2 - i\nu \frac{\partial \bar{p}_1}{\partial x}, \quad (19)$$

$$-i \frac{\partial \bar{p}_2}{\partial t} = -\frac{1}{2} \frac{\partial^2 \bar{p}_2}{\partial x^2} + \mu \overline{(Z_2^{(0)})^2} p_2 + 2\mu |Z_2^{(0)}|^2 \bar{p}_2 - \omega \bar{p}_2 - \gamma \bar{p}_1 - i\nu \frac{\partial \bar{p}_2}{\partial x}. \quad (20)$$

For the sake of simplicity, we substitute  $p_1 = \delta_1$ ,  $\bar{p}_1 = \sigma_1$ ,  $p_2 = \delta_2$ ,  $\bar{p}_2 = \sigma_2$  in equations (17), (18), (19), (20) and obtain

$$i \frac{\partial \delta_1}{\partial t} = -\frac{1}{2} \frac{\partial^2 \delta_1}{\partial x^2} + \mu(Z_1^{(0)})^2 \sigma_1 + 2\mu|Z_1^{(0)}|^2 \delta_1 - \omega \delta_1 - \gamma \delta_2 + iv \frac{\partial \delta_1}{\partial x} = \lambda \delta_1, \quad (21)$$

$$i \frac{\partial \delta_2}{\partial t} = -\frac{1}{2} \frac{\partial^2 \delta_2}{\partial x^2} + \mu(Z_2^{(0)})^2 \sigma_2 + 2\mu|Z_2^{(0)}|^2 \delta_2 - \omega \delta_2 - \gamma \delta_1 + iv \frac{\partial \delta_2}{\partial x} = \lambda \delta_2, \quad (22)$$

$$i \frac{\partial \sigma_1}{\partial t} = \frac{1}{2} \frac{\partial^2 \sigma_1}{\partial x^2} - \mu(\overline{Z_1^{(0)}})^2 \delta_1 - 2\mu|Z_1^{(0)}|^2 \sigma_1 + \omega \sigma_1 + \gamma \sigma_2 + iv \frac{\partial \sigma_1}{\partial x} = \lambda \sigma_1, \quad (23)$$

$$i \frac{\partial \sigma_2}{\partial t} = \frac{1}{2} \frac{\partial^2 \sigma_2}{\partial x^2} - \mu(\overline{Z_2^{(0)}})^2 \delta_2 - 2\mu|Z_2^{(0)}|^2 \sigma_2 + \omega \sigma_2 + \gamma \sigma_1 + iv \frac{\partial \sigma_2}{\partial x} = \lambda \sigma_2, \quad (24)$$

where the scalar  $\lambda$  represents the eigenvalues. We discretize the above four equations to get

$$-\frac{1}{2} \left( \frac{\delta_{1,j-1} - 2\delta_{1,j} + \delta_{1,j+1}}{h^2} \right) + \mu(Z_{1,j}^{(0)})^2 \sigma_{1,j} + 2\mu|Z_{1,j}^{(0)}|^2 \delta_{1,j} - \omega \delta_{1,j} - \gamma \delta_{2,j} + iv \left( \frac{\delta_{1,j+1} - \delta_{1,j-1}}{2h} \right) = \lambda \delta_{1,j}, \quad (25)$$

$$-\frac{1}{2} \left( \frac{\delta_{2,j-1} - 2\delta_{2,j} + \delta_{2,j+1}}{h^2} \right) + \mu(\overline{Z_{2,j}^{(0)}})^2 \sigma_{2,j} + 2\mu|Z_{2,j}^{(0)}|^2 \delta_{2,j} - \omega \delta_{2,j} - \gamma \delta_{1,j} + iv \left( \frac{\delta_{2,j+1} - \delta_{2,j-1}}{2h} \right) = \lambda \delta_{2,j}, \quad (26)$$

$$\frac{1}{2} \left( \frac{\sigma_{1,j-1} - 2\sigma_{1,j} + \sigma_{1,j+1}}{h^2} \right) - \mu(\overline{Z_{1,j}^{(0)}})^2 \delta_{1,j} - 2\mu|Z_{1,j}^{(0)}|^2 \sigma_{1,j} + \omega \sigma_{1,j} + \gamma \sigma_{2,j} + iv \left( \frac{\sigma_{1,j+1} - \sigma_{1,j-1}}{2h} \right) = \lambda \sigma_{1,j}, \quad (27)$$

$$\frac{1}{2} \left( \frac{\sigma_{2,j-1} - 2\sigma_{2,j} + \sigma_{2,j+1}}{h^2} \right) - \mu(\overline{Z_{2,j}^{(0)}})^2 \delta_{2,j} - 2\mu|Z_{2,j}^{(0)}|^2 \sigma_{2,j} + \omega \sigma_{2,j} + \gamma \sigma_{1,j} + iv \left( \frac{\sigma_{2,j+1} - \sigma_{2,j-1}}{2h} \right) = \lambda \sigma_{2,j}, \quad (28)$$

where  $j = 1, 2, \dots, N$ . Applying the Neumann boundary conditions  $\delta_{n,0} = \delta_{n,1}$  and  $\sigma_{n,N} = \sigma_{n,N+1}$ ,  $n = 1, 2$ , the above system of equations (25), (26), (27) and (28) can be written as an eigenvalue problem

$$CY = \lambda Y,$$

where

$$C = \begin{bmatrix} C_1 & -E & D_1 & 0 \\ -E & C_2 & 0 & D_2 \\ -D_1 & 0 & C_3 & E \\ 0 & -D_2 & E & C_4 \end{bmatrix},$$

$$C_1 = \begin{bmatrix} \frac{1}{2h^2} + 2\mu|Z_{1,1}^{(0)}|^2 - \omega - \frac{iv}{2h} & \frac{-1}{2h^2} + \frac{iv}{2h} & 0 & 0 & \dots & 0 \\ \frac{-1}{2h^2} - \frac{iv}{2h} & \frac{1}{h^2} + 2\mu|Z_{1,2}^{(0)}|^2 - \omega & \frac{-1}{2h^2} + \frac{iv}{2h} & 0 & \dots & 0 \\ 0 & \frac{-1}{2h^2} - \frac{iv}{2h} & \frac{1}{h^2} + 2\mu|Z_{1,3}^{(0)}|^2 - \omega & \frac{-1}{2h^2} + \frac{iv}{2h} & \dots & 0 \\ \vdots & \vdots & \vdots & \vdots & \ddots & \vdots \\ 0 & 0 & \dots & \frac{-1}{2h^2} - \frac{iv}{2h} & \dots & \frac{1}{2h^2} + 2\mu|Z_{1,N}^{(0)}|^2 - \omega + \frac{iv}{2h} \end{bmatrix},$$

$$C_2 = \begin{bmatrix} \frac{1}{2h^2} + 2\mu|Z_{2,1}^{(0)}|^2 - \omega - \frac{iv}{2h} & \frac{-1}{2h^2} + \frac{iv}{2h} & 0 & 0 & \dots & 0 \\ \frac{-1}{2h^2} - \frac{iv}{2h} & \frac{1}{h^2} + 2\mu|Z_{2,2}^{(0)}|^2 - \omega & \frac{-1}{2h^2} + \frac{iv}{2h} & 0 & \dots & 0 \\ 0 & \frac{-1}{2h^2} - \frac{iv}{2h} & \frac{1}{h^2} + 2\mu|Z_{2,3}^{(0)}|^2 - \omega & \frac{-1}{2h^2} + \frac{iv}{2h} & \dots & 0 \\ \vdots & \vdots & \vdots & \vdots & \ddots & \vdots \\ 0 & 0 & \dots & \frac{-1}{2h^2} - \frac{iv}{2h} & \dots & \frac{1}{2h^2} + 2\mu|Z_{2,N}^{(0)}|^2 - \omega + \frac{iv}{2h} \end{bmatrix},$$

$$C_3 = \begin{bmatrix} -\frac{1}{2h^2} - 2\mu|Z_{1,1}^{(0)}|^2 + \omega - \frac{iv}{2h} & \frac{1}{2h^2} + \frac{iv}{2h} & 0 & 0 & \dots & 0 \\ \frac{1}{2h^2} - \frac{iv}{2h} & -\frac{1}{h^2} - 2\mu|Z_{1,2}^{(0)}|^2 + \omega & \frac{1}{2h^2} + \frac{iv}{2h} & 0 & \dots & 0 \\ 0 & \frac{1}{2h^2} - \frac{iv}{2h} & -\frac{1}{h^2} - 2\mu|Z_{1,3}^{(0)}|^2 + \omega & \frac{1}{2h^2} + \frac{iv}{2h} & \dots & 0 \\ \vdots & \vdots & \vdots & \vdots & \ddots & \vdots \\ 0 & 0 & \dots & \frac{1}{2h^2} - \frac{iv}{2h} & \dots & -\frac{1}{2h^2} - 2\mu|Z_{1,N}^{(0)}|^2 + \omega + \frac{iv}{2h} \end{bmatrix},$$

$$C_4 = \begin{bmatrix} -\frac{1}{2h^2} - 2\mu|Z_{2,1}^{(0)}|^2 + \omega - \frac{iv}{2h} & \frac{1}{2h^2} + \frac{iv}{2h} & 0 & 0 & \dots & 0 \\ \frac{1}{2h^2} - \frac{iv}{2h} & -\frac{1}{h^2} - 2\mu|Z_{2,2}^{(0)}|^2 + \omega & \frac{1}{2h^2} + \frac{iv}{2h} & 0 & \dots & 0 \\ 0 & \frac{1}{2h^2} - \frac{iv}{2h} & -\frac{1}{h^2} - 2\mu|Z_{2,3}^{(0)}|^2 + \omega & \frac{1}{2h^2} + \frac{iv}{2h} & \dots & 0 \\ \vdots & \vdots & \vdots & \vdots & \ddots & \vdots \\ 0 & 0 & \dots & \frac{1}{2h^2} - \frac{iv}{2h} & \dots & -\frac{1}{2h^2} - 2\mu|Z_{2,N}^{(0)}|^2 + \omega + \frac{iv}{2h} \end{bmatrix},$$

$$D_1 = \begin{bmatrix} \mu (Z_{1,1}^{(0)})^2 & 0 & 0 & \dots & 0 \\ 0 & \mu (Z_{1,2}^{(0)})^2 & 0 & \dots & 0 \\ 0 & 0 & \mu (Z_{1,3}^{(0)})^2 & \dots & 0 \\ & & \ddots & & \\ 0 & 0 & 0 & \dots & \mu (Z_{1,N}^{(0)})^2 \end{bmatrix},$$

$$D_2 = \begin{bmatrix} \mu (Z_{2,1}^{(0)})^2 & 0 & 0 & \dots & 0 \\ 0 & \mu (Z_{2,2}^{(0)})^2 & 0 & \dots & 0 \\ 0 & 0 & \mu (Z_{2,3}^{(0)})^2 & \dots & 0 \\ & & \ddots & & \\ 0 & 0 & 0 & \dots & \mu (Z_{2,N}^{(0)})^2 \end{bmatrix},$$

$$E = \begin{bmatrix} \gamma & 0 & 0 & \dots & 0 \\ 0 & \gamma & 0 & \dots & 0 \\ 0 & 0 & \gamma & \dots & 0 \\ & & & \ddots & \\ 0 & 0 & 0 & \dots & \gamma \end{bmatrix}.$$

The solution will be stable if all the eigenvalues are real. But, if, atleast one of the eigenvalues is imaginary, the solution will be unstable.

The eigenvalues of the stability matrix  $C$  are evaluated and are depicted in Fig. 2. It is easy to see that a few of the eigenvalues are lying vertically while all the remaining eigenvalues are lying horizontally. The eigenvalues lying vertically shows that the travelling coupled dark soliton is unstable. For the verification of the results obtained, we perform the numerical integration of the system of equations (3) and (4) by perturbing the solution shown in Fig. 1. In particular, the numerical integration is done by applying the fourth order Runge-Kutta method. The contour plot of the time evolution of travelling coupled dark soliton is shown in Fig.3. The radiation are emerging at nearly  $t = 35$  and reveals that the solution is unstable which justifies the results already obtained. The instability causes the solution to move away from the centre. Moreover, the density of the atoms in one of the panels go on increasing with time.

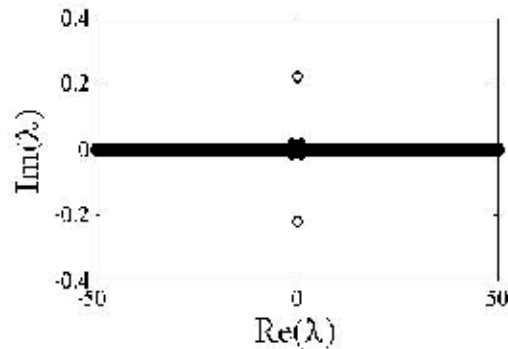


**Fig. 2.** The layout of eigenvalues for the solution presented in Fig. 1. Some of the eigenvalues are not on the horizontal axis and indicate the instability of the solution.

We then investigate the stability of the travelling coupled dark soliton for different values of velocity  $v$ . It is observed that the critical value  $\gamma_c$  of the coupling parameter  $\gamma$  at which the solution becomes stable varies with  $v$ . When  $v = 0$ , the critical value of the coupling strength is  $1/3$ . This agrees with the result in [13] and is shown in Fig. (4) by brown dotted curve. For different nonzero values of  $v$ , we find the critical values  $\gamma_c$  by plotting the stability curves as displayed in Fig. (4). One can see that  $\gamma_c$  decreases with  $v$  and tends to zero as  $v$  goes to 1. The graph of  $\gamma_c$  versus  $v$  is shown in Fig. (5). The travelling coupled dark soliton exists and is unstable below the curve while it is stable above the curve in its domain of existence. This means that the instability of travelling coupled dark soliton can be managed by having a control over the coupling strength.

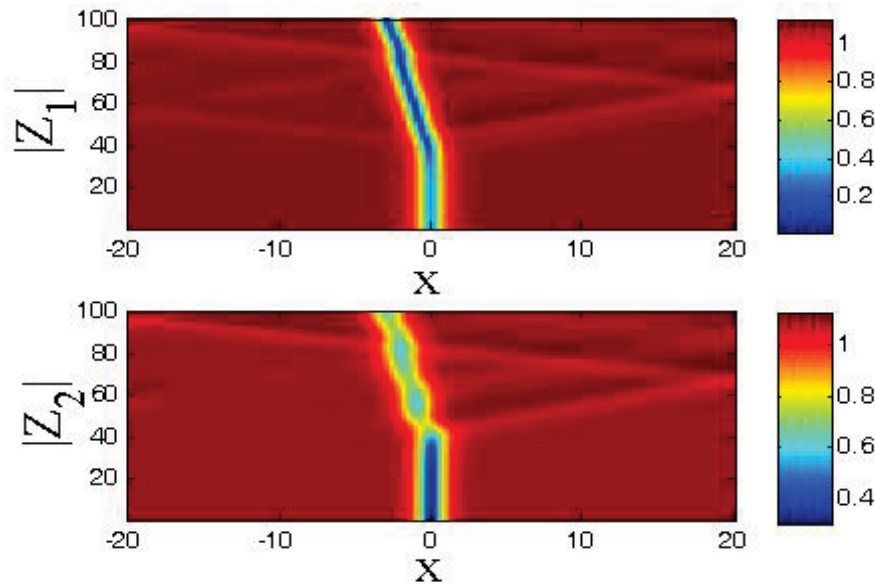


**Fig. 3.** The contour plot for the time evolution of the solution shown in Fig. (1). Radiation are emerging and the solution shifts away from the centre due to instability.

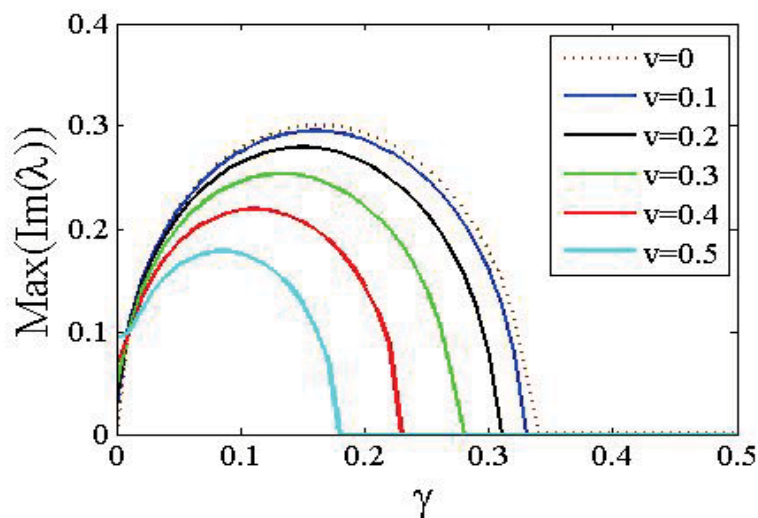


**Fig. 4.** The graph of coupling strength versus the maximum value of the imaginary parts of the eigenvalues corresponding to different values of velocity. The dotted curve is for zero velocity and shows that the value of critical coupling is  $1/3$ . The other curves correspond to the non zero velocity and depict that the value of critical coupling decreases with velocity.

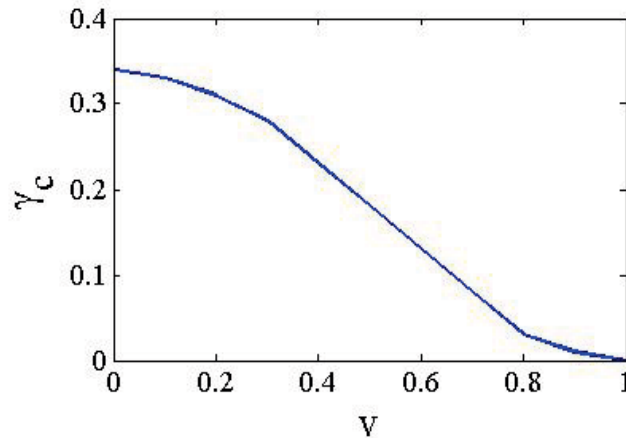


**Fig. 5.** The graph of velocity versus the corresponding values of critical coupling  $\gamma_c$ . Below the curve, the coupled dark soliton solutions exist and are unstable, while they are stable above the curve in their domain of existence.

#### 4. CONCLUSIONS

In this paper, we have examined the existence and stability of matter wave travelling coupled dark solitons in two quasi one-dimensional parallel coupled BEC. It has been found that the travelling coupled dark solitons moving with velocity  $v$  exist for  $v \leq 1$ . The stability of travelling coupled dark soliton solutions has been investigated while varying the value of coupling strength. The region in the  $v\gamma_c$  -plane was determined in which the travelling coupled dark solitons were found to be unstable. However, the instability of travelling dark soliton can be controlled through the coupling strength.

#### 5. REFERENCES

1. Anderson, M.H., J.R. Ensher, M.R. Matthews, C.E. Wieman & E.A. Cornell. Observation of Bose-Einstein condensation in a dilute atomic vapor. *Science* 269: 198-201 (1995).
2. Davis, K.B., M. -O. Mewes, M. R. Andrews, N.J. van Druten, D. S. Durfee, D. M. Kurn & W. Ketterle. Bose-Einstein condensation in a gas of sodium atoms. *Physical Review Letters* 75: 3969-3973 (1999).
3. Griffin, A., D. W. Snoke & S. Stringari. *Bose- Einstein Condensation*. Cambridge University Press, UK (1995).
4. Pethick C.J., & H. Smith. *Bose- Einstein Condensation in Dilute Gases*. Cambridge University Press, UK (2001).
5. Burger, S., K. Bongs, S. Dettmer, W. Ertmer, K. Sengstock, A. Sanpera, G. V. Shlyapnikov & M. Lewenstein. Dark solitons in Bose-Einstein condensates. *Physical Review Letters* 83: 5198-5201 (1999).
6. Muryshv, A.E., H.B. Heuvell & G.V. Shlyapnikov. Stability of standing matter waves in a trap. *Physical Review A* 60: R2665-R2668 (1999).
7. Fetter, A.L., & A.A. Svidzinsky. Vortices in a trapped dilute BEC. *Journal of Physics: Condensed Matter* 13: R135-R194 (2001).
8. Josephson, B.D.. Possible new effects in superconductive tunneling. *Physics Letters* 1: 251-253 (1962).
9. Smerzi, A., S. Fantoni, S. Giovanazzi & S.R. Shenoy. Quantum coherent atomic tunneling between two trapped Bose-Einstein condensates. *Physical Review Letters* 79: 4950-4953 (1997).
10. Raghavan, S., A. Smerzi, S. Fantoni & S. R. Shenoy. Coherent oscillations between two weakly coupled Bose-Einstein condensates: Josephson effects,  $\pi$  oscillations, and macroscopic quantum self-trapping. *Physical Review A* 59: 620-633 (1999).
11. Giovanazzi, S., A. Smerzi & S. Fantoni. Josephson effects in dilute Bose-Einstein condensates. *Physical Review Letters* 84: 4521-4524 (2000).
12. Cataliotti, F.S., S. Burger, C. Fort, P. Maddaloni, F. Minardi, A. Trombettoni, A. Smerzi & M. Inguscio. Josephson junction arrays with Bose-Einstein condensates. *Science* 293: 843-846 (2001).
13. Kaurov, V.M., & A. B. Kuklov. Josephson vortex between two atomic Bose-Einstein condensates. *Physical Review A* 71: 011601-011604 (2005).
14. Kaurov V.M., & A. B. Kuklov. Atomic Josephson vortices. *Physical Review A* 73: 013627 (2006).
15. Ustinov, A.V.. Solitons in Josephson junctions. *Physica D: Nonlinear Phenomena* 123: 315-329 (1998).





# Characterizing Semirings using Their Quasi and Bi-Ideals

Mohammad Munir<sup>\*1</sup>, and Mustafa Habib<sup>2</sup>

<sup>1</sup>Department of Mathematics, Government Postgraduate College, Abbottabad, Pakistan

<sup>2</sup>Department of Mathematics, University of Engineering and Technology, Lahore, Pakistan

**Abstract:** Quasi-ideals in a semiring are the generalization of one-sided right ideals and left ideals. Bi-ideals are generalized form of the quasi-ideals. This paper is concerned with these two types of ideals in the semirings from pure algebraic point of view. We shall characterize three important classes of semirings namely regular semirings, intra-regular semirings and weakly regular semirings by the characteristics of their quasi and bi-ideals along with their right and left-ideals.

**Keywords:** Quasi-ideal, bi-ideal, regular semiring, intra-regular semiring, weakly-regular semiring

## 1. INTRODUCTION

Regular rings were introduced by Von Neumann in 1936, in order to clarify certain aspects of Operator Algebras. Since then regular rings have been very extensively studied for their own sake and for the sake of their links with the Operator Algebras. Semirings as generalized rings having no negative elements were initially defined by Vandiver in 1934 [1]. They have wide range applications in theoretical computer science. The algorithms for dynamic programming uses the theory of semirings.

Steinfeld initially defined the quasi-ideals for semigroups and rings respectively in [2] and [3]. Iseki [4] introduced this concept for semirings without zero and proved some results. Shabir et al. [5] characterized semirings by the properties of their Quasi-ideals.

Lajos and Szasz [6] introduced the concept of bi-ideals for the associative rings. Quasi-ideals are the one-sided ideals and bi-ideals are their generalization. In this way, the study of the quasi-ideals and bi-ideals become as important as other ideals.

We present some basic concepts used in the context of semiring theory from the literature for

our later pursuit in Section 2. Section 3 deals with the characterization of regular semirings by the properties of their quasi and bi-ideals. The intra-regular and weakly regular semirings are characterized in Sections 4 and 5 respectively. For undefined terms, we refer to [7] and [8].

## 2. FUNDAMENTAL CONCEPTS

**Definition 2.1.** A semiring is a nonempty set  $A$  possessing two binary operations  $+$  (Addition) and  $*$  (Multiplication) such that  $(A, +)$  is a commutative semigroup and  $(A, *)$  is generally a non-commutative semigroup; connecting the two algebraic structures are the distributive laws;  $a(b + c) = ab + ac$  and  $(a + b)c = ac + bc$ ,  $\forall a, b, c \in A$ .

**Definition 2.2.** A subsemiring of a semiring  $(A, +, *)$  is its nonempty subset  $S$  provided it is itself a semiring under the operation of  $A$ .

**Definition 2.3.** A nonempty subset  $I$  of a semiring  $(A, +, *)$ , is called a right(left) ideal of  $A$  if it satisfies the conditions that  $x + y \in I$ ,  $x * y \in I \forall x, y \in A$ , and  $xa \in I (ax \in I), \forall x \in I, a \in A$ .  $I$  is called an ideal of  $A$  if it is both left and right ideal.

**Definition 2.4.** Let  $(A, +, *)$  be a semiring. A

quasi-ideal  $Q$  of  $A$  is a subsemigroup  $(Q, +)$  of  $A$  such that  $AQ \cap QA \subseteq Q$  [4].

Each quasi-ideal of a semiring  $A$  is its subsemiring. Every one-sided ideal of  $A$  is its quasi-ideal. Since intersection of any family of quasi-ideals of  $A$  is its quasi-ideal [5], so intersection of a right ideal  $R$  and a left-ideal  $L$  of  $A$  is a quasi-ideal of  $A$ . Both the sum and the product of two or more quasi-ideals of  $A$  need not be its quasi-ideal [5].

**Definition 2.5.** Let  $(A, +, *)$  be a semiring. A bi-ideal  $B$  is a subsemiring of  $A$  if  $BAB \subseteq B$ .

Every quasi-ideal, product of two quasi-ideals e.g., the product  $RL$  of a semiring  $A$  is its bi-ideal. However, every bi-ideal is not its quasi-ideal [5]. The product  $TB$  and  $BT$  of an arbitrary subset  $T$  and bi-ideal  $B$  of a semiring  $A$  are its bi-ideals. Since the product of two bi-ideals of a semiring is a bi-ideal, so is the intersection of their any finite or infinite family.

### 3. CHARACTERIZING REGULAR SEMIRINGS

**Definition 3.1.** An element  $a$  of a semiring  $A$  is called regular if  $axa = a$  for some  $x \in A$ . Semiring  $A$  is called regular if each element of  $A$  is regular [9]. If  $a$  is regular element, then  $ax$  and  $xa$  are idempotent as  $ax.ax = (axa)x = ax$  and  $xa.xa = x(axa) = xa$ .

We begin to characterize the regular semirings by the following theorem.

**Theorem 3.1.** *The results given below are equivalents [5]:*

- (1)  $A$  is regular,
- (2)  $RL = R \cap L$  for every right-ideal  $R$  and left-ideal  $L$  of  $A$ ,
- (3) (a).  $R^2 = R$ , (b).  $L^2 = L$ , and (c).  $RL$  is a quasi-ideal of  $A$ ,
- (4) The set of quasi-ideals of  $A$  is a regular(multiplicative) semigroup,
- (5) Each quasi-ideal  $Q$  is expressed as  $QAQ = Q$ .

**Proof.** (1)  $\Rightarrow$  (2): If  $R$  and  $L$  are respectively the right and the left ideals of  $A$ , then clearly  $RL \subseteq$

$R \cap L$ . For the converse, let  $x \in R \cap L$ , then  $x \in A$  and as  $A$  is regular, so for some  $y \in A$ , we have  $x = xyx = (xy)x \in RL$  because  $R$  is right ideal. Thus  $R \cap L = RL$ .

(2)  $\Rightarrow$  (3): Let  $RL = R \cap L$ . Since  $R \cap L$  is a quasi-ideal [5],  $RL$  is a quasi-ideal of  $A$ . Now if  $A$  is a semiring, then the ideal generated by the right ideal  $R$  is  $R + AR$ , so by (2), we have  $R = R \cap (R + AR) = R(R + AR) = R^2 + (RA)R \subseteq R^2 + R^2 \subseteq R^2$ : i.e.,  $R \subseteq R^2$ , i.e.,  $R^2 = R$ . Similarly, we can prove that  $L^2 = L$ .

(3)  $\Rightarrow$  (4): Suppose (3) holds and let  $K$  be the set of quasi-ideals of  $A$ , then  $Q + AQ$  is its left-ideal generated by  $Q$ . So by (3), we get  $Q \subseteq Q + AQ = (Q + AQ)^2 = (Q + AQ)(Q + AQ) = Q^2 + QAQ + AQQ + AQAQ \subseteq AQ + AQ + AQ + AQ \subseteq AQ$  i.e.,  $Q \subseteq AQ$ . Similarly, we can show that  $Q \subseteq QA$ . So  $Q \subseteq AQ \cap QA$ . Since  $Q$  is Quasi-ideal,  $AQ \cap QA \subseteq Q$  i.e.,

$$AQ \cap QA = Q \dots \quad (3.1)$$

Now using 3(c) and (3.1), we get

$$RL = ARL \cap ARL \dots \quad (3.2)$$

for right-ideal  $R$  and left-ideal  $L$  of  $A$ . Now we shall prove that  $Q_1Q_2$  of two quasi-ideals  $Q_1$  and  $Q_2$  is a quasi-ideal of  $A$ . By property 3(a) and 3(b), we have  $AQ_1Q_2 = (AQ_1Q_2)(AQ_1Q_2) = (AQ_1Q_2)(A.AQ_1Q_2)$ , and  $Q_1Q_2A = (Q_1Q_2A)(Q_1Q_2A) = (Q_1Q_2AA)(Q_1Q_2A)$ . Thus using Equation (3.2), we get

$$\begin{aligned} Q_1Q_2A \cap AQ_1Q_2 &= (Q_1Q_2A)(AQ_1Q_2)A \\ &\cap A(Q_1Q_2A)(AQ_1Q_2) \end{aligned}$$

$$= (Q_1Q_2A)(AQ_1Q_2) \subseteq Q_1(Q_2AQ_2) \subseteq Q_1Q_2$$

i.e.,  $(Q_1Q_2)A \cap A(Q_1Q_2) \subseteq Q_1Q_2$ . So,  $Q_1Q_2$  is a quasi-ideal of  $A$ . Since the multiplication of quasi-ideals of the semiring  $A$  is associative in  $K$ , so  $K$  is a semigroup. Finally, we shall show that  $K$  is a regular semigroup. If  $Q$  is an arbitrary quasi-ideal of  $A$ , then the properties 3(a), 3(b) and the Relations (3.1) and (3.2) imply that  $Q = QA \cap AQ = (QA.AQ)A \cap A(QA.AQ) = QA.AQ = QAQ \subseteq Q$ . So  $Q = QAQ$ . Thus  $K$  is a regular semigroup.

(4)  $\Rightarrow$  (5): Let  $Q$  be a quasi-ideal of  $A$ . By assumption (4), we can find a Quasi-ideal  $X$  of  $A$  so that  $Q = QXQ \subseteq QAQ \subseteq AQ \cap QA \subseteq Q$ ; i.e.,  $Q = QAQ$ .

(5)  $\Rightarrow$  (1): Let  $b \in A$  and  $(b)_L$  and  $(b)_R$  be the principal left-ideal and the principal right-ideal of  $A$  generated by  $b$ , then since the intersection of a left and right ideal is a Quasi-ideal, so  $(b)_L \cap (b)_R$  is a quasi-ideal of  $A$ , so by (5), we have  $(b)_L \cap (b)_R = ((b)_L \cap (b)_R)A((b)_L \cap (b)_R) \subseteq (b)_L A (b)_R$ . Since  $b \in (b)_L \cap (b)_R$ , it follows that  $b \in (b)_R A (b)_L$ . But  $(b)_R A = bA$  and  $(b)_L = Ab$ , therefore  $b \in bA(b)_L = bAb$  i.e.,  $b \in bAb$  i.e.,  $A$  is regular.

The following theorem signifies when a bi-ideal of a semiring is a quasi-ideal.

**Theorem 3.2.** *Let  $A$  be a semiring. Then the following assertions hold [5]:*

- (1) Every quasi-ideal  $Q$  of  $A$  can be written in the form as  $Q = R \cap L = RL$ , where  $R$  is the right and  $L$  is the left-ideal,
- (2) If  $Q$  is a quasi-ideal of  $A$ , then  $Q^2 = Q^3$ ,
- (3) Every bi-ideal of  $A$  is its quasi-ideal,
- (4) Every bi-ideal of any two-sided ideal of  $A$  is a quasi-ideal of  $A$ .

**Proof:** (1) Let  $A$  be a semiring and  $Q$  be a quasi-ideal of  $A$  then  $R=(Q)_r = Q + QA = QA$ , and  $L = (Q)_l = Q + AQ = AQ$ . Clearly  $Q \subseteq R \cap L = QA \cap AQ \subseteq Q$  i.e.,  $Q = R \cap L$ . But  $A$  is a regular semiring, therefore  $Q = R \cap L = RL$  by Theorem 3.2.

(2)  $Q^3 \subseteq Q^2$  always holds. We have to show that  $Q^2 \subseteq Q^3$ . By Theorem 3.1,  $Q^2$  is a quasi-ideal of  $A$ . Furthermore  $Q^2 = Q^2 A Q^2 = Q Q A Q Q \subseteq Q Q Q = Q^3$  i.e.,  $Q^2 \subseteq Q^3$ .

(3) Let  $B$  be a bi-ideal of  $A$ , then  $AB$  respectively  $BA$  are left and right-ideal of  $A$ , therefore from Theorem 3.1, we have  $BA \cap AB = BAAB = BAB \subseteq B$  i.e.,  $BA \cap AB \subseteq B$  i.e.,  $B$  is a quasi-ideal of  $A$ .

(4) Finally let  $C$  be an ideal of  $A$  and  $B$  be a bi-ideal of  $C$ . Then obviously  $C$  is a regular subsemiring of  $A$ . By (3),  $B$  is a quasi-ideal of  $C$ . Now  $BAB \subseteq BAC \subseteq CAB \subseteq BC \cap CB \subseteq B$

i.e.,  $BAB \subseteq B$  i.e.,  $B$  is a bi-ideal of  $A$ . Again by (3),  $B$  is a bi-ideal of  $A$ .

**Theorem 3.3.** *Let  $A$  be a semiring with 1, then  $A$  is a division semiring if and only if it has no proper bi-ideals.*

**Proof.** Let  $A$  be a semiring with 1 and  $B \neq 0$  be a bi-ideal of  $A$ . Let  $0 \neq b \in B$ . Since  $A$  is a division ring, so  $bA = Ab = A$ . But  $bA$  is a right-ideal and  $A$  is regular, so  $bA \cap Ab = (bA)(Ab)$  [5]. Therefore, Theorem 3.1 gives,  $A = bAb \subseteq BAB \subseteq B$  i.e.,  $A \subseteq B$ . But  $B \subseteq A$ , so  $A = B$ . Hence  $A$  has no proper bi-ideal.

Conversely, if  $A$  has no proper bi-ideal. Let  $0 \neq a \in A$ , then  $aA$  and  $Aa$  are respectively the right and left-ideal of  $A$  and so are bi-ideals. Thus either  $aA = A(Aa = A)$  or  $aA = 0(Aa = 0)$ . But  $a \in aA(a \in Aa)$ , so  $aA = A$  and  $Aa = A$ . Thus  $A$  is a division semiring.

**Theorem 3.4.** *For the semiring  $A$ , the following conditions are equivalent:*

- (1)  $A$  is regular,
- (2) For any bi-ideal  $B$  of  $A$ ,  $B = BAB$ ,
- (3) For any quasi-ideal  $Q$  of  $A$ ,  $Q = QAQ$ .

**Proof.** (1) if and only if (3) proved in Theorem 3.1. For a regular semiring, the concept of quasi-ideal coincides with the concept of bi-ideal, so (1) if and only if (2).

**Theorem 3.5.** *The following results are equivalent for a semiring  $A$  for all bi-ideals  $B$ , quasi-ideals  $Q$  and any ideal  $A$ :*

- (1)  $A$  is regular,
- (2)  $I \cap B = BIB$ ,
- (3)  $I \cap Q = QIQ$ .

**Proof:** (1)  $\Rightarrow$  (2): Suppose  $A$  is a semiring and  $I$  is any ideal of  $A$  and  $B$  is any bi-ideal of  $A$  then  $BIB \subseteq I$  and  $BIB \subseteq BAB \subseteq B$ . Thus  $BIB \subseteq I \cap B$ . Let  $x \in I \cap B$  then  $x = xyx$  for some  $y \in A$ . Now  $x = xyx = x(yxy)x \in BIB$ . Thus  $I \cap B = BIB$ .

(2)  $\Rightarrow$  (3): Let  $I$  be any ideal of  $A$  and  $Q$  any quasi-ideal of  $A$ . As every quasi-ideal is bi-ideal, therefore by (2),  $I \cap Q = QIQ$ .

(3)  $\Rightarrow$  (1): Since  $A$  is an ideal of itself, therefore by (3),  $A \cap Q = QAQ$ , i.e.,  $Q = QAQ$ . Hence by Theorem 3.1,  $A$  is a regular semiring.

**Theorem 3.6.** *The following conditions are equivalent for a semiring  $A$  for all its right-ideal  $R$ , left-ideal  $L$ , Quasi-ideal  $Q$  and bi-ideal  $B$ :*

- (1)  $A$  is regular,
- (2)  $R \cap B \subseteq RB$ ,
- (3)  $R \cap Q \subseteq RQ$ ,
- (4)  $L \cap B \subseteq BL$ ,
- (5)  $L \cap Q \subseteq QL$ ,
- (6)  $R \cap B \cap L \subseteq RBL$ ,
- (7)  $R \cap Q \cap L \subseteq RQL$ .

**Proof.** (1)  $\Rightarrow$  (2): Let  $x \in R \cap B$ , so  $x \in R$  &  $x \in B$ . Since  $A$  is regular, there is  $y \in A$  such that  $x = xyx$ . Now  $x = (xy)x \in RB$ . Thus  $R \cap B \subseteq RB$ .

(2)  $\Rightarrow$  (3): Since every quasi-ideal is a bi-ideals, therefore by (2),  $R \cap Q \subseteq RQ$ .

(3)  $\Rightarrow$  (1): Since every one-sided ideal is a quasi-ideal, therefore by (3),  $R \cap L \subseteq RL$ . But  $RL \subseteq R \cap L$ . Therefore,  $R \cap L = RL$ . Hence by Theorem 3.2,  $A$  is a regular semiring. Similarly, we can show that (1) if and only if (4) if and only if (5) if and only if (1).

(1)  $\Rightarrow$  (6):  $R \cap B \cap L \subseteq (R \cap B) \cap L \subseteq (RB) \cap L$  by (2). Now  $RB$  is a bi-ideal, so by (4),  $L \cap (RB) \subseteq (RB)L$ . Thus  $R \cap B \cap L \subseteq RBL$ .

(1)  $\Rightarrow$  (7): Since every quasi-ideal is a bi-ideal, therefore by (6),  $R \cap Q \cap L \subseteq RQL$  for right-ideal  $R$ , left-ideal  $L$  and quasi-ideal  $Q$  of  $A$ .

(7)  $\Rightarrow$  (1): Then by (7),  $R \cap A \cap L \subseteq RAL = (RA)L \subseteq RL$ . Also  $R \cap L = R \cap A \cap L$ . Thus  $R \cap L \subseteq RL$ . But  $RL \subseteq R \cap L$  always. Hence  $R \cap L = RL$ . Thus by Theorem 3.1,  $A$  is a semiring.

**Proposition 3.1.** *Let  $A$  be a semiring with multiplicative identity 1, then the*

*following are equivalent:*

(1).  $R \cap L \subseteq LR$  for any right-ideal  $R$  and left-ideal  $L$  of  $A$ ,

(2). Every  $a \in A$  can be written as  $a = \sum_{i=1}^n x_i a^2 y_i$ , where  $x_i, y_i \in A$ .

**Proof.** (1)  $\Rightarrow$  (2): let  $a \in A$ . Let  $R = aA$  and  $L = Aa$  be the right and the left-ideal generated by  $a$  respectively. Then by  $R \cap L \subseteq LR$ ,  $a \in R \cap L$   $a \in LR$ . So  $a = \sum_{i=1}^n x_i a^2 y_i$ , where  $x_i, y_i \in A$ .

(2)  $\Rightarrow$  (1): Let  $a \in R \cap L$ . Then  $a \in R$  and  $a \in L$ . By (2),  $a = \sum_{finite} x_i a^2 y_i = \sum_{finite} (x_i a)(a y_i) \in RL$ . So  $R \cap L \subseteq LR$ .

#### 4. CHARACTERIZING INTRA-REGULAR SEMIRINGS

Intra-regular semiring is also an important class of semirings which can be studied by the properties of their quasi and bi-ideals.

**Definition 4.1.** A semiring  $A$  with multiplicative identity 1 is called intra-regular if every  $a \in A$  can be written as  $a = \sum_{i=1}^n x_i a^2 y_i$ , where  $x_i, y_i \in A$ .

Thus a semiring  $A$  with multiplicative identity 1 is called intra-regular if it satisfies one of the conditions of Proposition (3.1).

The next theorem states that the bi-ideals and quasi-ideal are idempotent for intra-regular and regular semiring.

**Theorem 4.1.** *For a semiring with 1, the following are equivalents:*

- (1)  $A$  is both regular and intra-regular,
- (2)  $B^2 = B$  for every bi-ideal  $B$  of  $A$ ,
- (3)  $Q^2 = Q$  for every quasi-ideal  $Q$  of  $A$ .

**Proof:** (1)  $\Rightarrow$  (2): Let  $B$  be any bi-ideal of  $A$ , then  $B^2 \subseteq BAB$ , since  $A$  contains multiplicative identity 1. But  $BAB \subseteq B$ . Thus  $B^2 \subseteq B$ . Let  $b \in B$  then  $b = bxb$  for some  $x \in A$ , since  $A$  is regular. Also since  $A$  is intra-regular,  $b = \sum_{finite} x_i b^2 y_i$ , for some  $x_i, y_i \in A$ . Thus

$b = bxb = bxbxb = bx(\sum_{finite} x_i b^2 y_i)xb = \sum_{finite} (bxx_i b) (by_i xb)$ . Since  $b \in B$ , therefore  $b(xx_i)b \in BAB \subseteq B$  and  $b(y_i x)b \in BAB \subseteq B$ . Thus  $= \sum_{finite} (bxx_i b) (by_i xb) \in BB = B^2$ . Hence  $B \subseteq B^2$ . Consequently  $B = B^2$ .

(2)  $\Rightarrow$  (3): As every quasi-ideal is a bi-ideal, therefore by (2),  $Q = Q^2$ .

(3)  $\Rightarrow$  (1): Since  $R \cap L$  being the intersection of two quasi-ideals is a quasi-ideals, so from (3),  $R \cap L = (R \cap L)(R \cap L) \subseteq RL$ . But  $RL \subseteq R \cap L$ . So  $R \cap L = RL$ . Now from Theorem (3.1),  $A$  is regular. Now  $R \cap L = (R \cap L)^2 = (R \cap L)(R \cap L) \subseteq LR$ . So by Proposition (3.1),  $A$  is intra-regular.

**Theorem 4.2.** *The following conditions are equivalent for a semiring  $A$  with identity :*

- (1)  $A$  is both regular and intra-regular,
- (2)  $B_1 \cap B_2 \subseteq (B_1 B_2) \cap (B_2 B_1)$  for any bi-ideal  $B_1$  and  $B_2$  of  $A$ ,
- (3)  $B \cap Q \subseteq (BQ) \cap (QB)$  for any bi-ideal  $B$  and quasi-ideal  $Q$  of  $A$ ,
- (4)  $Q_1 \cap Q_2 \subseteq (Q_1 Q_2) \cap (Q_2 Q_1)$  for any quasi-ideals  $Q_1$  and  $Q_2$  of  $A$ ,
- (5)  $B \cap R \subseteq (BR) \cap (RB)$  for any bi-ideal  $B$  and right-ideal  $R$  of  $A$ ,
- (6)  $Q \cap R \subseteq (QR) \cap (RQ)$  for any quasi-ideal  $Q$  and right-ideal  $R$  of  $A$ ,
- (7)  $B \cap L \subseteq (BL) \cap (LB)$  for any bi-ideal  $B$  left-ideal  $L$  of  $A$ ,
- (8)  $Q \cap L \subseteq (BQ) \cap (QB)$  for any quasi-ideal  $Q$  and left-ideal  $L$  of  $A$ ,
- (9)  $R \cap L \subseteq (LR) \cap (RL)$  for any right-ideal  $R$  and left-ideal  $L$  of  $A$ ,

**Proof.** (1)  $\Rightarrow$  (2): Since  $B_1 \cap B_2$  is a bi-ideal of  $A$ , so by Theorem 4.2 ,  $B_1 \cap B_2 = (B_1 \cap B_2)(B_1 \cap B_2) \subseteq B_1 B_2$ . Also  $B_1 \cap B_2 \subseteq B_2 B_1$ . Thus  $B_1 \cap B_2 \subseteq (B_1 B_2) \cap (B_2 B_1)$ .

(1)  $\Rightarrow$  (3): As every quasi-ideal is bi-ideal, therefore by (2),  $B \cap Q \subseteq (BQ) \cap (QB)$ .

(2)  $\Rightarrow$  (4): As every quasi-ideal is bi-ideal, therefore by (3),  $Q_1 \cap Q_2 \subseteq (Q_1 Q_2) \cap (Q_2 Q_1)$

(3)  $\Rightarrow$  (6): As every right-ideal is quasi-ideal, therefore by (4),  $Q \cap R \subseteq (QR) \cap (QR)$ .

(6)  $\Rightarrow$  (9): As every left-ideal is quasi-ideal, therefore by (6),  $L \cap R \subseteq (LR) \cap (RL)$ .

(9)  $\Rightarrow$  (1): As  $L \cap R \subseteq (LR) \cap (RL)$ , so  $R \cap L \subseteq RL$ . But  $RL \subseteq R \cap L$ , therefore  $R \cap L = RL$ . Hence  $A$  is regular.  $R \cap L \subseteq LR$  implies that  $A$  is intra-regular. Thus we have shown that

(1)  $\Rightarrow$  (2)  $\Rightarrow$  (3)  $\Rightarrow$  (4)  $\Rightarrow$  (6)  $\Rightarrow$  (9)  $\Rightarrow$  (1). Similarly we can show that (1)  $\Rightarrow$  (2)  $\Rightarrow$  (5)  $\Rightarrow$  (9)  $\Rightarrow$  (1) and

(1)  $\Rightarrow$  (2)  $\Rightarrow$  (7)  $\Rightarrow$  (8)  $\Rightarrow$  (9)  $\Rightarrow$  (1).

**Theorem 4.3.** *The following are equivalent for a semiring  $A$  with 1 for its any right-ideal  $R$ , left-ideal  $L$ , bi-ideal  $B$  and quais-ideal  $Q$ :*

- (1)  $A$  is both regular and intra-regular,
- (2)  $B \cap L \subseteq BLB$ ,
- (3)  $B \cap R \subseteq BRB$ ,
- (4)  $Q \cap L \subseteq QLQ$ ,
- (5)  $Q \cap R \subseteq QRQ$ .

**Proof.** (1)  $\Rightarrow$  (2): Take  $a \in B \cap L$ , then  $a \in B$  &  $a \in L$ . Since  $A$  is regular and intra-regular, therefore  $a = axa$  and  $a = \sum_{finite} x_i a^2 y_i$ , where  $x, x_i, y_i \in A$ . Now  $a = axa = axaxa = ax(\sum_{finite} x_i a^2 y_i)xa = a(\sum_{finite} xx_i a^2 y_i xa) = a(\sum_{finite} xx_i a)(a y_i xa) \in BLB$ , because  $ay_i xa \in BAB \subseteq B$ .

(2)  $\Rightarrow$  (4): Since a quasi-ideal is a bi-ideal, therefore by (2),  $Q \cap L \subseteq QLQ$ .

(4)  $\Rightarrow$  (1):  $R$  being right ideal is a quasi-ideal, so by (4),  $R \cap L \subseteq RLR \subseteq LR$ . Thus by Proposition (3.1),  $A$  is intra-regular. Now let  $I$  be any ideal of  $A$ , then  $I$  is a left-ideal so by (4),  $Q \cap I \subseteq QIQ$ : On the other hand,  $QIQ \subseteq QAQ \subseteq Q$  and  $QIQ \subseteq I$ , so  $QIQ \subseteq Q \cap I$ . Thus  $Q \cap I \subseteq QIQ$ . So by Theorem (3.5),  $A$  is regular. Similarly, we can show that (1)  $\Rightarrow$  (3)  $\Rightarrow$  (5)  $\Rightarrow$  (1).

## 5. CHARACTERIZING WEAKLY-REGULAR SEMIRINGS

Analogous to von Neumann regular rings, a ring  $R$  is weakly-regular if  $x \in (xR)^2$  for each  $x \in R$ . These rings were introduced by Brown and McCoy [10], later investigated by Rammamurthy [11]. Here we characterize weakly-regular semirings using their quasi-ideals and bi-ideals.

**Definition 5.1.** A semiring  $A$  is called a right weakly-regular semiring if for each  $x \in A$ ,  $x \in (xA)^2$ . Thus, if  $A$  is commutative then  $A$  is weakly-regular if and only if  $A$  is regular. In general, however, regular semirings form a proper subclass of weakly-regular semirings.

We start to give their characterization by following theorem.

**Theorem 5.1.** *The following are equivalent for a semiring  $A$  with  $I$ :*

- (1)  $A$  is weakly-regular,
- (2)  $R^2 = R$  for all right-ideal  $R$  of  $A$ ,
- (3) For every ideal  $I$  of  $A$ ,  $R \cap I = RI$ .

**Proof:** (1)  $\Rightarrow$  (2): Clearly  $R^2 \subseteq R$ . For the converse, let  $x \in R$ ; so  $x \in (xR)^2$ . Hence  $x \in R^2$ , so  $R = R^2$ .

(2)  $\Rightarrow$  (3): let  $x \in I$ . Since  $x \in (xA) = (xA)^2$ , it follows that  $x = xy$ , for some  $y \in I$ . For a right-ideal  $R$  of  $A$ , clearly  $RI \subseteq R \cap I$ . Let  $x \in R \cap I$ . Then there exists  $y \in I$  such that  $x = xy$ . Thus  $x \in RI$  i.e.,  $R \cap I \subseteq RI$ , so  $R \cap I = RI$ .

(3)  $\Rightarrow$  (1): Let  $x \in A$ , Then  $x \in (xA) \cap (AxA) = (xA)(AxA) \subseteq (xA^2)(xA) \subseteq (xA)(xA)$  i.e.,  $x \in (xA)^2$ . Hence  $A$  is right weakly-regular.

**Theorem 5.2.** *For a semiring  $A$  with identity 1, the following conditions are equivalent for all bi-ideal  $B$ , quasi-idea  $Q$ , ideal  $I$  and right-ideal  $R$  of  $A$ ,*

- (1)  $A$  is right weakly-regular,
- (2)  $B \cap I \cap R \subseteq BIR$ ,
- (3)  $Q \cap I \cap R \subseteq QIR$ .

**Proof.** (1)  $\Rightarrow$  (2): Let  $x \in B \cap I \cap R \Rightarrow x \in B, x \in I$  and  $x \in R$ . Since  $x \in A$  and  $A$  is right weakly-regular, therefore  $x \in (xA)^2$ . i.e.,  $x = \sum_{finite} xr_i xs_i$  for some,  $s_i \in A$ . Now,  $x = \sum_{finite} xs_i xr_i = \sum_{finite} xs_i (\sum_{finite} xs_i xr_i) r_i = \sum_{finite} xa_i xb_i xc_i$ , where  $a_i, b_i, c_i \in A$ . Thus  $x = \sum_{finite} x(a_i xb_i x)c_i \in BIR$ . Hence  $B \cap I \cap R \subseteq BIR$ .

(1)  $\Rightarrow$  (3): Every quasi-ideal is a bi-ideal, therefore by (2),  $Q \cap I \cap R \subseteq QIR$ .

(3)  $\Rightarrow$  (1): Taking  $Q = R, I = I$  and  $R = A$ , we get from (3),  $R \cap I \cap A \subseteq RIA$ . As  $R \cap I \cap A = RIA$ , and  $RIA \subseteq RI$ . Thus  $R \cap I \subseteq RI$ . But  $RI \subseteq R \cap I$ , so by Theorem (5.1),  $A$  is right weakly-regular.

**Theorem 5.3.** *For a semiring  $A$  with identity, the following are equivalent for all bi-ideals  $B$  and two-sided ideals  $I$ :*

- (1)  $A$  is right weakly-regular,
- (2)  $B \cap I \subseteq BI$ ,
- (3)  $Q \cap I \subseteq QI$ .

**Proof.** (1)  $\Rightarrow$  (2): Let  $x \in B \cap I$ , then  $x \in B$  and  $x \in I$ . Since  $x \in A$  and  $A$  is right weakly-regular, therefore  $x \in (xA)^2$  i.e.,  $x = \sum_{finite} xr_i xs_i$  for some  $r_i, s_i \in A$ . Now  $x = \sum_{finite} x(r_i xs_i) \in BI$ . Thus  $B \cap I \subseteq BI$ .

(2)  $\Rightarrow$  (3): Since a quasi-ideal is a bi-ideal, therefore by (2),  $Q \cap I \subseteq QI$ .

(3)  $\Rightarrow$  (1): Since a one-sided ideal is a quasi-ideal, therefore by (3),  $R \cap I \subseteq RI$ . But  $RI \subseteq R \cap I$ . Therefore  $R \cap I = RI$ . Hence by Theorem (5.1),  $A$  is a right weakly-regular.

## 6. REFERENCES

1. Vandiver, H.S. Note on a simple type of algebra in which the cancellation law of addition does not hold. *Bulletin of the American Mathematical Society* 40(12): 914-920 (1934).
2. Steinfeld, O. *Über die quasiideale von Halbgruppen*. Institutum Mathematicum Universitatis Debreceniensis (1956).
3. Steinfeld, O. *Quasi-Ideals in Rings and Semigroups*. Akad. Kiadó, Budapest (1978).
4. Iséki, K. Quasiideals in semirings without zero. *Proceedings of the Japan Academy* 34(2): 79-81 (1958).

5. Shabir, M., A. Ali & S. Batool. A note on quasi-ideals in semirings. *Southeast Asian Bulletin of Mathematics* 27(5): 923-928 (2004).
6. Lajos, S & F.A. Szasz. On the bi-ideals in associative rings. *Proceedings of the Japan Academy* 46(6): 505-507 (1970).
7. Howie, J. M. *An Introduction to Semigroup Theory*. Academic Press, New York (1976).
8. Golan, J.S. *The Theory of Semirings with Applications in Mathematics and Theoretical Computer Science*. Addison-Wesley Longman Ltd (1992).
9. Subramanian, H. Von neumann regularity in semirings. *Mathematische Nachrichten* 45(1-6):73-79 (1970).
10. Brown, B.& N. H. McCoy. Some theorems on groups with applications to ring theory. *Transactions of the American Mathematical Society* 69(2): 302-311 (1950)
11. Ramamurthi, V. Weakly regular rings. *Canadian Mathematical Bulletin* 16(3): 317 ( 1973).





## Obituary

### Prof. Dr. Muzaffer Ahmad (1920–2016)

With great sorrow and profound grief, the Pakistan Academy of Sciences announces the sad demise of its Senior Fellow Dr. Muzaffer Ahmad who breathed his last on November 22, 2016 at the age of 97. He was Professor Emeritus of Zoology at University of the Punjab, Lahore, which he joined in 1949 and retired from there in 1980 as Mian Afzal Hussain Professor of Zoology. As Professor Emeritus, he continued to go to his Department at the University till his death.

Prof. Dr. Muzaffer Ahmad was elected Fellow of Pakistan Academy of Sciences as early as in 1970.

Dr. Ahmad was born in India on 20<sup>th</sup> September 1920 and opted for Pakistan in 1947 while he was studying in USA as a Government of India scholar. He studied at the University of the Lucknow, India; Muslim University, Aligarh; and The University of Chicago.

Dr. Ahmad was recipient of several awards, including *Aizaz-i-Kamal* from the President of Pakistan, Gold Medal (Fellowship), Gold Medal (research publications) and Felicitation from Pakistan Academy of Sciences; Gold Medal jointly awarded by USDA and PARC and Life-time Achievement Award from the Zoological Society of Pakistan.

Dr. Ahmad made valuable contributions to promote the science of Zoology in Pakistan. He was Founder of the Zoological Society of Pakistan and The Pakistan Congress of Zoology. He was the

first Editor of Pakistan Journal of Zoology and The Proceedings of Pakistan Congress of Zoology and then their Editor-in-Chief. He piloted the scheme recommended by the committee appointed by the Ministry of



Science and Technology, Government of Pakistan to establish a museum of Natural History at Islamabad, which is now a full-fledged institution.

He built up one of the world's finest termite collections, mostly from South-East Asia (Pakistan, Sri Lanka, Bangladesh, Thailand, Malaysia, Malaya, Sarawak and North Borneo).

Dr. Ahmad's decades-long research on termites has been prominently included (with his photograph) in the 7-volume, 2704-page *Treatise on the Isoptera of the World*, published by the American Museum of Natural History, New York. According to the *Treatise* "his 1950 consideration of termite phylogeny remains as one of the most cited and classic works of the Isoptera".

May the departed soul rest in peace. Aameen.

**Prof. Dr. A.R. Shakoori, FPAS**

## Obituary

### Prof. Dr. Syed Qasim Mehdi

(1941–2016)

We are grieved on the demise of an eminent scientist and a senior Fellow of the Pakistan Academy of Sciences, Prof. Dr. Syed Qasim Mehdi, who breathed his last on 27 September, 2016 in Lahore after a protracted illness. Dr. Mehdi was a renowned molecular biologist and was elected Fellow of the Pakistan Academy of Sciences in 1999.

Dr. Qasim Mehdi was born in British India on 13th February, 1941. He obtained his MS in 1966 from Massachusetts Institute of Technology (MIT), USA and D.Phil. in 1969 from University of Oxford, UK. Prof. Mehdi served as Director General, Biomedical and Genetic Engineering Division of Dr. A. Q. Khan Labs; Head, National Institute of Biotechnology and Genetic Engineering, Biomedical Division, Lahore, 1986-1991; Director (Scientific), The Alexandar Medical Foundation, Woodside, California, USA, 1980-1992; Senior Research Fellow and Research Professor, Department of Chemistry and Radiology, Cancer Biology Research Labs, Stanford University, California, USA, 1980-1986; Senior Research Associate, Department of Radiology, Nuclear Medicine Division, Stanford University, School of Medicine, California, USA, 1976-1980; and Visiting Professor, Klinikum Steglitz, The Free University, Berlin, Germany, 1974-1976. Currently, he was heading the Centre for Human Genetics and Molecular Medicine at Sindh Institute of Urology (SIU), Karachi.

Dr. Qasim Mehdi was recipient of *Hilal-e-Imtiaz* in 2003, *Sitara-i-Imtiaz* in 1998, Sigma Xi Award by American Society for the Promotion of Research in 1966, and Best Student Award by Lucknow University in 1962 and 1963. He was Nuffield Committee Fellow, Oxford University, UK, 1970; Wellcome Trust Fellow, Oxford

University, UK, 1972; Fellow, National Academy of Medical Sciences, Pakistan; Fellow, New York Academy of Sciences; Fellow, Chemical Society of Pakistan; Member, Biochemical Society, UK; Member, The American Thyroid



Association; Member (Life) The Oxford Union Society; Member, The Oxford-Cambridge Society; Member, Human Genome Organization (HUGO), USA; Member, International Executive Committee, Human Genome Diversity Project (HGDP), USA; Member, Governing Body, The Liaquat National Hospital, Karachi; Member, Prime Minister's Cabinet Committee for Evaluation of S&T Development in Pakistan, 1993; Member, Board of Governors, Shaukat Khanum Memorial Trust, Lahore, 1998; Chairman, Southwest Asian Committee, HGDP, USA; UNESCO Bioethics Committee, 2002-2005; and Uttar Pradesh Association for Science and Technology Advancement (UPASTA), India.

Dr. Qasim Mehdi's areas of research were Molecular Biology and Genetics with special interest in Molecular Biology of Diseases, Biotechnology and Human Genome Diversity. In the death of Dr. Qasim Mehdi, Pakistan has lost a stalwart in the area of human genomics.

May the Allah Almighty rest his soul in eternal peace and give fortitude to his family to bear this irreparable loss! Aameen.

**Dr. Abdul Rashid, FPAS**

# *Proceedings of the Pakistan Academy of Sciences*

## **Instructions for Authors**

**Aims and Scope:** *Proceedings of the Pakistan Academy of Sciences* is official journal of the Academy, published quarterly, in English. This open access journal publishes research papers in *Engineering Sciences & Technology, Life Sciences, Medical Sciences, and Physical Sciences*. State-of-the-art reviews (~20 pages, supported by recent references) summarizing R&D in a particular area of science, especially in the context of Pakistan, and suggesting further R&D are also considered. Manuscripts undergo double-blind review. Authors are not required to be Fellows or Members of the *Pakistan Academy of Sciences* or citizens of Pakistan.

### **Manuscript Format**

*Manuscript may contain Abstract, Keywords, INTRODUCTION, MATERIALS AND METHODS, RESULTS, DISCUSSION (or RESULTS AND DISCUSSION), CONCLUSIONS, ACKNOWLEDGEMENTS and REFERENCES and any other information that the author(s) may consider necessary.* The Manuscript sections must be numbered, i.e., **1. INTRODUCTION, 2. MATERIALS AND METHODS,** and so on.

Manuscripts, in *Times New Roman*, 1.5-spaced (but single-space the Tables), with line numbering and one-inch margins on all sides on A-4 size paper, should not exceed 20 pages including Tables and Figures. Number manuscript pages throughout. The text (in **Font Size 11**, except for the sections mentioned in **Font Size 10**) must be typed in a single column across the paper width. All Tables and Figures must be placed after the text, i.e., after REFERENCES section.

(a) **Title** of the article (Capitalize initial letter of each main word; font size 16; **bold**), max 160 characters (no abbreviations or acronyms), depicting article's contents; (b) Author's first name, middle initial and last name (font size 12, **bold**), and professional affiliation (i.e., each author's Department, Institution, Mailing address and Email; but no position titles) (font size 12); (c) Indicate the corresponding author with \*; (d) **Short running title**, max 50 characters (font size 10). The **next Page** should start with **Title** of the Article, followed by entire manuscript. **Headings and Subheadings** (font size 11): All flush left

**LEVEL-1: ALL CAPITAL LETTERS; bold**

**Level-2: Capitalize each main word; bold**

**Level-3: Capitalize each main word; Bold, Italic**

**Level-4: Run-in head; Italics, in the normal paragraph position. Capitalize the initial word only and end in a colon (i.e., :)**

**Abstract** (font size 10; max 250 words): Must be self-explanatory, stating rationale, objective(s), methodology, main results and conclusions of the study. Abbreviations, if used, must be defined on first mention in the Abstract as well as in the main text. Abstract of review articles may have variable format.

**Keywords** (font size 10): Three to eight keywords, depicting the article.

**INTRODUCTION:** Provide a clear and concise statement of the problem, citing relevant recent literature, and objectives of the investigation.

**MATERIALS AND METHODS:** Provide an adequate account of the procedures or experimental details, including statistical tests (if any), in a concise manner but sufficient enough to replicate the study.

**RESULTS:** Be clear and concise with the help of appropriate Tables, Figures and other illustrations. Data should not be repeated in Tables and Figures, but must be supported with statistics.

**DISCUSSION:** Provide interpretation of the RESULTS in the light of previous relevant studies, citing published references.

**ACKNOWLEDGEMENTS** (font size 10): In a brief statement, acknowledge financial support and other assistance.

**REFERENCES** (font size 10): Cite references in the text **by number only in square brackets**, e.g. "Brown et al [2] reported ..." or "... as previously described [3, 6–8]", and list them in REFERENCES section, in the order of citation in the text, Tables and Figures (not alphabetically). Only published (and accepted for publication) journal articles, books, and book chapters qualify for REFERENCES.

List of REFERENCES must be prepared as under:

a. **Journal Articles** (*Name of journals must be stated in full*)

1. Golding, I. Real time kinetics of gene activity in individual bacteria. *Cell* 123: 1025–1036 (2005).
2. Bialek, W. & S. Setayeshgar. Cooperative sensitivity and noise in biochemical signaling. *Physical Review Letters* 100: 258–263 (2008).
3. Kay, R.R. & C.R.L. Thompson. Forming patterns in development without morphogen gradients: differentiation and sorting. *Cold Spring Harbor Perspectives in Biology* 1: doi: 10.1101/cshperspect.a001503 (2009).

b. **Books**

4. Luellen, W.R. *Fine-Tuning Your Writing*. Wise Owl Publishing Company, Madison, WI, USA (2001).
5. Alon, U. & D.N. Wegner (Ed.). *An Introduction to Systems Biology: Design Principles of Biological Circuits*. Chapman & Hall/CRC, Boca Raton, FL, USA (2006).

c. **Book Chapters**

6. Sarnthein, M.S. & J.D. Stanford. Basal sauropodomorpha: historical and recent phylogenetic developments. In: *The Northern North Atlantic: A Changing Environment*. Schafer, P.R. & W. Schluter (Ed.), Springer, Berlin, Germany, p. 365–410 (2000).
7. Smolen, J.E. & L.A. Boxer. Functions of Europhiles. In: *Hematology*, 4<sup>th</sup> ed. Williams, W.J., E. Butler & M.A. Litchman (Ed.), McGraw Hill, New York, USA, p. 103–101 (1991).

**Tables**, with concise but self-explanatory headings must be numbered according to the order of citation (like **Table 1**, **Table 2**). Round off data to the nearest three significant digits. Provide essential explanatory footnotes, with superscript letters or symbols keyed to the data. Do not use vertical or horizontal lines, except for separating column heads from the data and at end of the Table.

**Figures** may be printed in two sizes: column width of 8.0 cm or page width of 16.5 cm; number them as **Fig. 1**, **Fig. 2**, ... in the order of citation in the text. Captions to Figures must be concise but self-explanatory. Laser printed line drawings are acceptable. Do not use lettering smaller than 9 points or unnecessarily large. Photographs must be of high quality. A scale bar should be provided on all photomicrographs.

**Declaration:** Provide a declaration that: (i) the results are original; (ii) the same material is neither published nor under consideration elsewhere; (iii) approval of all authors has been obtained; and, (iv) in case the article is accepted for publication, its copyright will be assigned to *Pakistan Academy of Sciences*. Authors must obtain permission to reproduce, where needed, copyrighted material from other sources and ensure that no copyrights are infringed upon.

**Reviewers:** Authors may suggest four relevant reviewers, two local and two from scientifically advanced countries.

Manuscripts must be submitted in Microsoft Word (.doc or .docx format; **pdf** files not acceptable). Figures can be submitted in Word format, TIFF, GIF, JPEG, EPS, PPT.

Manuscripts may be submitted as email attachment at the following email address. In case of any difficulty while submitting your manuscript, please get in touch with:

**Editor-in-Chief**  
**Pakistan Academy of Sciences**  
**3-Constitution Avenue, G-5/2, Islamabad, Pakistan**  
**Email:** [editor@paspk.org](mailto:editor@paspk.org)  
**Tel:** +92-51-920 7140  
**Website:** [www.paspk.org](http://www.paspk.org)



# PROCEEDINGS

## OF THE PAKISTAN ACADEMY OF SCIENCES:

### A. Physical and Computational Sciences

## CONTENTS

Volume 53, No. 4, December 2016 Page

### Research Articles

Enhanced Performance of Consensus Fault-tolerant Schemes for Decentralized Unmanned Autonomous Vehicle System — <i>Naeem Khan, Aitzaz Ali, and Wasi Ullah</i>	363
Identification of Factors Affecting Modal Shift in Lahore — <i>Sulaiman Majeed and Zahara Batool</i>	373
Generating EXPRESS Data Models from SBVR — <i>Imran Sarwar Bajwa, Nadeem Sarwar, and M. Asif Naeem</i>	381
CFD Analysis to Study the Effect of Geometry in Flow Behavior of Wing Structure with Additional Riblets — <i>Muhammad Zia Ullah Khan, Rumeel A. Bhutta, Tahir Asif, Muhammad Farooq, and Adnan Qamar</i>	391
Palm and Finger Segmentation of High Resolution Images using Hand Shape and Texture — <i>Momna Asghar, Irfan Arshad, Imtiaz Ahmad Taj, Gulistan Raja, and Ahmad Khalil Khan</i>	401
An Empirical Study and a Framework for Effective Risk Management in Scrum — <i>Muneeb Ali, Yasir Hafeez, and Bushra Hamid</i>	417
Fabrication and Identification of Graphene Layers on Silicon Dioxide and Flexible PMMA Substrates — <i>Zeba Khanam, Ibtisam Riaz, Adeel Rasheed, and Rashid Jalil</i>	431
Product and Exponential Product Estimators in Adaptive Cluster Sampling under Different Population Situations — <i>Muhammad Shahzad Chaudhry, and Muhammad Hanif</i>	447
Matter Wave Travelling Dark Solitons in a Coupled Bose-Einstein Condensate — <i>Muhammad Irfan Qadir and Sumreen Naz</i>	459
Characterizing Semirings using Their Quasi and Bi-Ideals — <i>Mohammad Munir, and Mustafa Habib</i>	469
<b>Obituaries</b>	
Prof. Dr. Muzaffer Ahmad	477
Prof. Dr. Syed Qasim Mehdi	478
<b>Instructions for Authors</b>	479

PAKISTAN ACADEMY OF SCIENCES, ISLAMABAD, PAKISTAN

HEC Recognized, Category X; PM&DC Recognized

Website: [www.paspk.org](http://www.paspk.org)